

STELLINGEN

1. Het baculovirus GP64 eiwit bevat signalen die het uitreden van virusdeeltjes via de basolaterale zijde van geïnfecteerde middendarmcellen regelen.

Dit proefschrift

2. De concentratie van GP64 aan de uiteinden van het staafvormige 'budded virion' suggereert dat GP64 een rol speelt bij de membraanroning ter initiatie van virus 'budding'.

Dit proefschrift

3. Alle NPV virussen die op basis van fylogenetische analyses ondergebracht worden in de gepostuleerde NPV subgroep I bevatten een *gp64* gen.

Dit proefschrift

Zanotto et al. (1993). *J. Invert. Pathol.* 62: 147-164

Hu, Z.H. (1998). *Ph.D. thesis*

4. Het effect van cytochalasine B en D op de 'budding' van AcMNPV is moeilijk te interpreteren en de conclusie dat het cytoskelet geen rol speelt bij dit proces is derhalve voorbarig.

Volkman et al. (1987). *Virology* 156: 32-39

5. Chimeraplastie biedt mogelijkheden bij de genezing van erfelijke ziekten, o.a. door het nauwkeurig aanbrengen van gewenste mutaties via het gebruik van niet-virale carriers (liposomen). Het gebruik van virussen, van op virus gebaseerde carriers of van een combinatie van liposomen en virale componenten, verhoogt de efficiëntie van chimeraplastie op organismaal niveau.

Gura (1999). *Science* 285: 316-318

6. Het bewijs, dat het niet-incorporeren van het HIV gp120/160 in VSV virions wordt veroorzaakt doordat dit glycoproteïne wordt verankerd op plaatsen van het plasmamembraan die afwijken van de plaats van VSV 'budding', is niet overtuigend.

Johnson et al. (1998). *Virology* 251: 244-252

7. In het streven naar publiekelijk begrip en ondersteuning voor verdere ontwikkeling van wetenschapsgebieden die genetische modificatie betreffen, zou als eerste het verband tussen research en technologie enerzijds en reeds geconsumeerde genetisch gemodificeerde producten zoals voedsel, medicijnen en vaccins anderzijds, moeten worden benadrukt.

8. GP64 fungeert voor een baculovirus als 'huissleutel'. Zonder sleutel komt het virus de cel slechts in of uit als per toeval de deur wordt opgedaan.

9. Het eeuw-oud advies (1897) van Ramón y Cajal (een grondlegger van de moderne neurobiologie) voor de jonge onderzoeker om geen rijke vrouw te trouwen, is niet meer van deze tijd.

J.H. Kaas (1999). *Science* 284: 2097

S. Ramón y Cajal. *Precepts and counsels in scientific investigation: Stimulants of the spirit* (1951). Translated by Ma. Sanchez-Perez. C.B Courville, Ed. (Pacific, Mountain View, CA).

10. Een significant verschil tussen Nederland en de VS is de franje op de friet.

Stellingen behorend bij het proefschrift

Functional and structural analysis of GP64, the major envelope glycoprotein of the budded virus phenotype of *Autographa californica* and *Orgyia pseudosugata* multicapsid nucleopolyhedroviruses

door A.G.P. Oomens, te verdedigen op 20 september 1999

Functional and structural analysis of GP64, the major
envelope glycoprotein of the Budded Virus phenotype
of *Autographa californica* and *Orgyia pseudotsugata*
Multicapsid Nucleopolyhedroviruses

Promotor: Dr. J.M. Vlak
Persoonlijk Hoogleraar bij de leerstoelgroep Virologie

Co-promotor: Gary W. Blissard, Ph.D.
Associate Molecular Biologist at the Boyce Thompson Institute

W 008201, 2532

Functional and structural analysis of GP64, the major
envelope glycoprotein of the Budded Virus phenotype
of *Autographa californica* and *Orgyia pseudotsugata*
Multicapsid Nucleopolyhedroviruses

Antonius G.P. Oomens

Proefschrift

ter verkrijging van de graad van doctor
op gezag van de rector magnificus van de
Universiteit Wageningen
Dr. C.M. Karssen
in het openbaar te verdedigen
op maandag 20 september 1999
des namiddags te vier uur in de Aula

99/0029

The work presented in this thesis was carried out at the Boyce Thompson Institute for Plant Research at Cornell University, Ithaca, New York, U.S.A. The work was supported by NIH grants AI 31130 and AI 33657

Oomens, A.G.P.

Functional and structural analysis of GP64, the major envelope glycoprotein of the Budded Virus phenotype of *Autographa californica* and *Orgyia pseudotsugata* Multicapsid Nucleopolyhedroviruses -

A.G.P. Oomens

Thesis Wageningen, - with summary in Dutch

ISBN 90-5808-061-7

Subject headings: Baculovirus, GP64

BIBLIOTHEEK
LANDBOUWUNIVERSITEIT
WAGeningen

Preface

Let me begin by saying that I am very excited to soon finish my graduate work and (by the time the thesis will be printed) to have begun a post-doctoral position in pursuit of a Ph.D. career track. Despite the excitement, the decision to follow such a track did not come easily. For a long time I have been trying to figure out, in a somewhat philosophical fashion, whether pursuing a Ph.D. degree was the right thing to do for me, and some of my 'stellingen' (statements) may reflect that. My first thanks go out to the people who have, through the many years, discussed with me their personal experiences during and after obtaining their Ph.D., in particular Gary Blissard and Peter Roelvink. It is, needless to say, unpredictable what a Ph.D. will bring or lead to, nevertheless these discussions were always very helpful and well appreciated. Ultimately, entering the Ph.D. track has enhanced my thinking and enthusiasm with regards to virology in many ways, and I am happy to be where I am. To get where I am, I have had help and support from a great many people. From our lab and Cornell I would like to thank for good collegueship John Wenz, Phil Kogan, Xiaoying Chen, Jeff Slack, David Garrity, Min-Ju Chang, Kathy Hefferon, Guangyun Lin, Debbie Letham, Casey Finnerty, Marlinda Lobo de Souza, Pat Lilja, Jodie Mangor, Rodolfo Lopez-Gomez, Bob Granados, Alan Wood, Pat Hughes, Ping Wang, Marc Harper, Lokesj Joshi, and last but not least Scott Monsma. For my Ithaca friends, I'll simply say thanks to Paul and to the Gary (Matassarini) group, which includes just about everybody else I know. A special thank you go out to the Boyce Thompson Institute for providing excellent opportunities and an encouraging scientific environment, to Andy Grefig for putting me up in his house for several years, to my promotor Just Vlak for all of the timely arrangements and tasks carried out in Wageningen on my behalf in preparation of the defense, to my Dutch friends Toon Rijkers, Belinda Oude-Essink and Inca Kusters for their enduring friendship, and to my supervisor Gary Blissard for the never ending enthusiasm and encouragement and for giving me the opportunity to develop my skills. Gary, it has been a (intense :)) privilege to get introduced to virology in your laboratory. Finally, I'd like to thank my family for a life-long support, everybody I have not mentioned above, and most of all Katie, my wife, for all of the patience, understanding, and encouragement.

Contents

Chapter 1	Introduction and scope of the thesis	1
	- Introduction to the Baculoviridae and their life cycle	1
	- A history of GP64 literature preceding the thesis	4
	- Scope of the thesis	11
Chapter 2	The baculovirus GP64 envelope fusion protein: Synthesis, oligomerization, and processing	15
Chapter 3	The GP64 envelope fusion protein is an essential baculovirus protein required for cell-to-cell transmission of infection	35
Chapter 4	Requirement for GP64 to drive efficient budding of <i>Autographa californica</i> Multicapsid Nucleopolyhedrovirus	57
Chapter 5	Host cell receptor binding by baculovirus GP64 and kinetics of virion entry.	83
Chapter 6	Characterization of the <i>lef7-gp64-p74</i> locus of <i>Anticarsia gemmatalis</i> Multicapsid Nucleopolyhedrovirus	103
Chapter 7	General discussion	125
	- Carbohydrate and lipid modifications of GP64 and their role in GP64 function	125
	- Glycoprotein targeting in polarized epithelial cells, the initial site of ODV infection: a role for GP64?	129
	- The role of viral spike proteins and their cytoplasmic tail domains in virus budding	132
	- Evolution of GP64, and current and future avenues of GP64 research	147
References		153
Summary		169
Samenvatting		173
List of publications		176
Curriculum vitae		179

Abbreviations

General

BV	Budded Virus
CTD	Cytoplasmic tail domain
Env	Envelope glycoprotein
ER	Endoplasmatic reticulum
gag	Retrovirus polyprotein Pr55gag
GV	Granulovirus
HA	Influenza virus hemagglutinin
Ld	<i>Lymantria dispar</i>
MAB	Monoclonal antibody
NA	Influenza virus neuraminidase
NC	Nucleocapsid
NPV	Nucleopolyhedrovirus
OB	Occlusion body
ODV	Occlusion Derived Virus
ORF	Open reading frame
Sf	<i>Spodoptera frugiperda</i>
TM	Transmembrane
Tn	<i>Trichoplusia ni</i>

Viruses

AcMNPV	<i>Autographa californica</i> Multicapsid Nucleopolyhedrovirus
AfMNPV	<i>Anagrapha falcifera</i> Multicapsid Nucleopolyhedrovirus
AgMNPV	<i>Anticarsia gemmatalis</i> Multicapsid Nucleopolyhedrovirus
BmNPV	<i>Bombyx mori</i> Nucleopolyhedrovirus
BsNPV	<i>Buzura suppressaria</i> Singlecapsid Nucleopolyhedrovirus
CfMNPV	<i>Choristoneura fumiferana</i> Multicapsid Nucleopolyhedrovirus
DHO virus	Dhori virus
EpNPV	<i>Epiphyas postvittana</i> Multicapsid Nucleopolyhedrovirus
HIV	Human Immunodeficiency virus
LdMNPV	<i>Lymantria dispar</i> Multicapsid Nucleopolyhedrovirus
LsNPV	<i>Leucania separata</i> Multicapsid Nucleopolyhedrovirus
MbMNPV	<i>Mammestra brassicae</i> Multicapsid Nucleopolyhedrovirus
MoMuLV	Moloney Murine Leukemia virus
NDV	Newcastle Disease virus
OpMNPV	<i>Orgyia pseudotsugata</i> Multicapsid Nucleopolyhedrovirus
SeMNPV	<i>Spodoptera exigua</i> Multicapsid Nucleopolyhedrovirus
SFV	Semliki Forest virus
SpINPV	<i>Spodoptera litura</i> Multicapsid Nucleopolyhedrovirus
SpItNPV	<i>Spodoptera littoralis</i> Multicapsid Nucleopolyhedrovirus
THO virus	Thogoto virus
VSV	Vesicular Stomatitis virus

Chapter 1

Introduction and scope of the thesis

Introduction to the Baculoviridae and their life cycle

The field of baculovirology has advanced rapidly in recent years. One reason for this advance was the potential to use baculoviruses for insect pest control, as the main target of baculoviruses, Lepidopteran larvae, cause feeding damage to agricultural crops and forests. Along with an increased understanding of the molecular biology of baculoviruses came the potential to use baculoviruses as systems for foreign gene expression and to study fundamental virological questions. It is within the latter category that the focus of this thesis falls.

The Baculoviridae are a family of large, enveloped, double-stranded DNA viruses that are found almost exclusively in insects. Most baculoviruses have a narrow host range, and infect hosts within the order Lepidoptera. Some have been identified in other insect orders such as Hymenoptera and Diptera, as well as in crustaceans. The virions of the Baculoviridae are typically rod-shaped (~ 30-60 x 250-300 nm), and are often found embedded within proteinaceous occlusion bodies (Fig. 1). All known baculoviruses are currently classified in one of two genera: the Nucleopolyhedroviruses (NPVs), or the Granuloviruses (GVs), which can be differentiated (among others) by the size of their occlusion bodies. The GV's occlude single virions within smaller occlusion bodies called 'granules', whereas the NPVs contain multiple virions within each large occlusion body (OB) or 'polyhedron'. The NPVs are designated SNPV or MNPV depending on whether single (S) or multiple (M) nucleocapsids (NCs) are packaged within each virion. Virions of the NPVs derived from polyhedra, are termed 'occlusion derived virus' or 'ODV'. Not all NPV virions however are occluded within polyhedra. Characteristic for the NPVs is the production of a second, non-occluded phenotype during their infection cycle: the 'budded virus' (BV). While apparently containing identical NCs, BV and ODV differ in composition of their envelopes, and serve distinctly different roles in the infection cycle. Whereas the ODV is highly infectious only to the epithelial cells of the midgut and is responsible for the spread of the virus from insect to insect, the apparent role of the BV in the infection cycle is to spread the infection from cell to cell within the insect (128, 265). BV is highly infectious to cells and tissues (except midgut) *in vivo* as well as in tissue culture.

Baculovirus occlusion bodies are released into the environment upon cell lysis and death of an insect host. Horizontal transmission occurs through feeding on foliage contaminated with occlusion bodies. After ingestion, ODVs are released in the insect midgut when the occlusion bodies dissolve upon exposure to the alkaline pH (Fig. 2). Upon entering the epithelial cells, NCs are released into the cytoplasm and migrate to

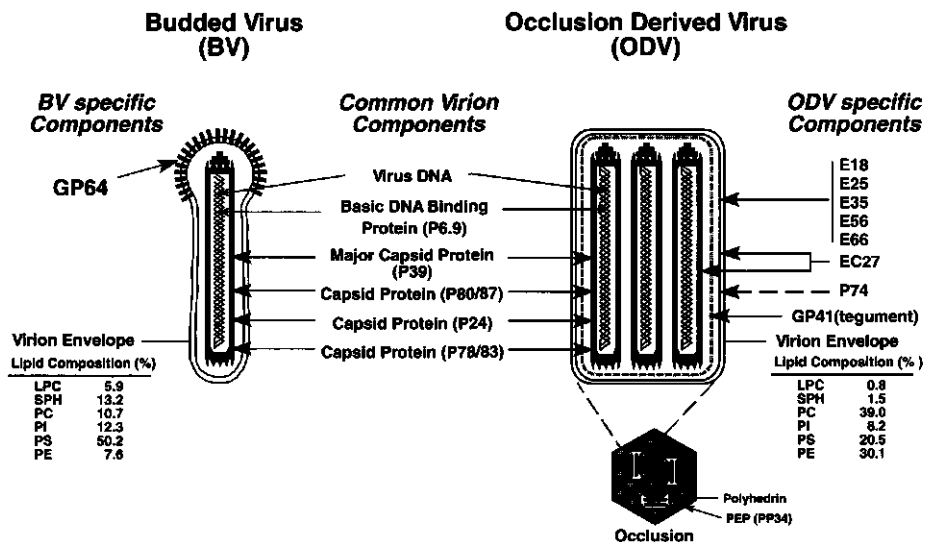


FIG. 1. Structural composition of the two baculovirus phenotypes, 'budded virus' (BV) and 'occlusion-derived virus' (ODV) (adapted from Blissard, 1996). The ODV structure in this illustration represents the Multicapsid (M) Nucleopolyhedrovirus (NPV) group. Proteins specific to either BV or ODV are indicated on the left and right of the diagrams. Proteins common to both virion phenotypes are indicated in the center. The baculovirus capsid is of a polar nature, illustrated by a structure described as claw-like at the bottom, and by a ring-like nipple structure at the top. Although the specific locations of most capsid proteins are not known, the P78/83 capsid protein was reported to be localized at one end of the capsid. The possible location of the P74 protein is indicated by a dashed line. Lipid compositions of the BV and ODV envelopes derived from AcMNPV infected-Sf9 cells (14) are indicated (LPC, lysophosphatidylcholine; SPH, sphingomyelin; PC, phosphatidylcholine; PS, phosphatidylserine; PE, phosphatidylethanolamine)

the nucleus where transcription of viral genes and replication of the viral genome takes place. The ~ 134,000 bp genome of the prototype baculovirus, *Autographa californica* Multicapsid Nucleopolyhedrovirus (AcMNPV), was recently sequenced and contains 154 open reading frames (ORF) potentially encoding proteins of ≥ 50 amino acids (2). Genes are expressed sequentially, in a cascade-like fashion in which each successive phase is dependent on the previous one (for reviews, see (7, 167)). Regulation of baculovirus gene expression occurs primarily at the transcriptional level, and three separate phases are distinguished during a baculovirus infection: early, late and very late. Early genes are transcribed by a host cell-encoded RNA polymerase II, and contain typical eukaryotic consensus transcription signals such as the TATA box and CAGT motif. Among the early gene products are powerful transcriptional regulators, such as the immediate-early gene *ie1* (81). Late genes are transcribed by an alpha-amanitin resistant virus-encoded RNA polymerase (56, 82), and this transcription initiates at a consensus A/GTAAG motif. Many late genes are involved in virion structure

Midgut Epithelium

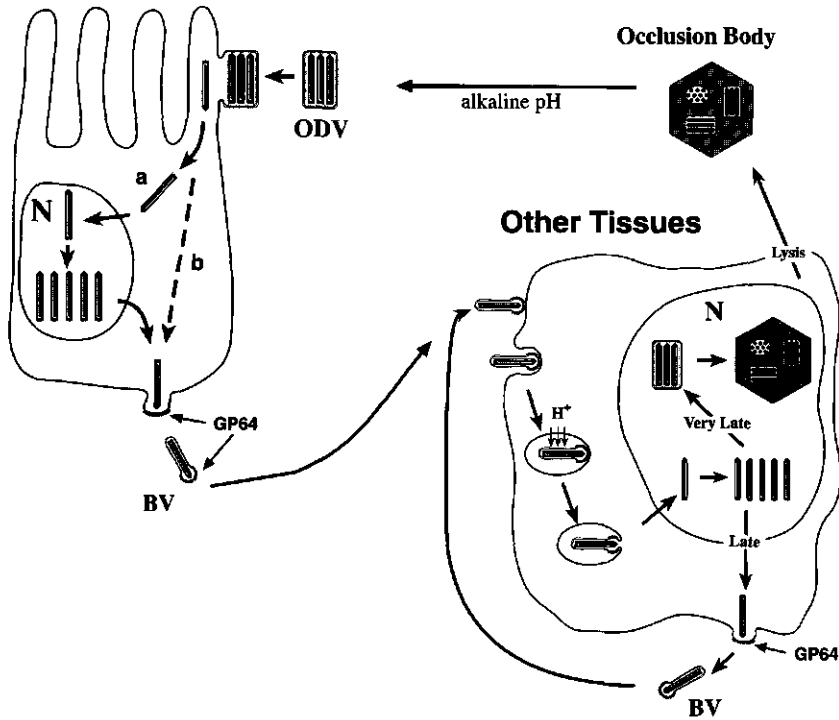


FIG. 2. The baculovirus infection cycle (from Blissard, 1996). On the left, the infection of midgut epithelial cells by the occlusion derived Virus (ODV) is illustrated. After fusion of the ODV at the plasma membrane, two possible routes of nucleocapsid migration are indicated (a and b). In what is thought to be the typical route (a), nucleocapsids (NCs) are transported to the nucleus where gene expression, DNA replication, and assembly of progeny NCs occur. Newly assembled NCs then migrate from the nucleus towards the plasma membrane. A portion of the incoming NCs may bypass the nucleus (b), and migrate directly to the basolateral plasma membrane. NCs bud from the basal side of the epithelial cell at sites where GP64, the major envelope glycoprotein of the BV phenotype (indicated by arrows), has accumulated. During the budding process, GP64 is acquired along with a loosely adhering envelope. The right side of the figure represents the infection of insect cells, other than midgut epithelial, by the 'budded virus' (BV) phenotype. After BV binding and uptake into the endosome, the acidification of the endosome triggers fusion of the viral and endosomal membrane, after which the NCs are released into the cytoplasm. Although the modes of entry of the ODV and BV are different and specific for each virus phenotype, once NCs are released into the cytoplasm, progression of infection appears similar. Except for midgut epithelial cells, at the very late stage of the infection cycle nucleocapsids become embedded within proteinaceous occlusion bodies (OBs) in the nucleus. Upon death and liquefaction of the host, OBs are released into the environment to initiate a new round of infection.

and morphogenesis, whereas the very late genes such as *polyhedrin* and *p10*, are associated with virus occlusion (253, 255). The very late genes are expressed from very strong viral promoters, and these promoters are extensively utilized in baculovirus systems for heterologous protein production. When viral DNA has been replicated and structural proteins are produced in sufficient quantities, NCs are assembled within the nucleus, and subsequently migrate towards the plasma membrane. NCs line up along the plasma membrane (90) at sites where GP64, the major envelope glycoprotein of the BV, has accumulated (258). As NCs egress by budding through the plasma membrane, they acquire from the host cell a loosely adhering envelope (249), and GP64 is acquired by the BV in the process of budding. The BV phenotype then, is responsible for the spread of infection beyond the initially infected midgut epithelium. This is thought to occur by budding of the BV from the initially infected midgut epithelial cell at the basal plasma membrane, as this was experimentally observed by several groups (for example (74, 249)). Recent studies suggest that the BV may also use the tracheal system to spread the infection beyond the midgut epithelium, since tracheoblasts are among the first cells infected after midgut epithelial cells (47, 51, 127). The mechanism of virus budding and the role of GP64 in this process are not well understood, and this is one of the research topics (chapter 4) of this thesis. Contrary to epithelial cells, at the very late stage of infection of non-epithelial cells, a portion of the newly assembled NCs remain in the nucleus where they are occluded within proteinaceous occlusion bodies (OB), termed polyhedra. Upon death and liquefaction of an infected insect, these OBs remain in the environment to initiate a new infection upon ingestion by a susceptible insect larva.

A history of GP64 literature preceding the thesis

The early history. One of the earliest reports of the baculovirus protein currently known as GP64, GP64/67, or GP64 envelope Fusion Protein (GP64 EFP) was a study by Carstens (21). In that study, a protein of an estimated molecular weight of 67 was shown to be a major structural BV component, and could be detected in AcMNPV infected *Spodoptera frugiperda* (Sf) cells as early as 6-8 h pi, peaking at 24 h pi. Other studies found a similarly sized BV protein to be phosphorylated (161) and glycosylated (68). Monoclonal antibodies (MAb) were raised against the non-occluded or BV phenotype of AcMNPV (97). Two antibodies from that study, AcV5 and AcV1, have since been extensively utilized in the quest for GP64 structure and function. These two antibodies differed in their reactivity for GP64. In Western blot analyses of β -mercaptoethanol-reduced BV proteins, MAb AcV5 displayed strong reactivity for a protein with an estimated molecular weight of 64, but did not neutralize BV infectivity. In contrast, AcV1 neutralized BV infectivity but did not react with any viral proteins on Western blots. Neither of the two antibodies reacted with proteins derived from ODV. In a later study (264), the target antigen for AcV1 was further investigated: AcV1 was

shown to immunoprecipitate proteins of various molecular weight (among which a protein of 64 kD), all of which were glycosylated. In retrospect some of these were likely degradation products of GP64 with the exception of some high molecular weight bands, which were speculated to represent dimeric, trimeric, and tetrameric forms of GP64 (258, 260). The AcV1 epitope on BV was destroyed when viral proteins were denatured in the presence of β -mercaptoethanol. GP64 was (again) shown to be phosphorylated, and reported to have an isoelectric point of 3.15 and therefore to be highly acidic. It was suggested that the phosphate groups might contribute to the acidity of GP64. Unpublished data from our laboratory however suggest that the isoelectric point is between 5.6 and 6.0, contradicting the earlier assertion that GP64 might be a highly acidic protein (Monsma, unpublished data).

GP64 and virus exit from the host cell. A study by Volkman (264) was among the first to demonstrate the location of GP64 in a baculovirus infected insect cell, and to give clues about one of its possible roles in the baculovirus infection cycle. AcV1 was shown to react with the surface of infected cells at a stage of the infection cycle prior to

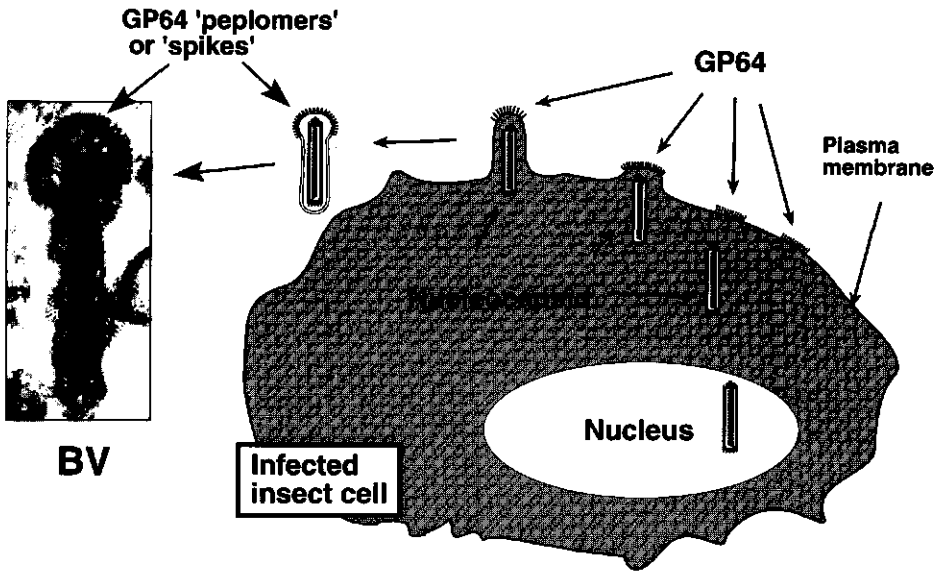


FIG. 3. Baculovirus BV budding and presence of 'spike-like' proteins or 'peplomers' on the BV phenotype as seen by electron microscopy (from Blissard(7)). In the late phase of the infection cycle, progeny NCs migrate from the nucleus and bud through the plasma membrane at sites where GP64 (indicated by arrows), the major envelope glycoprotein of the BV phenotype, has accumulated. GP64 is acquired during the budding process, along with an apparently loosely adhering plasma membrane-derived envelope. The resulting virions display 'spike-like' proteins or 'peplomers' at the virion surface. These spike-like proteins appear to be concentrated at one end of the virion and are believed to be composed of the major envelope glycoprotein GP64.

polyhedra formation, a period of active virus budding. Also, immuno-electron microscopy indicated that AcV1 reacted with a protein present at or in the viral envelope, more concentrated at one end of the virion with 'peplomers' (264)(Fig. 3). The accumulation of 'peplomers' or 'spike' glycoproteins at the plasma membrane coincident with budding of virus particles from the cell surface, was a process observed with several other enveloped viruses (129). In addition, while NCs were observed budding only from the basolateral side of ODV- infected midgut epithelial cells (74, 249), GP64 was detected in AcMNPV- infected columnar epithelial cells in a polar fashion as well (127). Hence, it was suggested that GP64 might be a potentially important factor in the budding process of AcMNPV. The role of GP64 in virus exit was extensively studied in this thesis, see chapters 4 and 3.

GP64 and virus entry into the host cell. In an attempt to better understand the entry mechanism of BV, the mechanism by which MAb AcV1 neutralized BV infectivity was examined (261). Binding of radiolabeled BV to Sf21 cells appeared unaffected when BV was pre-incubated with AcV1, showing that the neutralizing capacity of AcV1 was not at the level of virus binding to cells. In the same study, a valuable insight into the mechanism by which the BV phenotype enters its host cell was gained, when the effect of lipophilic amines on BV infectivity was examined. These agents (for example chloroquine and ammonium chloride, also called lysosomotropic reagents) prevent the acidification of the endosome when added to cells (89, 148). As such, these reagents identified viruses that enter by endocytosis, such as the enveloped viruses Semliki Forest virus (SFV, Togaviridae)(158), Influenza virus (Orthomyxoviridae)(148), and Vesicular Stomatitis virus (VSV, Rhabdoviridae)(35). When insect cells were treated with these lipophilic amines, BV infectivity was drastically reduced, and it was therefore concluded that baculovirus BV also enters its host cell by endocytosis. MAb AcV1 then, neutralized BV at a stage of endocytosis beyond binding, possibly in the endosome. In the model of entry by endocytosis (see also Fig. 2), virus first binds to cells, and is then taken up via clathrin coated pits to follow an endocytic pathway. During uptake through the endocytic pathway, the pH of the endosome decreases at least partly as a result of vacuolar proton ATPases (83). The lowered pH triggers a conformational change in the viral glycoprotein, which in some cases has been shown to expose a hydrophobic fusion peptide/domain. Based on recent studies with Influenza virus following a comparison of the three-dimensional structure of portions of HA at the physiological and low pH conformations (18, 279), some of the important conformational changes believed to occur are a) formation of a triple-stranded coiled coil, and b) the transition of a loop region within each HA monomer to an alpha-helix structure. These structural changes in turn translocate the alpha-helical hydrophobic peptide, and insert the peptide into the target membrane. The top of the acid-induced coiled coil is then thought to spread apart, thereby bringing the viral and cellular membrane closer together ('apposition' (20, 285)). This ultimately leads to fusion of the viral and endosomal membrane by a process that is poorly understood, and after which the viral NC is

thought to be released into the cytoplasm. The fact that uptake through an endocytic pathway (after binding to the host cell) requires energy and can be prevented by using low temperatures, was utilized to further examine the kinetics of viral entry by endocytosis and the role of GP64 in viral entry (chapter 5). Adsorption of viruses to the surface of cells is generally thought to occur by interaction of the virus and a specific receptor, and this has been demonstrated for several virus species. However, negatively charged liposomes have also been shown to enter cells by adsorptive endocytosis, suggesting that specific receptor interaction may not be necessary (238). Alternative to adsorptive endocytosis to enter cells, it is possible that baculoviruses may utilize fluid endocytosis, one of the uptake mechanisms for low molecular weight solutes and soluble macromolecules such as enzymes, hormones, and antibodies (228), or a combination of adsorptive and fluid endocytosis. It may however not seem beneficial that a virus would depend on a non-specific interaction such as fluid endocytosis for entry into its host cell.

In another study (262), GP64 was found to be resistant to functional inactivation by proteolysis. Protease treatments with proteinase K and trypsin each resulted in a 35 kD soluble GP64 fragment, and 36 and 37 kD fragments of GP64 that were retained with the BV, and the AcV1 epitope was lost by this protease treatment. The fragments retaining with the BV also appeared to be more sensitive to β -mercaptoethanol, however the protease-treated BV proved as infectious as control BV containing the full length GP64. Assuming that in this case, GP64 in the viral envelope was effectively and quantitatively cleaved, and that consequently the fragments retained with the BV represent one side of the GP64 molecule only, this would imply that the necessary, biologically relevant domains of GP64 for entry are located in the 36 and 37 kD fragments retained with the BV. It may however seem unlikely that ~ half of the GP64 molecule would be dispensable for its functions within the baculovirus infection cycle.

DNA and amino acid sequences, and predicted domains of GP64. Molecular aspects of GP64 were first addressed, when the coding sequences for OpMNPV and AcMNPV GP64 were cloned after locating the genes by using GP64-specific antibodies to screen a lambda gt11 expression library (9) and (273). Subsequent sequence analyses revealed ORFs with 1527 and 1539 nt respectively for OpMNPV and AcMNPV, predicting a protein with a molecular weight of ~ 58. (The difference between predicted and observed molecular mass is mostly due to glycosylation.) A high degree of nucleotide (74%) and amino acid (78%) identity was observed between these two GP64s. Translated ORFs contained 7 and 5 potential N-linked glycosylation sites, for OpMNPV and AcMNPV GP64 respectively. The GP64 promoter region contained early as well as late transcription consensus motifs, and primer extension analyses showed transcription initiation at the early (CAGT) as well as two out of the four late (ATAAG) consensus motifs. Western blot analysis and immunofluorescence microscopy of infected cells demonstrated that GP64 was expressed in both early and late stages of the infection cycle, and was present as diffuse patches in the cytoplasm or at the plasma

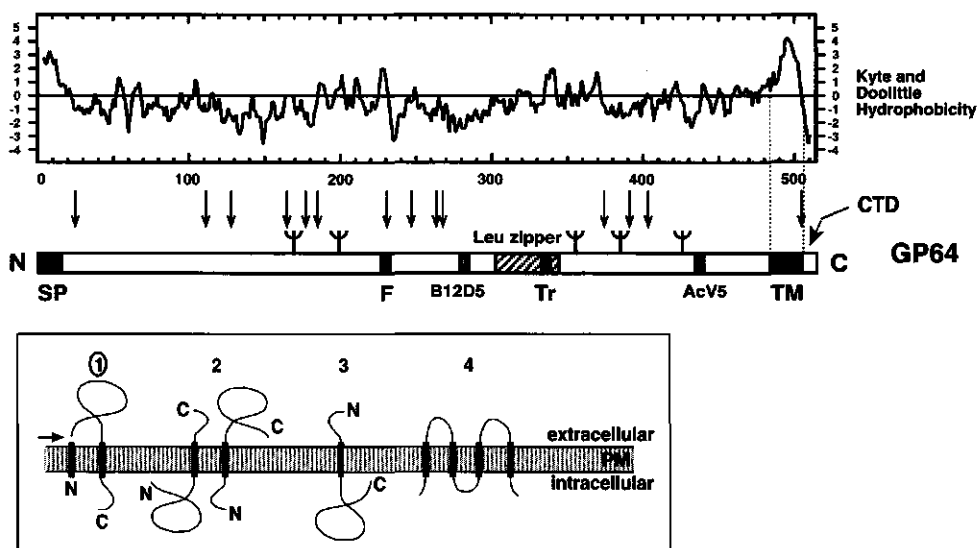


FIG. 4. Features of AcMNPV GP64. Various domains, antibody epitopes, and hydrophobicity profile of AcMNPV GP64 are shown: N (N-terminus), C (C-terminus), SP (signal peptide), TM (transmembrane domain), CTD (cytoplasmic tail domain), leu zipper (heptad repeat of leucines, predicting an amphipathic alpha-helix), AcV5 (linear epitope of Monoclonal antibody [MAb] AcV5), B12D5 (linear epitope of MAb B12D5), F (domain involved in fusion), Tr (domain involved in trimerization), Y (consensus N-linked glycosylation sites). Indicated fusion and oligomerization domains are the corresponding locations in AcMNPV GP64 to those mapped in the OpMNPV GP64 protein (171). Vertical arrows indicate the locations of cysteine residues. The hydrophobicity profile is based on Kyte and Doolittle (142); The vertical axis indicates Kyte-Doolittle hydrophobicity values (+ hydrophobic; - hydrophilic) and numbers on the horizontal axis represent GP64 amino acid numbers. For the complete 512 amino acid primary sequence of AcMNPV GP64, see Fig. 3, chapter 6. (**Insert**) Classification of integral membrane proteins adapted from Von Heijne and Gavel (267). Mature GP64 is a type 1 membrane glycoprotein, with a large N-terminal ectodomain, membrane anchoring domain (TM), and a C-terminal cytoplasmic domain. The site where the signal peptide is cleaved is indicated by an arrow.

membrane (9). Hydrophobicity profiles (142) predicted that GP64's topology resembled that of a type 1 transmembrane protein (Fig. 4): A signal peptide preceding a large N-terminal ectodomain and a membrane anchoring (transmembrane, TM) domain at the C-terminus followed by a short cytoplasmic tail domain (CTD). A TM domain of a type I membrane envelope protein is generally defined as a highly hydrophobic domain near the C-terminus, and there are no consensus sequences known that indicate beginning or end of a TM domain. Based on hydrophobicity alone, residues leu480 to phe483 may represent the N-terminal end of the AcMNPV GP64 TM domain. The first charged residue beyond the hydrophobic domain, arg506, may represent the C-terminal boundary and start of the cytoplasmic tail domain (CTD). With the above considerations, the TM domain was predicted to be 23 amino acids long, while the CTD domain was

predicted to be only 7 amino acids long, of which several residues are positively charged. Due to its predicted cytoplasmic location, it was speculated that this CTD might be involved in virion assembly (273). A non-protein modification of GP64 that might alter the hydrophobicity of the TM domain was reported (207). Palmitic acid was found to be the fatty acid responsible for a detected acylation of GP64, and two candidate amino acid residues were selected (ser482 and cys503) for this modification. Based on the characteristics of chemical release, it was proposed that this modification most likely occurs post-translationally through a thio-ester linkage at ser482. Suggested functions and location of acylation of GP64 are addressed in the general discussion.

GP64 mediates low pH-dependent membrane fusion. Enveloped viruses (such as Influenza and VSV) that enter their host cells by receptor-mediated endocytosis, possess surface glycoproteins which (after endocytosis) fuse the viral envelope with the membrane of the endocytic vesicle upon exposure to low pH (see section 'GP64 and entry of the host cell'). Entry of baculovirus BV resembled that of the enveloped viruses mentioned above ((261), see earlier), and GP64 was implied in the entry process

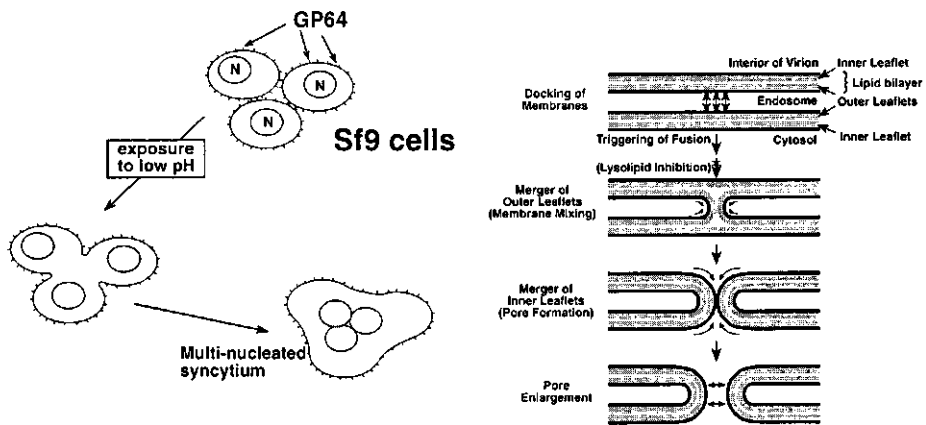


FIG. 5. Low pH-induced membrane fusion assay and model for fusion pore formation (from Blissard (5)). On the left: Infected or transfected Sf9 cells which express GP64, are incubated with pH 5 medium for 5 min. After 5 min, the pH 5 medium is replaced with TNM-FH and cells are further incubated. The exposure to low pH triggers GP64 to induce fusion between adjacent membranes, resulting in the formation of multi-nucleated syncytia. The low pH-triggered membrane fusion assay can serve as an indicator for the capacity of a particular envelope protein to fuse viral and cellular membranes in the endosome during viral entry by endocytosis. On the right: Before NCs can enter the cytosol, viral and endosomal membrane must fuse, and form a pore (or pores) wide enough to allow passage of the NC. In BV entry, membrane fusion is mediated by GP64. In the ODV, a viral protein mediating membrane fusion has not yet been identified. A hypothetical model for fusion pore formation shows that opposing membranes must first be docked or held in close 'apposition'. Subsequent steps include a merging of outer membrane leaflets (membrane mixing), a merging of inner membrane leaflets (pore formation), followed by pore enlargement. Small arrows indicate the steps that are presumably catalyzed by viral membrane fusion proteins. A step at which lysolipids are able to inhibit membrane fusion is also indicated.

because AcV1, a MAb that was known to immunoprecipitate a protein of 64 kD, neutralized BV infectivity at an entry step beyond binding (see earlier). Moreover, GP64's hydrophobicity profile resembled that of type 1 membrane proteins such as Influenza HA. Blissard and Wenz (10) examined the capacity of OpMNPV GP64 to mediate low pH-triggered membrane fusion by syncytium formation assays. Ability to fuse plasma membranes in this assay generally serves as an indicator of the capacity to fuse viral and cellular membranes in the endosome during viral entry. When expressed alone in *Lymantria dispar* (Ld) cells (i.e. in the absence of viral infection), and exposed to low pH medium, OpMNPV GP64 was capable of inducing membrane fusion, with formation of multi-nucleated syncytia (Fig. 5). This suggested that one function of GP64 was to induce membrane fusion during entry, presumably to release the NC into the cytosol. A drop in pH from 6.2 (physiological) to ≤ 5.5 was necessary to induce membrane fusion, and as little as 5 seconds exposure to low pH was sufficient for this induction. Several studies showed that the neutralization of AcMNPV by MAb AcV1 was likely the result of inhibition of fusion between the viral and endosomal membrane: Lysis of red blood cells by AcMNPV BV at low pH was inhibited by pre-incubating BV with AcV1 (261), and Sf9 cells pre-incubated with AcV1, no longer formed syncytia when exposed to low pH (25). In OpMNPV GP64 a domain was identified, involved in or responsible for the low pH-dependent membrane fusion, by examining the effect of single or multiple amino acid substitutions in predicted hydrophobic domains on low pH-triggered membrane fusion (171). The identified domain was one of two small, locally hydrophobic domains of GP64 (termed I and II; Fig. 4) that are present in addition to the signal peptide and TM domain. Nonconservative substitutions of amino acids leu226 or leu227, which represent the core of hydrophobic domain I (amino acids 223 to 228), completely abolished fusion while the stability and surface expression of GP64 were unaffected. Hydrophobic region II was also examined in that study. Region II shows characteristics typical of a leucine zipper, a structure with heptad repeats of leucine, predicted to be an amphipathic alpha helix with local hydrophobicity along one face of the helix. When multiple leucines of the heptad repeats were replaced with alanines or prolines (helix destabilizing), GP64 no longer oligomerized, indicating that this region is required for oligomerization. In the same study, the epitope for MAb AcV5 was mapped to 9 amino acids (431 to 439) within GP64.

Evolution of GP64: A remarkable homology between GP64 and an orthomyxovirus glycoprotein. Thogoto (THO) and Dhori (DHO) viruses are tick-transmitted viruses that replicate in both ticks and mammals. Both are classified as THO-like viruses within the Orthomyxoviridae, based on several morphological and biochemical similarities, while displaying biological properties divergent from other orthomyxoviruses (26). When the sequence of RNA segment 4 of THO virus was determined (173), a protein of 512 amino acids was predicted, with a type 1 membrane topology. The THO envelope glycoprotein (THO env) has extensive homology with the previously published putative envelope glycoprotein of the DHO virus (54), but did not

display significant homology with any of the envelope glycoproteins of other orthomyxoviruses. Instead a remarkable homology was found between the glycoproteins of THO and DHO virus and baculovirus GP64 (173). Overall amino acid identity was between 28 and 33%, and clusters of strong homology were present. Hydrophobicity profiles were strikingly similar, and some glycosylation sites as well as most cysteines were conserved between DHO/THO env, and GP64 from AcMNPV and OpMNPV, indicative of a significant conservation. Upon characterization of THO viral proteins, Portela (201) found a membrane associated glycoprotein with a molecular mass of 75, which likely represents the glycoprotein predicted by Morse (173). In addition, the THO virus showed low pH-induced membrane fusion, hemagglutination, and hemolytic activity with a pH optimum of 6, when infecting mammalian cells, grown at pH 7. The 75 kD protein (THO env) was implicated in these functions because MAbs against this protein inhibited these activities.

We have cloned the THO env coding sequence into an insect and a mammalian expression vector and performed transient analysis in insect cells (Ld652Y; at physiological pH, 6.2) as well as several mammalian cell lines (NIH3T3, BHK, and COS; at physiological pH 7). When exposed to low pH, only minimal syncytium formation could be detected in Ld cells, and none in NIH3T3, or BHK cells. However, in COS cells, expression of THO env alone was sufficient for robust, low pH-induced syncytia formation (Oomens, unpublished data). Together these data indicate that THO env and baculovirus GP64 are structurally and functionally similar. Evolutionary implications are discussed in the general discussion.

Scope of the thesis

The aim of this thesis is to lay out my experimental contribution to understanding GP64 structure and function in the baculovirus life cycle, and to put this contribution in the perspective of the processes of exit and entry of enveloped viruses in general. Previous literature reports (see 'A history of GP64 literature preceding the thesis') suggested that GP64 might be involved in two important events in the baculovirus life cycle: BV entry into, and exit from the host cell. One function was demonstrated when GP64 was shown to induce plasma membrane fusion when expressed alone in insect cells, and thus likely to be the protein responsible for fusion between the viral and endosomal membrane upon entry by endocytosis (10). However, direct roles in other aspects of exit or entry of the baculovirus BV phenotype were suspected but never demonstrated. The research presented in this thesis contributes to elucidating the role of GP64 in virus exit, viral transmission, and virus entry.

First I conducted some basic experiments addressing temporal expression, oligomerization, and carbohydrate processing of GP64, as well as certain structural features of GP64 from the baculovirus OpMNPV (chapter 2). Next, the role of GP64 in the infection cycle was addressed by examining AcMNPV infectivity in the complete

absence of GP64. This was accomplished by deleting the gene from the viral genome and the generation of a gp64null virus, which was complicated by the fact that the GP64 turned out to be an essential baculovirus protein. An important function of GP64 was revealed by this gp64null virus: Without GP64, the virus was unable to transmit infection from cell-to-cell in cell culture as well as in insect larvae. Whether this effect was due to decreased virus budding or whether the absence of GP64 resulted in defective virions, was the next question addressed (chapter 4). When it was shown that this defect in viral transmission was caused primarily by a reduction in virus budding in the absence of GP64, the focus shifted towards the CTD of GP64. The CTD is predicted to be in a position to interact with cytoplasmic viral and/or cellular factors and hence a logical target for BV exit/assembly studies. Recombinant viruses carrying deletions or modifications in the CTD and/or portions of the TM domain were generated and examined for their role in virus budding (chapter 4). Switching direction, the role of GP64 in BV entry into host cells was addressed in chapter 5. Data of those studies suggest that AcMNPV GP64 is a host cell receptor binding protein, and demonstrate half-times of AcMNPV entry, and release from endosomes. In the last experimental chapter (chapter 6) we mapped the GP64 homolog in baculovirus *Anticarsia gemmatalis* Multicapsid Nucleopolyhedrovirus (AgMNPV). This virus is extensively utilized in the protection of soybean crop in Brazil, and demonstrates well the baculovirus potential for insect pest control. To examine the relatedness of AgMNPV to other NPVs, a genomic region of AgMNPV, containing the *gp64* gene and 18 additional ORFs, was analyzed and compared to the corresponding regions in other baculoviruses. Finally, because virus budding is a poorly understood area of baculovirology, the general discussion includes a review of selected literature regarding the role of viral spike proteins in exit of enveloped viruses from host cells. A few additional GP64 research areas are also included in the discussion. These are not or to a lesser degree addressed experimentally in this thesis, but are touched upon with the aim of complementing the experimental contribution towards our understanding of GP64 structure and function. The discussion is concluded with a note on current and future avenues of GP64 research.

Chapter 2

The baculovirus GP64 envelope fusion protein: Synthesis, oligomerization, and processing

Abstract

The baculovirus GP64 envelope fusion protein (GP64 EFP) is a class I integral membrane protein that enters the secretory pathway, and is oligomerized and extensively processed during transport to the plasma membrane. The kinetics of GP64 EFP biosynthesis, oligomerization and processing in OpMNPV-infected *Lymantria dispar* cells, were examined by pulse label, pulse-chase, and immunoprecipitation experiments. Relative rates of GP64 EFP synthesis in OpMNPV infected *L. dispar* cells were examined at various times throughout the infection cycle. Using pulse labeling and immunoprecipitation, GP64 EFP synthesis was detected within 2 hr p.i., and the maximal rate of synthesis was observed in the period of 24-26 hr p.i., a time coincident with the onset of high level production of budded virus in OpMNPV-infected *L. dispar* cells. To determine the oligomeric structure of GP64 EFP, a soluble form of *Orgyia pseudotsugata* Multicapsid Nuclear Polyhedrosis virus (OpMNPV) GP64 EFP was produced, and examined by a combination of gel filtration chromatography, non-reducing SDS-PAGE, and mass spectrometry. Oligomeric GP64 EFP was identified as a trimeric molecule, that migrates as 2 discrete bands on non-reducing SDS-PAGE. Pulse-chase studies, performed at both early (12 hr p.i.) and late (36 hr p.i.) stages of the infection cycle, showed that GP64 EFP oligomerization is complete within 15 min after synthesis. Efficiency of oligomerization however was relatively low, with less than 28% of the synthesized GP64 EFP converted to trimers. The majority of monomeric GP64 EFP remaining in the cell appeared to be degraded within 30 to 45 min after synthesis. Analysis of the kinetics of carbohydrate processing at early (12 hr p.i.) and late (36 hr p.i.) times post infection showed that for both early and late phases of infection, carbohydrate was rapidly added, and processing began within 10 to 20 min after GP64 EFP synthesis. Although carbohydrate processing was completed within ~ 90 min after synthesis during the early phase, the same process required ~ 150 min during the late phase. Thus, carbohydrate processing appeared to become less efficient as infection progressed. These studies thus show that GP64 EFP undergoes a rapid but inefficient oligomerization step that results in a homo-trimeric structure for GP64 EFP. While carbohydrate addition is rapid, carbohydrate processing requires prolonged periods of time (with half-times of 45 to 75 min) and appears to become less efficient during the late phase of the infection.

This chapter has been published as:

Oomens, A.G.P., S.A. Monsma, and G.W. Blissard (1995). The Baculovirus GP64 envelope fusion protein: Synthesis, oligomerization, and processing. *Virology* 209, 592-603

Introduction

The Baculoviridae are a family of enveloped animal viruses that are pathogenic to invertebrates, primarily insects in the order Lepidoptera. Baculoviruses have large circular double-stranded DNA genomes ranging from approximately 80 to 180 kbp. Transcription, replication, and nucleocapsid assembly take place in the nuclei of infected cells. Baculoviruses are characterized by an infection cycle that produces two virion phenotypes that are structurally and functionally distinct (7, 265). The first virion phenotype produced in the infection cycle is the budded virus (BV). Production of the BV begins when nucleocapsids bud through the plasma membrane into the extracellular space. BV is responsible for the systemic infection of insect cells and tissues *in vivo*, and is highly infectious in cell culture systems. Production of the second virion phenotype, the occlusion-derived virus (ODV), occurs in the very late phase of the infection cycle when nucleocapsids become enveloped within the nucleus. The process of ODV envelopment is not well characterized, and is followed by occlusion of ODV virions within proteinaceous occlusion bodies (termed polyhedra in the nuclear polyhedrosis viruses, and granules in granulosis viruses). Although BV and ODV appear to be identical in nucleocapsid structure, they differ in the sources of their envelopes. This difference results in differences in biochemical compositions (14), and correlates with observed differences in relative infectivities for different tissues within the insect and in tissue culture (128, 265).

Infectivity of BV is dependent on a major BV-specific envelope glycoprotein known as the GP64 Envelope Fusion Protein (GP64 EFP). Some monoclonal antibodies and polyclonal antisera directed against the GP64 EFP are capable of neutralizing infectivity (97, 171, 206, 264). Transcription of the *gp64 efp* gene is regulated by both early and late promoters, which results in the appearance of GP64 EFP in infected cells at both early and late times post infection. This temporal pattern of *gp64 efp* transcriptional expression has been demonstrated in both OpMNPV (8, 9, 13) and *Autographa californica* multicapsid nuclear polyhedrosis virus (AcMNPV) (112, 273). Similarities in regulatory sequence arrangements between the *gp64 efp* genes of OpMNPV, AcMNPV and *Choristoneura fumiferana* multicapsid nuclear polyhedrosis virus (CfMNPV) suggest that transcriptional regulation is similar in these three baculoviruses (9, 112, 273). Regulation of early transcription has been studied in detail for the OpMNPV *gp64 efp* gene (8-10, 132, 133). After viral DNA replication and late gene expression, nucleocapsids assemble in the nucleus. Nucleocapsids then migrate through the cytoplasm, and bud through the plasma membrane at sites where GP64 EFP appears to be concentrated (264). A number of biochemical properties of the GP64 EFP protein of AcMNPV have been described: GP64 EFP is a phosphorylated, acylated, and glycosylated homo-oligomer with subunits that are covalently linked by disulfide bonds (207, 260, 264). The OpMNPV, AcMNPV and CfMNPV GP64 EFP's have very similar hydrophobicity profiles, and show a high degree of amino acid sequence similarity (9, 93) with the predicted ectodomains showing at least 82% identity across all

three baculovirus GP64 EFP proteins. The OpMNPV and CfMNPV proteins have 7 potential sites for N-linked glycosylation, whereas AcMNPV has 5. The locations of the 5 potential glycosylation sites in AcMNPV are conserved in both OpMNPV and CfMNPV (9, 93, 273). Recent studies of the AcMNPV GP64 EFP show that at least some of the N-linked glycosylation sites contain carbohydrates that are Endo H resistant (112) and thus may be processed into complex sugars.

Previous studies utilizing a neutralizing monoclonal antibody (MAb), AcV1, and the lipophilic amine chloroquine, showed that GP64 EFP is required for viral entry by endocytosis (97, 261). Later, it was demonstrated that GP64 EFP expressed on the surface of uninfected cells is sufficient to mediate membrane fusion in a pH dependent manner (10). These studies showed that GP64 EFP is necessary and sufficient for low pH activated membrane fusion activity, consistent with the role of GP64 EFP in viral entry through the low pH environment of the endosome. Recent studies of GP64 EFP mediated membrane fusion have identified a hydrophobic 'fusion domain' which is required for pH-dependent membrane fusion activity (171).

Although the kinetics of folding, oligomerization, and transport have been characterized for a diverse group of animal and viral membrane proteins (43), little is known about similar kinetics of baculovirus membrane proteins. Here, we report a study of the kinetics of production, oligomerization and processing of OpMNPV GP64 EFP in infected *L. dispar* cells. Because GP64 EFP is a highly processed viral protein that enters the secretory pathway, studies of the kinetics of GP64 EFP biosynthesis, oligomerization, and processing will aid our understanding of baculovirus infection mechanisms, and may also yield insights into the use of recombinant baculoviruses to express secreted or membrane proteins that are highly processed.

Materials and methods

Anti-GP64 EFP polyclonal antiserum. To generate a polyclonal antiserum (PAs) directed against the GP64 EFP, we cloned the OpMNPV *gp64 efp* open reading frame in the pMalcR1 plasmid vector (New England Biolabs), and expressed GP64 EFP as a protein fusion in *E. coli*. For cloning, pMalcR1 was digested with *Hind*III, repaired with Klenow polymerase, then digested with *Pst*I. A 1685 bp *Pst*I-*Sma*I fragment (containing the *gp64 efp* gene) was excised from plasmid p64-166 (10), and ligated into the pMalcR1 vector. The resulting plasmid, pMalcR1-EFP, encodes a protein fusion consisting of amino acids 1-384 of the *E. coli* maltose binding protein (MBP) fused to amino acids 45-509 of OpMNPV GP64 EFP. This resulted in a protein of 857 amino acids with a predicted size of approximately 92 kDa. *E. coli* expressing the MBP-EFP protein were sonicated, then centrifuged for 20 min at 1500 x *g*. The MBP-EFP protein was purified from the supernatant by affinity chromatography on amylose columns, followed by size fractionation on preparative 6% SDS-PAGE, and electroelution from gel purified bands. The MBP-EFP protein was concentrated in Centricon-30 micro-

concentrators (Amicon, Inc.) and used for injections into a Flemish Giant/Chinchilla rabbit. Prior to use, anti-GP64 EFP PAs was preadsorbed with an MBP extract prepared from *E. coli* cells. To prepare the MBP extract, *E. coli* cells expressing MBP were sonicated, cleared by centrifugation (20 min at 1500 x *g*), and supernatants were stored at -20°C. The anti-GP64 EFP PAs was preadsorbed by adding 5 µl MBP extract (approximately 3 mg MBP/ml extract) to 250 µl of a 1:100 dilution of the anti-GP64 EFP PAs, and incubating at 4°C for 1 hr, followed by ultra centrifugation at 84,000 x *g* for 30 min to remove insoluble complexes.

Cell culture, infections, and virus purification. *L. dispar* cells (IPLB-LD-652Y) were propagated in TNM-FH medium (95) and infected with OpMNPV at a multiplicity of infection (m.o.i.) of 20. The time defined as 0 hr p.i. corresponds to the timepoint at the end of a 1 hr viral absorption period. Mock-infected cells were treated similar to infected cells but no virus was added. BV virions were collected at 7 days post infection from the medium of cells infected at a low m.o.i. (0.01). Debris were removed by low speed centrifugation at 3000 x *g* for 1 hr, and BV virions were purified by sucrose density gradient centrifugation (177).

Metabolic labeling and immunoprecipitation. An EXPRE^{35S} protein labeling mix (containing 72% L-^{35S}-methionine and small amounts of L-^{35S}-cysteine; DuPont NEN) was used for metabolic labeling of protein. Prior to labeling, *L. dispar* cells (5x10⁵ per well in a 24 well plate) were starved by incubation in Graces without methionine (Graces^{-met}) for 30 min (pulse labeling experiments) or 60 min (pulse-chase experiments), then labeled by incubation in Graces^{-met} supplemented with EXPRE^{35S} protein labeling mix, at a final concentration of 75 µCi (pulse label experiments) or 100 µCi (pulse-chase experiments) of EXPRE^{35S} per 250 µl labeling medium. For immunoprecipitation of GP64 EFP, pulse labeled *L. dispar* cells (5x10⁵ cells) were lysed in 300 µl RIPA buffer (150 mM NaCl, 1% NP-40, 0.5% deoxycholic acid, 0.1% SDS, and 50 mM Tris, pH 8) for 1 hr at 4°C with agitation. Insoluble material was cleared from the lysate by centrifugation for 10 min at 16,000 x *g*, followed by a 30 min centrifugation at 84,000 x *g* at 4°C. To 250 µl of the cleared supernatant, 250 µl of preadsorbed anti-GP64 EFP PAs (1:100 in RIPA buffer) was added and incubated for 40 min at 4°C. Insoluble protein A (Staph A, in 40 mM sodium phosphate buffer, pH 7.2) was added (25 µl / 250 µl lysate), and incubated at 4°C for 45 min with agitation. The Staph A complexes were then pelleted, washed 3x in 0.7 ml RIPA buffer, and boiled in disruption buffer. For electrophoresis under non-reducing conditions (6% polyacrylamide) the disruption buffer contained 8% SDS, 37.5 mM iodoacetamide (IA), and no β-mercaptoethanol. For electrophoresis under reducing conditions (9% polyacrylamide) the disruption buffer contained 2% SDS and 5% β-mercaptoethanol.

Oligomeric structure of GP64 EFP. For studies of the oligomeric structure of GP64 EFP, a soluble form of OpMNPV GP64 EFP (GP64 EFP^{sol}) was prepared and purified. Full details of expression vector construction and GP64 EFP^{sol} purification will be published elsewhere (87). Briefly, a recombinant virus expressing GP64 EFP^{sol} was constructed as follows. A stop codon was engineered into the OpMNPV *gp64 efp* gene

in plasmid p64-166 (10), immediately upstream of the predicted transmembrane domain. The Tyr478 codon (TAC) was converted to TGA using the long-primer unique site elimination protocol (171, 203) to create plasmid p64-166STOP. Next, a *Bgl*II restriction site was created 10 nt upstream of the translation initiation codon of the *gp64 efp* gene in plasmid p64-166STOP, to create plasmid p64-166BglATG-STOP. To place the *gp64 EFP^{sol}* gene under control of the polyhedrin promoter, the 1820 bp *Bgl*II-*Bam*HI restriction fragment of plasmid p64-166BglATG-STOP was ligated into the *Bam*HI site of tr *EFP^{sol}* nsfer vector pAcDZ1 (177, 295) to create transfer plasmid pAc-OpEFP^{sol}. A recombinant AcMNPV virus was then generated by standard methods (177) using linearized AcMNPV viral genomic DNA (BacPak6, Clontech Inc.). A recombinant virus (*EFP^{sol}* C2) was purified by three rounds of cloning by end point dilution.

GP64 *EFP^{sol}* was expressed and purified from supernatants of *EFP^{sol}*C2 infected BTI-Tn-5B1-4 cells (75), grown in spinner cultures. Cells were grown in serum-free Excell 405 liquid medium (JRH Bioscience) at 27°C to a density of 1×10^6 cells/ml, then infected at m.o.i. 10. Infected cells were maintained at 27°C, and media was harvested at 48 hr p.i.. GP64 *EFP^{sol}* was purified from the media by a combination of lectin-binding, anion-exchange, hydrophobic interaction, and gel filtration chromatography. Purity as assessed on silver-stained SDS-PAGE gels typically exceeded 95%.

For analysis of the oligomeric structure of GP64 *EFP^{sol}*, purified GP64 *EFP^{sol}* was examined by both gel filtration and mass spectrometry. For gel filtration, purified GP64 *EFP^{sol}* was loaded onto a 70 cm x 1.6 cm Sephacryl S400-HR column (Pharmacia) equilibrated with 200 mM NaCl, 20 mM Sodium phosphate, 0.02% azide (pH 7.0) and run at a flow rate of 20 ml/hr. For molecular weight estimates, the following gel filtration standards were used to calibrate the column: Carbonic anhydrase (29 kDa), albumin (66 kDa), alcohol dehydrogenase (150 kDa), β -amylase (200 kDa), apoferritin (443 kDa), and blue dextran (2000 kDa). The protein concentration was monitored by spectrophotometry (UV-absorption at 280 nm). Column fractions of 3 ml each were collected, and aliquots were denatured in non-reducing lysis buffer and examined on 6% SDS-PAGE gels by Coomassie blue staining. Molecular weight markers, run in parallel on the non-reducing SDS-PAGE gels, included myosin (200 kDa), β -galactosidase (116.25 kDa), and phosphorylase b (97.4 kDa). Although bovine serum albumin (BSA, 66 kDa) was also run, BSA contains disulfide bonds and therefore was not utilized for calculations of molecular weight under non-reducing conditions. For mass spectrometry, the three peak fractions from the gel filtration indicated in Fig. 3B were pooled, dialyzed to distilled H₂O, and concentrated. The sample (approximately 20 pmol) was prepared in sinnapinic acid and analyzed on a Finnegan-Matt matrix-assisted laser desorption/ionization time of flight (MALDI-TOF) mass spectrometer at the Cornell Biotechnology service facility, using BSA (66,431 MW) for calibration.

Analysis of carbohydrate processing. For studies of N-linked glycosylation, addition of N-linked carbohydrates was inhibited by adding tunicamycin (TM, Boehringer) to the medium to a final concentration of 10 μ g/ml. TM containing medium was added to cells 1 hr prior to pulse labeling and was maintained throughout the

experiment. For endoglycosidase treatments, immunoprecipitated ³⁵S-labeled GP64 EFP samples were first boiled for 4 min in the presence of 0.5% SDS and then for 4 min in the presence of 0.75% n-octylglucoside and 0.1% SDS. For each immunoprecipitate (from 4x10⁵ cells), 0.5 units of endoglycosidase F/N-glycanase F (endo F, Boehringer) or 10 milliunits of endoglycosidase H (endo H, Boehringer) were added and incubated for 24 hr at 37°C. After endoglycosidase treatments, samples were mixed with an equal volume of 2x disruption buffer (0.25 M Tris, pH 6.8; 4% SDS; 20% glycerol; 0.002% bromophenol blue; 10% β-mercaptoethanol), boiled for 5 min, and run on a 9 or 10% SDS-polyacrylamide gel.

Analysis of immunoprecipitated GP64 EFP. For analysis of GP64 EFP labeling, SDS-PAGE gels were fixed in 25% isopropanol, 10% acetic acid for 30 min, then treated with a fluorographic reagent (Amplify, Amersham) for 30 min before drying under vacuum. Dried gels were used to expose both x-ray film and phosphorimager screens. For phosphorimager analysis, screens were exposed for times ranging from 0.5 - 3 days and scanned on a Molecular Dynamics phosphorimager. Analysis of SDS-PAGE images and quantification of individual bands were performed with the Imagequant software package (Molecular Dynamics, Inc.).

Results

Anti-GP64 EFP antiserum. To examine the relative rates of synthesis and the kinetics of oligomerization and processing of GP64 EFP in OpMNPV infected *L. dispar* cells, we generated a PAs specific for GP64 EFP. Preliminary studies showed that the available MAbs to GP64 EFP varied in cross-reactivity and their capacities to recognize native and denatured forms of the protein. To generate a PAs with broad specificity for GP64 EFP, a protein fusion of MBP and GP64 EFP, MBP-EFP, was expressed in *E. coli*, purified, and used to produce rabbit anti-GP64 EFP antibodies. Specificity of the anti-GP64 EFP PAs was examined by Western blot analysis and immunoprecipitation of GP64 EFP from OpMNPV infected *L. dispar* cells and purified OpMNPV BV (Fig. 1). On Western blots treated with pre-immune serum, no proteins of 64 kDa were detected from BV, infected cells, or uninfected cells, although two minor cross-reacting proteins of lower molecular weight were detected in infected cells (Fig. 1, lane 1). In Western blots treated with the anti-GP64 EFP PAs, a 64 kDa protein corresponding to the 64 kDa GP64 EFP was detected in infected cells and from purified BV (Fig. 1, lanes 4 and 5). The identity of the reactive band was confirmed on parallel blots using the well-characterized anti-GP64 EFP MAb, AcV5 (9, 97) (data not shown). The anti-GP64 EFP PAs was also used to immunoprecipitate native GP64 EFP. Uninfected and infected *L. dispar* cells were metabolically labeled with ³⁵S-methionine for 14 hours, and proteins were immunoprecipitated with either the anti-GP64 EFP PAs or pre-immune serum. A 64 kDa protein was immunoprecipitated from infected *L. dispar* cells (Fig. 1, lane 11), but not from uninfected cells or when pre-immune serum was used (Fig. 1, lanes 8 and

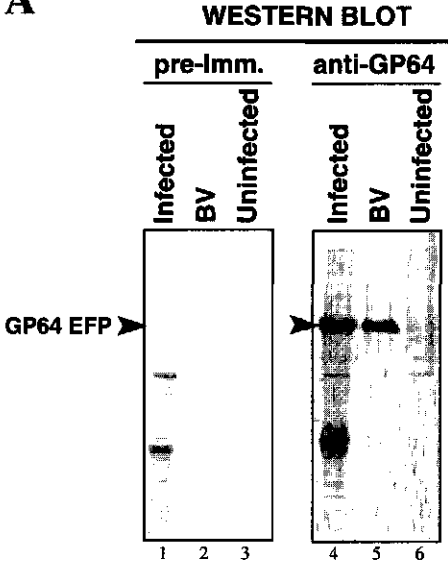
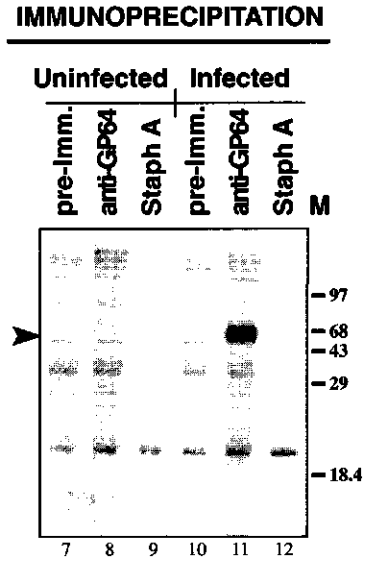
A**B**

FIG. 1. Specificity of the anti-GP64 EFP polyclonal antiserum. An anti-GP64 EFP polyclonal antiserum (anti-GP64) was generated from a MBP-EFP fusion expressed in *E. coli* (see Materials and Methods). Specificity of the anti-GP64 EFP PAs was examined by Western blot analysis (panel A) and immunoprecipitation (panel B). (A) Western blot analysis of protein from uninfected and infected *L. dispar* cells, and purified budded virions (BV). Sources of proteins are indicated immediately above each lane. The left panel (lanes 1 to 3) shows reactivity of pre-immune serum (pre-Imm.) and the right panel (lanes 4 to 6) shows reactivity of anti-GP64 EFP polyclonal antiserum (anti-GP64). The location of GP64 EFP, as determined by incubation of similar blots with monoclonal antibody AcV5, is indicated by an arrowhead on the left of each blot. (B) Immunoprecipitation analysis of anti-GP64 EFP antiserum. Uninfected and infected *L. dispar* cells were metabolically labeled with ^{35}S -methionine for 14 hr, then lysed and immunoprecipitated with either anti-GP64 EFP polyclonal antiserum (anti-GP64; lanes 8 and 11), pre-immune serum (pre-Imm.; lanes 7 and 10), or with no serum (Staph A; lanes 9 and 12). Infected cells were prepared at 40 hr p.i. The location of GP64 EFP is indicated by an arrowhead on the left. The positions and sizes of marker proteins (M) are indicate on the right.

10, respectively). Because the anti-GP64 EFP PAs reacted with denatured and reduced forms of GP64 EFP on Western blots, and also immunoprecipitated non-denatured GP64 EFP from infected cells, these data indicate that the anti-GP64 EFP PAs has a broad specificity for both native and denatured forms of the protein.

GP64 EFP synthesis early and late in infection. To examine the relative rate of GP64 EFP synthesis during various periods of the infection cycle, *L. dispar* cells were infected at an m.o.i. of 20, then metabolically labeled with ^{35}S for 2-hr periods between 0 and 120 hr p.i. At the end of each 2-hr labeling period, GP64 EFP was immunoprecipitated from cell lysates with anti-GP64 EFP PAs (Fig. 2). GP64 EFP was

detected at a relatively low level during the first time period examined (Fig. 2A, 0-2 hr p.i.), indicating either a low level of synthesis over the entire 2 hr period or the onset of synthesis within this period. However, by 6 hr p.i., GP64 EFP synthesis had increased dramatically, as evidenced by a more than 6-fold increase in the quantity of GP64 EFP detected during that period (Fig. 2A, 2B; 0-2 vs. 6-8 hr p.i.). Peak rates of early phase expression were observed in the periods of 12-14 and 18-20 hr p.i.. The highest overall rate of synthesis was detected in the 24-26 hr p.i. period, a time immediately after late transcription of the GP64 EFP begins (9). The rate of GP64 EFP synthesis decreased gradually between 36 and 72 hr p.i. and low but detectable GP64 EFP synthesis was

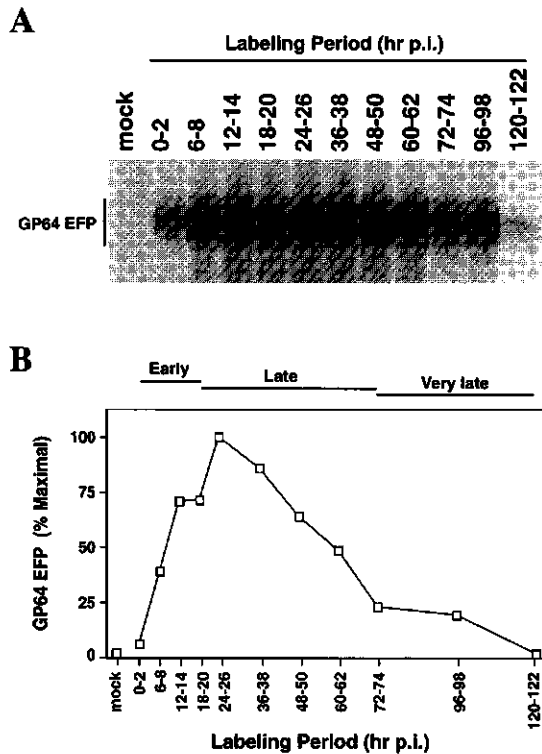


FIG. 2. Relative rate of GP64 EFP synthesis in infected *L. dispar* cells. **(A)** *L. dispar* cells were infected with OpMNPV at an m.o.i. of 20, and metabolically labeled with ^{35}S -methionine for 2-hr periods (indicated above the lanes) between 0 and 122 hr p.i. At the end of each 2-hr labeling period, GP64 EFP was immunoprecipitated, denatured in the presence of β -mercaptoethanol and electrophoresed on a 9% SDS-PAGE gel. A control immunoprecipitation from uninfected 2-hr pulse labeled cells is shown in the first lane (mock). The location of GP64 EFP is indicated by a bar on the left of the panel. Closed circles indicate the different size classes of immunoprecipitated GP64 EFP. **(B)** Quantitative analysis of immunoprecipitated GP64 EFP. Relative band intensities, as measured by phosphorimager analysis (Molecular Dynamics, Inc) are indicated as a percentage of the maximal rate of GP64 EFP synthesis (Y-axis) and are plotted as a function of the 2-hr labeling periods (X-axis). Early, late, and very late phases of the infection cycle are indicated above the graph.

observed in the 72-74 and 96-98 hr p.i. periods. The extremely low levels of GP64 EFP synthesis detected at 120 hr p.i. may result from cellular lysis at this late stage of infection. Some cellular lysis was observed by light microscopy at 120 hr p.i., but not at the earlier time periods examined (data not shown). With a plateau in the early phase and a peak observed after the late phase begins (Fig. 2B), the rates of OpMNPV GP64 EFP synthesis correlate well with the known transcriptional regulation of the *gp64 efp* gene. It is likely that the plateau in rate of GP64 EFP synthesis between the 12-14 and 18-20 hr p.i. periods results from maximal steady state levels of accumulated GP64 EFP early mRNAs. The further increase in the rate of GP64 EFP synthesis observed between the 18-20 and 24-26 hr p.i. periods likely results from increased levels of GP64 EFP mRNA produced from the late promoter, as late transcripts are first detected at 24 hr p.i. (9). In most 2-hr periods examined, the detected GP64 EFP consisted of 3-4 distinct size classes (Fig. 2A, filled circles). Because the labeling periods were long (2 hr), the multiple sizes of GP64 EFP detected may likely represent GP64 EFP in various states of glycosylation and processing (see below).

Oligomeric structure. Like many other viral membrane proteins, the baculovirus GP64 EFP is present in the virion and functions as an oligomer. However, little information is available on the oligomeric structure of GP64 EFP. GP64 EFP forms disulfide-bonded oligomers that migrate at positions equivalent to approximately 172 and 229 kDa (based on linear non-disulfide bonded marker proteins) on non-reducing SDS-PAGE gels (260). Because these sizes correspond approximately to homotrimers and homotetramers of GP64 EFP, and the presence of both forms would be unusual, we used a soluble form of GP64 EFP to more closely examine its oligomeric structure. For these studies, we produced a recombinant AcMNPV baculovirus (EFP^{sol}C2) that expresses a soluble form of the OpMNPV GP64 EFP (GP64 EFP^{sol}). A stop codon was inserted after codon 477 (of the OpMNPV *gp64 efp* ORF), which is immediately upstream of the predicted transmembrane domain and predicted acylation site. GP64 EFP^{sol} was collected from supernatants of cells infected with EFP^{sol}C2 and purified as described (see Materials and Methods). In reduced samples, the size of secreted GP64 EFP^{sol} corresponded to the predicted size of mature GP64 EFP without the C-terminal 32 amino acids (data not shown). On non-reducing gels, GP64 EFP^{sol} showed a migration pattern similar to native GP64 EFP from purified OpMNPV BV, appearing as two major high molecular weight bands (Fig. 3C). To examine a possible difference between the two observed bands in more detail, purified GP64 EFP^{sol} was fractionated by gel filtration chromatography, and fractions were analyzed by electrophoresis on non-reducing SDS-PAGE gels. On S400 gel filtration columns, GP64 EFP^{sol} eluted as a single peak centered at an estimated mass of approximately 200 kDa (Fig. 3A). Analysis of multiple fractions across the single peak by non-reducing gel electrophoresis and Coomassie blue staining showed that both high molecular weight bands of GP64 EFP^{sol} were represented in all fractions from this peak (Fig. 3B). In addition, the ratio of protein in the 2 bands (quantitated by densitometric scanning) did not vary significantly across

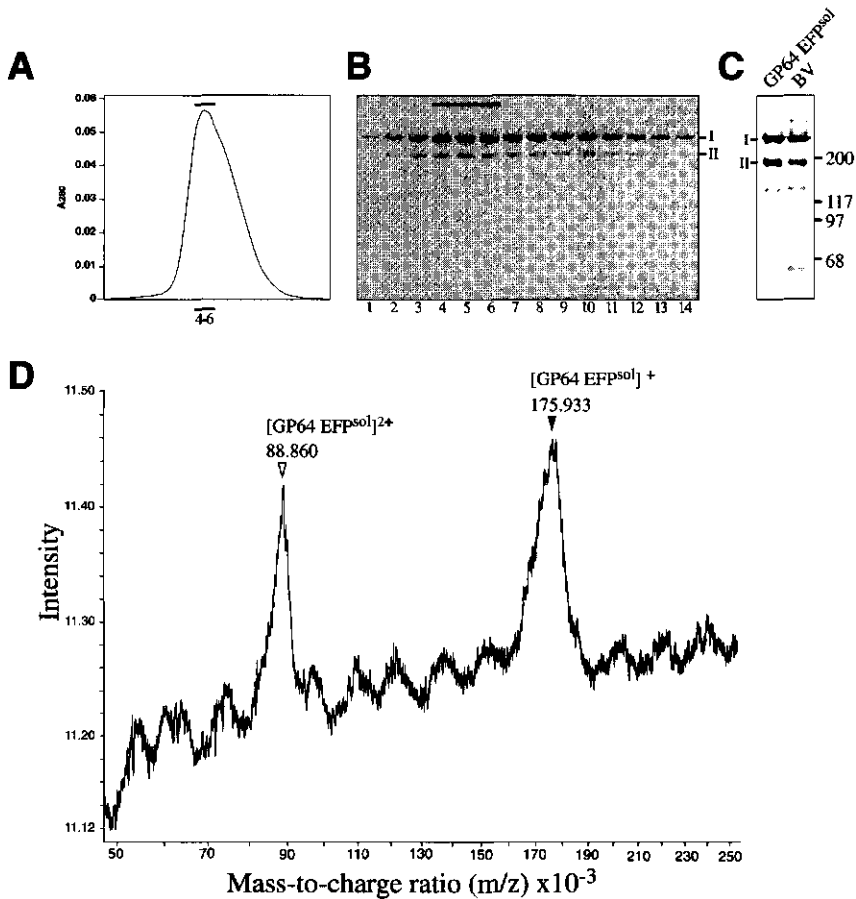


FIG. 3. Physical analysis of the oligomeric structure of a purified, soluble form of GP64 EFP (GP64 EFP^{sol}). A soluble form of OpMNPV GP64 EFP, expressed from a recombinant baculovirus, was used for physical studies of the oligomeric state of GP64 EFP using gel filtration chromatography, non-reducing SDS-PAGE, and mass spectrometry. (A) The elution profile of GP64 EFP^{sol} obtained from S400 gel filtration chromatography is illustrated. Absorbance at 280 nm is shown on the Y-axis, and 14 fractions collected from the single broad GP64 EFP^{sol} peak are indicated on the X-axis. Three peak fractions selected and pooled for further analysis are indicated by a thick line above and below the peak. (B) Fourteen fractions (lanes 1-14) from the major peak of GP64 EFP^{sol} isolated by S400 column chromatography (panel A) were electrophoresed on a non-reducing SDS-PAGE and stained with Coomassie blue. Three fractions selected and pooled for analysis by mass spectrometry are indicated by a thick line above lanes 4-6, and correspond to peak fractions indicated in panel A. The two protein bands are identified as I and II. (C) The S400 purified GP64 EFP^{sol} and wt GP64 EFP were compared on non-reducing SDS-PAGE. GP64 EFP was identified by Western blot analysis, using monoclonal antibody AcV5. The two major GP64 EFP bands are identified as I and II. The migrations of reduced protein markers on the same gel are shown on the right. (D) Matrix-assisted laser desorption/ionization mass spectrum of a >98% pure preparation of oligomeric GP64 EFP^{sol}. The measured molecular mass of 175.933 kDa represents the mass of oligomeric GP64 EFP^{sol} with one attached proton ([GP64 EFP^{sol}]⁺) and corresponds to a trimeric species. A second peak (88.860 kDa, [GP64 EFP^{sol}]²⁺) represents a doubly protonated form of the trimer. Mass-to-charge ratios (m/z) x 10⁻³ are indicated along the X-axis and signal intensity is indicated on the Y-axis.

the peak (data not shown). Analysis by gel filtration therefore suggested that the two bands detected on non-reducing SDS-PAGE do not differ in molecular mass. To determine whether the two bands observed on non-reducing SDS-PAGE corresponded to oligomeric proteins composed of different numbers of subunits, a >98% pure preparation of GP64 EFP^{sol}, containing both bands (Fig. 3B, lanes 4 to 6, pooled), was analyzed by MALDI-TOF mass spectrometry. Data from the mass spectrometry analysis showed that the largest singly-charged species of GP64 EFP^{sol} has an approximate molecular mass of 175.9 kDa (Fig. 3D, [GP64 EFP^{sol}]⁺, filled arrowhead). The mass-to-charge (*m/z*) ratio of the doubly-protonated species (Fig. 3D, [GP64 EFP^{sol}]²⁺, open arrowhead) also agrees closely, (within approximately 1%) with this mass measurement. Because N-terminal amino acid sequencing of GP64 EFP^{sol} showed that the mature peptide backbone begins at amino acid 18 (Ala18, (87)), the molecular mass of monomeric, unglycosylated GP64 EFP^{sol} is predicted (from the amino acid sequence) to be 52.525 kDa. Since mature GP64 EFP^{sol} contains approximately 6-8 kDa of carbohydrate per monomer (determined by endoglycosidase treatment, data not shown), the mass determination by mass spectrometry corresponds to a homo-trimeric form of GP64 EFP^{sol} ($3 \times [52.525 + 6] = 175.6$ kDa). As no larger species were detected by mass spectrometry, there is no evidence for the presence of a tetrameric form in this preparation. Thus, the analysis of oligomeric GP64 EFP^{sol} by gel filtration and mass spectrometry indicates that the largest oligomeric form of GP64 EFP^{sol} is trimeric. Based on these data, the two major forms of GP64 EFP and GP64 EFP^{sol} detected on non-reducing SDS-PAGE gels (Fig. 3C) are designated trimer I and trimer II.

Oligomerization and processing in infected cells. To examine oligomerization and processing of GP64 EFP in different phases of the infection cycle, pulse-chase experiments were performed at both early (12 hr p.i.) and late (36 hr p.i.) times post infection. Infected cells were pulse labeled for 5 min with ³⁵S-methionine, and chased with unlabeled amino acids for times ranging from 0 to 300 min. To examine the oligomerization state, GP64 EFP was immunoprecipitated after pulse-chase and examined on SDS-PAGE gels under reducing and non-reducing conditions.

Oligomeric forms of GP64 EFP consisted primarily of the two trimer forms (Fig. 4A, trimer I, II). Based on migration in non-reducing gels, a small amount of apparently dimeric GP64 EFP was also detected (Fig. 4A, dimer). Oligomeric GP64 EFP was detected immediately after the 5 min pulse period, indicating that oligomerization occurs very rapidly (Fig. 4, lane 2, trimer I, II). At this time (0 min chase), the monomeric form accounted for approximately 74% of the total GP64 EFP detected (Fig. 4A, lane 2, trimer I, II vs. monomer). Levels of oligomeric GP64 EFP increased slightly with extended chase times, and the largest quantity of oligomeric GP64 EFP was detected after a 10 min chase (Fig. 4A, lane 3, trimer I, II). Between 0 and 45 min chase the amount of total detectable GP64 EFP decreased substantially (approximately 67%) (Fig. 4A and 4B, lanes 2 vs. 6). Because DNA replication and budding of progeny virus have not yet occurred at 12 hr p.i. (13), this approximately 67% decrease in detection of GP64 EFP

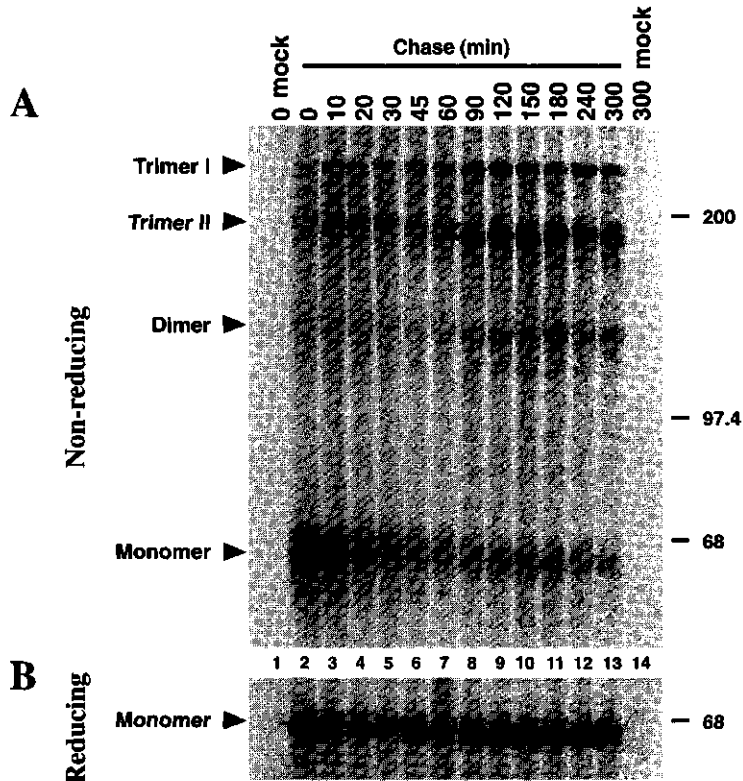


FIG. 4. Oligomerization and processing of GP64 EFP in OpMNPV infected *L. dispar* cells at 12 hr p.i.. *L. dispar* cells were infected at an m.o.i. of 20. At 12 hr p.i. cells were pulse labeled for 5 min with ^{35}S -methionine, then chased with unlabeled medium. GP64 EFP was immunoprecipitated at various time points between 0 and 300 min chase. Immunoprecipitates were divided into equal portions and examined under non-reducing (Panel A) and reducing (Panel B) conditions. **(A)** Analysis of GP64 EFP under non-reducing conditions. Immunoprecipitated GP64 EFP was boiled in the presence of 37.5 mM IAA and electrophoresed on a 6% SDS-polyacrylamide gel. Numbers above the lanes represent chase times (min) at which GP64 EFP was immunoprecipitated. Lane 1 and 14 (mock) are immunoprecipitates from uninfected cells, pulse labeled and chased for 0 and 300 min, respectively. The positions and sizes of linear (reduced) protein markers are indicated on the right. On the left the positions of different oligomerization products of GP64 EFP are indicated (Trimer I, Trimer II, Dimer, Monomer). The two closed circles in Panel A indicate the migrations of pre-processed and processed forms of GP64 EFP Trimer II. **(B)** Analysis of GP64 EFP under reducing conditions. Immunoprecipitated GP64 EFP was boiled in the presence of 5% β -mercaptoethanol and electrophoresed on a 9% SDS-polyacrylamide gel. The lanes correspond to those directly above on the non-reducing gel, and the position of a marker protein is indicated on the right.

was not due to loss of surface GP64 EFP through viral budding. On non-reducing gels, the decrease in total GP64 EFP detected between 0 and 45 min chase was due primarily to a loss of monomeric, not oligomeric GP64 EFP (Fig. 4A, lanes 2-6,

monomer). An approximately 86% decrease in monomeric GP64 EFP was detected between 0 and 45 min chase. Surprisingly, no equivalent increase in oligomeric GP64 EFP was observed during the same time, indicating that monomeric GP64 EFP was not chased into the oligomeric form. These data therefore suggest that a large proportion of the newly synthesized monomeric GP64 EFP is degraded within 30 to 45 min after synthesis. Together, these data indicate that, while oligomerization occurs very rapidly and is completed in less than 15 min, the efficiency of oligomerization appears to be relatively low. Less than 28% of the synthesized GP64 EFP is converted to the trimer forms, and the majority of monomeric GP64 EFP appears to be degraded within the cell.

A change in the migration of the oligomeric forms was observed from 30 to 90 min chase (Fig. 4A, lanes 5-8, trimer II). A slower migrating trimer II form was predominant from 0 to 30 min, whereas a faster migrating form appeared at 45 to 60 min and was the primary form at 90 min chase and beyond. This reduction in size was observed for all oligomeric forms on non-reducing gels (Fig. 4A, lanes 5-8), and also for denatured GP64 EFP on reducing gels (Fig. 4B, lanes 5-8). Mature OpMNPV GP64 EFP contains 7 potential sites for N-linked glycosylation in the ectodomain. To determine if the observed reduction in size resulted from carbohydrate processing, we examined GP64 EFP before the change in migration (15 min chase) and after the change (120 min chase), using either a) treatments that prevented carbohydrate addition (tunicamycin, TM), or b) treatments that removed N-linked carbohydrates (endoglycosidase F/N-glycanase F [Endo F], or endoglycosidase H [Endo H]). For carbohydrate analysis at 12 hr p.i., cells were pulse labeled for 10 min with ³⁵S-methionine, then chased for either 15 min (pre-transition) or 120 min (post-transition),

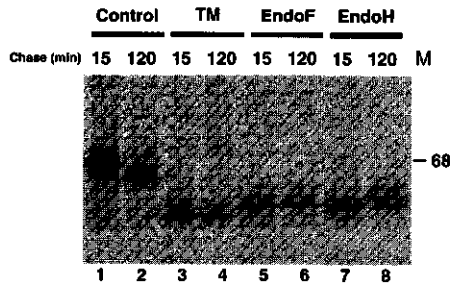


FIG. 5. Carbohydrate processing on GP64 EFP. The N-linked carbohydrate content of GP64 EFP was examined by pulse chase analysis in combination with an inhibitor (Tunicamycin, TM) and two endoglycosidases. OpMNPV infected *L. dispar* cells, at 12 hr p.i., were pulse labeled for 10 min with ³⁵S-methionine, and subsequently chased in unlabeled medium for 15 or 120 min. After the chase, GP64 EFP was immunoprecipitated, reduced by boiling in β -mercaptoethanol, and electrophoresed on a 9% SDS-polyacrylamide gel. The closed circles in lanes 1 and 2 (control) indicate a shift in size of GP64 EFP between 15 and 120 min chase. Lanes 3 and 4 represent samples in which tunicamycin (TM) was added to the cells before and during the experiment. Lanes 5-8 represent samples treated with either endoglycosidase F/N-glycanase F (endo F, lanes 5 and 6), or endoglycosidase H (endo H, lanes 7 and 8). Chase times (min) and treatments are indicated above the lanes. The migration of a protein size marker (M) is indicated on the right.

and immunoprecipitated. Samples were reduced in disruption buffer containing 5% β -mercaptoethanol and visualized on an SDS-PAGE gel. At 15 min chase with no inhibitors (Fig. 5, lane 1), 3 bands were detected. The majority of the labeled protein was present in a central band of approximately 67 kDa (Fig. 5, lane 1, filled circle). By 120 min chase, the migration of labeled GP64 EFP had changed significantly: the majority of labeled GP64 EFP was detected as a faster migrating band of 64 kDa (Fig. 5, lane 2, filled circle). This is consistent with earlier observations on reducing gels (Fig. 4B, lane 4 vs. 9). To compare the molecular weight of reduced GP64 EFP at 15 and 120 min chase in the absence of N-linked sugars, GP64 EFP proteins were either treated with endo F or endo H; or synthesized in the presence of TM. While the sizes of untreated GP64 EFP at 15 and 120 min chase differed (Fig. 5, compare lanes 1 and 2), treatment with either TM (Fig. 5, lanes 3 and 4) or endo F (Fig. 5, lane 5 and 6) resulted in proteins of equal size (approximately 56 kDa for TM, and 58 kDa for endo F treatments) at both chase times. Thus, the differences in the size of GP64 EFP at 15 and 120 min chase resulted from changes in the carbohydrate portions of the glycoprotein. The increased mobility at 120 min is therefore likely caused by the processing of carbohydrates during the process of transport through the Golgi complex. The difference of approximately 2 kDa in GP64 EFP mass between endo F and TM treatments presumably results from the fact that TM prevents the transfer of oligosaccharides (linked to dolichol phosphate) to protein, whereas endo F cleavage results in a residual N-acetyl-D-glucosamine molecule at each glycosylation site. Endo H treatment showed results similar to endo F treatment, although a slightly slower migrating and more diffuse GP64 EFP band was observed at 120 min chase. This indicates that between 15 and 120 min chase, at least a portion of the 7 potential N-linked carbohydrates are processed to a more complex endo H-resistant form.

Extensive cellular modifications are associated with viral infection and the transition between early and late stages of infection. Therefore, we also examined GP64 EFP oligomerization and processing during the late phase of the infection cycle (36 hr p.i., Fig. 6), after the initiation of viral DNA replication and late transcription. Similar to observations at 12 hr p.i., biosynthesis of GP64 EFP at 36 hr p.i. was followed by rapid oligomerization (Fig. 6, lane 2), and degradation of the majority of the monomeric GP64 EFP between 0 and 45 min chase (Fig. 6A, monomer, lanes 2-6). Carbohydrate processing was also examined at early and late times post infection. In contrast to the observations at 12 hr p.i., the period during which processing occurred was significantly extended. At 36 hr p.i., processing was extended through approximately 150 min chase, when the majority of oligomeric GP64 EFP was detected in a more discrete and faster migrating band (Fig. 6A, lanes 5-11, trimer II). To compare the kinetics of GP64 EFP carbohydrate processing at 12 and 36 hr p.i., the pre-processed and processed forms of the GP64 EFP trimer II bands shown in Figures 4A and 6A were quantified, and plotted as a function of chase times (Fig. 7). For both 12 and 36 hr p.i. a decrease in the pre-processed form began between 10 and 20 min chase. Thus, the initiation of carbohydrate processing was similar at early and late times

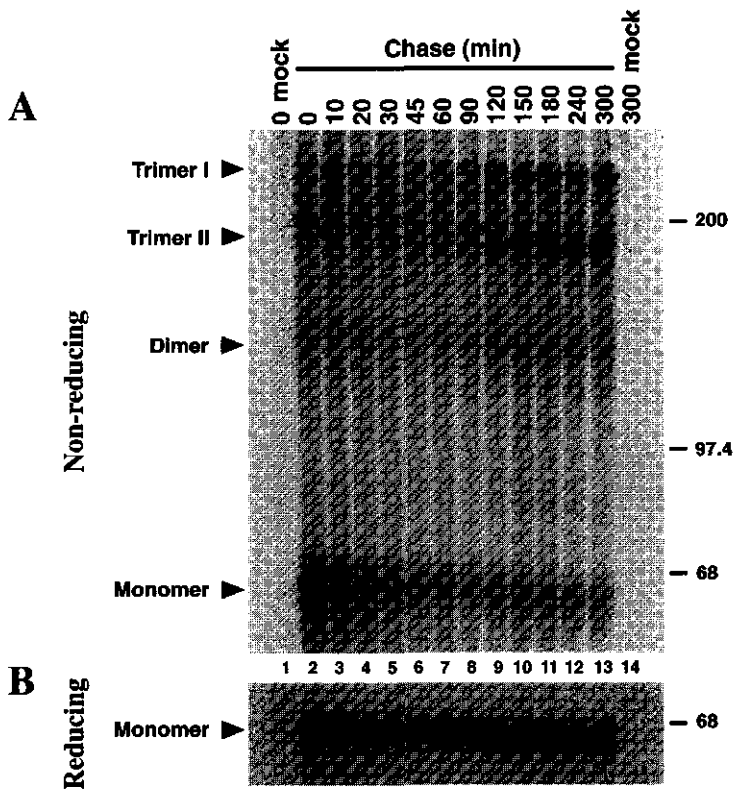


FIG. 6. Oligomerization and processing of GP64 EFP in OpMNPV infected *L. dispar* cells at 36 hr p.i.. *L. dispar* cells were infected at an m.o.i. of 20. At 36 hr p.i. cells were pulse labeled for 5 min with ^{35}S -methionine, then chased with unlabeled medium. GP64 EFP was immunoprecipitated at various time points between 0 and 300 min chase. Immunoprecipitates were divided into equal portions and examined under non-reducing (Panel A) and reducing (Panel B) conditions. (A) Analysis of GP64 EFP under non-reducing conditions. Immunoprecipitated GP64 EFP was boiled in the presence of 37.5 mM IAA and electrophoresed on a 6% SDS-polyacrylamide gel. Numbers above the lanes represent chase times (min) at which GP64 EFP was immunoprecipitated. Lane 1 and 14 (mock) are immunoprecipitates from uninfected cells, pulse labeled and chased for 0 and 300 min, respectively. The positions and sizes of linear (reduced) protein markers are indicated on the right. On the left the positions of different oligomerization products of GP64 EFP are indicated (Trimer I, Trimer II, Dimer, Monomer). The two closed circles in Panel A indicate the migrations of pre-processed and processed forms of GP64 EFP Trimer II. (B) Analysis of GP64 EFP under reducing conditions. Immunoprecipitated GP64 EFP was boiled in the presence of 5% β -mercaptoethanol and electrophoresed on a 9% SDS-polyacrylamide gel. Lanes correspond to those directly above on the non-reducing gel, and the position of a marker protein is indicated on the right.

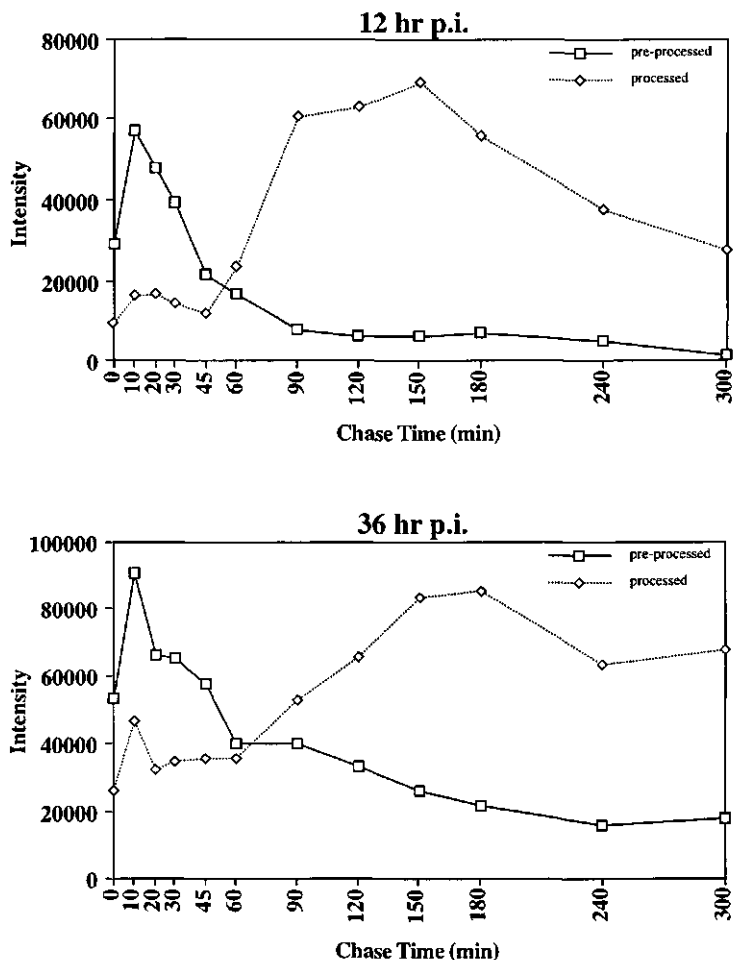


FIG. 7. Processing of GP64 EFP at early (12 hr p.i., upper panel) and late (36 hr p.i., lower panel) times post infection. The quantities of pre-processed and processed forms of GP64 EFP trimer II, as detected in Fig. 4A and 6A (12 hr p.i. and 36 hr p.i., respectively) by phosphorimager analysis, are graphically illustrated. Relative band intensities (Intensity) are indicated on the Y-axis, and chase times (min) are indicated on the X-axis. The slower migrating pre-processed form of GP64 EFP Trimer II is indicated by a solid line and the processed form is indicated by a dashed line in each graph.

post infection. However, early and late phases differed with respect to how rapidly processing was completed. In the early phase (12 hr p.i.), maximal levels of processed GP64 EFP were detected by 90 min chase, indicating that the half-time for carbohydrate processing was approximately 45 min. In the late phase (36 hr p.i.), near maximal levels of processed GP64 EFP were observed only after 150 min, indicating that the half-time

for processing was approximately 75 min. This increase in the half-time required for carbohydrate processing suggests that processing of carbohydrates may become less efficient in the late phase of the infection cycle.

Discussion

Synthesis. GP64 EFP is critical for infectivity of the BV, which mediates the systemic portion of baculovirus infections in insects. Although it has been shown that GP64 EFP is expressed early in infection (Fig. 2) (9, 13, 112), the precise role of GP64 EFP expressed during the first few hours after infection is not known. Studies showing BV budding from the basal side of midgut epithelial cells within 0.5 hr of infection (74, 76) suggest that one possible role of early GP64 EFP expression may be the rapid production of BV from midgut cells prior to DNA replication. Thus, early expression of GP64 EFP may support rapid movement of the virus through the midgut epithelium. Expression of GP64 EFP is driven by both early and late promoters. In combination with transcription data from a previous study (9), data from pulse labeling experiments (Fig. 2) show that early *gp64 efp* transcription results in increasing rates of GP64 EFP synthesis between 0 and 12 hr p.i., and a plateau in the rate of synthesis between 12 and 18 hr p.i.. This early phase plateau in the rate of GP64 EFP synthesis is followed by a further increase in synthesis between 18 and 24 hr p.i.. Transcription from *gp64 efp* late promoters is first detected at approximately 24 hr p.i. (9) and this correlates well with data showing that the maximal rate of GP64 EFP synthesis is observed at approximately 24-26 hr p.i. (Fig. 2). The initiation of late transcription also marks the beginning of BV production. GP64 EFP synthesis decreased substantially by 48 hr p.i., and this likely resulted from lower steady state levels of GP64 EFP mRNA at that time (9). Preliminary experiments utilizing long (4 hr) pulse labeling periods, followed by GP64 EFP immunoprecipitation from culture supernatants (data not shown) indicate that decreased synthesis and not virion budding is responsible for decreased levels of GP64 EFP detected in the late phase in the experiment in Fig. 2. GP64 EFP synthesis decreases further between 48-72 hr p.i. and remains at a relatively low level throughout the remainder of the infection cycle. The decreased synthesis of GP64 EFP at 48 hr p.i. appears to be coordinated with the onset of the very late phase of infection, which is characterized by high level synthesis of structural proteins of the occlusion body. In a previous study of OpMNPV infected *L. dispar* cells, capsid protein (P39, a late gene product) was first detected at 36 hr p.i., while polyhedrin (a very late gene product) was first detected at 48 hr p.i. (13). Thus, GP64 EFP synthesis is highest in the late phase, and decreases but does not cease in the very late phase. These observations of GP64 EFP synthesis correlate well with the observation that in OpMNPV infected *L. dispar* cells, BV production reaches maximal levels between 24 and 48 hr p.i. and remains high between 48 and 96 hr p.i. (13).

Oligomeric structure. Previous studies demonstrated that GP64 EFP of AcMNPV was present in the BV envelope as homo-oligomers in which the subunits were associated by disulfide bonds (260). Similar to the AcMNPV protein, oligomers of OpMNPV GP64 EFP show resistance to boiling in 8% SDS (Fig. 4, upper panel), but dissociate into monomers in the presence of a reducing agent (5% β -mercaptoethanol) (Fig. 4B). These data demonstrate that, in addition to very high conservation of primary amino acid sequence, the AcMNPV and OpMNPV GP64 EFP proteins oligomerize in a similar, if not identical, manner. Based on migrations in non-reducing gels, it was initially proposed that GP64 EFP oligomers might consist of trimers and tetramers (260). In order to study the oligomeric structure of GP64 EFP, we produced a highly purified soluble form of OpMNPV GP64 EFP (GP64 EFP^{sol}), and showed that GP64 EFP^{sol} was oligomerized in a manner similar to native GP64 EFP. On non-reducing SDS-PAGE, migration patterns of GP64 EFP^{sol} were identical to those of GP64 EFP from budded virions (Fig. 3C). Physical analysis of purified, oligomeric GP64 EFP^{sol} by gel filtration and mass spectrometry (Fig. 3) showed that its mass corresponds to a trimeric form. Thus, the two high molecular weight bands detected on non-reducing gels (Fig. 3C, 4A, 6A) both represent trimeric GP64 EFP. One possible explanation for the migration of trimeric GP64 EFP as two species on non-reducing gels is the presence of disulfide isomers. Since the OpMNPV GP64 EFP contains 16 cysteine residues and may be extensively disulfide bonded, differential migrations in non-reducing gels may result from differential patterns of disulfide bonding during synthesis or folding of the individual GP64 EFP chains, or during oligomerization.

Kinetics of oligomerization. Protein folding is an event that typically occurs cotranslationally. In contrast, the process of oligomerization commonly takes place posttranslationally inside the ER (106). The kinetics of oligomerization can differ significantly between various membrane proteins (43, 106). Pulse-chase analysis of GP64 EFP shows that oligomerization is complete or near-complete within 15 min, a timing that is relatively rapid and similar to that of the hemagglutinin protein of Influenza virus and VSV-G protein (29, 42), other homo-trimeric fusion proteins. Subunit concentration and complexity are factors that may influence the rate of oligomerization (107). GP64 EFP can be considered non-complex with respect to assembly, since trimers of GP64 EFP are assembled from identical subunits. While GP64 EFP is oligomerized rapidly, the efficiency of this process is very low. Less than 28% of the synthesized GP64 EFP reaches the trimeric state. In most cases, oligomeric membrane proteins must assemble in order to become transport-competent (106). Although the requirement of oligomerization for transport is not universal, monomers of oligomeric viral membrane proteins are often restricted to the ER (30). In the case of GP64 EFP, it is likely that monomeric forms are not transported to the cell surface. Evidence for this includes the fact that GP64 EFP found in the virion is predominantly, if not exclusively, in the trimeric form. In addition, recent studies of GP64 EFP proteins containing mutations that interfere with oligomerization showed that these mutant proteins failed to

accumulate normally at the cell surface (171), indicating that oligomerization deficient GP64 EFP proteins were also transport deficient. It is therefore likely that the majority of monomeric GP64 EFP detected in pulse chase experiments, represents a fraction that is either misfolded or unable to oligomerize and is subsequently degraded within the cell. Thus GP64 EFP appears to be highly sensitive to misfolding and/or oligomerization defects and the low natural efficiency of oligomerization results in a low efficiency of synthesis of the mature, functional protein.

Glycosylation and carbohydrate processing. Glycosylation of GP64 EFP appears to occur cotranslationally, since proteins migrating at the size of unglycosylated (TM treated) GP64 EFP were not detected in pulse-chase experiments (Fig. 4, 5, and 6). Processing of carbohydrates was detected as a change in the mobility of oligomerized GP64 EFP, beginning within 10 to 20 min after synthesis (Fig. 4 and 6). This carbohydrate processing probably occurs within the Golgi compartment, since most carbohydrate processing events are mediated by Golgi-associated enzymes (136). Changes in carbohydrate presence or content may affect the stability or conformation of glycoproteins, and thus may be a possible explanation for the diffuse nature of the GP64 EFP-oligomer bands in non-reducing gels during the period of carbohydrate processing (Fig 4, lanes 6 and 7; Fig. 6, lanes 5-10). At both 12 and 36 hr p.i., the amount of the pre-processed trimer II begins to decrease within 10-20 min chase, and thus the beginning of carbohydrate processing does not appear to be affected by the phase of infection. However, early and late phases differ with respect to how rapidly processing is completed. At 12 hr p.i. near maximal quantities of processed GP64 EFP were detected at 90 min chase, whereas at 36 hr p.i., near maximal levels of processed GP64 EFP were not observed until 150 min chase. This difference in the time required to complete processing suggests that processing of carbohydrates is more efficient at 12 hr than at 36 hr p.i., possibly reflecting a reduction in the cell's capacity to process carbohydrates at later times post infection. We do not know when, in the process of maturation, GP64 EFP appears on the surface of a cell, or which factors determine the speed and efficiency of this process. However, relative to carbohydrate addition and oligomerization of subunits, carbohydrate processing appears to be a slow process and may be the rate-limiting step in the process of GP64 EFP maturation and transport.

Acknowledgments

The authors thank Peter Faulkner for providing hybridoma line AcV5 and David Garrity and Leslie Lepore for comments on the manuscript. This research was supported by NIH grants AI 33657 and 31130, and Boyce Thompson Institute projects 1250-01 and 1255-01.

Chapter 3

The GP64 envelope fusion protein is an essential baculovirus protein required for cell to cell transmission of infection

Abstract

To demonstrate the essential nature of the baculovirus GP64 Envelope Fusion Protein (GP64 EFP), and to further examine the role of this protein in infection, we inactivated the *gp64* gene of *Autographa californica* Multicapsid Nuclear Polyhedrosis virus (AcMNPV), and examined the biological properties of this virus *in vivo*. To provide GP64 EFP during construction of the recombinant GP64 EFP-null AcMNPV baculovirus, we first generated a stably transfected insect cell line (Sf9^{Op64-6}) that constitutively expressed the GP64 EFP of *Orgyia pseudotsugata* MNPV (OpMNPV). The AcMNPV *gp64* gene was inactivated by inserting the bacterial *lacZ* gene in frame after codon 131 of the *gp64* gene. The inactivated *gp64* gene was cloned into the AcMNPV viral genome by replacement of the wild-type *gp64* locus. When propagated in the stably transfected insect cells (Sf9^{Op64-6}), budded virions produced by the recombinant AcMNPV GP64 EFP-null virus (vAc^{64Z}) contained OpMNPV GP64 EFP supplied by the Sf9^{Op64-6} cells. Virions propagated in Sf9^{Op64-6} cells were capable of infecting wild-type Sf9 cells, and cells infected by vAc^{64Z} exhibited a blue phenotype in the presence of X-gal. Using cytochemical staining to detect vAc^{64Z} infected cells, we demonstrate that this GP64 EFP-null virus is defective for cell to cell propagation in cell culture. Although defective for cell to cell propagation, vAc^{64Z} produces occlusion bodies and infectious occlusion derived virions within the nucleus. Occlusion bodies collected from cells infected by vAc^{64Z} were infectious to midgut epithelial cells of *Trichoplusia ni* larvae. However, in contrast to a control virus, infection by vAc^{64Z} did not proceed into the hemocoel. Analysis of vAc^{64Z} occlusion bodies in a standard neonate droplet feeding assay showed no viral-induced mortality, indicating that occluded virions produced from vAc^{64Z} could not initiate a productive (lethal) infection in neonate larvae. Thus, GP64 EFP is an essential virion structural protein that is required for propagation of the budded virus from cell to cell and for systemic infection of the host insect.

This chapter has been published as:

Monsma, Scott A., A.G.P. Oomens and Gary W. Blissard (1996). The GP64 envelope fusion protein is an essential baculovirus protein required for cell to cell transmission of infection. *Journal of Virology* 70 (7), 4607-4616

Introduction

Baculoviruses are large double stranded DNA viruses that are pathogens of insects. Infection of the host begins when insect larvae acquire the virus orally. Infection is first observed in the epithelial cells of the midgut and is followed in most cases by systemic infection. One hallmark of the baculovirus infection cycle is the production of two structurally and functionally distinct virion phenotypes. One virion phenotype, the occlusion derived virus (ODV), is found within the protective "occlusion bodies". Once released from the occlusion body by the alkaline pH of the gut, the ODV initiates infection of the animal by infecting epithelial cells of the midgut. A second virion phenotype, the budded virus (BV), is produced by budding from the surface of infected cells. The BV is initially produced from infected midgut epithelial cells (74, 127) and is believed to be essential for systemic infection, mediating movement of the virus from midgut to other tissues and propagating the infection from cell to cell within the infected animal. BV are highly infectious to tissues of the hemocoel and to cultured cells, whereas ODV appear to be less infectious in cell culture or when injected into the hemocoel (265, 266). The two virion phenotypes also differ in entry mechanisms, as the BV enter cells via endocytosis (261), while the ODV appear to fuse directly with the plasma membrane at the cell surface (74, 99).

The major envelope protein of the BV is the GP64 Envelope Fusion Protein (GP64 EFP, also known as GP67), which is an extensively processed type I integral membrane glycoprotein that has been studied in some detail (10, 25, 112, 171, 184, 206, 207, 260, 262, 273). Densely packed peplomers found on the surface of BV are believed to be composed of the GP64 EFP protein (264) and these peplomers are acquired by the virion during budding. Recent studies of a soluble form of GP64 EFP indicate that the native form of GP64 EFP is trimeric (184) and thus, each peplomer is likely comprised of a single trimer of GP64 EFP. The important role of GP64 EFP in BV infectivity is demonstrated by the neutralization of BV infectivity with antibodies specific to GP64 EFP (97, 171, 206, 264). Using syncytium formation assays and cells expressing GP64 EFP, it was shown that the GP64 EFP protein is both necessary and sufficient for low pH activated membrane fusion activity (10, 171). In addition, two functional domains have been identified in GP64 EFP: an oligomerization domain necessary for trimerization and transport, and a small internal hydrophobic membrane fusion domain (171). Thus, functional studies of GP64 EFP show that GP64 EFP mediates membrane fusion in a pH dependent manner, consistent with an essential role for GP64 EFP during viral entry by endocytosis.

While indirect data on the role of GP64 EFP in the infection cycle strongly suggest that GP64 EFP is essential for infectivity of the BV, conclusive data have been lacking. No temperature sensitive mutants in the GP64 EFP gene are known, and previous attempts to generate a helper-independent virus containing a GP64 EFP deletion were unsuccessful (J. Kuzio, personal communication). To demonstrate the essential nature of GP64 EFP and to further characterize the role of GP64 EFP in

infection, we generated a stably-transfected cell line that constitutively expresses the GP64 EFP of OpMNPV, and used the cell line to generate a recombinant GP64 EFP-null AcMNPV baculovirus. We then examined the effect of the GP64 EFP-null mutation on viral transmission in both cell culture and insect larvae.

Materials and methods

Cells, insects and antibodies. For production of stably transfected cell lines and propagation of AcMNPV, *Spodoptera frugiperda* Sf9 cells were cultured in TNM-FH complete medium containing 10% fetal bovine serum at 27° C (95, 244). For neonate and larval bioassays, larvae of *Trichoplusia ni* were reared as described previously (105). Monoclonal antibody AcV5 (97) was used to detect GP64 EFP of both AcMNPV and OpMNPV. Monoclonal antibody OpE4A was raised against a purified soluble form of OpMNPV GP64 EFP (184). Because OpE4A recognizes both native and denatured forms of OpMNPV GP64 EFP, and does not cross react with GP64 EFP of AcMNPV, OpE4A was used to distinguish between OpMNPV and AcMNPV GP64 EFP. Monoclonal antibody MA6 39 (274) was used to detect the AcMNPV capsid protein, P39. A commercially available anti- β -galactosidase monoclonal antibody (Promega) was used to detect the GP64- β -galactosidase fusion protein. A rabbit polyclonal antiserum was generated against a soluble form of OpMNPV GP64 EFP (GP64 EFP^{sol}) that was expressed and purified as previously described (184). The anti-GP64 EFP^{sol} antiserum reacts with both SDS-denatured and native GP64 EFPs of both OpMNPV and AcMNPV.

Virus preparation. Viral DNA used for the generation of recombinant viruses was prepared from the E2 strain of AcMNPV (232) by standard methods (177). For production of budded virus (BV) stocks and occlusion bodies of the wild type and recombinant viruses, cells (Sf9 or Sf9^{OP64-6}, see below) were infected at a multiplicity of infection (MOI) of 0.1 and incubated at 27° C for 5 to 7 days. Supernatants were harvested and titered by end-point dilution. The recombinant AcMNPV virus lacking *gp64* expression was titered on the Sf9^{OP64-6} cells, and the wild type AcMNPV virus and recombinant virus vAc^{h5Z} were titered on Sf9 cells. Occlusion bodies were purified from infected cells by sequential washing with 0.5 % SDS, 0.5 M NaCl and distilled water as described previously (177). For analysis of budded virion structural proteins, budded virions were isolated from viral stocks by pelleting through a 25% sucrose pad followed by centrifugation on 25%-60% sucrose gradients (177). The budded virus band was collected, diluted in PBS pH 6.2, pelleted and resuspended in SDS lysis buffer for SDS-PAGE on 10% acrylamide gels.

Isolation of stably transfected insect cell lines expressing OpMNPV GP64 EFP. To generate stably transfected insect cells, Sf9 cells were transfected with two plasmids. One plasmid (p64-166, (10)) encodes the OpMNPV *gp64 efp* ORF under the control of its own 166 bp promoter. The second plasmid (pAc ie1-Neo) encodes a bacterial

neomycin resistance gene under the control of the AcMNPV *ie1* promoter, and was constructed using the approach described by Jarvis *et al.* (111). Transfection and G418 selection were performed essentially as described previously (113, 233). Briefly, Sf9 cells were plated at a density of 1×10^6 cells per well (34 mm diameter). The cells were transfected with 2 μ g p64-166 plasmid plus 1 μ g pAc *ie1*-Neo using calcium phosphate precipitation (244). One day after transfection, the cells were replated at low density in 75 cm² flasks and maintained for 2 weeks in TNM-FH complete media containing 1 mg/ml G418 (Geneticin, GIBCO-BRL). During this period, mock-transfected Sf9 control cells died due to the G418 selection. The G418-resistant transfected cells were replated in TNM-FH complete medium (lacking G418) at low density. Single colonies were isolated and transferred to individual wells of a 24 well plate. Isolated lines were screened for GP64 EFP expression by cell-surface staining of paraformaldehyde-fixed cells using MAb AcV5 and an alkaline phosphatase-conjugated goat-anti-mouse secondary antibody. Isolated lines were also screened for GP64 EFP fusion activity using a syncytium formation assay (10, 171).

Quantification and analysis of GP64 EFP expression in stably transfected cell lines. To analyze GP64 EFP expression in stably transfected cell lines, we quantified the levels of GP64 EFP expressed in stably transfected Sf9 cells, transiently transfected Sf9 cells, and AcMNPV infected Sf9 cells, using quantitative enhanced chemiluminescence (ECL) Western blots, cell-surface ELISA, and flow cytometry. For all three assays, the following cells were analyzed under the following conditions: a) two cell lines (Sf9^{OP64-6} and Sf9^{OP64-2}) constitutively expressing OpMNPV GP64 EFP were plated at passage number 39, and analyzed at 44 h after plating, b) Sf9 cells transfected with plasmid p64-166 (encoding OpMNPV GP64 EFP) at 3.75 μ g plasmid/ 3×10^5 cells were analyzed at 44 h post-transfection, c) Sf9 cells infected with AcMNPV (MOI 10) were analyzed at 24 h post-infection (pi), and d) Sf9 cells were analyzed at 44 h after plating as a negative control. Values for this negative control were subtracted as background in quantitative analysis of CELISA and ECL-Western blots.

Quantitative ECL-Western blot analyses were performed by comparison of cell lysates to a standard dilution series of purified GP64 EFP^{sol}, using MAb AcV5 to detect GP64 EFP and GP64 EFP^{sol}. A preparation of GP64 EFP^{sol} (purity >95% as judged by SDS-PAGE and coomassie blue staining) was quantified by absorption at 280 nm. The predicted molar extinction coefficient of pure, native GP64 EFP^{sol} at 280 nm was calculated as 77,510 M⁻¹ cm⁻¹, based on the predicted amino acid content of 14 Cys, 11 Trp and 11 Tyr residues per molecule (65). The molecular weight of mature GP64 EFP^{sol} predicted from the amino acid sequence is 52,519 Da (amino acids 18-477 of OpMNPV GP64 EFP). To prepare a standard curve, purified GP64 EFP^{sol} was added to Sf9 cell lysates in SDS lysis buffer (30,960 cells/20 μ l lysate) at concentrations of 0.1 ng to 40 ng GP64 EFP^{sol}/20 μ l lysate (equivalent to 1.3×10^4 to 5×10^6 trimers of GP64 EFP^{sol}/cell). Triplicate cell samples and standard curve samples were electrophoresed on SDS-PAGE gels, blotted to PVDF membranes, and GP64 EFP was detected with MAb AcV5 by ECL (Amersham). For quantification of films by densitometry, ECL

exposure times were chosen to avoid film saturation. Exposed films were digitized on a flat-bed scanner and the ECL signals (below saturation) were quantified using Imagequant software (Molecular Dynamics). Quantitative measurements of GP64 EFP expression from the samples of infected, transiently transfected, or stably transfected cells were performed by comparison of the mean ECL signal to the GP64 EFP^{sol} standard curve. The mean ECL signal from each triplicate cell sample was divided by the estimated number of cells in the sample, determined by counting the cells present in triplicate wells of an identically treated replicate plate. Conversion from ng GP64 EFP^{sol}/cell to trimers/cell used the predicted mass of GP64 EFP^{sol}: (52,519 g/mole)/(6.02 x 10²³ molecules/mole) = 8.72 x 10⁻²⁰ g/molecule of GP64 EFP^{sol} = 2.62 x 10⁻¹⁹ g/trimer of GP64 EFP^{sol}. Because both GP64 EFP^{sol} and GP64 EFP were detected using a monoclonal antibody that recognizes a single defined epitope (171) the ECL signal is proportional to the number of molecules rather than the mass.

Relative levels of GP64 EFP localized on the cell surface were determined by a previously described whole cell ELISA (CELISA) technique (171) with minor modifications. Cells were fixed for 10 minutes at room temperature with 0.5% glutaraldehyde in PBS pH 7.4, and surface GP64 EFP was detected using MAb AcV5. The mean CELISA signal from each triplicate cell sample was normalized to the estimated number of cells per well, as determined above for quantitative ECL analysis.

To examine variation of GP64 EFP surface density in populations of cells, uninfected Sf9 cells, AcMNPV infected Sf9 cells, the stably transfected cell lines, and transiently transfected Sf9 cells were analyzed by flow cytometry using anti-GP64 EFP^{sol} antiserum. For flow cytometry, cells were gently suspended in TNM-FH complete medium containing 0.02% w/v sodium azide (NaN₃) and incubated for 20 min at RT. Cells (1 x 10⁶ cells/250 µl) were incubated with anti-GP64 EFP^{sol} antiserum (diluted 1:20,000 in binding buffer; binding buffer is PBS pH 7.0 containing 1% w/v gelatin and 0.02% NaN₃) for 40 min at RT. After washing twice with PBS-NaN₃ (PBS pH 7.0 containing 0.02% NaN₃), the cells were incubated with FITC-conjugated goat-anti-rabbit secondary antibody (diluted 1:100 in binding buffer; Pierce). Cells were washed four times in PBS-NaN₃, and resuspended in 350 µl PBS-NaN₃ for flow cytometry. For each cell type, control samples were incubated without antibodies, or with only secondary antibody. Fluorescence was analyzed by flow cytometry (EPICS, Coulter Corp.), and fluorescence data were collected for 1 x 10⁴ cells from each sample. Dead cells were excluded from analysis by gating of the live cell population based on the ratio of forward to side scatter.

Generation of a GP64 EFP-null AcMNPV baculovirus. To construct a transfer vector for allelic replacement of the *gp64 efp* locus of the AcMNPV genome, the 4718 bp *EcoRI-SmaI* fragment (corresponding to nucleotides 107,326 to 112,043 from the *EcoRI* H fragment (2)) of AcMNPV strain E2 was cloned into the pBS vector (Stratagene) to generate the plasmid pAcEcoHΔSma. This plasmid contains 2327 bp upstream of the *gp64 efp* ORF, the *gp64 efp* ORF, and 853 bp downstream of the *gp64 efp* ORF. To disrupt the AcMNPV *gp64 efp* gene by insertional mutagenesis, we

generated an in-frame fusion between GP64 EFP and the *Escherichia coli lacZ* gene in an AcMNPV GP64 EFP expression plasmid pAcNru(BKH). The pAcNru(BKH) expression plasmid contains an 18 bp in-frame linker encoding unique *Bgl*II, *Kpn*I and *Hind*III restriction sites, inserted at the *Nru*I restriction site within the *gp64 efp* ORF of plasmid p166B+1 Ac Spe/Bgl (171). A 3072 bp *Bam*HI fragment containing the *lacZ* ORF (derived from pMC1871, (22) was subcloned into *Bgl*II digested pAcNru(BKH). The resulting construct (pAcNru(*lacZ*)) contains a GP64-*lacZ* fusion after codon 131 of *gp64 efp* (4, 43), and the fusion gene open reading frame terminates at the end of the *lacZ* insertion. The 3447 bp *Bsm*II/*Sac*II fragment of pAcNru(*lacZ*) (containing the *lacZ* cassette and the flanking portions of *gp64 efp*) was subcloned into *Bsm*II/*Sac*II digested pAcEcoHΔSma, to generate plasmid pAcGP64Z (Fig. 2A). Finally, to ensure inactivation of the *gp64 efp* gene, the downstream portion of the *gp64 efp* ORF was truncated by digesting pAcGP64Z with *Nco*I, removing the resulting 54 bp *Nco*I-*Nco*I fragment, then blunting and religating to generate pAcGP64ZΔ*Nco*. This deletion results in a frame shift mutation and terminates the *gp64 efp* open reading frame after codon 452, 30 codons upstream of the predicted transmembrane domain. Recombinant viruses were generated using standard protocols (177), by cotransfecting viral DNA from wild-type AcMNPV strain E2 and pAcGP64ZΔ*Nco* plasmid DNA into the GP64 EFP expressing Sf9^{OP64-6} cells. A recombinant virus (vAc^{64Z}) was isolated from culture supernatant by plaque purification on Sf9^{OP64-6} cells, using X-gal in the agarose overlay to identify the recombinant plaques.

The structure of the *gp64 efp* locus in vAc^{64Z} was analyzed by PCR amplification and restriction mapping. DNA was extracted from infected Sf9 cells at 24 h pi, or viral DNA was isolated from BV pelleted through a 25% sucrose cushion (177). For PCR analysis, the following primers homologous to the 5' and 3' ends of the *gp64 efp* ORF were used (Fig. 2A): GB111, 5'-GAGCTGATCGACCGTTGGGG-3' and GB152, 5'-CGGTTTCTGATCATAACAGTACA-3'. To verify the presence of the *Nco*I deletion in vAc^{64Z}, PCR amplification was performed using primers flanking the deletion site (Fig. 2A; GB53, 5'-CCAGCGGCTGGTCGTTTATCGCCC-3' and GB152).

For comparisons of infection in Sf9 cells and *T. ni* larvae, a control virus (vAc^{hsZ}; kindly provided by Dr. P. Roelvink) was used. vAc^{hsZ} contains the bacterial *lacZ* gene (under the control of the *Drosophila hsp70* promoter) in the *p10* locus, and lacks a functional *p10* gene (vAc^{hsZ} is identical to recombinant virus AcNPV/As3 (256).

Assays:

Cell-cell transmission in cell culture. To monitor the cell to cell transmission of infection in cell culture, Sf9 cells were infected at MOI 0.1 with vAc^{64Z} or vAc^{hsZ}. After a 1 h incubation at room temperature, the inoculum was removed and the cells were rinsed twice with complete TNM-FH media, then placed in complete TNM-FH media and incubated at 27° C. At 20, 48, and 72 h pi, the cells were fixed and stained for β-galactosidase activity to detect cells infected by the *lacZ*-marked viruses (247).

Larval feeding assays. Neonate bioassays were performed by the droplet feeding assay (105), using occlusion bodies prepared from either wild type AcMNPV-

infected Sf9 cells or from vAc^{64Z}-infected Sf9^{OP64-6} cells. Occlusion bodies were suspended in distilled water, counted in a hemacytometer, then diluted to the indicated concentrations in distilled water containing blue food coloring. After droplet feeding, larvae that had imbibed were identified by their blue color, and were placed in individual cups with artificial diet and maintained at 29° C in darkness. Because a low level of non-viral neonate mortality is sometimes observed, larvae that died within the first 24 h post-feeding were discarded from analysis. Viral-induced mortality was scored at 4 d post-feeding. For late larval bioassays, newly molted 4th instar *T. ni* larvae were starved for 1.5-2 h after molting, then fed occlusion bodies prepared from either vAc^{64Z} infected Sf9^{OP64-6} cells, or from vAc^{hsZ} infected Sf9 cells. Each larva was fed 1 µl of a suspension containing 1000 occlusion bodies/µl, 5% w/v sucrose and blue food coloring. Larvae were kept in empty cups for 2 h after feeding, then were placed in individual cups with artificial diet and maintained at 27° C in darkness. At the indicated times post-feeding, larvae were dissected in PBS (pH 7.4) by a single longitudinal incision through the dorsal cuticle and pinned to expose the gut and hemocoel. Dissected larvae were fixed for 30 min at RT by immersion in 0.01% w/v gluteraldehyde and 2% w/v paraformaldehyde in PBS pH 7.4. After fixation, larvae were rinsed 3 times for 5 min in PBS (pH 7.4), and stained with X-gal (1 mg/ml) in PBS (pH 7.4) containing 3 mM K₃Fe(CN)₆ and 3 mM K₄Fe(CN)₆ (51). Staining times were typically 2 h at RT (Fig. 5 panels A, C and D), but were extended to 18 h at RT to verify the lack of systemic infection with vAc^{64Z} (Fig. 5 panel B).

Results

Generation of stably transfected cell lines. Because previous studies using anti-GP64 EFP antibodies suggested that GP64 EFP might be an essential component of budded virions, we used a strategy in which the GP64 EFP protein was provided *in trans*, to complement the inactivation of the *gp64 efp* gene in the virus. To provide GP64 EFP *in trans*, a stably transfected cell line that constitutively expresses the OpMNPV GP64 EFP protein was generated by transfection with plasmids encoding GP64 EFP and the bacterial neomycin resistance gene, followed by selection for G418 resistance. To express the OpMNPV GP64 EFP, we used a GP64 EFP expression plasmid (p64-166) that contains the OpMNPV *gp64 efp* ORF under control of an OpMNPV *gp64 efp* early promoter construct that has been studied in detail (6, 8, 132, 133). Transfected Sf9 cells that were resistant to G418 were selected, and isolated cell lines were established.

Quantitative analysis of GP64 EFP expression in stably transfected cell line. Expression of GP64 EFP from two stably transfected cell lines (Sf9^{OP64-6} and Sf9^{OP64-2}) was compared to AcMNPV infected Sf9 cells (at 24 h pi), and to transient GP64 EFP expression from Sf9 cells transfected with plasmid p64-166 (at 44 h post-transfection) (5). For these analyses, we used several quantitative techniques to determine absolute

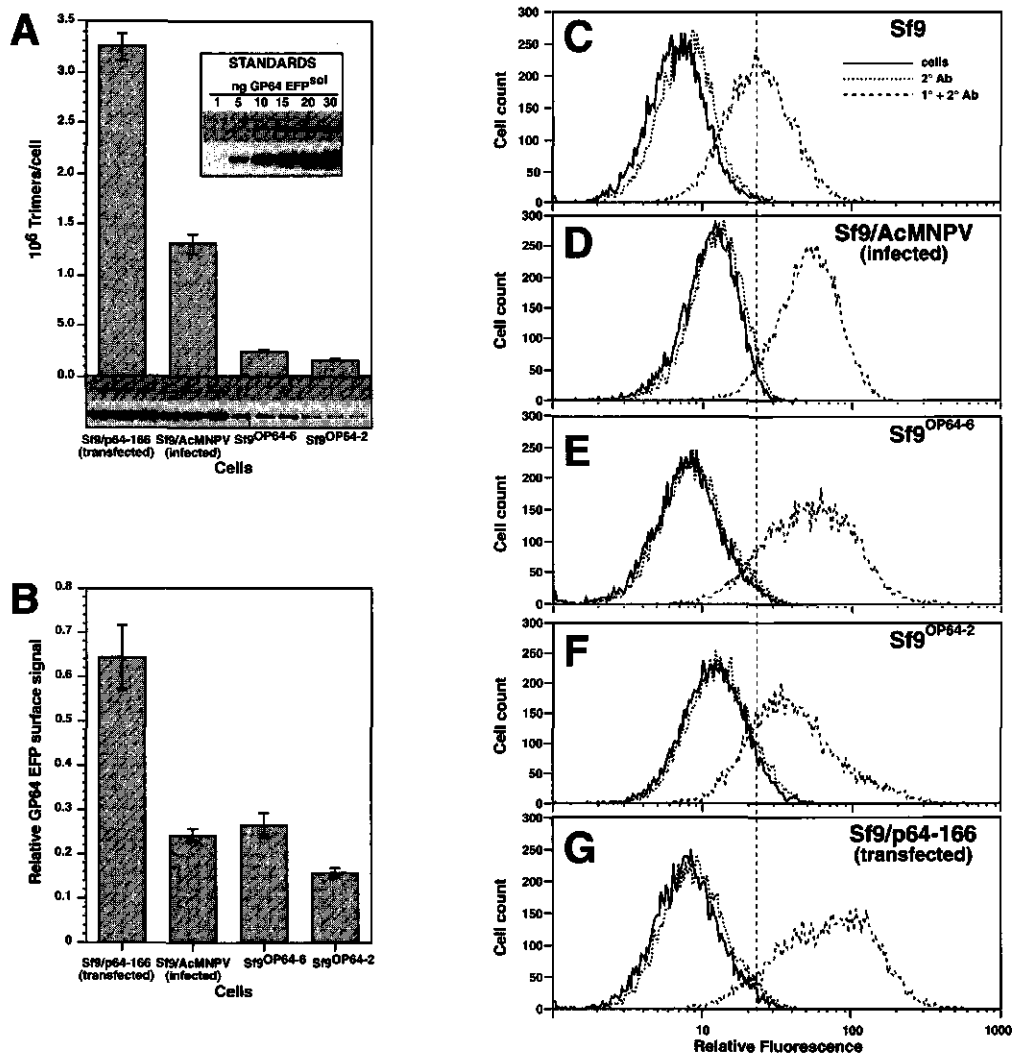


FIG. 1. Expression of GP64 EFP by transiently transfected Sf9 cells (transfected), AcMNPV infected Sf9 cells (infected), and two stably transfected Sf9 cell lines (Sf9^{OP64-6} and Sf9^{OP64-2}). For analysis of infected cells, Sf9 cells were infected with wild type AcMNPV at an MOI of 10 and analyzed at 24 h pi. Transiently transfected cells were transfected with plasmid p64-166 (encoding OpMNPV GP64 EFP) and analyzed at 44 h post transfection. Stably transfected cell lines Sf9^{OP64-6} and Sf9^{OP64-2} were analyzed at 44 h after plating. **(A)** ECL-Western blot quantification of total GP64 EFP. Cell lysates were prepared from triplicate samples of each cell type and analyzed by Western blot with enhanced chemiluminescence detection using MAb AcV5. Two exposures of the triplicate samples of each cell type are shown below the graph. Absolute quantities of GP64 EFP per cell were determined by densitometry and extrapolation from a standard curve prepared with purified GP64 EFP^{sol} (inset). The inset shows two exposures of a series of standard concentrations (ng/20 μ) of GP64 EFP^{sol}. Each bar in the graph represents the calculated mean number of GP64 EFP trimers per cell; error bars represent the standard deviations of triplicate samples for

and relative levels of GP64 EFP: a) absolute levels of GP64 EFP from whole cells were determined by quantitative ECL-Western blots, b) relative surface levels of GP64 EFP were determined by CELISA, and c) variation in average surface density of GP64 EFP was determined by flow cytometry (Figure 1).

A soluble secreted form of GP64 EFP (GP64 EFP^{sol}) was used to generate a standard curve for quantitative ECL analysis (see Methods; Fig. 1A inset). Comparisons of GP64 EFP present in the whole cell extracts from transiently transfected Sf9 cells, AcMNPV infected Sf9 cells, and two stably transfected cell lines are indicated in Figure 1A. The quantity of GP64 EFP detected in AcMNPV infected Sf9 cells at 24 h pi corresponds to approximately 1.3×10^6 trimers of GP64 EFP per cell. The quantity of GP64 EFP detected from stably transfected line Sf9^{OP64-6} (2.5×10^5 trimers/cell) was approximately 19% of that detected from AcMNPV infected cells at 24 h pi. Total GP64 EFP levels from line Sf9^{OP64-2} were lower (1.6×10^5 trimers/cell), corresponding to approximately 12% of that detected from AcMNPV infected cells. Interestingly, transiently transfected Sf9 cells assayed at 44 h post-transfection (included as a control) showed the highest average levels of GP64 EFP expression, approximately 3.2×10^6 trimers/cell, or 2.5 times that detected from AcMNPV infected Sf9 cells.

Detection and quantification (by CELISA) of average relative levels of surface-localized GP64 EFP (Figure 1B) showed that the level of surface-localized GP64 EFP from Sf9^{OP64-6} cells was similar to that detected at the surface of AcMNPV infected Sf9 cells at 24 h pi, a time when virion budding is occurring. Average surface levels of GP64 EFP on Sf9^{OP64-2} cells were lower, corresponding to approximately 70% of that detected from AcMNPV infected Sf9 cells or Sf9^{OP64-6} cells. Transiently transfected Sf9 cells assayed at 44 h post-transfection expressed the highest average levels of surface GP64 EFP, corresponding to approximately 2.7 times that detected from AcMNPV infected Sf9 cells at 24 h pi.

Because GP64 EFP expression levels may vary between individual cells in a population, we also used flow cytometry to determine the degree of variation. The degree of variation (of GP64 EFP surface densities) within populations was compared

each indicated cell type. All data were normalized to Sf9 cells analyzed at 44 h after plating. (B) CELISA of surface-localized GP64 EFP. Relative levels of surface localized GP64 EFP were determined by CELISA of gluteraldehyde fixed cells using MAb AcV5. Each bar in the graph represents the mean CELISA signal of triplicate samples, normalized to the estimated mean number of cells present in each sample. Error bars represent the standard deviations of triplicate samples for each indicated cell type. All data were normalized to Sf9 cells analyzed at 44 h after plating. (C-G) Flow cytometry analysis of surface-localized GP64 EFP on individual cells. Unfixed cells from each indicated population were incubated with an anti-GP64 EFP^{sol} polyclonal serum in the presence of sodium azide. Bound antibodies were detected with an FITC-conjugated secondary antibody. Each graph plots the cell count (y axis) versus relative fluorescence level (x-axis). For each population, samples analyzed included cells incubated without antibodies (solid black line), cells incubated with secondary antibody only (fine dotted line), and cells incubated with both primary and secondary antibodies (dashed line). For reference, the mean fluorescence intensity for the negative control (Sf9 cells incubated with anti-GP64 EFP primary antibody and FITC-conjugated secondary antibody) is indicated by the vertical dashed line.

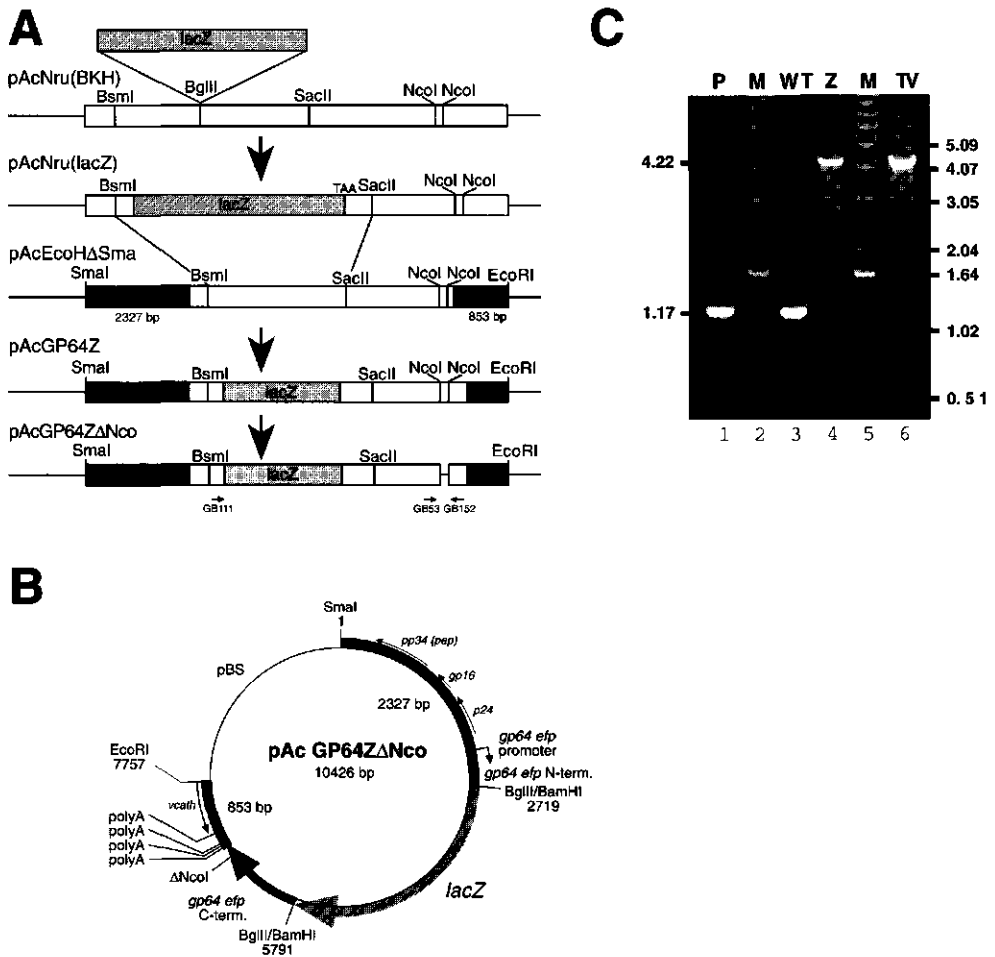


FIG. 2. Insertional mutagenesis of the AcMNPV *gp64 efp* gene. **(A)** Construction of the GP64-*lacZ* transfer vector pAcGP64 Δ Nco. Plasmid names are indicated for each construct (diagrams not to scale). The *lacZ* ORF is shaded gray, the *gp64 efp* ORF is indicated in white, and AcMNPV sequences flanking the *gp64 efp* ORF are indicated in black. Small arrows below the bottom diagram indicate the locations of primers (GB111, GB53, GB152) used for PCR analysis. **(B)** Map of the GP64-*lacZ* transfer vector pAcGP64 Δ Nco. The transfer vector contains 2327 bp of flanking sequences upstream of the *gp64 efp* ORF, and 853 bp of flanking sequences downstream of the wild type *gp64 efp* stop codon. Also indicated are the locations and orientations of genes flanking the *gp64 efp* locus (*vCath*, *p24*, *gp16* and *pp34 (pap)*). **(C)** PCR amplification of the *gp64 efp* locus of wild type AcMNPV or vAc^{64Z}. Primers flanking the *lacZ* insertion (GB111 and GB152, indicated in panel A) were used to amplify the *gp64 efp* locus. The templates used for PCR amplification were: plasmid DNA containing a wild type AcMNPV *gp64 efp* gene (P; lane 1); DNA extracted from Sf9 cells infected with wild type AcMNPV (WT; lane 3); DNA extracted from Sf9 cells infected with vAc^{64Z} (Z; lane 4); and plasmid DNA from the transfer vector pAcGP64 Δ Nco (TV; lane 6). The intact *gp64 efp* ORF is predicted to yield a 1.17 kb PCR product, while the disrupted *gp64 efp* ORF resulting from *lacZ* insertion and the *NcoI* deletion is predicted to yield a 4.22 kb product. Lanes 2 and 5 contain molecular weight standards (M), indicated in kb on the right.

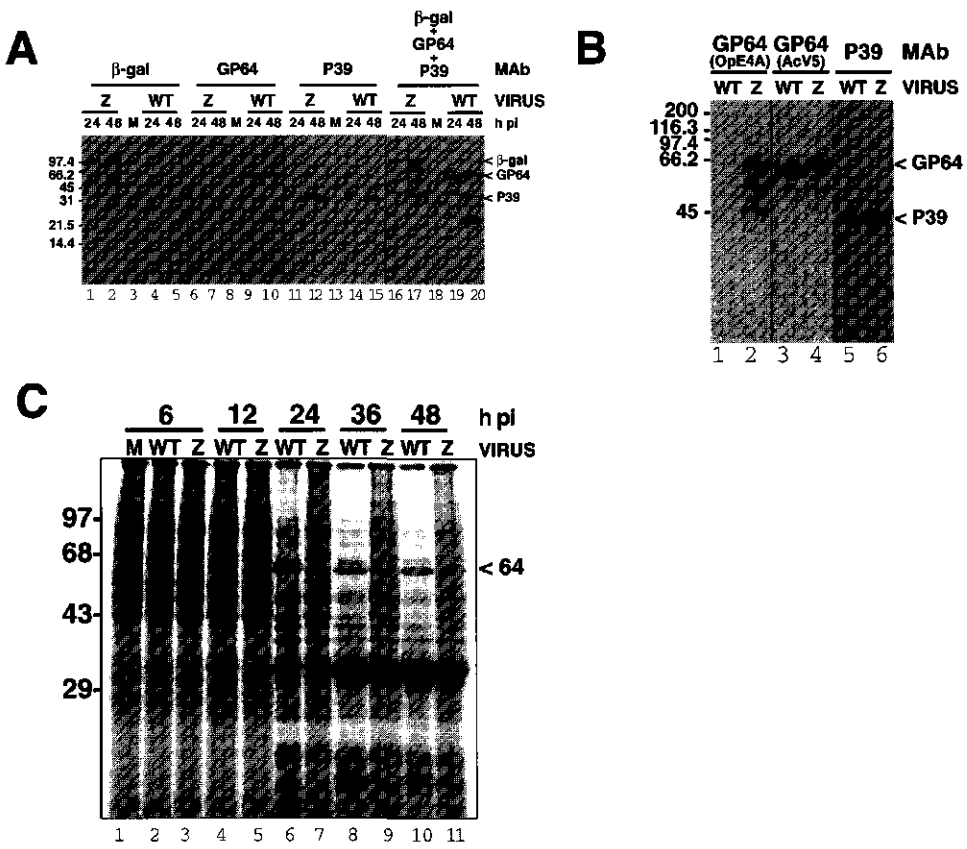
between AcMNPV infected Sf9 cells at 24 h pi, stably transfected cell lines Sf9^{OP64-6} and Sf9^{OP64-2}, and transiently transfected cells at 44 h post-transfection (Fig. 1C-G). Analysis of cells from each population showed that both stably transfected cell lines (Sf9^{OP64-6} and Sf9^{OP64-2}) and transiently transfected Sf9 cells contain a significantly wider variation in GP64 EFP surface densities than do AcMNPV infected Sf9 cells, as indicated by the broader peaks (Fig. 1, compare panels E, F and G to panel D). A small proportion of cells in both of the stably transfected cell populations and in the transiently transfected cell population showed higher levels of surface GP64 EFP (relative fluorescence intensities of approximately 200-300) than did infected Sf9 cells (maximum fluorescence intensity of approximately 150).

Thus by several measurements, the average surface density of GP64 EFP on stably transfected Sf9^{OP64-6} cells appears to be comparable to that on AcMNPV infected Sf9 cells at 24 h pi, a time at which active budding of virions is occurring. Therefore, the level of GP64 EFP expressed by Sf9^{OP64-6} cells was judged to be sufficient to complement inactivation of the *gp64 efp* gene in the AcMNPV viral genome.

Generation of vAc^{64Z}. To inactivate the *gp64 efp* gene in AcMNPV, we used insertional mutagenesis. The AcMNPV *gp64 efp* gene was inactivated by inserting the bacterial *lacZ* ORF (in frame) into the *gp64 efp* ORF after codon 131 (Fig. 2A). Although the *lacZ* ORF contains a translation termination codon, we also created a frame-shift mutation after codon 452 of *gp64 efp*, by removing a 54 bp *NcoI* restriction fragment. This frame shift resulted in a translation termination codon immediately upstream of the GP64 EFP transmembrane domain and insured inactivation of the *gp64 efp* gene. The *gp64-lacZ* fusion gene was then cloned into a transfer vector containing sequences flanking the *gp64 efp* locus in AcMNPV (Fig. 2B; pAcGP64ZΔNco). Recombination of this transfer vector into the *gp64 efp* locus of wild type AcMNPV results in a virus wild type for all genes except *gp64 efp*. To generate recombinant viruses defective for GP64 EFP, transfections, recombination and viral growth were carried out in the Sf9^{OP64-6} cell line. A recombinant virus (vAc^{64Z}) was isolated by plaque purification on Sf9^{OP64-6} cells, using X-gal in the plaque overlay to detect β-galactosidase expression. Although the *gp64 efp* promoter is active in both early and late phases of infection, β-galactosidase activity was not detectable before 5-7 days pi, unless the plaque assay plates were subjected to a freeze-thaw cycle to disrupt the infected cells. This result suggested that active GP64-β-galactosidase fusion protein was not secreted into the medium, despite the presence of the GP64 EFP signal peptide in the GP64-β-galactosidase fusion protein.

To confirm the location of the *gp64-lacZ* insertion in vAc^{64Z}, the *gp64 efp* locus of the vAc^{64Z} recombinant virus was examined by PCR amplification using primers complementary to the 5' and 3' ends of the *gp64 efp* gene (Fig. 2A; GB111, GB152). As control templates for PCR, we used a plasmid containing the wild-type AcMNPV *gp64 efp* gene (negative control), DNA from cells infected with wild type AcMNPV, or plasmid DNA of the transfer vector pAcGP64ZΔNco (positive control). Amplification from the

plasmid containing the wild type *gp64 efp* gene or AcMNPV viral DNA resulted in a 1.17 kb product, as predicted from the sequence (Fig. 2C, lanes 1 and 3). Amplification from the pAcGP64ZΔNco transfer vector or DNA from cells infected by vAc^{64Z} resulted in a single 4.22 kb product, as predicted from allelic replacement of the *gp64 efp* locus by the *gp64-lacZ* fusion gene (Fig. 2C, lanes 4 and 6). PCR analysis (using primers GB53 and GB152; Fig. 2A) was also used to verify that the recombinant virus vAc^{64Z} lacked the NcoI fragment deleted from the downstream region of the *gp64 efp* ORF (data not shown). The structure of the recombinant virus vAc^{64Z} was also examined by restriction enzyme digestion of viral genomic DNA. As expected, the *Eco*RI and *Bam*HI restriction profile of vAc^{64Z} differed from wild type AcMNPV only in the *Eco*RI H and *Bam*HI G fragments, confirming replacement of the *gp64 efp* locus (data not shown). Thus, PCR



analysis, restriction mapping and β -galactosidase activity indicate that the recombinant virus vAc^{64Z} contains only the *gp64-lacZ* fusion gene in the *gp64 efp* locus, and cells infected with vAc^{64Z} express β -galactosidase activity.

To verify that the *gp64 efp* gene was inactivated, vAc^{64Z} infected Sf9 cells were examined by ECL-Western blot analysis (Fig. 3A). Cells were infected with either vAc^{64Z} or wild type AcMNPV, and cell lysates were prepared at 24 and 48 h pi. Replicate blots were probed with monoclonal antibodies specific to β -galactosidase (Fig. 3A, lanes 1-5), GP64 EFP (Fig. 3A, lanes 6-10), or P39 capsid protein (Fig. 3A, lanes 11-15). A replicate blot was also probed with a mixture of all three antibodies (Fig. 3A, lanes 16-20). Expression of β -galactosidase was detected only in cells infected with vAc^{64Z} (Fig. 3A, lanes 1 and 2) and not in cells infected with wild type AcMNPV (Fig. 3A, lanes 4, 5). GP64 EFP expression was not detectable in cells infected with vAc^{64Z} (Fig. 3A, lanes 6, 7). However, expression of the capsid protein P39 was detected in cells infected with either vAc^{64Z} or wild type AcMNPV (Fig. 3A, lanes 11, 12, 14 and 15).

To demonstrate the presence of OpMNPV GP64 EFP on budded virions produced by vAc^{64Z} infected Sf9^{OP64-6} cells, budded virions were purified from tissue culture supernatants by sucrose gradient centrifugation and examined by Western blot analysis (Fig. 3B, lanes 2, 4 and 6). As a control, budded virions were also purified from tissue culture supernatants of AcMNPV infected Sf9 cells (Fig. 3B, lanes 1, 3 and 5). Replicate blots were probed with either a) a monoclonal antibody that reacts only with

FIG. 3. Analysis of GP64 EFP in infected Sf9 cells (panel A) and purified budded virions (panel B), and protein synthesis in infected Sf9 cells (panel C). (A) Western blot analysis of expression of GP64- β -galactosidase fusion protein (β -gal), GP64 EFP (GP64), and the major capsid protein (P39) in Sf9 cells infected with either vAc^{64Z} (Z) or wild type AcMNPV (WT). Sf9 cells were infected at MOI 10 with vAc^{64Z} (Z; lanes 1, 2, 6, 7, 11, 12, 16, 17) or with wild type AcMNPV (WT; lanes 4, 5, 9, 10, 14, 15, 19, 20); mock infected cells were included as a negative control (M, lanes 3, 8, 13 and 18). Cell lysates were prepared for SDS-PAGE and Western blot analysis at 24 h pi (24; lanes 1, 4, 6, 9, 11, 14, 16, 19) or 48 h pi (48; lanes 2, 5, 7, 10, 12, 15, 17, 20). Replicate blots were probed with either a MAb directed against *E. coli* β -galactosidase (β -gal; lanes 1-5), MAb AcV5 which is directed against GP64 EFP (GP64; lanes 6-10), or MAb 39 which is directed against P39 Capsid protein (P39; lanes 11-15). Lanes 16-20 were probed with a mixture of all three MAbs. Bound antibodies were detected by ECL. Positions of protein size standards are indicated along the left in kDa. (B) Detection of OpMNPV GP64 EFP on vAc^{64Z} budded virions. Budded virions were purified from supernatants of AcMNPV infected Sf9 cells (lanes 1, 3 and 5) or vAc^{64Z} infected Sf9^{OP64-6} cells (lanes 2, 4 and 6) by centrifugation on 25-60% sucrose gradients. The budded virion bands were collected and analyzed by SDS-PAGE and Western blot. Duplicate blots were probed with MAb OpE4A, which recognizes only the GP64 EFP of OpMNPV (lanes 1 and 2); with MAb AcV5 (lanes 3 and 4) which recognizes the GP64 EFPs of both AcMNPV and OpMNPV; or with MAb 39 which recognizes the P39 capsid protein (lanes 5 and 6). Bound antibodies were detected by ECL. Positions of protein size standards are indicated along the left in kDa. (C) Kinetics of infection-specific protein expression. Sf9 cells were infected at MOI 20 with either vAc^{64Z} (Z; lanes 3, 5, 7, 9, 11) or wild type AcMNPV (WT; lanes 2, 4, 6, 8, 10). At the indicated times pi, the cells were pulse-labeled for 2 h with ³⁵S-methionine. As a negative control, mock-infected cells were labeled at the first time point (M; lane 1). After the labeling period, the cells were lysed and labeled proteins were analyzed by SDS-PAGE and Phosphorimager analysis. Positions of protein size standards are indicated along the left in kDa.

the OpMNPV GP64 EFP (Fig. 3B, lanes 1 and 2; OpE4A), b) a monoclonal antibody that reacts with GP64 EFPs of both OpMNPV and AcMNPV (Fig. 3B, lanes 3 and 4; AcV5), or c) a monoclonal antibody that reacts with the P39 capsid protein (Fig. 3B, lanes 5 and 6). GP64 EFP was detected in purified budded virions of both AcMNPV and vAc^{64Z} by monoclonal antibody AcV5 (which cross reacts with GP64 EFPs of both AcMNPV and OpMNPV), and capsid protein P39 was also detected in both budded virion preparations (Fig. 3B, lanes 3-6). Using the OpMNPV GP64 EFP-specific monoclonal antibody (OpE4A), we detected the OpMNPV GP64 EFP in purified budded virions of vAc^{64Z} (Fig. 3B lane 2), but not in budded virions of AcMNPV (Fig. 3B lane 1). Thus vAc^{64Z} budded virions produced from Sf9^{OP64-6} cells contained the OpMNPV GP64 EFP protein.

To verify that the infection cycle proceeds normally in vAc^{64Z} infected cells, the kinetics of the infection cycle were examined by pulse-labelling of proteins (Fig. 3C). In vAc^{64Z} infected Sf9 cells, the overall pattern of protein synthesis was similar to that from Sf9 cells infected with wt AcMNPV. At 24 h pi, a labeled band of approximately 64 kD was observed in wt AcMNPV infected cells but not in vAc^{64Z} infected cells (Fig. 3C, compare lanes 6 and 7). Because 24 h pi is the time of maximal GP64 EFP synthesis in AcMNPV infected Sf9 cells (112) this 64 kD band is likely GP64 EFP. Comparison of the temporal progression of infection confirms progression into the late phase between 6 and 12 h pi and therefore suggests that the viral infection cycle of vAc^{64Z} is not significantly affected by the lack of GP64 EFP expression.

Because sequences flanking the *gp64 efp* genes of AcMNPV and OpMNPV are present in the recombinant virus vAc^{64Z} and in the Sf9^{OP64-6} cell line, respectively, and the two genes are highly similar (9), the formal possibility exists that recombination between the heterologous genes in the virus and cell line might result in replacement of the *gp64-lacZ* fusion gene with a functional (OpMNPV) *gp64 EFP* gene. In addition, selection pressure might force integration of the OpMNPV *gp64 EFP* gene at random sites within the genome. Such recombination products were not detected in DNA from the vAc^{64Z} viral stocks, using PCR amplification with primers specific for the OpMNPV *gp64 efp* gene (data not shown). In control experiments, OpMNPV viral DNA was detectable with the OpMNPV specific primers when mixed with AcMNPV DNA at a molar ratio of 1 part OpMNPV to 10⁴ parts AcMNPV DNA, but was not detectable at 1:10⁵. Our inability to detect OpMNPV *gp64 efp* in vAc^{64Z} viral stocks therefore indicates that if any recombinant viruses carrying the OpMNPV *gp64 efp* gene were present, they occurred at a frequency of less than 1 in 10⁴ particles. Because the most likely recombination events that might restore the *gp64 efp* gene would also remove the *lacZ* gene, expression of the *lacZ* marker gene was used as the indicator of infection in subsequent analyses of vAc^{64Z} infectivity.

Cell to cell transmission. To determine if GP64 EFP is required for the production of infectious virions and cell to cell transmission of the virus, Sf9 cells were infected at a low MOI (MOI 0.1) with vAc^{64Z} or with a *lacZ*-marked control virus (vAc^{hsZ}). At various times post-infection, the cells were fixed and stained with X-gal to detect spread of the *lacZ*-marked viruses from the initially infected cells (Fig. 4). At 20 h pi, single infected cells were detected in the cultures infected with vAc^{64Z} (Fig. 4A) or with the control virus (Fig. 4D). At 48 h pi, the control virus had spread from the initially infected cells resulting in large clusters of infected cells (Fig. 4E), and by 72 h pi the control virus had infected most or all cells in the culture (Fig. 4F). In contrast, cultures infected with vAc^{64Z} showed no evidence of cell to cell movement, with only single infected cells detected at 48 and 72 h pi (Fig. 4B and C). Thus these data indicate that GP64 EFP is required for the production of infectious virions, and for cell to cell movement in cell culture.

To examine the role of GP64 EFP during infection in the animal, vAc^{64Z} occlusion bodies were purified from infected Sf9^{OP64-6} cells and fed to early 4th instar *T. ni* larvae (1.5-2 h post-molt). As a control, a second group of larvae was fed occlusion bodies

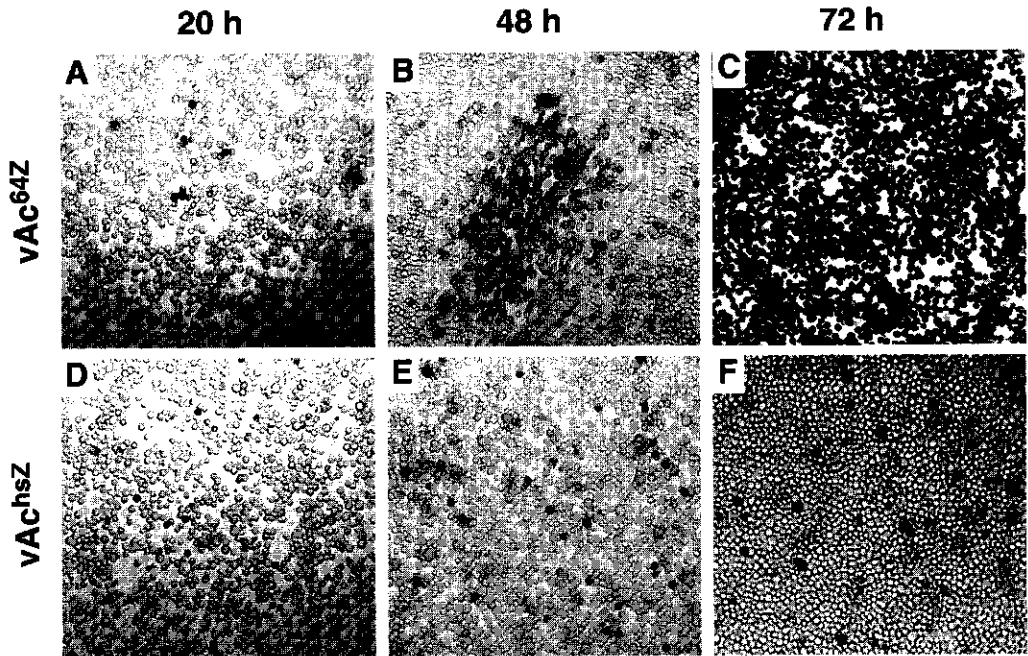


FIG. 4. GP64 EFP role in cell to cell transmission in cell culture. Sf9 cells were infected at a low MOI (0.1) with either virus containing an inactivated *gp64 efp* gene (vAc^{64Z}; panels A, B and C) or a control virus expressing β -galactosidase from the *hsp70* promoter (vAc^{hsZ}; panels D, E and F). To identify infected cells, β -galactosidase activity was detected. Cells were fixed with glutaraldehyde and stained with X-gal at 20 h pi (panels A and D), 48 h pi (panels B and E) or 72 h pi (panels C and F).

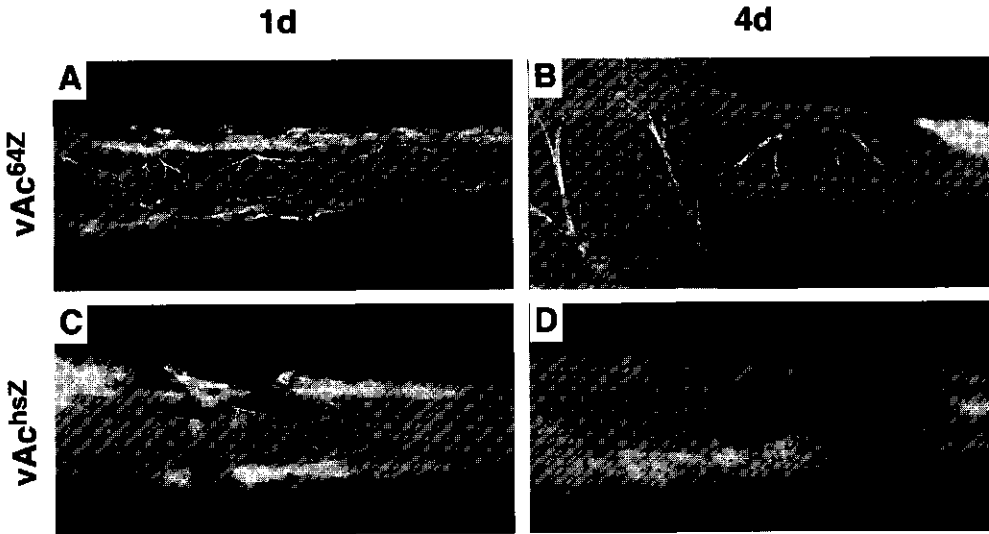


FIG. 5. GP64 EFP role in systemic infection in the insect host. Newly molted 4th instar *T. ni* larvae were fed a suspension of occlusion bodies (1000 occlusion bodies/ μ l) from either the GP64 EFP-null virus (vAc^{64Z}; panels A and B) or the control virus (vAc^{hsZ}; panels C and D). The larvae were dissected, fixed and stained with X-gal to detect β -galactosidase expression in infected cells at either 1 day postfeeding (panels A and C), or 4 days postfeeding (panels B and D). Infected midgut epithelial cells were observed as blue cells in the midgut at 1 d postfeeding in larvae fed either the GP64 EFP-null virus (vAc^{64Z}; panel A) or the control virus (vAc^{hsZ}; panel C). By 4 d postfeeding, larvae fed vAc^{64Z} appeared healthy, and only occasional infected cells were detected in the midgut epithelium (panel B, inset is higher magnification). The larvae fed the control virus vAc^{hsZ} (panel D) exhibited widespread systemic infection of many tissues and this was consistent with their moribund state.

from the *lacZ*-marked control virus (vAc^{hsZ}). At various times post-feeding, animals were dissected and fixed, and infected cells were identified by whole mount X-gal staining (Fig. 5). Infected cells in the midgut epithelium were detected at 4 h postfeeding in 5 of 6 animals fed vAc^{64Z} occlusion bodies and in 5 of 6 animals fed vAc^{hsZ} occlusion bodies (data not shown). By 24 h postfeeding, many midgut cells contained β -galactosidase activity in animals fed either vAc^{64Z} occlusion bodies (Fig. 5A, 3 of 5 animals) or vAc^{hsZ} occlusion bodies (Fig. 5C, 4 of 5 animals), indicating infection. By 4 d postfeeding, all animals fed the control virus vAc^{hsZ} were quiescent and moribund (5 of 5 animals). After X-gal staining, these animals exhibited extensive β -galactosidase staining in many tissues, indicating systemic infection (Fig. 5D). In parallel experiments, all animals fed vAc^{hsZ} occlusion bodies underwent tissue liquification (typical of late stage infection by NPVs) by 5 days postfeeding. In contrast, animals fed vAc^{64Z} occlusion bodies appeared healthy at 5 days postfeeding and continued to develop normally. When examined at 4 days postfeeding by X-gal staining, these animals did not exhibit infection in any tissues, except for occasional isolated midgut cells containing β -galactosidase activity (Fig. 5B, inset). Thus, occluded virions of vAc^{64Z} were infectious to midgut cells and

Table I. Comparative mortalities of neonates fed vAc^{64Z} and AcMNPV in droplet feeding assays

Exp	Virus	Dose (OBs ^a / 10nl)	n	% Mortality
I	AcMNPV	1	30	30.0
		5	30	80.0
		10	30	93.3
	vAc ^{64Z}	1	30	0
		5	30	0
		10	30	(3.3) ^b
II	Control	0	57	0
	AcMNPV	0.1	57	1.8
		1	58	20.7
		10	57	65.0
	vAc ^{64Z}	10	53	0
		100	55	0
1,000		52	0	

^a OB, occlusion body

^b One animal died, but not because of polyhedrosis

established a primary infection, but the infection by vAc^{64Z} failed to escape the midgut. Thus GP64 EFP was not required for infection by occlusion derived virions (ODV), but was essential for the escape of the infection from the midgut into the hemocoel.

To further assess the biological effects of GP64 EFP inactivation, we used a sensitive neonate droplet feeding assay to determine the lethality of vAc^{64Z} to neonate larvae (Table I). *T. ni* neonates were allowed to feed on a suspension of occlusion bodies of either vAc^{64Z} or wild type AcMNPV. Because each larva typically consumes a volume of 8-13 nl (104, 105), occlusion bodies were diluted to a concentration of 1, 5 or 10 occlusion bodies per 10 nl, and neonate larvae were allowed to feed for estimated doses of 1, 5 or 10 occlusion bodies per larva. By 4 d pi, neonates fed 5 or 10 occlusion bodies of wild type AcMNPV exhibited 80% and 93% mortality respectively, while larvae fed an average of 1 occlusion body of wild type AcMNPV exhibited 30% mortality (Table I Experiment I). These observations are consistent with previously published data from wild type AcMNPV in the droplet feeding assay (78). In contrast, larvae fed vAc^{64Z} occlusion bodies at doses of 1 or 5 occlusion bodies per 10 nl exhibited no viral induced mortality. In the group of larvae fed 10 vAc^{64Z} occlusion bodies, one animal died but upon microscopic examination, no evidence of polyhedrosis was found. In a second experiment, doses of 10 occlusion bodies of wild type AcMNPV per 10 nl resulted in 65% mortality (Table I Experiment II). However, doses of vAc^{64Z} as high as 1000

occlusion bodies per 10 nI (100x the measured LD₆₅ of wt AcMNPV in this experiment) resulted in no viral induced mortality by 4 d pi. Thus, the vAc^{64Z} virus was not lethal to *T. ni* neonate larvae at any dose tested.

Discussion

Generation of a virus lacking GP64 EFP. To study the role of the baculovirus GP64 EFP protein in the context of a viral infection, we generated a recombinant baculovirus that contains an insertionally inactivated *gp64 efp* gene and examined the effects of that mutation on viral infectivity, and propagation of the virus in cell culture and in animals. Previous studies of the GP64 EFP protein demonstrated that some anti-GP64 antibodies are capable of neutralizing infectivity of the virus (97, 171, 206, 264). Because of the likelihood that inactivation of the *gp64 efp* gene would be difficult, we chose to supply the GP64 EFP protein *in trans*, from a stably transfected cell line, and to then use homologous recombination for generating an inactivated *gp64 efp* gene in the context of an otherwise wild type AcMNPV baculovirus.

One disadvantage of this approach is that if the *gp64 efp* gene is essential, a very strong selection pressure for regenerating a GP64 EFP⁺ virus may result in recombination between the virus and the *gp64 efp* gene within the cell line. To reduce this possibility and insure that we examined only virus containing the inactivated *gp64 efp* gene, we used the following strategies: a) For generating the stably transfected cell line, we selected a heterologous *gp64 efp* gene (derived from a different baculovirus, OpMNPV), b) Recombinant vAc^{64Z} virus stocks were screened by restriction analysis, Western blots and PCR for significant levels of any revertant virus, c) A *lacZ* marker gene was fused in-frame with the wt AcMNPV *gp64 efp* gene, and analyses of the "loss-of-function" phenotype of the recombinant virus relied on detection of the β -galactosidase marker. Thus, the analysis of only cells expressing the *lacZ* marker gene insured that we exclusively analyzed viruses carrying the inactivated *gp64 efp* gene.

Constitutive expression of GP64 EFP on Sf9^{OP64-6} cells. The first step in the above strategy involved the production of cell lines that constitutively expressed the GP64 EFP protein from OpMNPV. In addition to facilitating the construction of the recombinant virus, the use of a heterologous *gp64 efp* gene also allowed us to determine whether the highly conserved (but not identical) OpMNPV GP64 EFP could functionally replace the AcMNPV GP64 EFP protein. After constructing the OpMNPV GP64 EFP expressing cell lines, we performed several quantitative studies to compare GP64 EFP expression from AcMNPV infected cells, stably transfected cells and transiently transfected cells. For one aspect of these studies, we measured the quantities of GP64 EFP expressed on a per cell basis. At 24 h pi, AcMNPV infected Sf9 cells contained on average approximately 3.9×10^6 molecules of GP64 EFP per cell (equivalent to 1.3×10^6 trimers). Stably transfected Sf9^{OP64-6} cells contained only approximately 7.6×10^5

molecules (equivalent to 2.5×10^5 trimers) of GP64 EFP per cell. While the total quantity of GP64 EFP per infected cell was approximately 5 times higher than the quantity detected per Sf9^{OP64-6} cell, a further (CELISA) analysis of the average levels of GP64 EFP at the surface of these cells indicated that the level of GP64 EFP at the surface of the Sf9^{OP64-6} cells was similar to that of infected cells. Flow cytometry analysis of surface GP64 EFP levels on individual cells in each population indicated that there was less cell to cell variability among AcMNPV infected cells than among Sf9^{OP64-6} cells. Greater variability of GP64 EFP surface density appeared to be a general feature of transfected cells, since both the Sf9^{OP64-2} cell line and transiently transfected cells also exhibited wider variations in GP64 EFP surface levels. The narrower range of GP64 EFP surface levels in infected Sf9 cells is likely due to the synchronization of GP64 EFP expression during infection, since at 24 hours postinfection, GP64 EFP expression is primarily from the late promoter. In contrast, GP64 EFP in transfected cells results from constitutive expression by the early promoter and accumulation of the protein in a population of asynchronously dividing cells. In transient transfections, variable levels of GP64 EFP expression may also arise from cell to cell variations in DNA uptake during transfection.

Because cell surface levels of GP64 EFP from infected and Sf9^{OP64-6} cells were similar, yet an approximately 5 fold difference was detected in the total quantity of GP64 EFP, these data suggest that no more than 20% of the total GP64 EFP protein detected from AcMNPV infected Sf9 cells (at 24 h pi) is found at the cell surface. Using this estimate of surface localization (20%) in combination with quantitative ECL data derived from whole cell measurements of GP64 EFP, we estimate that AcMNPV infected Sf9 cells (MOI 10, 24 h pi) contain an average surface density of 2.6×10^5 trimers of GP64 EFP per cell, at most. These preliminary studies suggested that the Sf9^{OP64-6} cell line produces sufficient quantities of surface localized GP64 EFP to yield reasonable titers of budded virions when infected by a virus lacking a *gp64 efp* gene. Production of infectious vAc^{64Z} budded virus from Sf9^{OP64-6} cells was on the order of $2-3 \times 10^7$ infectious units/ml (determined by TCID₅₀ on Sf9^{OP64-6} cells). The presence of GP64 EFP on the surface of the Sf9^{OP64-6} cells apparently did not interfere with infection, since the TCID₅₀ titer of the wild type AcMNPV stock determined on the Sf9^{OP64-6} cells was approximately 1.3 fold higher than the titer determined on Sf9 cells. In addition to production of recombinant baculoviruses containing deletions or mutations in GP64 EFP, these stably transfected cell lines constitutively expressing GP64 EFP will also be useful for studies of GP64 EFP mediated membrane fusion.

gp64 efp is an essential baculovirus gene. The production of infectious budded virions by vAc^{64Z} infected Sf9^{OP64-6} cells demonstrates that the OpMNPV GP64 EFP can functionally substitute for the AcMNPV GP64 EFP in the production of budded virions. In addition, vAc^{64Z} virions (produced in Sf9^{OP64-6} cells) were infectious to Sf9 cells indicating that this aspect of host range was apparently unaffected. Thus the GP64 EFP protein from these two related baculoviruses appears to be interchangeable. Of particular importance, we demonstrate that vAc^{64Z} budded virions produced in Sf9^{OP64-6} cells are

able to enter and infect Sf9 cells, but in the absence of the *gp64 efp* gene, the vAc^{64Z} virus is unable to transmit the infection to uninfected neighboring cells. Thus *gp64 efp* is an essential baculovirus gene, and the GP64 EFP protein is required for the cell to cell transmission of the infection. Studies are now in progress to identify the cause of the defect in viral transmission. Preliminary studies suggest that virion budding is defective in the absence of GP64 EFP.

GP64 EFP is not essential for infectivity of occluded virions. In previous studies, the transmission of virus from the midgut to hemocoel has been studied using marker genes to follow the progression of tissues infected (47, 51). Virions have been observed budding from the basal side of the midgut epithelial cells (74) and virion budding is believed to serve as the primary mode of viral movement from midgut epithelium to hemocoel. Hemocytes (127) cells of the tracheal system (47), and basal lamina associated muscle and tracheal cells (51) have been proposed as the primary cells infected after the first round of replication in midgut epithelial cells. It has also recently been suggested that the tracheal system may serve as a "conduit" for budded virus transmission across the basal lamina of the midgut epithelium to other tissues within the hemocoel (47).

In the current study, we examined the role of GP64 EFP during infection in the animal by feeding occlusion bodies prepared from vAc^{64Z} infected cells to either neonate or early 4th instar *T. ni* larvae. Using whole mount histological staining of 4th instar *T. ni* larvae to detect infection, we found that the vAc^{64Z} occlusion derived virions were capable of infecting cells of the midgut epithelium, but infection by vAc^{64Z} did not move beyond the midgut. The ability of vAc^{64Z} to produce infectious occluded virions in the absence of GP64 EFP expression is consistent with previous studies that found no detectable GP64 EFP protein associated with the occluded virus (14, 97) and clearly demonstrates the virion phenotype specificity of the GP64 EFP protein.

As perhaps the most sensitive indicator of systemic propagation of viral infection, we examined mortality in neonate larvae fed occlusion bodies of vAc^{64Z}. At doses of up to 100x the LD₆₅ of AcMNPV, the vAc^{64Z} virus was non-lethal to *T. ni* neonates. The lack of vAc^{64Z} induced mortality in *T. ni* neonate larvae thus confirms the observations in tissues of whole 4th instar larvae, and demonstrates that the inability of the vAc^{64Z} virus to escape from the midgut epithelium results in a non-lethal phenotype *in the animal*. These results therefore demonstrate an absolute requirement for GP64 EFP in the progression of the infection from the midgut epithelium to the systemic form of the disease in tissues of the hemocoel.

Acknowledgements

We thank P. R. Roelvink for providing the control virus vAc^{hsZ}, R. R. Granados and K. McKenna for providing larvae and for assistance with the neonate assays, D.

Theilman for providing the *lacZ* cassette, and J. R. Manning for kindly providing anti-P39 MAb 39. This research was supported by NIH grants AI 33657 and AI 31130, and Boyce Thompson Institute projects 1250-01 and 1255-17.

Chapter 4

Requirement for GP64 to drive efficient budding of *Autographa californica* Multicapsid Nucleopolyhedrovirus

Abstract

Budded virions (BV) of *Autographa californica* Multicapsid Nucleopolyhedrovirus (AcMNPV) contain a major envelope glycoprotein (GP64) that is present on the plasma membrane of infected cells. GP64 is acquired by virions during budding from the plasma membrane, the final step in assembly of the budded virion at the cell surface. Previous studies (172) showed that insertional inactivation of the AcMNPV *gp64* gene resulted in a virus unable to move from cell to cell and non-lethal to orally infected *Trichoplusia ni* larvae. To determine if GP64 is involved in virion budding, we measured BV production from Sf9 cells infected with a *gp64*null virus. Sf9 cells infected with *gp64*null virus vAc⁶⁴ were pulse labeled and progeny BV were isolated on equilibrium sucrose gradients and quantified. BV production from vAc⁶⁴ was reduced to ~ 2% of that from wild-type AcMNPV. Thus, the GP64 protein is important for efficient virion budding. To determine if the highly charged 7 amino acid cytoplasmic tail domain (CTD) of GP64 was required for virion production, we generated a series of GP64 constructs containing C-terminal truncations or substitutions. Modified forms of GP64 were analyzed in transfected cells, and in recombinant viruses in which the wild-type *gp64* gene was replaced with a modified *gp64*. Deletion of 1 to 7 amino acids from the CTD did not affect GP64 trimerization, protein transport to the cell surface, or membrane fusion activity. However, deletions of 11 or 14 amino acids, which removed the CTD and portions of the predicted TM domain, were trimerized but were present at lower levels on the cell surface due to shedding of these truncated proteins. Comparisons of growth curves and quantitative measurements of labeled progeny BV production from recombinant viruses expressing either wild-type or mutant GP64 proteins showed that deletion of the 7 residue CTD only moderately reduced the production of infectious virions (~ 50%). However, deletions of the C-terminal 11 or 14 amino acids had more substantial effects. Removal of the C-terminal 11 amino acids reduced titers of infectious virus by 78-96% and labeled progeny virions were reduced by 91-92%. Removal of 14 amino acids from the C-terminus resulted in an ~ 98% reduction in progeny BV and a virus that was apparently incapable of efficient propagation in cell culture. Thus, the GP64 CTD is not essential for production of infectious BV, but removal of the CTD results in a measurable reduction in budding efficiency. Deletion of the CTD plus small portions of the TM domain resulted in shedding of GP64, reduced surface levels, and a dramatic reduction in the production of BV. Together, these data indicate that GP64 is an important and limiting factor in BV production.

This chapter has been published as:

Oomens, A.G.P., and G.W. Blissard (1999). Requirement for GP64 to drive efficient budding of *Autographa californica* Multicapsid Nucleopolyhedrovirus. *Virology* 254, 297-314.

Introduction

During the infection cycle, baculoviruses such as the *Autographa californica* Multicapsid Nucleopolyhedrovirus (AcMNPV) and the *Orgyia pseudotsugata* MNPV (OpMNPV) produce two types of infectious virus particles which are referred to as virion phenotypes (reviewed in (5, 167, 209)). The two virion phenotypes are termed Budded Virus (BV) and Occlusion Derived Virus (ODV). Each consists of enveloped nucleocapsids, but the envelopes differ in source and composition (14). BV and ODV serve distinctly different roles in the life cycle of the virus and are assembled by different mechanisms and at different sites in the infected cell. BV are assembled at the cell surface as nucleocapsids bud through the plasma membrane. In contrast, ODV are assembled within the nucleus when nucleocapsids are enveloped within membranes that appear to be derived from the nuclear membrane (52, 98). Very late in infection, ODV become embedded within an abundantly expressed viral protein, polyhedrin, to form highly stable occlusion bodies. Animal-to-animal transmission of baculovirus infections is typically by the oral route and is mediated by ODV which are highly infectious to the epithelial cells of the midgut (265). ODV enter and infect host midgut epithelial cells and infection results in assembly and budding of BV from the basal side of these polarized cells (74, 127). BV is highly infectious to tissues within the hemocoel and in cell culture (266) and mediates the spread of infection from cell to cell within the animal. BV from viruses such as AcMNPV and OpMNPV have a loosely adhering envelope that contains a major spike protein known as GP64. On the surface of infected cells and in the BV envelope, GP64 is present as a homotrimer (184). GP64 is thought to serve critical roles during viral entry into host cells. After binding, BV enter cells by endocytosis (261) and previous studies have demonstrated that GP64 is necessary and sufficient for low pH triggered membrane fusion, a process that is required for release of nucleocapsids from endosomes (10, 25, 147, 171, 172). During budding and assembly of BV, GP64 concentrates in discrete areas on the plasma membrane (9) and these sites appear to represent the sites of BV budding (260). In many cases, viral envelope proteins are important in budding and assembly of progeny virions at the cell surface (236). However, the role of the envelope proteins in virion budding may differ substantially in different virus groups. Recent studies of virion budding in two rhabdovirus systems showed that virion budding is severely reduced (approximately 30 fold) in the absence of the major envelope glycoprotein, G protein (163, 223). In contrast, the budding of some retroviruses is independent of the major envelope protein (Env), requiring only the gag protein for budding (64, 72, 215, 226).

In a previous study, we generated a gp64null AcMNPV baculovirus using a stably transfected cell line to provide the GP64 protein during construction and propagation of the virus (172). Using the gp64null virus, it was demonstrated that GP64 is necessary for cell-to-cell transmission of infection in cell culture, and for movement of infection from the insect midgut into the hemocoel. However, the precise mechanism of this defect in the gp64null virus was not known. Possible explanations included: a) a

defect in production of BV, or b) production of BV that were not infectious. To address these possibilities in the current study, we used a biochemical approach to examine BV production from a *gp64*null virus. We show that virion production is almost completely eliminated in the absence of GP64. Our results indicate that GP64 plays an important role in virion budding from the plasma membrane, and that the observed defect in cell-to-cell transmission by the *gp64*null virus results primarily from a defect in virion budding. We also examined the role of the predicted cytoplasmic tail domain (CTD) of GP64 in virion budding from the plasma membrane. A series of GP64 constructs containing deletions or substitutions within the CTD region was generated, analyzed, and used for constructing recombinant viruses in which the wild type *gp64* gene was replaced with modified forms of *gp64*. We found that the GP64 CTD was not required for either transport to the cell surface, trimerization, low pH-triggered membrane fusion activity, budding of progeny virions, or infectivity of BV. However, deletions of the CTD and portions of the transmembrane domain resulted in less efficient anchoring of GP64 in the plasma membrane, which was accompanied by a decrease in virion assembly at the cell surface.

Results

GP64null virus construction. In a previous study (172) we generated a *gp64*null baculovirus (*vAc*^{64Z}) in which the *gp64* gene was inactivated by insertion of a *lacZ* cassette into the AcMNPV *gp64* ORF. The *vAc*^{64Z} virus was generated and propagated in a cell line (Sf9^{OP64-6}) that constitutively expresses the OpMNPV GP64 protein. We found that upon prolonged passage of *vAc*^{64Z} in Sf9^{OP64-6} cells, low frequency homologous recombination of the virus with the OpMNPV *gp64* gene in the cell line resulted in rescue and generation of a low level of virus expressing a functional GP64 protein. To avoid the potential problem of *gp64*null rescue by homologous recombination, we generated a second recombinant AcMNPV, in which the entire *gp64* ORF was removed. To remove the *gp64* ORF, we generated a transfer vector plasmid containing a *lacZ* cassette (under the control of the OpMNPV IE1 promoter), flanked by sequences found upstream and downstream of the AcMNPV *gp64* ORF (Fig. 1). Cotransfection of the transfer vector and wild type AcMNPV DNA in stably transfected cells that express OpMNPV GP64 (Sf9^{Op1D}), resulted in discrete removal of the AcMNPV *gp64* ORF plus a small amount of flanking sequence, and replacement with the *lacZ* cassette (Fig. 1). The resulting virus (*vAc*⁶⁴⁻), lacking the *gp64* gene and containing a *lacZ* cassette in the *gp64* locus, was confirmed by PCR and restriction enzyme analysis as described earlier (172). Following extensive passaging of *vAc*⁶⁴⁻ in Sf9^{Op1D} cells, we did not detect production of GP64 when Sf9 cells were subsequently infected with *vAc*⁶⁴⁻ (data not shown).

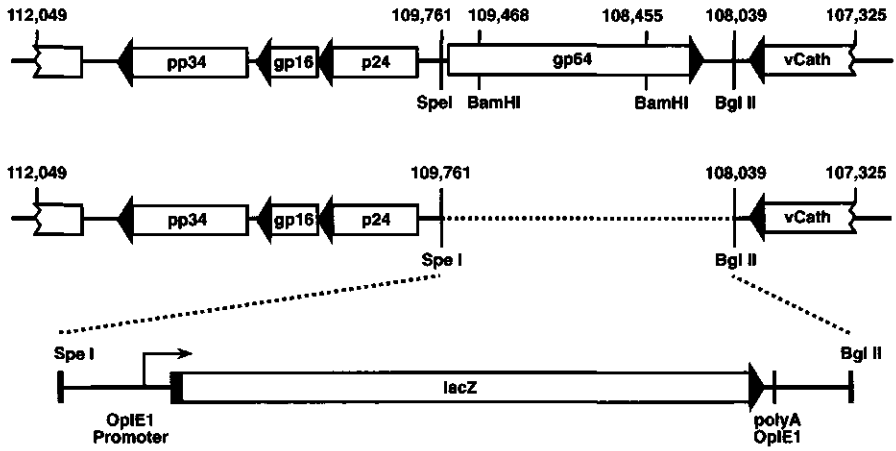
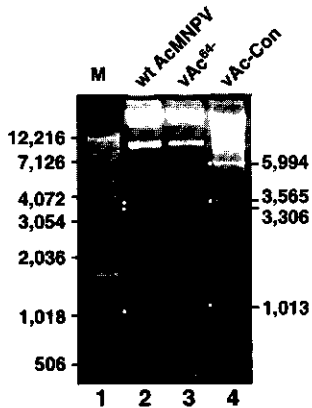
A**B**

FIG. 1. Construction and analysis of *vAc*⁶⁴⁻, a *gp64* null virus containing a complete deletion of the AcMNPV *gp64* ORF. **(A)** Construction of *gp64* null virus *vAc*⁶⁴⁻. The top line represents the 4718 bp *Eco*RI-*Sma*I fragment (corresponding to nt 107325 to 112049) from plasmid pAcEcoHΔSma. This fragment contains the AcMNPV *gp64* locus plus flanking genes (open arrows indicate AcMNPV ORFs). The *gp64* ORF was removed from pAcEcoHΔSma as a 1722 bp *Spe*I-*Bgl*II fragment (dashed horizontal line), and replaced with a 4195 bp cassette containing the *E. coli lacZ* ORF under the control of the OpMNPV IE1 early promoter (lower line). The resulting transfer vector as named pAcEcoHΔSmaSpe(*OptE1Z*+)Bgl and was used to generate *gp64* null virus *vAc*⁶⁴⁻ by cotransfection and homologous recombination with wild type AcMNPV E2 DNA in Sf9^{Opt1D} cells. *vAc*⁶⁴⁻ contains a discrete deletion of the AcMNPV *gp64* gene between nt 108,039 and 109,761, and replacement with the 4195 bp *lacZ* expression cassette. **(B)** Restriction enzyme analysis of genomic DNAs from wild type and recombinant baculoviruses. Lanes 2-4 compare *Bam*HI restriction enzyme profiles of genomic DNA's from wt AcMNPV E2 (Lane 2), *vAc*⁶⁴⁻ (Lane 3), and *vAc*-Con (Lane 4). The fragments containing portions of the GP64 ORF are indicated on the left of lane 2. Fragments containing the replacement *gp64* gene and GUS gene are indicated on the left of lane 4. Lane 1 contains a DNA ladder (M).

Studies of a previous gp64null virus (vAc^{64Z}) showed that the absence of GP64 expression resulted in a virus unable to move from cell to cell. However, the nature of the defect was not known. Possible explanations included: a) a defect in virion budding, or b) production of virions that were not infectious. To determine if GP64 was involved in BV budding or assembly, we used a biochemical approach to compare relative quantities of BV production in Sf9 cells infected with either wild type AcMNPV or the gp64null recombinant virus, vAc⁶⁴⁻. Since vAc⁶⁴⁻ is propagated in Sf9^{Op1D} cells, the virions carry OpMNPV GP64 in their envelope and are therefore infectious in cell culture. However, after infection of Sf9 cells, vAc⁶⁴⁻ is unable to produce GP64. As an internal control to confirm infection of Sf9 cells by each virus, cell extracts were examined by Western blot analysis, using a combination of anti-VP39 and anti-GP64 antibodies (Fig. 2, Lower panels, lanes W). Polyhedra formation in infected cells was also monitored (not shown) as a control for productive infection. As expected, the major

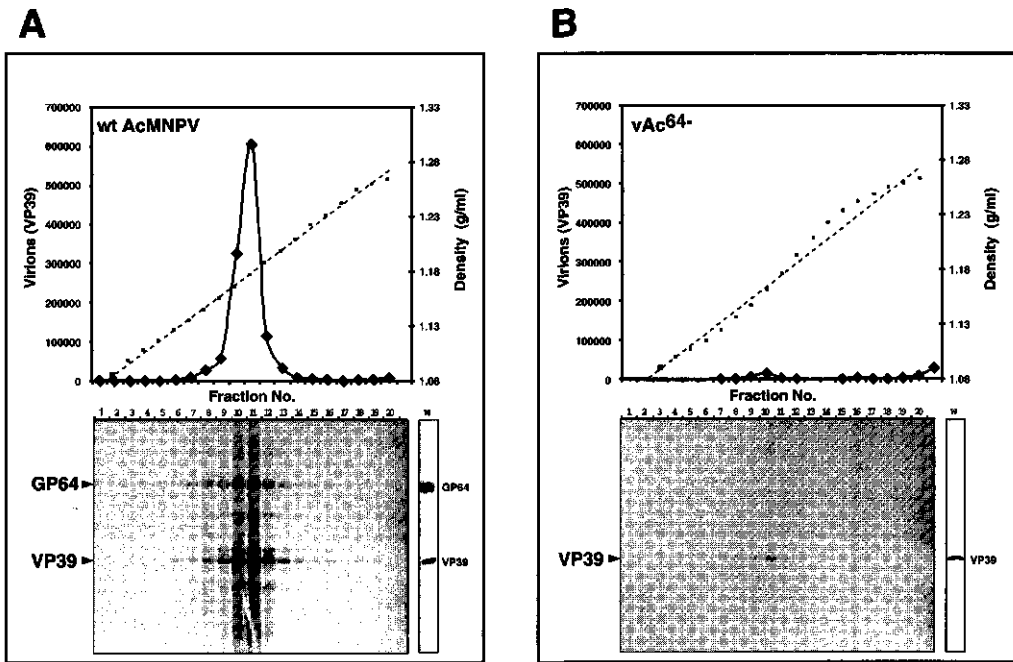
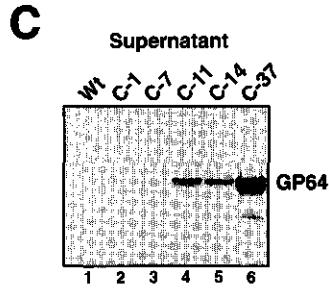
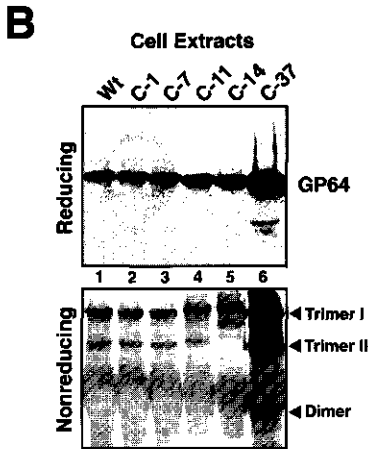
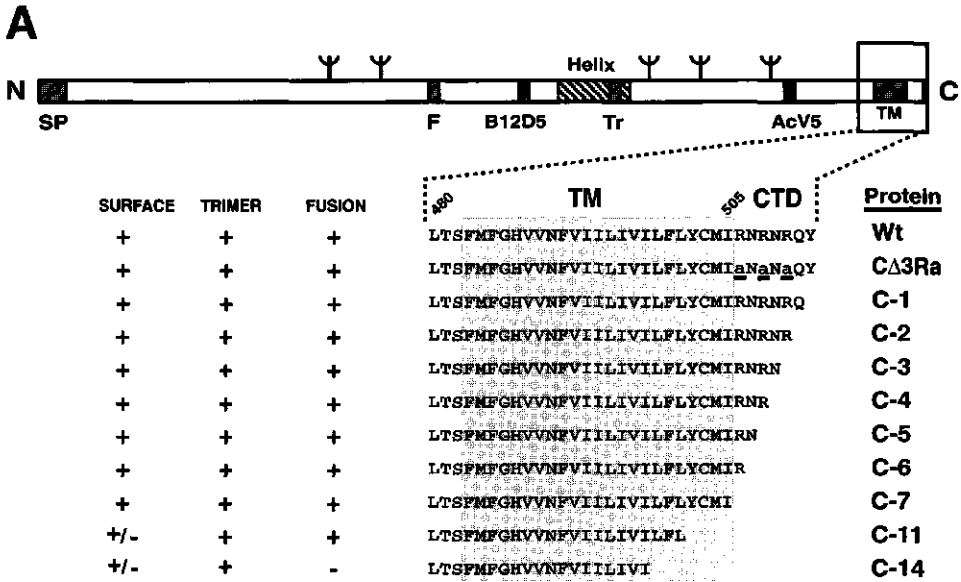


FIG. 2. Quantitative analysis of ³⁵S-methionine labeled BV production from wild type AcMNPV (A) and vAc⁶⁴⁻ (B) infected Sf9 cells. Sf9 cells infected with each virus were pulse labeled with ³⁵S-methionine from 16 to 30 h pi and labeled progeny virions were isolated from supernatants by purification through a sucrose cushion, followed by separation on equilibrium sucrose density gradients. Gradients were fractionated and the density of each gradient fraction was measured. Equal amounts of gradient fractions were analyzed by electrophoresis on SDS-PAGE gels and proteins were quantified by phosphorimager analysis (bottom panels, left). To confirm infection in each experiment, infected cell extracts were examined by Western blot analysis using anti-GP64 and anti-VP39 antibodies (lane W). In each panel (A and B) the top panels show the measured density (g/ml, dashed line) and the relative quantity of VP39 (solid line, determined by phosphorimager analysis) in each fraction.

capsid protein, VP39, was detected from cells infected with both viruses, and GP64 was not detected from Sf9 cells infected with vAc⁶⁴, confirming the GP64null virus phenotype. Because the antibody used for these experiments cross reacts with OpMNPV GP64, these data also show that we could not detect any remaining OpMNPV GP64 from the inoculum.

To distinguish between the virions used to infect cells and potential progeny virions, infected Sf9 cells were pulse labeled with ³⁵S-methionine from 16 to 30 h post infection (p.i.) and supplemented with unlabeled methionine as a chase at 22 h p.i.. Supernatants harvested at 30 h p.i. were used for virion isolation, fractionation, and quantitative analysis. Virions present in supernatants from cells infected with wild type AcMNPV or vAc⁶⁴ were pelleted through a 25% sucrose cushion, resuspended, then layered onto a linear 25-60% sucrose gradient and centrifuged to equilibrium. Equal fractions were collected from the gradient, the densities were measured, and proteins were analyzed on SDS-PAGE gels. Relative quantities of labeled virion proteins in each fraction were determined by phosphorimager analysis, using the characteristic polypeptide profile to identify virion fractions. The VP39 capsid protein in virion fractions was used as an internal indicator of the relative number of virions. Figure 2 shows the results of this analysis. Virion fractions isolated from the supernatants of Sf9 cells infected with wild type AcMNPV were identified by the presence of GP64 and VP39 in standard virion profiles (Fig. 2A; fractions 8-13). Wild type AcMNPV virions were identified at a peak density of approximately 1.18 g/ml. Although abundant virion production was detected from wild type AcMNPV, only trace amounts of the VP39 protein were detected at similar densities when supernatants from vAc⁶⁴ infected Sf9 cells were similarly analyzed (Fig. 2B, fractions 9-11). Long exposures of the gel in the lower panel of Figure 2B showed that other virion proteins were also present in fractions

FIG. 3. Construction and analysis of plasmid constructs expressing GP64 proteins with truncations or substitutions in the cytoplasmic tail domain (CTD) and the transmembrane (TM) domain. **(A)** A schematic representation of the GP64 protein shows the locations of the signal peptide (SP), fusion domain (F), B12D5 and AcV5 epitopes, trimerization domain (TR), transmembrane domain (TM), and cytoplasmic tail domain (CTD). The various deletions and substitutions in the CTD and TM domain used in this study, and their names, are indicated. The indicated constructs were generated in plasmids, examined in transient expression assays, and used to generate recombinant viruses (see Fig. 5). A summary of the properties of each GP64 construct is shown on the left of each construct (see Fig. 5). **(B)** Expression and trimerization of representative GP64 constructs. Sf9 cells were transfected with plasmids expressing either wild type GP64 (Wt) or modified GP64 (C-1, C-7, C-11, C-14, and C-37), and expression and trimerization of GP64 were examined by Western blot analysis of cell extracts on reducing SDS-PAGE (top panel) or non-reducing SDS-PAGE (bottom panel). The positions of GP64 and oligomeric forms (Trimer, Dimer, Monomer) are indicated on the right. **(C)** Detection of modified GP64 proteins from the supernatants of Sf9 cells transfected with plasmids expressing either wild type GP64 (Wt) or modified GP64 (C-1, C-7, C-11, C-14, and C-37). Supernatants were collected from transfected Sf9 cells examined in panel B, and GP64 was immunoprecipitated using an anti-GP64sol antiserum. Plasmid pΔCia-C-37, which expresses a secreted soluble form of AcMNPV GP64 (C-37), was used as a positive control for secretion. All constructs were expressed from the wild type AcMNPV GP64 early promoter, except C-37 in plasmid pΔCia-C-37, which contains a truncated early promoter.



9-11 (not shown) confirming that the VP39 detected in these fractions resulted from BV. As expected, no labeled GP64 was detected from these progeny virions as the *gp64* gene was deleted from vAc⁶⁴⁻ (Fig. 2B). Quantitative measurements of VP39 in all virion-containing fractions indicated that virion production from the vAc⁶⁴⁻ virus was approximately 2 % of that detected from wild type AcMNPV. This dramatic reduction in virion production in the absence of GP64 indicates that GP64 is necessary for efficient virion budding. However, the detection of small quantities of labeled VP39 in virion fractions from vAc⁶⁴⁻ supernatants also indicates that a very low level of budding occurred even in the absence of GP64.

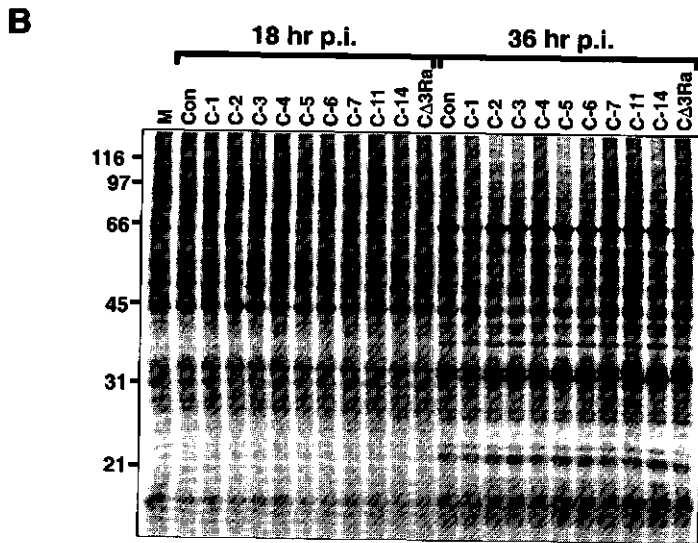
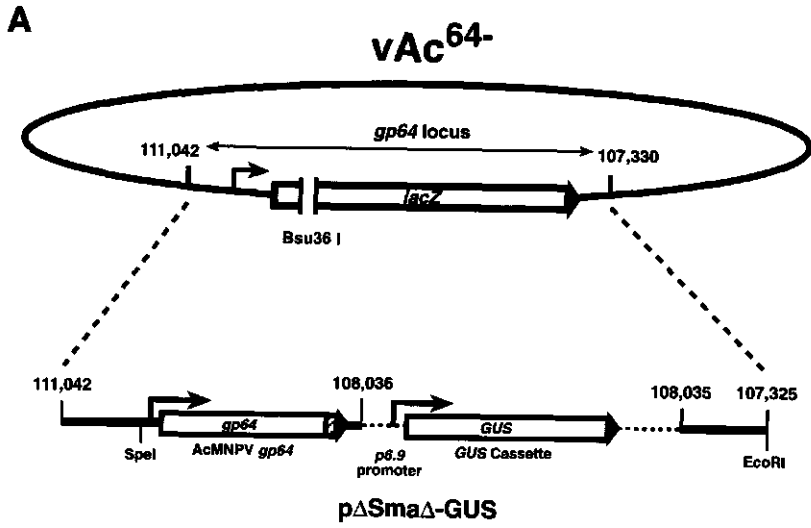
Construction and analysis of GP64 CTD mutations. The predicted structure of the AcMNPV GP64 protein includes a 20 amino acid hydrophobic N-terminal signal peptide (SP), a large ectodomain of 459 amino acids (present on the cell or virion surface), a hydrophobic transmembrane (TM) domain of 23 residues, and a short hydrophilic cytoplasmic tail domain (CTD) of 7 amino acids (Fig. 3A). By convention, the TM and CTD are defined as follows: the TM is defined as the highly hydrophobic domain near the C-terminus, and the CTD is defined as the hydrophilic domain which begins with the first charged residue following the hydrophobic TM domain. Because the cytoplasmic tail of GP64 is the only domain thought to be in direct contact with the cytoplasm, and was considered most likely to interact with other viral or cellular proteins during budding, we examined the functional role of the predicted 7 amino acid AcMNPV GP64 CTD. To examine the function of the AcMNPV GP64 CTD, we generated a series of constructs in which amino acid residues were sequentially deleted from the C-terminus, with deletions extending through the CTD and into the predicted TM domain (Fig. 3A, C-1 to C-14). For constructs designated C-1 through C-37, numbers represent the number of amino acids removed from the C-terminus of AcMNPV GP64. To examine the potential role of a cluster of basic residues within the CTD, we also generated a construct in which each of the 3 arginine residues was replaced with alanine (Fig. 3A, CA3Ra).

Because previous studies showed that a number of GP64 ectodomain modifications resulted in unstable proteins, representative constructs containing CTD and TM mutations were initially examined by transient expression in transfected cells. Expression and trimerization of mutant constructs were compared to that of wild type GP64 (Fig. 3B; wt vs C-1, C-7, C-11, C-14). The two characteristic trimeric forms (Trimer I and II) were identified in the extract of cells transfected with each construct (Fig. 3B, bottom panels) when examined under non-reducing conditions. All constructs except C-37 were transiently expressed under the control of the wild type AcMNPV *gp64* early promoter region. Control construct (C-37), which contains a complete deletion of the CTD and TM, was expressed from a truncated promoter and was expressed in higher quantities. Because deletions of the CTD and portions of the predicted TM domain might affect protein anchoring, supernatants from transfected cells were also examined for the presence of GP64 that may be shed from the cell surface. Control construct C-37

contains a deletion of the complete CTD and TM and therefore represents a secreted soluble form of GP64 and served as a positive control for secretion or shedding. Supernatants from transfected cells were collected at 48 h post transfection and GP64 was immunoprecipitated with an anti-GP64sol polyclonal antiserum. The wt, C-1, and C-7 GP64 proteins were detected in abundance in cell extracts (Fig. 3B, lanes 1-3), and in only trace amounts from supernatants (Fig. 3C, lanes 1-3). In contrast, the GP64 C-11 and C-14 proteins were detected in the supernatants of transfected cells at much higher levels than wt, C-1 or C-7 proteins, suggesting that C-11 and C-14 were shed from the cell surface (Fig. 3C, lanes 4-5). Thus, initial analyses of AcMNPV GP64 with CTD and TM truncations showed that the modified proteins were expressed and trimerized in a manner similar to wild type GP64, and that truncations into the TM domain resulted in less stable anchoring in the membrane.

Construction of recombinant viruses with GP64 CTD mutations. To generate recombinant AcMNPV viruses in which modified forms of *gp64* replaced the wild type *gp64* gene, viral DNA derived from the *gp64*null virus vAc⁶⁴ was cotransfected into Sf9 or Sf9^{Op1D} cells with transfer vectors containing the modified *gp64* genes and sequences flanking the *gp64* locus. A wild type *gp64* gene was also included for parallel construction of a control virus. Each transfer vector also contained a GUS marker gene under the control of the AcMNPV p6.9 promoter, inserted downstream of the *gp64* gene (Fig. 4A). Because the *gp64*null virus contains a *lacZ* gene in the *gp64* locus, double recombination events resulted in viruses in which the *lacZ* gene was replaced with the modified *gp64* gene and GUS gene, and exhibiting a *lacZ*/GUS⁺ phenotype. Virus isolates were identified and plaque purified based on this phenotype and were subsequently examined by PCR analysis, restriction enzyme profiles of genomic DNA's (Fig. 1, lane 4), and sequencing to confirm correct insertion of the wild type or modified *gp64* gene. Sf9 cells were used to generate viruses containing all constructs shown in Figure 3A, except the C-14 construct. This construct apparently did not produce infectious virions in sufficient quantities to sustain a multiple-round plaque purification procedure. Therefore, Sf9^{Op1D} cells (a line that constitutively expresses wild type OpMNPV GP64) were used for generation and propagation of the vAc-C-14 virus.

To confirm that the infection cycle proceeded normally in each of the recombinant viruses, viral infections were analyzed by pulse labeling. Sf9 cells were infected with each virus at an m.o.i. of 10, then pulse labeled with ³⁵S-Methionine for 1.5 hours preceding the indicated times (Fig. 4B, 18 and 36 h p.i.). Cell lysates were then examined for the presence and relative intensities of infected cell specific proteins (ICSPs). Profiles of ICSPs from viruses carrying modified *gp64* genes were similar to those from a control virus (Fig. 4B, lanes Con) in which the wild type *gp64* gene was inserted in the same manner as modified *gp64* constructs (Fig. 4A).



Analysis of mutant GP64 proteins in recombinant viruses. The expression, localization, and function of wild type and modified GP64 proteins were examined in infected Sf9 cells. To compare relative quantities of each GP64 protein construct at the cell surface, Sf9 cells infected with each recombinant virus were examined by cell surface ELISA (CELISA) using an anti-GP64 Mab, AcV5. Data from CELISA at 30 h p.i. are shown in Figure 5A. GP64 levels at the surface of cells infected with viruses expressing constructs C-1 through C-7 and CΔ3Ra were similar to that of wild type GP64 from either a control virus (Con) or wild type AcMNPV. The surface levels of GP64 among these constructs ranged from approximately 80 - 130% of that observed from wild type GP64 in the control virus, vAc-Con. In contrast, the C-11 and C-14 proteins were detected at substantially lower levels, approximately 19 and 24%, respectively, relative to the level of wild type GP64 from the control virus. This is consistent with the earlier data demonstrating increased levels of GP64 in the supernatants of transfected cells expressing the C-11 and C-14 (Fig. 3C). Thus, CELISA and immunoprecipitation data indicate that the C-11 and C-14 truncations affected anchoring of these protein constructs to the cell membrane.

To confirm that truncated and modified GP64 proteins were trimerized in Sf9 cells infected with recombinant viruses, infected cell extracts were examined under reducing and non-reducing conditions (Fig. 5B). Previous studies showed that trimer forms I and II both represent homotrimeric forms of GP64 (184) although the physical differences that result in different electrophoretic mobilities are not understood. All constructs were detected from infected cells at levels similar to those observed in the control virus expressing wild type GP64 and all constructs were trimerized (Fig. 5B, right panel). We also asked whether low pH triggered membrane fusion was affected by the C-terminal truncations or substitutions. Sf9 cells were infected with each of the recombinant viruses, then assayed at 36 h p.i. for membrane fusion activity using a

FIG. 4. Construction and analysis of recombinant AcMNPV viruses expressing modified forms of the GP64 protein and GUS. (A) To generate recombinant AcMNPV viruses expressing modified GP64 proteins, gp64null virus DNA (vAc⁶⁴, shown as a circle; not drawn to scale) was linearized with unique site Bsu36I (located in the lacZ ORF), and cotransfected with transfer vectors containing inserts as indicated below. Each transfer vector contained an AcMNPV gp64 gene with modifications of the cytoplasmic tail domain (CTD) and/or transmembrane (TM) domain, a GUS gene cassette containing the GUS gene under the control of the AcMNPV p6.9 promoter, and flanking sequences for recombination into the gp64 locus (nt 107,325 to 111,042). Dashed lines represent the boundaries of the area exchanged between vAc⁶⁴ and transfer vector pΔSmaΔ-GUS by double homologous recombination. This results in replacement of the lacZ cassette of vAc⁶⁴ with the modified gp64 and GUS marker gene. Sequences in the transfer vector derived from the gp64 locus of the AcMNPV genome are represented as a solid line whereas sequences associated with the GUS cassette are represented by a dashed line. Numbers indicated above the sequence represent the standard nomenclature for AcMNPV (2). (B) Pulse labeling of proteins from Sf9 cells infected with viruses expressing wild type or modified forms of GP64. Cells were infected (m.o.i. 10) and labeled with ³⁵S-methionine at 18 and 36 h p.i. Extracts from infected cells were electrophoresed on SDS-PAGE gels and examined by phosphorimager analysis. (M, mock infection; Con, Control virus vAc-Con; C-1 to CΔ3Ra, recombinant viruses expressing modified forms of GP64).

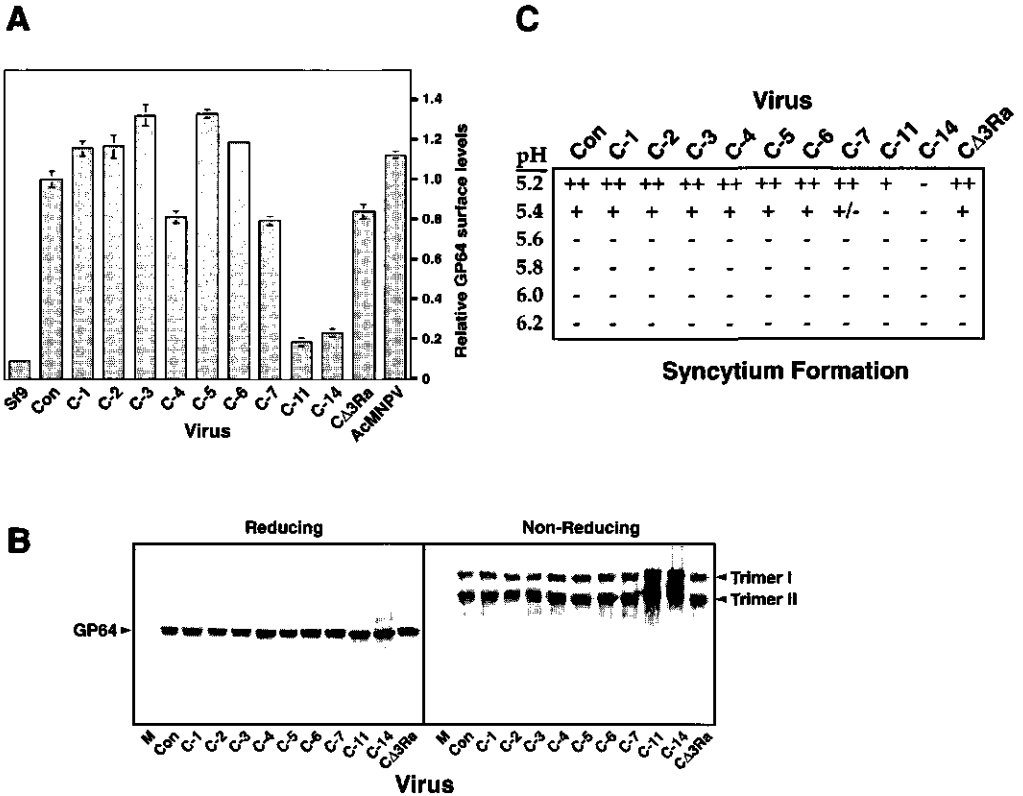


FIG. 5. Expression and functional analysis of wild type and modified forms of GP64 in infected Sf9 cells. **(A)** Quantitation of GP64 on the cell surface of Sf9 cells infected with recombinant viruses expressing modified forms of GP64 (C-1 to C-14, and CΔ3Ra) at 30 h p.i. by CELISA. The background CELISA signal from uninfected Sf9 cells is indicated on the left (Sf9); Positive controls are a control virus that expresses the wild type GP64 protein (Con) and wt AcMNPV. **(B)** Expression and trimerization of modified forms of GP64 in Sf9 cells infected with the recombinant viruses listed in A. Western blots of cell extracts (48 h pi) electrophoresed under reducing (left) and non-reducing (right) conditions, and detected with Mab AcV5. **(C)** Syncytium formation assays with recombinant viruses listed in A. Sf9 cells were infected at m.o.i. 10. At 36 h pi, medium was removed and replaced for 5 minutes with PBS adjusted to a range of pH values from 5.2 to 6.2, then fresh medium was added and incubated for 2 h prior to scoring for syncytium formation. Syncytium formation requires ≥ 5 nuclei in each syncytial mass. (++) syncytia abundant; + syncytia present but not abundant; +/- syncytia rare but present; - no syncytia observed.)

syncytium formation assay. Triggering of fusion was examined over a range of pH values (Fig. 5C). The pH required to trigger membrane fusion activity in the syncytium formation assays was between 5.4 and 5.6 and was similar for constructs C-1 through C-7 and the wt GP64 protein (Con). Interestingly, membrane fusion activity was detected from construct C-11 only at pH 5.2 and no activity was detected from construct

C-14. While this effect may be partially explained by lower levels of C-11 and C-14 at the cell surface (Fig. 5A), the levels of cell surface GP64 C-11 and C-14 were similar in CELISA experiments that were performed in parallel (Fig. 5A,C). Thus, the truncation of additional amino acids in the TM domain in construct C-14 may specifically affect the ability of the protein to mediate fusion. Further studies will be necessary to confirm this preliminary result.

Effects of CTD mutations on infectious BV production. The GP64 protein is necessary for virion entry into host cells by receptor-mediated endocytosis, and studies of a GP64 deletion virus showed that GP64 was important for efficient virion budding. To study the role of the cytoplasmic tail domain (CTD) on production of infectious progeny virus, we examined yields of infectious virions from cells infected with virus constructs containing the truncated or modified GP64 CTDs described above. Except for virus vAc-C-14 (which was propagated in Sf9^{Op1D} cells) relatively high levels of virus production were observed from all other constructs, even when the CTD was truncated by 11 amino acids (Fig. 6A). These data provided an initial but clear indication that the GP64 CTD was not essential for viral propagation in cell culture. To examine potential differences in virion production in more detail, we generated viral growth curves for selected viruses (vAc-Con, vAc-C-7, vAc-C-11, and vAc-CΔ3Ra). For these studies, BV production was measured during 6 hour periods throughout the course of infection. Sf9 cells were infected with each virus (m.o.i. 10) and cells were washed 6 hours prior to each indicated time point and fresh medium was added. Supernatants containing infectious virions that accumulated in the supernatant (during the subsequent 6 hour period) were collected and infectious BV quantified by TCID₅₀ assay. BV production curves were similar for viruses vAc-Con, and vAc-CΔ3Ra (Fig. 6B). The production of infectious BV from vAc-C-7 infected cells was also high but was lower than the control virus (vAc-Con). Significantly lower titers were recorded from vAc-C-7 at a number of time points (18, 36, 48, and 60 h p.i.). Thus, growth curve data suggested that production of infectious BV from vAc-C-7 was slightly reduced from that of the control virus that expresses a wild type GP64 protein. Production of infectious BV from virus vAc-C-11 was further reduced and was consistently 78 to 96% lower than that measured from the control virus (vAc-Con) at 18-60 h p.i. (Fig. 6B). These reductions in yield of infectious BV are correlated with the deletions from the C-terminus of GP64, and the lower levels of the C-11 construct detected at the surface of vAc-C-11 infected Sf9 cells (Fig. 5A).

Biochemical analysis of virion production. The reduction in virus titers from cells infected with vAcC-7, vAcC-11, and vAc-C-14 could result from either a) normal production of virion particles but reduced infectivity per virion; or b) a reduction in the quantity of virions budded from the cell surface. To determine if the observed effects of GP64 truncations C-7, C-11, and C-14 were due to a reduction in the quantity of progeny virions, we pulse labeled infected cells, then purified and measured the

A

Virus	Titre	Cells
vAc-Con	5.58×10^8	Sf9
vAc-C-1	4.97×10^8	Sf9
vAc-C-2	2.69×10^8	Sf9
vAc-C-3	2.86×10^8	Sf9
vAc-C-4	8.29×10^8	Sf9
vAc-C-5	1.93×10^8	Sf9
vAc-C-6	3.64×10^8	Sf9
vAc-C-7	1.93×10^8	Sf9
vAc-C-11	1.59×10^8	Sf9
vAc-C-14	3.20×10^7	Sf9 ^{Op1D}
vAc-CΔ3Ra	4.97×10^8	Sf9

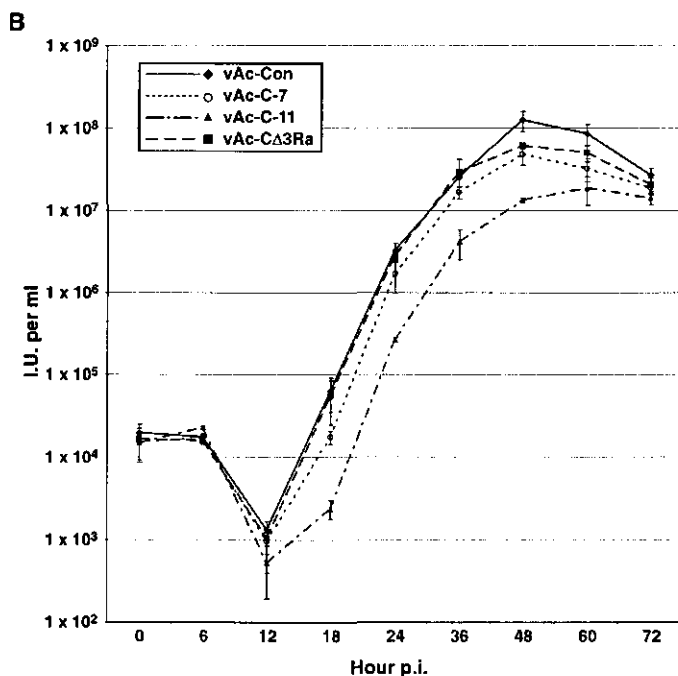


FIG. 6. Production of infectious virions by recombinant viruses expressing wild type or C-terminally modified forms of GP64. **(A)** Comparison of virus stock titers. All viruses except vAc-C-14 were titrated in Sf9 cells. Virus vAc-C-14 was titrated in Sf9^{Op1D} cells which constitutively express OpMNPV GP64. **(B)** Comparison of virus growth curves for selected recombinant viruses with C-terminal modifications. Viruses expressed either a wt GP64 (vAc-Con), a complete deletion of the GP64 CTD (vAc-C-7), a deletion of the complete CTD plus 4 amino acids of the TM domain (vAc-C-11), or substitutions of all three arginines within the CTD with alanine (vAc-CΔ3Ra). Each data point represents virion production in the preceding 6 hour period. Data points represent triplicate infections and titrations and error bars represent standard deviation from the mean.

relative quantities of labeled virions that accumulated in cell culture supernatants as described earlier (see also Materials and Methods). The control virus (vAc-Con) used for these studies was generated in parallel with other GP64 replacement viruses, and

contains a *GUS* marker gene and a wild type *gp64* gene inserted into the *gp64* locus. Infection and the expression of the GP64 construct from each recombinant virus was confirmed by western blot analysis of infected cell supernatants (Fig. 7; lower panels, lanes W). As before, VP39 in virion fractions was used as an indicator of relative virion quantity. Phosphorimager analysis and comparisons of virion fractions from vAc-C-7 and vAc-Con infected cells indicated that vAc-C-7 virion production was approximately 53% of that detected from vAc-Con (Fig. 7A,B). These findings parallel the data from growth curves where a small but notable reduction in infectious virus yield was measured for virus vAc-C-7 (Fig. 6B). This indicates that the 7 amino acid GP64 CTD plays a significant role in virion production, although relatively high titers of infectious virions are still produced in its absence (Fig. 6B, vAc-C-7). A more substantial reduction in infectious BV production was observed from growth curve data for virus vAc-C-11, which expresses a more severely truncated GP64 protein. Biochemical analysis of BV production (Fig. 7C) showed that vAc-C-11 produced only approximately 8-9% of the BV generated from the control virus that expresses wild type GP64 (Fig. 7C vs. 7A). Thus, the measured reduction by quantitative analysis of virion proteins (91-92%) closely parallels the reduction in infectious BV observed from growth curves (78-96%).

We also examined potential virion production from vAc-C-14 which expressed a C-terminal truncation of 14 amino acids. In our studies, insertion of this GP64 mutant into the AcMNPV genome was not sufficient for propagation of a recombinant virus in Sf9 cells (vAc-C-14 was generated and propagated in Sf9^{Op1D} cells). Analysis of virions prepared from supernatants from vAc-C-14 infected Sf9 cells resulted in detection of only trace quantities of BV, approximately 2% of that detected from the control virus, vAc-Con (Fig. 7D vs. 7A). These data were similar to earlier results from the *gp64*null virus which contained a complete deletion of GP64 (Fig. 2). Long exposures of gels containing virion fractions from vAc-C-14 revealed that these virions contained the mutant C-14 GP64 protein, albeit in very low quantities.

Effects of GP64 mutations on GP64 incorporation into BV. In addition to the effects of GP64 and the GP64 CTD on virion production, we also analyzed the effects of the CTD and TM truncations on the incorporation of GP64 into virions. As a measure of the concentration of GP64 in each virion, we examined the ratio of GP64 to the major capsid protein, VP39, in virion fractions (Fig. 7; Table 1). The ratio of GP64:VP39 in the peak fraction of the control virus (vAc-Con; Fig. 7, fraction 12) that expresses the wild type GP64 protein was 0.762 (Table 1). Comparison of this ratio to that from the peak BV fractions from viruses vAc-C-7, vAc-C-11, and vAc-C-14 indicated that the GP64:VP39 ratio was substantially lower for each of the viruses containing C-terminal truncations (Table 1, column 3). When data from all fractions containing BV were similarly analyzed, similar results were obtained (Table 1, column 4). Because the mature GP64 protein and the VP39 protein contain different numbers of methionine residues (16 and 9 residues, respectively), and the amount of incorporated label is proportional to the number of methionine residues, protein labeling data were adjusted

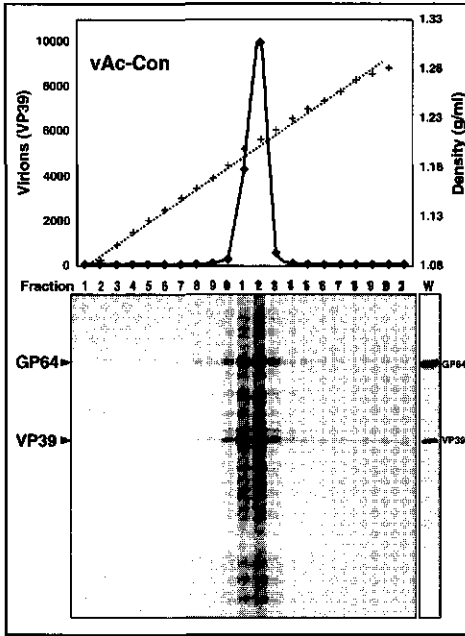
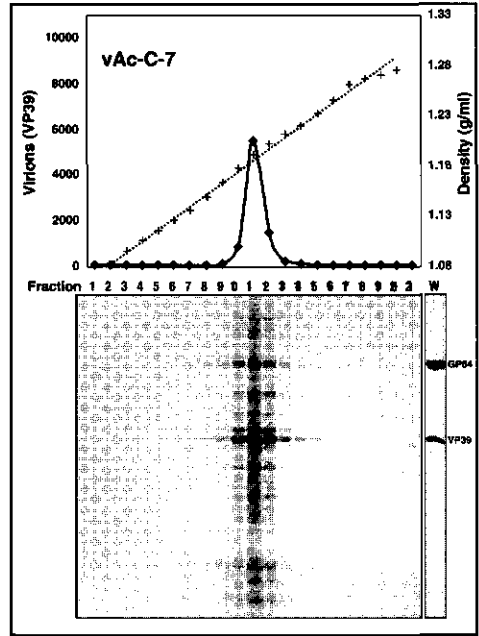
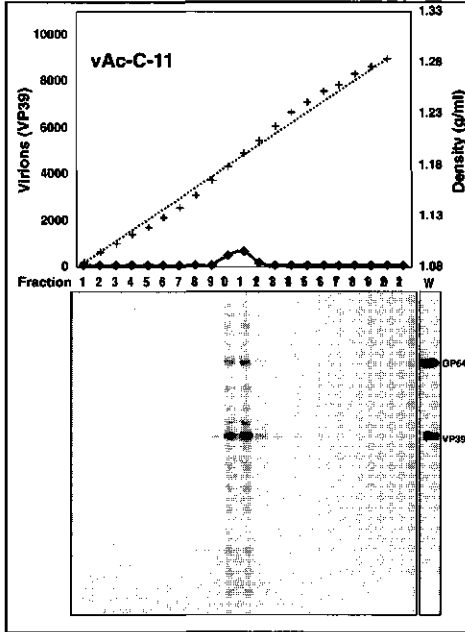
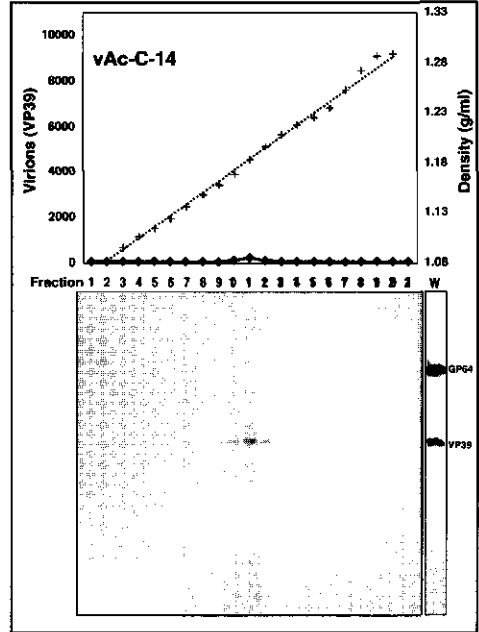
A**B****C****D**

FIG. 7. Quantitative analysis of ³⁵S-methionine labeled progeny BV production from recombinant baculoviruses expressing wild type (vAc-Con) or C-terminal truncations of GP64 (vAc-C-7, vAc-C-11, vAc-C-14). Sf9 cells infected with each virus were pulse labeled with ³⁵S-methionine from 15 to 40 h p.i. and labeled progeny virions were isolated from supernatants by centrifugation through a sucrose cushion, followed by separation on equilibrium sucrose density gradients, and fractionation. Gradients were fractionated and the density of each gradient fraction was measured. Equal amounts of gradient fractions were analyzed by electrophoresis on SDS-PAGE gels and proteins were quantified by phosphorimager analysis (bottom panels, left). To confirm infection in each experiment, infected cell extracts were examined by Western blot analysis using anti-GP64 and anti-VP39 antibodies (lane W). In each panel (A, B, C, and D) the top panels show the measured density (g/ml; dashed line) and the relative quantity of VP39 (solid line, determined by phosphorimager analysis) in each fraction.

to represent relative molar quantities of the two proteins (Table 1, column 5). In all cases, truncation of the GP64 CTD resulted in a reduction (50-63%) in the concentration of GP64 in virions. In the case of C-11 and C-14, reduced quantities of GP64 on the cell surface may account for this difference since cell surface levels of GP64 were reduced by approximately 81 and 76% respectively (Fig. 5A). However, in the case of the C-7 protein, cell surface GP64 levels were similar to that from wt GP64 (Fig. 5A), yet the GP64 concentration in the virion was decreased by approximately 63%. Thus, the absence of C-terminal residues and not reduced cell surface levels, appear to result in

Table 1

Virus	Percent Budding	GP64:VP39 Ratio		
		Peak Virion Fraction	All Virion Fractions	Molar Ratios
vAc-Con	100.0%	0.762	0.684	0.129
vAc-C-7	52.5%	0.233	0.255	0.048
vAc-C-11	8.6%	0.233	0.354	0.068
vAc-C-14	1.4%	0.256	0.256	0.051

Percent Budding represents a comparison of the ³⁵S-Met labeled VP39 capsid protein present in virion fractions from each virus construct (Fig. 7). GP64:VP39 ratios were calculated from phosphorimager data (GP64 and VP39 bands) from either the "Peak Virion Fraction" or "All Virion Fractions" for each virus. Molar ratios of GP64:VP39 were calculated for virions of each virus (using data from All Virion Fractions) based on 16 methionine residues (mature wtGP64), 15 methionine residues (constructs vAc-C-11 and vAc-C-14), or 9 methionine residues (VP39).

a reduction in the concentration of GP64 in the virions of vAc-C-7. Together, these data suggest that the CTD influences the incorporation of GP64 into the virion, but is not essential for GP64 incorporation.

	TM	CTD
OpMNPV-	GGHTTSLSDIADMAK	GELNATLYSFMFLGHGFTFVLIVGVILFLVCM
CfMNPV-	GGHTTSLSDITDMAK	GELNAKLWSEFMLGHAFSFLMTVGVIIFLPCMV
AcMNPV-	GGVGTSLSDITSMAE	GELAAKLTSFMFGHVNFVILIVILFLYCM
BmNPV -	GGVGTSLNDITSMAE	GELAAKLTSFMFGHVATFVIVFIVILFLYCM
DHO-	GGKGTSLIEDVLYG	PSCWINGKLQQLLNCAISWVVVIGVVLVGVCLM

FIG. 8. Alignment of the C-terminal regions of baculovirus GP64 proteins and Dhori virus GP75 of the Orthomyxoviridae. The hydrophobic predicted transmembrane (TM) domain of each protein is indicated by the box and the cytoplasmic tail domains are aligned to demonstrate the conservation of charged arginine residues and prevalence of the terminal tyrosine residue in baculovirus proteins. (CfMNPV, *Choristoneura fumiferama* MNPV; BmNPV, *Bombyx mori* NPV; DHO, Dhori virus).

Discussion

Using recombinant AcMNPV baculoviruses containing either a deletion of the *gp64* gene, or modified forms of *gp64*, we examined the role of the GP64 protein in virion budding. By labeling and quantifying progeny virions from cells infected with either wild type AcMNPV or a *gp64*null virus, we showed that GP64 is necessary for efficient production of BV. Therefore, the previously observed defect in cell-to-cell transmission in a *gp64*null virus (172) is caused primarily by a defect in virus budding. In the current study, we detected only very low quantities of BV in the absence of the *gp64* gene, and this result may be explained by one of two possible mechanisms. One possibility is that GP64 is not absolutely required for budding and a low level of budding may occur in the absence of GP64. A second possible explanation is that GP64 is essential for budding and the low level of progeny BV observed in these experiments results from recycling of GP64 present on infecting *gp64*null virus particles of the inoculum. Because we were unable to detect recycled GP64 (by Western blots), we currently favor the former explanation. It is not known whether GP64 is recycled or whether it is degraded after virion disassembly during entry. Our observation that the major AcMNPV BV envelope protein is required for efficient budding is similar to results from recent studies of the rhabdovirus G protein. In those studies, virion budding by VSV and Rabies viruses was reduced approximately 30 fold in the absence of G-protein (163, 223).

In several cases, it has been proposed that virion budding is driven by interactions between the cytoplasmic domains of viral envelope proteins and capsid or matrix proteins. We therefore examined the role and function of the GP64 cytoplasmic tail domain (CTD) in this process. The predicted CTD of the AcMNPV GP64 protein

consists of only 7 amino acids. In comparison, the predicted CTDs of membrane proteins such as Influenza HA and NA, VSV G-protein, and human CD4 are 10 and 6, 29, and 38 amino acids in length, respectively. The small size of the GP64 CTD may be an important characteristic since the small size (7-8 amino acids) is conserved in GP64 proteins identified from *Bombyx mori* NPV (BmNPV), *Choristoneura fumiferama* MNPV (CfMNPV), and OpMNPV (Fig. 8). In addition, the closely related GP75 protein from an arthropod vectored orthomyxovirus (Dhori virus) contains a predicted CTD of only 4 amino acids. In each of these proteins (baculovirus and Dhori virus), the very short CTD contains 2-3 arginine residues which confer a basic charge on the CTD. To examine the role of the AcMNPV GP64 CTD, we generated alanine substitutions for the 3 arginine residues in the CTD, and generated a series of sequential deletions through the CTD and into the TM domain. An initial concern was that the modified GP64 constructs might be unstable. In a previous study, a number of GP64 constructs containing insertions and deletions in the AcMNPV and OpMNPV GP64 ectodomain were analyzed and in many cases, changes in the internal spacing of the ectodomain rendered the protein unstable (171). In the current study, representative GP64 mutants were examined using assays for transport, anchoring, and membrane fusion. We observed no significant differences in expression or stability of GP64 constructs containing deletions or substitutions of the CTD and TM, when compared with wild type GP64 (Fig. 3 and 5). Studies of protein transport and accumulation at the cell surface, and membrane fusion identified no apparent effect of the three arginine to alanine substitutions (C Δ 3Ra) or the deletions of the CTD (C-1 to C-7). Because previous studies have shown that deletions or modifications of the Influenza HA CTD can result in modified membrane fusion activity (164, 180), we therefore asked whether the AcMNPV GP64 CTD mutations affected triggering of membrane fusion by low pH. No apparent changes were observed for GP64 constructs that were present on the cell surface at or near wild type levels (C-1 to C-7 and C Δ 3Ra). Because we examined only the pH requirement for triggering, we cannot exclude the possibility that the kinetics or magnitude of GP64 mediated pore formation may be affected by changes in the CTD. Whether the GP64 CTD plays a role in fusion pore formation after triggering remains unknown and awaits further more detailed analyses of these constructs. Anchoring of GP64 to the cell membrane did not appear to be substantially affected by the deletion of the 7 amino acid CTD or by alanine substitutions for three arginine residues in the CTD, as little GP64 was detected in the supernatants of cells transfected with plasmids expressing those constructs. In contrast, cells transfected with constructs C-11 and C-14, which contain deletions of the 7 amino acid CTD plus removal of 4 or 7 additional amino acids from the predicted TM domain, had significantly lower levels of cell surface GP64 (Fig. 3A, C-11 and C-14), and increased levels of GP64 in the supernatants (Fig. 3B; C-11 and C-14). These data support the predicted locations of the boundaries of the TM and CTD. Relatively short deletions into the predicted TM domain (C-11) resulted in rather dramatic effects on anchoring of the protein in the membrane. Thus, these data show that the region

immediately upstream of amino acid 506 clearly serves as an anchoring domain for the GP64 protein.

We next examined the effects of these C-terminally modified GP64 proteins in the context of viral infection. To accomplish this, we retained wild type AcMNPV *gp64* transcriptional and translational regulatory control for mutant GP64 constructs, and used a *gp64*null virus to insert genes encoding these modified GP64 proteins into the *gp64* locus of the AcMNPV genome (Fig. 4). To examine the ability of modified GP64 constructs to facilitate virion assembly and budding, we analyzed the recombinant baculoviruses for production of infectious virions in growth curve experiments (Fig. 6), and by quantitative analysis of labeled BV production (Fig. 7). The virus carrying the three arginine-to-alanine substitutions in the GP64 CTD (vAc-C Δ 3Ra) showed no detectable change in production of infectious virions in growth curve experiments. Virion production was however, affected when the entire CTD was removed. Separate assays for infectious virions and labeled progeny virions both showed an approximately 50% decrease in virion production in the absence of the GP64 CTD (Fig. 6,7; vAc-C-7). These data indicate that the CTD is important for efficient virus budding, but not indispensable. Similar studies have examined the roles of CTDs from the Influenza virus HA and NA proteins, and the VSV G protein. Deletion of the CTD of either HA or NA does not cause substantial effects on budding and assembly, although altered morphology of virions was observed when the NA CTD was deleted (116, 118, 170). An Influenza virus in which the CTDs were deleted from both the HA and NA proteins, resulted in altered particle morphology, and budding was substantially reduced but remained at approximately 10% of wild type virus (117). Deletion of the majority of the VSV G protein CTD (28 of 29 residues) also results in a severe reduction in virion budding, with virion production reduced to approximately 11% of that from wt VSV (221). Interestingly, when the VSV G protein CTD and TM domains were replaced with the CTD and TM domains from a heterologous cellular membrane protein (Human CD4), virion production recovered to approximately 50% of wild type levels. Although the AcMNPV GP64 protein is necessary for efficient budding, the CTD does not appear to play a critical role in budding since deletion of the entire predicted CTD resulted in only a 50% reduction in budding. The role of the TM domain in virion budding remains unclear since deletion of the CTD plus small portions of the predicted TM resulted in poorly anchored GP64. The correlation of reduced budding with a reduction in cell surface levels of GP64 suggests that cell surface GP64 serves as a limiting factor in budding. However differences in BV production between vAc-C-11 and vAc-C-14 (Fig. 7C,D) cannot be explained by differences in surface levels and therefore suggest a possibly specific role for sequences within the TM. More definitive studies of the function of the TM in virion budding will require replacement of the GP64 TM domain with TM domains from heterologous membrane proteins.

In addition to examining the effect of the CTD on production of infectious BV, we also asked whether The GP64 CTD affected GP64 incorporation into virions. We therefore compared viruses expressing wild type and truncated GP64 proteins. The

GP64:VP39 ratio in virus vAc-C-7 was reduced in comparison to the control virus expressing wild type GP64 (Table 1, vAc-Con vs. vAc-C-7) indicating a lower level of GP64 in each virion. Reduced GP64 in vAc-C-7 virions did not appear to result from a limitation in available GP64 since the level of GP64 measured at the cell surface was similar for vAc-C-7 and the control virus, vAc-Con (Fig. 5A). Therefore, the absence of the CTD in vAc-C-7 resulted in both a reduced efficiency of budding and a decreased incorporation of GP64 into progeny virions. These data suggest that the GP64 CTD promotes efficient budding and is involved in concentrating GP64 within the particle.

In combination, the data presented in this study show that the GP64 protein is necessary for efficient budding of progeny virions. Because we detected low levels of virions containing no labeled GP64 in the absence of a *gp64* gene, we cannot rule out the possibility that incoming GP64 is recycled in these experiments. Therefore, it is not known whether the requirement for GP64 in the budding process is absolute. However quantitative measurements of BV progeny showed a 98-99% decrease in budding in the absence of GP64. We also found that the CTD was not required for budding, but appears to moderately affect the efficiency of budding. In comparison, removing the CTD plus small portions of the TM domain resulted in dramatic reductions in budding efficiency and this appears to result primarily from a limitation in the available GP64 due to the poor retention of these truncated proteins in the membrane. Because GP64 is required for efficient budding, yet removal of the CTD did not reduce budding dramatically, these data suggest that the GP64 protein contains an additional domain that facilitates efficient virion budding and that the domain is located either within the transmembrane portion of the protein or within the ectodomain.

The AcMNPV baculovirus has been developed and used extensively as an expression vector for heterologous proteins, as a biological control agent, and as a model virus system. Recent studies have also suggested that it may be possible to utilize AcMNPV in human gene therapy applications. If such applications are to be realized and developed, further studies of the function of the GP64 envelope protein will be necessary in order to understand the requirements for virion entry into host and non-host cells, and the role of this protein in the production of budded virions. For the current studies, we developed and used a recombinant baculovirus system for replacing the essential *gp64* gene with genes expressing modified forms of the GP64 protein. This system permits the insertion of modified GP64 proteins that would otherwise produce a lethal phenotype. The development of this system for examining mutant envelope proteins in the context of the virion and the infection cycle will allow us to address a number of important questions on virus entry, assembly, budding, and infection. Baculoviruses produce two virion phenotypes utilizing what appears to be the same nucleocapsid structure to generate virions in two quite different processes. Although little is known of the process and mechanisms of baculovirus BV assembly and budding, the identification of GP64 as a key component in the process of BV assembly will allow us to further examine and dissect the interactions that occur during this critical process.

Materials and Methods

Cells, transfections, and infections. *Spodoptera frugiperda* (Sf9) cells were used to propagate wild type (wt) AcMNPV virus as well as most recombinant viruses. Cells were cultured at 27°C in TNM-FH medium (95) containing 10% fetal bovine serum. Viruses without a functional copy of GP64 (*vAc*⁶⁴⁻ and *vAc*-C-14, see below) were propagated in a cell line (Sf9^{Op1D}) that constitutively expresses the OpMNPV GP64 protein. Cloning and characterization of cell line Sf9^{Op1D} were described previously (195). Wild type virus used in these studies was AcMNPV strain E2. AcMNPV nucleotide numbers listed in this study are according to the nomenclature of Ayres *et al.* (1994). For transient transfections, 6 µg of DNA was introduced into 0.6 x 10⁶ cells by CaPO₄ precipitation as described earlier (8). For viral infections, virus was incubated on cells for a 1 hr viral adsorption period. Times post infection (p.i.) were calculated from the time the viral inoculum was added.

*Generation of gp64null virus vAc*⁶⁴⁻. For studies of virion production from a *gp64null* virus, the *gp64* gene was deleted from the AcMNPV genome using a modification of a previously described method (172). A transfer vector for recombination into the *gp64* locus was constructed as follows: Plasmid pOplE1-βgal-Sal (provided by Dr. D. Theilmann) contains a cassette consisting of a lacZ gene driven by an OpMNPV IE1 promoter, and flanked by Sall sites. Linkers (SpeI/Sse83871/Sall and Sall/sse83871/BglII) were inserted into each of the Sall sites to create an SpeI site upstream, and a BglII site downstream of the cassette. The SpeI/BglII lacZ cassette was excised and used to replace the wild type *gp64* ORF in SpeI/BglII digested plasmid pAcEcoHΔSma (172), creating transfer vector pAcEcoHΔSmaSpe(Opie1Z+)Bgl. This transfer vector contains 2325 bp (nt 109761 to 112049) of sequence from the region immediately upstream of the AcMNPV *gp64* ORF, and 851 bp (nt 107325 to 108039) of sequence from the region immediately downstream. Wild type AcMNPV viral DNA (1 µg) and pAcEcoHΔSmaSpe(Opie1Z+)Bgl (2 µg) were cotransfected into 1 x 10⁶ Sf9^{Op1D} cells, and overlaid with agarose in TNM-FH. Plaques were picked 3 days after transfection. In sequential plaque assays, plaques were generated in the presence of 120 µg/ml 5-bromo-4-chloro-3-indolyl-β-D-galactopyranoside (Xgal, Labscientific, Inc.), and blue plaques were selected from infected Sf9^{Op1D} cells. A plaque purified viral isolate was named *vAc*⁶⁴⁻. In *vAc*⁶⁴⁻, the complete *gp64* ORF plus an additional 43 bp of upstream and 140 bp of downstream sequence (nt 108039 to 109760) are removed and replaced by the 4195 bp OplE1-lacZ cassette, with the lacZ ORF in the same orientation as *gp64*. Homologous recombination into the *gp64* locus, replacing the *gp64* gene, was confirmed by PCR analysis as described earlier (172) and restriction enzyme profiles of genomic DNA's.

Generation of GP64 CTD mutations. To generate GP64 proteins containing truncations or single amino acid substitutions near the C-terminus, plasmid pAcEcoHΔCla (172), containing the wild type *gp64* gene, was used for site-directed mutagenesis with the MORPH mutagenesis kit (5 prime->3prime, Inc.). Substitution of nt

1514 of the *gp64* ORF (T) with C created a unique *BclI* site at the C-terminal end of the predicted TM domain (conserving isoleucine 505); Substitution of nt 1538 to 1543 (relative to the start of *gp64* ORF) with CCCGGG created a unique *SmaI/XmaI* site at the *gp64* ORF stop codon, resulting in plasmid p Δ Cla-*BclI/SmaI*. This modified *gp64* gene was then used to replace the wild type *gp64* gene in plasmid p Δ Sma Δ (a pBS plasmid, containing the *gp64* locus, AcMNPV nt 107341 to 111046), creating p Δ Sma Δ -*BclI/SmaI*. Oligonucleotide linkers corresponding to the various C-terminal deletions or substitutions were then synthesized and cloned into *BclI/XmaI* digested p Δ Sma Δ -*BclI/SmaI*. The resulting plasmids were used to generate transfer vectors for the construction of recombinant viruses (see below).

Budding assay. For a comparison of virion budding from cells infected with either wild type AcMNPV or vAc⁶⁴, Sf9 cells (5×10^6) were infected at m.o.i. 5 for 1 hr at 27°C, washed once with TNM-FH, and further incubated at 27°C. At 14 hr p.i., cells were washed once and starved by incubation in Graces without methionine (Graces^{met}) for 2 hr. At 16 hr p.i., the medium was replaced with 2.2 ml of Graces^{met} containing 1 mCi of EXPRE³⁵S protein labeling mix (Dupont, NEN). At 22 hr p.i., 0.8 ml of TNM-FH was added. Cells and supernatants were harvested for analysis at 30 hr p.i. Cells (5×10^6) were washed once in PBS, then lysed and boiled in 2 ml Laemmli buffer containing a cocktail of protease inhibitors (0.7 μ g/ml pepstatin; 1 mg/ml pefabloc; 10 μ g/ml leupeptin). Supernatants were cleared of cell debris by brief centrifugation (15 min at 2000 x g, 4°C), then loaded onto a 25% sucrose cushion and centrifuged at 80,000 x g for 80 min at 4°C in a SW60 rotor. Virus pellets were resuspended in 300 μ l PBS (pH 6.2; incubation at 4°C for 10 min on a shaker platform at low speed). Resuspended virions were loaded onto pre-chilled 12 ml, 25 to 60% linear sucrose gradients and centrifuged to equilibrium at 96,000 x g for 16 hr at 4°C. Gradients were fractionated at 4°C in a Model 640 Density Gradient Fractionator (Isco), in 0.6 ml fractions at 1 ml/min. A 35 μ l sample was removed from each 0.6 ml fraction for density measurements (ABBE-3L refractometer, Spectronic Instruments). The remainder of each fraction was diluted to 1.5 ml with cold PBS pH 6.2, and virions were pelleted by centrifugation at 36,200 x g for 1.5 hr at 4°C. Pelleted virus was resuspended in 30 μ l Laemmli buffer containing a cocktail of protease inhibitors (see above), and incubated at 100°C for 5 min. Samples from cell lysates and sucrose gradient fractions were electrophoresed simultaneously on 10% polyacrylamide gels. For cell lysates, approximately 1.9% (equivalent to approximately 93,000 cells) of the total sample was loaded per lane. For samples derived from sucrose gradient fractions, the entire sample was loaded in each lane. The portion of the gel containing the cell lysates was transferred to Immobilon-P (Millipore) membrane, and blots were incubated simultaneously with monoclonal antibody (Mab) AcV5 (97, 171) and Mab 39 (274) for simultaneous detection of GP64 and VP39 respectively. The portion of the gel containing gradient fractions was dried, exposed on a phosphorimager screen, and scanned on a Molecular Dynamics phosphorimager. Quantification of individual bands was performed with the Imagequant software package (Molecular Dynamics, Inc.).

For a comparison of virion budding from cells infected with recombinant viruses containing C-terminal truncations and substitutions, the following modifications to the above protocol were used: For metabolic labeling, infected cells were washed in Graces^{met}, and label was added at 15 hr p.i. TNM-FH was added at 30 hr p.i., and cells and supernatants were harvested for analysis at 40 hr p.i.

CELISA, Western blots, and fusion assays. Western blots and fusion assays were carried out as described previously (10). For detection and quantification of GP64 surface levels, a modified cell ELISA (CELISA) protocol was used: Cells were fixed in 0.5% glutaraldehyde for 10 min at RT, washed once with phosphate buffered saline (PBS pH 7.4) and blocked by incubation in PBS + 1% gelatin for 2 hr at 27°C. Cells were then incubated for 45 min at 27°C in Mab AcV5 tissue culture supernatant diluted 1:25 in PBS + 0.5% gelatin. Cells were washed once in PBS for 2 min, followed by incubation for 45 min at 27°C in a secondary goat-anti-mouse antibody conjugated to β -galactosidase (GAM- β gal, Fisher) diluted 1:750 in PBS + 0.5% gelatin. Cells were then washed four times (5 min/wash) in PBS, then incubated in 1 mM o-nitrophenyl- β -D-galactopyranoside (oNPG) in oNPG substrate buffer (0.01M of each of the following: Tris base, sodium chloride, magnesium chloride, β -mercaptoethanol) at 37°C. After addition of the substrate, the OD₄₀₅ was determined at several timepoints using an ELISA plate reader. Immunoprecipitations were performed as described previously using a polyclonal antiserum prepared against a purified soluble form of OpMNPV GP64 (184).

Generation of CTD recombinant viruses. Plasmids containing genes encoding GP64 C-terminal truncations or substitutions (described above) were used to generate transfer vectors for construction of AcMNPV recombinant viruses by recombination into the GP64 locus of the GP64null virus vAc⁶⁴. For that purpose a cassette, containing the β -glucuronidase (GUS) gene driven by the AcMNPV p6.9 promoter and followed by the AcMNPV polyhedrin polyA signal, was cloned as a BglIII fragment downstream of the modified *gp64* gene, into each of the p Δ Sma Δ plasmids (described above). The resulting transfer vectors (see Fig. 4) contain 1325 bp (AcMNPV nt 109717 to 111042) of sequence from the region immediately upstream of the AcMNPV *gp64* ORF, and 705 bp (AcMNPV nt 107330 to 108035) of sequence from the region immediately downstream. For each recombinant virus, vAc⁶⁴ viral DNA (1 μ g, linearized by Bsu36I digestion) and transfer vector (2 μ g) were cotransfected into 1.5×10^6 Sf9 cells, and supernatants were harvested 3 days after transfection. In sequential plaque assays, plaques were selected by blue color in the presence of 120 μ g/ml 5-bromo-4-chloro-3-indolyl- β -D-glucuronide (XGluc, Labscientific, Inc.), and viral isolates were named vAc-C-1 to -14, and vAc-C Δ 3Ra. Homologous recombination into the *gp64* locus and replacement of the lacZ cassette was confirmed by PCR analysis and restriction enzyme profiles of genomic DNA's. The mutations in the C-terminal region were confirmed by sequencing the PCR amplified C-terminal region of each recombinant virus.

Pulse labeling. Sf9 cells infected with the CTD recombinant viruses at m.o.i 10 were analyzed by pulse labeling proteins at 18 and 36 hr p.i. Two hr before each of

these timepoints, cells were washed once and starved by incubation in Graces without methionine (Graces^{-met}) for 30 min, followed by metabolic labeling in Graces^{-met} containing 25 μ Ci of EXPRE³⁵S protein labeling mix (Dupont, NEN) per 0.6×10^6 cells, for 1.5 hr at 27°C. At the end of the labeling period, cells were washed once in PBS, then lysed and boiled in 350 μ l Laemmli buffer containing a cocktail of protease inhibitors (see above). Each sample (45 μ l) was electrophoresed on a 12% polyacrylamide gel, dried, exposed to a phosphorimager screen, and scanned on a Molecular Dynamics phosphorimager.

Growth curves. To measure infectious BV production from four of the CTD recombinant viruses, viral growth curves were generated by collecting infected cell supernatants at 6 hour intervals at various times post infection. Sf9 cells (0.65×10^6 cells per well; 12 well plates) were infected at m.o.i. 10 for 1 hr at 27°C. For each timepoint post infection, and each virus, triplicate samples were generated, and all wells were infected simultaneously to minimize variability. After infection, cells were washed once with 0.8 ml TNM-FH, and incubated in 0.9 ml TNM-FH. At 6 hr before each timepoint (except timepoint '0'), cells were washed once, and incubated in fresh TNM-FH for six hours, followed by harvesting of the supernatant. All data therefore represent BV produced during the 6 hr time period preceeding the indicated timepoint. Supernatants were carefully removed from the infected cells, centrifuged at 20,800 x g for 5 min to remove debris, and titered by TCID₅₀ (177, 244). X-Gluc, the substrate for the GUS marker gene present in these viruses, was included in the TCID₅₀ assay at 120 μ g/ml, and cells were examined 8 days p.i. for blue color and polyhedra formation.

Acknowledgements

The authors thank Dr. D. Theilmann for providing plasmid construct pOplE1- β gal-Sal, Dr. J. Manning for antibody Mab 39, Dr. P. Faulkner for antibody AcV5, and Dr. S. Monsma for construction and preliminary analysis of vAc⁶⁴. This work was supported by NIH grant AI33657.

Chapter 5

Host cell receptor binding by baculovirus GP64 and kinetics of virion entry.

Abstract

GP64 is the major envelope glycoprotein from budded virions of the baculoviruses *Autographa californica* Multicapsid Nucleopolyhedrovirus (AcMNPV) and *Orgyia pseudotsugata* Multicapsid Nucleopolyhedrovirus (OpMNPV). To examine the potential role of GP64 in host cell receptor binding, we generated, overexpressed, and characterized a soluble form of the OpMNPV GP64 protein, GP64sol^{Op}. Assays for trimerization, sensitivity to Proteinase K, and reduction by DTT suggested that GP64sol^{Op} was indistinguishable from the ectodomain of the wild-type OpMNPV GP64 protein. Virion binding to host cells was analyzed by incubating virions with cells at 4° in the presence or absence of competitors, in a single cell infectivity assay. Purified soluble GP64 (GP64sol^{Op}) competed for binding of a recombinant AcMNPV marker virus (vAchsZ) to host cells, similar to control competition with psoralen-inactivated wild-type AcMNPV and OpMNPV virions. A non-specific competitor protein did not similarly inhibit virion binding. Thus, specific competition by GP64sol^{Op} for virion binding suggests that the GP64 protein is a host cell receptor binding protein. We also examined the kinetics of virion internalization into endosomes and virion release from endosomes by acid-triggered membrane fusion. Using a protease sensitivity assay to measure internalization of bound virions, we found that virions entered *Spodoptera frugiperda* (Sf9) cells between 10 and 20 minutes after binding, with a half-time of ~ 12.5 min. We used the lysosomotropic reagent ammonium chloride to examine the kinetics of membrane fusion and nucleocapsid release from endosomes after membrane fusion. An ammonium chloride inhibition assay indicated that AcMNPV BV were released from endosomes between 15 and 30 min after binding, with a half-time of ~ 25 min.

This chapter has been published as:

Hefferon, K.L., A.G.P. Oomens, S.A. Monsma, C.M. Finnerty, and G.W. Blissard (1999). Host cell receptor binding by baculovirus GP64 and kinetics of virion entry. *Virology* 258, 455-468

Introduction

Baculoviruses are enveloped viruses that contain large circular double-stranded DNA genomes ranging in size from ~ 80-180 kbp (259). Transcription, DNA replication and nucleocapsid assembly occur within the nuclei of infected host cells. Baculoviruses are characterized by an infection cycle that produces two virion phenotypes which are structurally and functionally distinct (reviewed in (5, 167, 209)). Budded virus (BV) is highly infectious in cell culture and mediates cell-to-cell transmission in the infected animal. Virions of the second phenotype, occlusion-derived virus (ODV), are embedded within large proteinaceous occlusion bodies that are produced in the very late phase of the infection cycle. Structurally, BV and ODV differ by the origin and composition of their envelopes (14). They also differ in the mechanisms by which they enter host cells. BV enter cells through the endocytic pathway (261), whereas ODV appear to enter the midgut epithelial cells by direct membrane fusion at the cell surface (73, 243). Although several studies have examined binding properties of the two virion phenotypes (99, 270, 276), the viral receptor-binding proteins and host cell receptors have not been identified for either ODV or BV.

The BV envelopes of AcMNPV and OpMNPV contain an abundant viral-encoded glycoprotein, GP64, that is not found in the ODV envelope (9, 14, 49, 84, 273). BV examined by EM contain characteristic spike-like peplomers within the envelope and these spike proteins appear to be concentrated at the end of the virion that is associated with virion budding. Immuno-electron microscopic studies of virions budding from AcMNPV infected cells suggest that spikes are composed of the GP64 protein (258) and it was recently shown that GP64 is necessary for efficient production of BV (183). Each spike or peplomer is believed to represent a single homotrimer of the GP64 protein (184) and antibodies directed against GP64 have been shown to neutralize infectivity of the BV (97, 264). However, the single neutralizing monoclonal antibody (MAb AcV1) that has been characterized in detail was shown to neutralize virion entry by inhibition of membrane fusion, a step after virion binding (25, 261). Monoclonal antibodies that inhibit virion binding have not been reported. Previous studies showed that the GP64 protein is necessary and sufficient for low pH-triggered membrane fusion activity, the process that occurs during virion entry by endocytosis (10, 147, 171). In addition, a small hydrophobic domain necessary for membrane fusion was identified and characterized by site-directed mutagenesis (171). By generating and examining a Gp64null virus containing a *gp64* knockout, it was demonstrated that GP64 is an essential viral structural protein of AcMNPV (172). In animals fed occlusion bodies from the *gp64*null virus (vAc64Z), midgut cells were efficiently infected by ODV but the infection was unable to move from the midgut epithelium into cells and tissues of the hemocoel. Similarly, infection by vAc64Z did not spread from cell to cell in tissue culture.

Envelope proteins from animal viruses mediate entry into host cells by facilitating two critical functions: binding to host cell receptors and fusion of the viral envelope with

the host cell plasma membrane. In some cases such as the well studied Influenza hemagglutinin (HA) protein, both functions are provided by a single protein. In other cases such as the paraInfluenza viruses, these two functions are segregated into two proteins: hemagglutinin/neuraminidase (HN) and fusion (F) proteins. Viral binding to a host cell receptor may serve two major functions. First, adhesion of the virus particle to the cell may be a necessary prerequisite for subsequent endocytosis. Second, the viral envelope and host plasma membrane must be closely apposed in order to fuse. For example, in some paraInfluenza viruses it has been demonstrated that the receptor binding activity of the HN protein is necessary for fusion induced by the F protein (143). In the case of the baculoviruses OpMNPV and AcMNPV, the GP64 protein was previously demonstrated to encode a low-pH activated membrane fusion activity (10, 184). However, host cell receptor binding has not been previously assigned to GP64 or any other BV envelope protein. A recent study of GP64 glycosylation mutants showed that decreased infectivity was observed when some glycosylation sites were eliminated, suggesting that the GP64 glycosylation state may affect virion binding (115). Perhaps most compelling is the observation that a closely related orthomyxovirus homolog of GP64 (the GP75 protein of the Thogoto virus) has hemagglutinating activity(173, 201). Because the GP64 protein contains primary sequence similarities across the entire predicted ectodomain of GP75, this suggests that the GP64 protein may also encode a host receptor binding function. In the present study, we examined the role of GP64 in virion binding at the cell surface. To determine whether GP64 was involved in virion binding to host cell receptors, we first generated, purified, and characterized a secreted soluble form of the GP64 protein, GP64sol^{Op}. We previously showed that GP64sol^{Op} was trimerized in a manner indistinguishable from native membrane-bound GP64 protein. In the current study, we used N-terminal sequencing, limited proteolysis, and DTT sensitivity assays to further demonstrate that GP64sol^{Op} is indistinguishable from the predicted ectodomain of native GP64. Using purified GP64sol^{Op} as a competitor for virion binding to Sf9 cells, we show that GP64sol^{Op} competes for binding of AcMNPV BV at the surface. To further characterize virion entry, we also examined the kinetics of BV entry by measuring the timing of BV internalization into endosomes and release of nucleocapsids from endosomes.

Results

Production of a secreted soluble form of GP64. A secreted soluble form of the OpMNPV GP64 protein was produced in an AcMNPV baculovirus expression vector system, by inserting a modified *gp64* ORF into the polyhedrin locus of AcMNPV. Site directed mutagenesis was used to insert a stop codon after Leu477, which is located immediately upstream of the predicted transmembrane domain of the OpMNPV *gp64* ORF (Fig. 1A). The resulting construct was placed under the control of the polyhedrin promoter in transfer vector pAcDZ1 (109) and a recombinant baculovirus was

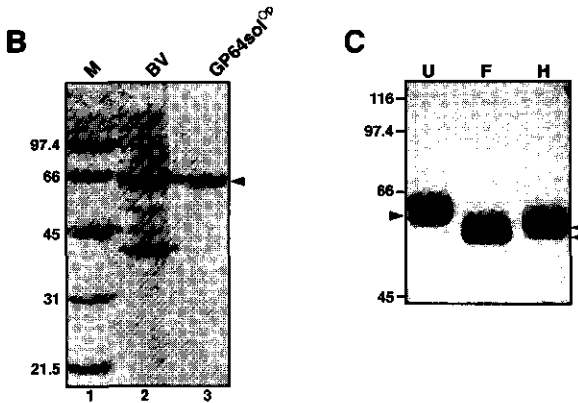
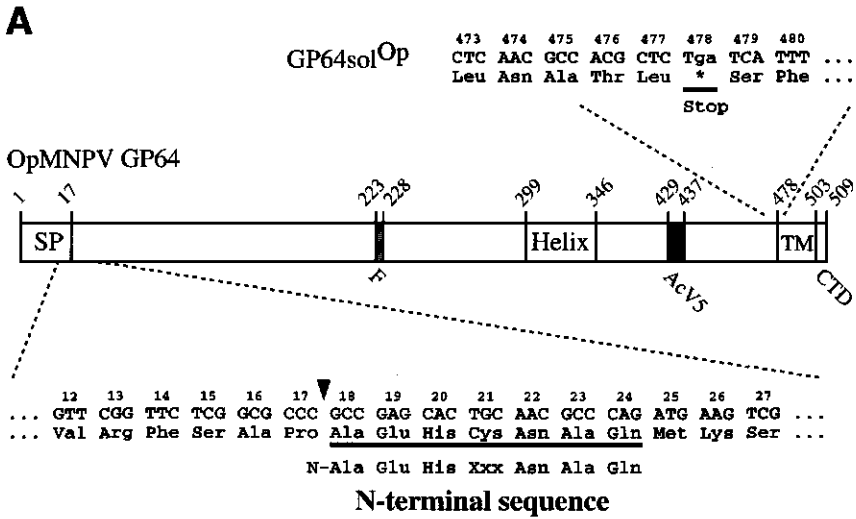


FIG. 1. (A) Construction of GP64sol^{Op}. The OpMNPV GP64 open reading frame is represented as an open bar with protein domains indicated on and below the bar. The gene encoding the secreted soluble form of GP64 (GP64sol^{Op}) contains a stop codon (*, Stop) introduced at Tyr 478, immediately upstream of the transmembrane domain (TM). The N-terminal sequence determined from the mature secreted soluble GP64 protein is indicated below the nucleotide sequence and the predicted N-terminal sequence. The signal peptide cleavage site is indicated by an arrowhead. SP, signal peptide; F, fusion domain; Helix, predicted amphipathic alpha-helical region; AcV5, monoclonal antibody epitope; CTD, cytoplasmic tail domain. **(B)** Highly purified GP64sol^{Op} (purified as described in Materials and Methods) was compared with GP64 from OpMNPV budded virions (BV) by SDS-PAGE and Coomassie blue staining. Lane 1, Protein markers; lane 2, OpMNPV BV; lane 3, Highly purified GP64sol^{Op}. **(C)** GP64sol^{Op} glycosylation. Purified GP64sol^{Op} (undigested, U) was compared with endoglycosidase F (F) or endoglycosidase H (H) digested GP64sol^{Op} on SDS-PAGE gels stained with Coomassie blue. The positions of protein markers and the mature GP64sol^{Op} (arrowhead) is indicated on the left and positions of major products of each digest are indicated on the right.

generated from BacPAK6 viral DNA. The secreted soluble form of GP64 (GP64sol^{Op}) was purified from supernatant collected from infected Tn5B1-4 cells at 48 h pi as described in the Materials and Methods section. Quantity and purity of GP64sol^{Op} were assessed by Bradford protein assay and by Coomassie blue and silver staining of GP64sol^{Op} electrophoresed on SDS-PAGE gels, followed by densitometric scanning of stained gels (Fig. 1B). Extensive purification of GP64sol^{Op} resulted in a preparation exceeding (93-95%) purity, which was used for all competition studies. A partially purified preparation of GP64sol^{Op} was used for protease resistance and oligomerization studies. We previously showed that this secreted soluble GP64sol^{Op} was trimerized in a manner indistinguishable from native OpMNPV GP64, suggesting that GP64sol^{Op} was identical to the ectodomain of native GP64 (184). To further confirm the native structure and processing of GP64sol^{Op}, we examined GP64sol^{Op} by N-terminal sequencing, endoglycosidase treatment, partial reduction with DTT, and protease treatment (below). For these studies GP64sol^{Op} was compared to GP64 derived from OpMNPV virions (Fig. 1,2).

Posttranslational modifications. The N-termini of baculovirus GP64 proteins are highly hydrophobic, although not well conserved in primary sequence (9, 93, 273). This is consistent with the presence of a signal peptide which is cleaved during entry into the secretory pathway. In a previous study (9), the signal peptide cleavage sites for the OpMNPV GP64 protein was predicted at a position between amino acids 17 and 18 (Fig. 1A) and this corresponds to a similar position (between amino acids 20 and 21) in the AcMNPV GP64 protein. N-terminal sequencing of highly purified GP64sol^{Op} resulted in the following N-terminal sequence, N-Ala-Glu-His-Xxx-Asn-Ala-Gln, demonstrating that the predicted peptide cleavage site is correct (Fig. 1A, arrowhead).

The native AcMNPV and OpMNPV GP64 proteins contain 5 and 7 potential sites for N-linked glycosylation, respectively, and previous studies have shown that the native proteins contain ~ 6 to 8 kDa of N-linked carbohydrate per monomer (9, 112, 184, 273). Digestion of purified GP64sol^{Op} with endoglycosidase F or endoglycosidase H resulted in increased mobility consistent with that reported from native OpMNPV GP64 (Fig. 1C)(184).

Proteinase K digestion and DTT reduction. To determine whether the secreted soluble form of GP64 retained a native conformation, GP64sol^{Op} was compared directly to GP64 from OpMNPV BV in Proteinase K resistance assays and DTT reduction assays (Fig. 2). Previous studies of GP64 from AcMNPV virions showed that Proteinase K digestion of native GP64 resulted in protease resistant peptides of ~ 34 to 37 kDa (262). To examine protease resistance, we used a monoclonal antibody (AcV5) that recognizes a defined, conserved linear epitope near the C-terminus of the GP64 ectodomain (171). When digested with proteinase K, an ~ 34 kDa protease resistant peptide (that encompasses the C-terminal portion of GP64) was identified from both wild-type OpMNPV GP64 and GP64sol^{Op} (Fig. 2A, lanes 2 and 4, respectively). These

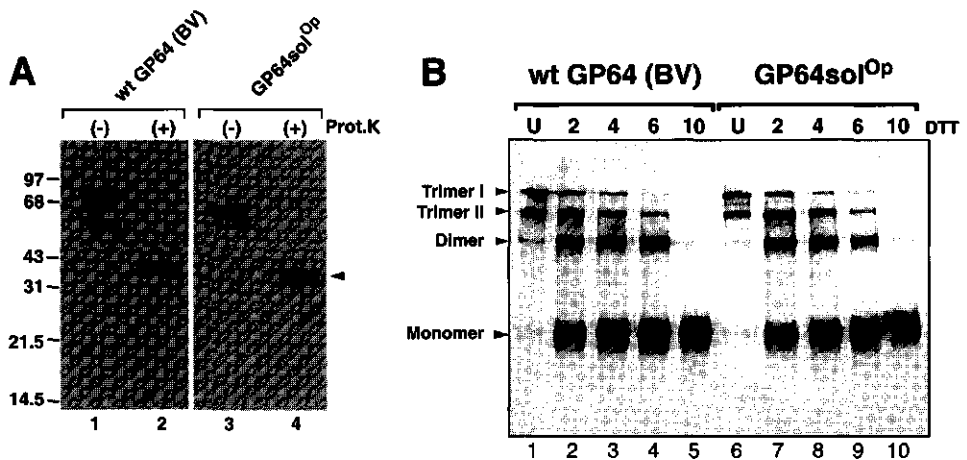


FIG. 2. (A) Protease resistance of OpMNPV GP64 and GP64sol^{Op}. GP64sol^{Op} (0.5 μ g) and OpMNPV budded virions (1 μ g) were digested with 0.1 mg/ml Proteinase K (Prot.K) for 10 min at 56^o, then examined by Western blot analysis using monoclonal antibody AcV5. Lane 1: Undigested OpMNPV BV; lane 2: OpMNPV BV digested with Proteinase K; lane 3, Undigested GP64sol^{Op}; lane 4, GP64sol^{Op} digested with Proteinase K. The position of the protease resistant C-terminal fragment of GP64 is indicated by the arrowhead. **(B)** DTT sensitivity of OpMNPV GP64 and GP64sol^{Op}. Purified GP64sol^{Op} and wild-type GP64 (wild-type GP64) from OpMNPV budded virions were reduced in various concentrations of DTT at 37^o for 5 min, then prepared under non-reducing conditions and electrophoresed on SDS-PAGE gels. Samples of GP64sol^{Op} (0.5 μ g) and OpMNPV BV (1 μ g) were treated with increasing concentrations of DTT (0-10 mM). GP64 proteins were identified by Western blot analysis using MAb AcV5. Lanes 1-5, OpMNPV BV; lanes 6-10, GP64sol^{Op}. Concentrations of DTT (mM) are indicated above each lane of the gel. Oligomeric forms of GP64 (Trimer I and II, Dimer, Monomer) which were characterized previously (184) are indicated on the left.

proteinas resistance data strongly suggest that analogous portions of both proteins are exposed to cleavage by proteinase K and that GP64sol^{Op} is found in the same conformation as native GP64 from BV.

GP64 is present in BV as disulfide linked homotrimers and a previous study demonstrated that two electrophoretic forms of trimeric GP64 are observed on nonreducing SDS-PAGE gels (184). The two trimer forms were designated Trimer I and Trimer II. Trimer I and II were also detected from GP64sol^{Op}. Thus trimers of GP64sol^{Op} were indistinguishable from those of wild-type GP64 derived from virions (see also Fig. 2B, lanes 1 vs. 6). To confirm the similarities and further examine GP64 trimerization, both GP64sol^{Op} and wild-type OpMNPV GP64 from BV were incubated in increasing concentrations of the reducing agent DTT, from 2 to 10 mM. In both cases, increasing concentrations of DTT resulted in a gradual loss of trimeric forms. At low DTT concentrations (2-4 mM), Trimer I appears to be more susceptible to reduction than Trimer II. This was observed for both GP64sol^{Op} and GP64 from OpMNPV BV (Fig. 2B

lanes 2-3 and 7-8). At higher concentrations of DTT (10 mM), both GP64s were almost completely reduced to monomers (Fig. 2B, lanes 5, 10). These similarities in sensitivity to DTT suggest that GP64sol^{Op} and wild-type OpMNPV GP64 are similar in structure.

Baculovirus BV binding and infectivity. To examine virion binding and entry in subsequent experiments, we used a recombinant AcMNPV virus containing a *lacZ* gene under the control of a promoter (*Drosophila hsp70*) that is active early in the infection cycle. The virus vAchsZ (172, 256) was used in a single cell infectivity assay to measure changes in virion binding. To generate a dose-response curve and identify assay conditions in which changes in virion binding could be detected and quantified, Sf9 cells (3×10^5) were infected with increasing concentrations of vAchsZ virions (MOIs ranging from 0.015 to 0.2), by binding BV at 4[°] for 1 hour. This resulted in a proportional linear increase in the number of single infected cells detected by staining for β -galactosidase at 24 hours pi (Fig. 3A). Thus, within this range of virion concentrations and under these conditions, virions are not present in saturating concentrations. Competition for virion binding can therefore be more readily detected by this method. Virion concentrations within the linear range of this assay were used in all subsequent experiments.

In these studies, virion entry was synchronized by binding BV to cells at 4[°] for 1 h, then shifting the temperature to 27[°] to permit endocytosis of virions. To confirm that the vAchsZ BV that were bound at 4[°] remained at the cell surface at the end of the 1 h binding period, virions were bound to cells at 4[°] for 1 h, then cells were washed and treated with the protease subtilysin (2 mg/ml) to inactivate or release virions at the cell surface. As a control, virions were bound at 4[°] for 1 hour, washed in TNM-FH medium, then incubated at 27[°] for one hour (allowing bound virions to internalize), and subsequently treated with subtilysin. Treatment of cells with subtilysin immediately after the 4[°] binding step resulted in a dramatic decrease in numbers of infected cells detected (Fig. 3B, column 2). In contrast, when virions were bound at 4[°], then allowed to enter endosomes by incubating at 27[°] for one hour before protease treatment, no detectable decrease in infectivity was observed (column 3). A control pretreatment of BV with subtilysin prior to binding (column 4) resulted in little binding and infectivity, as expected. These data indicate that during the 4[°] incubation period, virions remain at the cell surface, and that bound virions enter within one hour after the shift from 4[°] to 27[°]. Thus, entry by endocytosis (after binding) is efficiently synchronized in this manner.

Virion and GP64sol^{Op} competition. Because GP64 is the major envelope protein of the BV, we hypothesized that BV binding to the host cell receptor may be mediated by GP64. The OpMNPV and AcMNPV GP64 proteins are highly conserved, showing 84% sequence identity in the ectodomains. In addition, in previous studies (unpublished) we found that OpMNPV BV appear to bind and enter Sf9 cells, although Sf9 cells are not permissive for OpMNPV replication. Thus, if the GP64 protein encodes the host cell receptor binding activity, the OpMNPV GP64 protein may compete for the same

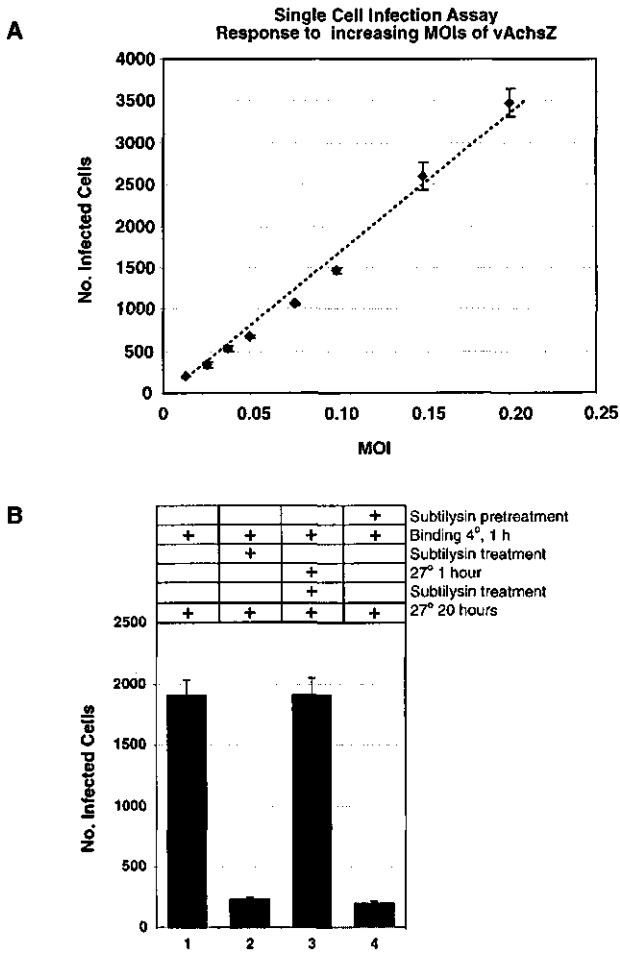


FIG. 3. (A) Dose-response curve for a single cell infectivity assay with virus vAchsZ. To develop a rapid single cell infectivity assay for detecting changes in virion binding, a range of virion concentrations were examined in a 1 hour viral binding assay. To identify a range of virion concentrations in which the response to increasing virion concentrations was linear, Sf9 cells (3×10^5) were incubated with increasing concentrations of vAchsZ (MOIs of 0.0125 to 0.2) for 1 hour at 4° C, then washed in TNM-FH, and incubated for 24 h in TNM-FH at 27°. Single cells were scored for expression of β -galactosidase as described in the Materials and Methods. In the dose-response curve, each data point represents the averaged results from three wells and bars represent standard deviation. **(B)** Protease sensitivity of virions bound at the cell surface. To determine whether virions remained at the cell surface at the end of a 1 h binding period at 4°, the sensitivity of surface bound virions to inactivation or release by treatment with the protease subtilysin was examined in a single cell infection assay. Virions of vAchsZ were bound to Sf9 cells at 4° for one hour, then cells were washed 3x with TNM-FH at 4° and either not treated (Lane 1), or treated with 2 mg/ml subtilysin (Lane 2) prior to shifting to 27° C and incubating for 24 hours. As a control, virions were bound at 4°, cells were washed as above, then virions were allowed to internalize by shifting to 27° for 1 hour prior to treatment with subtilysin (Lane 3). Pretreatment of vAchsZ virions with subtilysin prior to binding was sufficient to inactivate virions in the same single cell infection assay (Lane 4). Each data point represents average data from three wells and bars represent standard deviation.

binding sites used by AcMNPV or the AcMNPV recombinant, vAchsZ. To determine whether OpMNPV virions compete for the same binding sites used by AcMNPV, psoralen-inactivated virions of AcMNPV and OpMNPV were used as competitors in the virion binding assay described above. For these competition assays, Sf9 cells were incubated for 1.5 h at 4° with various concentrations of psoralen-inactivated AcMNPV or OpMNPV virions prior to addition and binding of vAchsZ at 4° for one hour. Prebinding of psoralen-inactivated AcMNPV or OpMNPV virions at 4° resulted in a dramatic decrease in the number of cells infected by vAchsZ, as detected in the single cell infection assay (Fig. 4). Results of these competition assays suggest that both AcMNPV and OpMNPV virions competed with vAchsZ for binding sites on Sf9 cells.

Competition studies with a soluble GP64 protein. Because both AcMNPV and OpMNPV appeared to compete for the same host cell receptor sites, we next asked whether secreted soluble GP64 (GP64sol^{Op}) would similarly compete for binding to the host cell receptor. To address this question, various concentrations of GP64sol^{Op} were

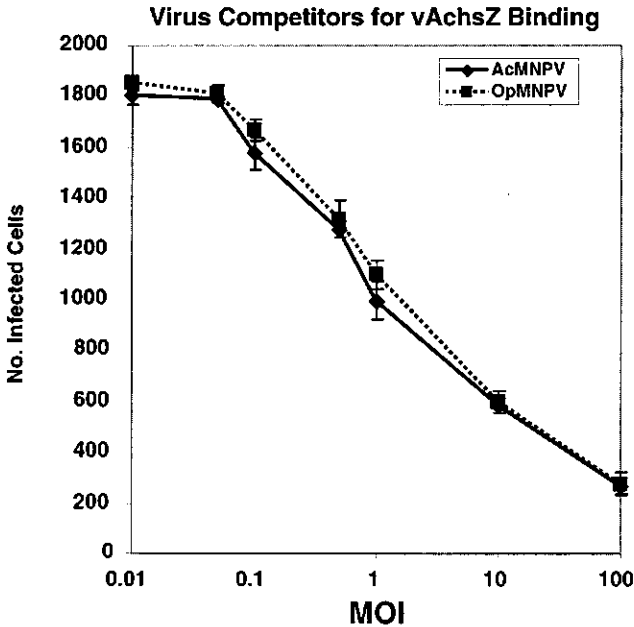


FIG. 4. Competition for virion binding by inactivated AcMNPV and OpMNPV BV. To determine whether OpMNPV and AcMNPV BV utilize the same host receptor binding sites on Sf9 cells, psoralen-inactivated BV of AcMNPV and OpMNPV were used as competitors for binding of BV from vAchsZ. Sf9 cells were preincubated with increasing concentrations of psoralen-treated AcMNPV and OpMNPV BV (X-axis, MOI) at 4° for 1 h, then vAchsZ (MOI 1) was added and allowed to bind for 1 h at 4°. Cells were washed in TNM-FH, fresh medium was added, and infection was allowed to proceed for 20 h. Numbers of infected cells were determined as described in Materials and Methods. Each data point represents average data from three wells and bars represent standard deviation.

Protein Competitors for vAchsZ Binding

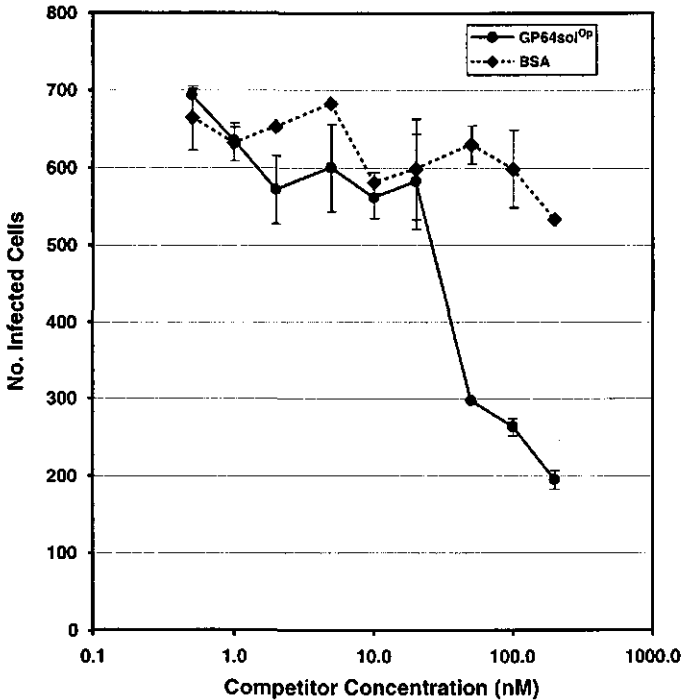


FIG. 5. GP64sol^{Op} competition for AcMNPV binding. GP64sol^{Op} was used as a competitor for virion binding in a single cell infectivity assay as described earlier. Sf9 cells were preincubated with increasing concentrations (X-axis) of either GP64sol^{Op} (solid line) or BSA (dashed line) at 4° for 1.5 h, then vAchsZ virions were added and bound for 1 h at 4°. Cells were washed at 4° in PBS, then incubated at 27° for 22 h. Numbers of infected cells (Y-axis) were quantified as described in Materials and Methods. Each data point represents average data from two wells and bars represent standard deviation.

incubated with Sf9 cells at 4° for 1.5 hours, then vAchsZ was added and bound to cells for an additional hour at 4°. As a control, identical molar concentrations of BSA were included in a parallel competition assay. Incubation of cells with increasing concentrations of GP64sol^{Op} resulted in a dramatic decrease in the number of infected cells (Fig. 5). Inhibition of virion binding was first detected at a GP64sol^{Op} concentration of 50 nM, and increasing concentrations of GP64sol^{Op} (100 and 200 nM) resulted in additional decreases in virion binding. Only a minor reduction in numbers of infected cells was observed when equivalent concentrations of BSA were used as a non-specific competitor (Fig. 5, dashed line). Competition by GP64sol^{Op} for virion binding was observed in at least 6 separate experiments. To determine whether native GP64sol^{Op} trimers were required for efficient binding, and as a further control to confirm

the role of GP64, purified GP64sol^{OP} trimers were reduced by treatment in 10 mM DTT prior to competition assays. Previous studies showed that these conditions were sufficient to reduce trimeric GP64sol^{OP} to monomers (Fig. 2B). For these experiments concentrated GP64sol^{OP} was reduced in 10 mM DTT, then diluted to a final concentration of 50 nM GP64sol^{OP} and 0.1 mM DTT for use as a competitor. Treatment of GP64sol^{OP} with 10 mM DTT resulted in a loss of competition by GP64sol^{OP} (Fig. 6). In a mock experiment, the same final dilution of DTT (0.1 mM DTT) added alone to cells did not affect infection in the absence of the competitor (not shown). The inability of reduced GP64sol^{OP} to effectively compete for virion binding sites suggests that disulfide bonds may be necessary for maintenance of a receptor binding domain of GP64 or that native trimeric GP64 is necessary for efficient receptor binding by GP64 (Fig. 6). As an additional control, GP64sol^{OP} was also pretreated with chymotrypsin, followed by addition of protease inhibitors, prior to use in competition assays. Protease treated GP64sol^{OP} did not compete for binding by vAchsZ (Fig. 6).

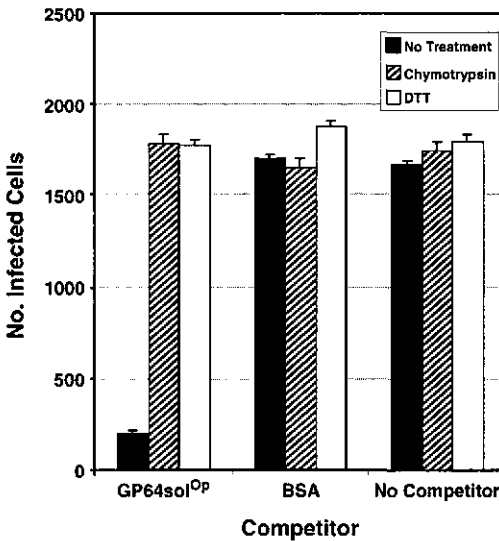


FIG. 6. Reduction in specific competition by GP64sol^{OP} after treatment with protease or reducing agent. GP64sol^{OP} was treated with either 1 mg/ml chymotrypsin (hatched bars) or 10 mM DTT (open bars) prior to use as a competitor in a virion binding assay, as in Figure 5. Competitor (GP64sol^{OP} or BSA) concentrations were 50 nM. Bovine serum albumin (BSA) was similarly treated. Treated and untreated protein competitors were preincubated with Sf9 cells at 4° for 1.5 h prior to incubation with BV of vAchsZ, as described in Figure 5. Numbers of infected cells were determined as described above. Each bar represents the average data from three wells and bars represent standard deviation.

Kinetics of virion entry. The timing of BV entry into endosomes was measured by first synchronizing BV binding at the cell surface at 4°, incubating for various periods at 27° to permit endocytosis, inactivating or releasing BV remaining at the cell surface with

subtilysin treatment, then measuring the virus that was internalized and therefore protected from subtilysin treatment. For these studies we used virus vAchsZ and the single cell infectivity assay described above. vAchsZ was bound to cells for 1 hr at 4^o, then the temperature was shifted to 27^o for increasing intervals of time from 0-120 min. At the end of each time interval, cells were treated with 2 mg/ml subtilysin to inactivate or release BV remaining at the cell surface. Cells were washed and then incubated at 27^o for 24 hours, and numbers of infected cells were determined as described earlier. The protease resistance curve shown in Fig. 7A (solid line) shows that between 0 and 10 min at 27^o, BV were highly sensitive to inactivation by exogenously applied subtilysin. Resistance to inactivation by subtilysin increased dramatically between 10

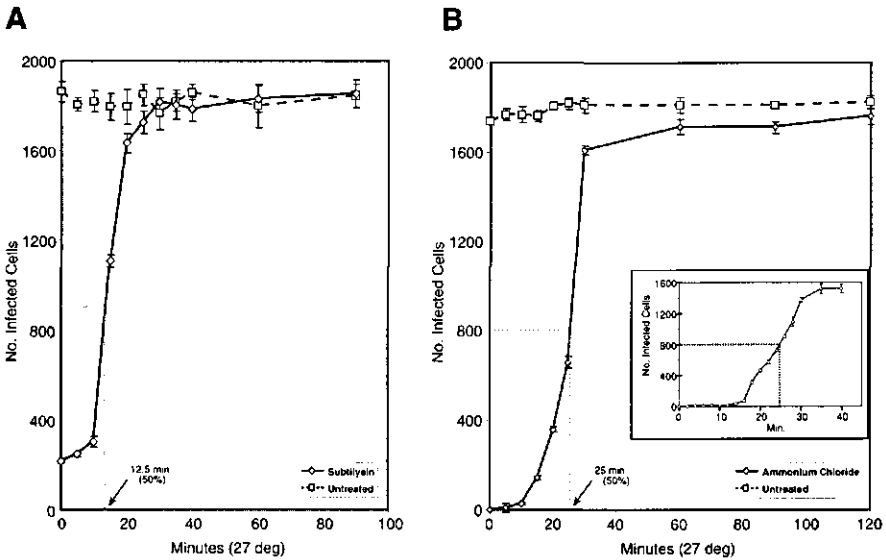


FIG. 7. (A) Kinetics of virion internalization into endosomes. The kinetics of virion internalization into endosomes were examined by synchronously binding virions to the cell surface at 4^o for 1 h, then shifting to 27^o for various periods of time, and treating with subtilysin. Resistance of internalized BV to inactivation by subtilysin was measured by the single cell infectivity assay described earlier. Synchronously bound virions of vAchsZ were incubated at 27^o for time periods ranging from 5-120 minutes. At the end of each time period, cells were treated with subtilysin, washed, and incubated at 27^o for 20 h. Numbers of infected cells were determined as described above and each data point represents the average of three wells. Error bars represent standard deviation. Subtilysin treated cells (solid line, solid diamonds); Untreated control cells (dashed line, solid squares). **(B)** Kinetics of virion release from the endosome. The kinetics of virion release from the endosome were examined by measuring the time after binding, required for acquisition of resistance to inhibitors of endosomal membrane fusion. Virions of vAchsZ were synchronously bound to Sf9 cells for 1 h at 4^o, then the temperature was shifted to 27^o for increasing time periods (2-120 min). At the end of each period, medium was replaced with medium containing 25 mM ammonium chloride or 0.75 mM chloroquine for the remainder of the assay (20 h). The numbers of infected cells were determined as described above. The inset shows an identical experiment in which chloroquine was added at 2 min intervals between 0 and 40 minutes.

and 20 min of incubation at 27°. As shown in Figure 7A the measured half-time for internalization of virions into endosomes was ~ 12.5 min.

Release of BV nucleocapsids from the endosome occurs when the BV envelope fuses with the membrane of the endosome, an event catalyzed by the pH triggered fusion activity of GP64. Studies using a syncytium formation assay indicate that AcMNPV and OpMNPV GP64s are triggered at pH values of ~ 5.5 - 5.7(10, 147). Lipophilic amines such as ammonium chloride or chloroquine buffer the endosomal pH and can be used to inhibit membrane fusion during endocytosis. For precise studies of timing, ammonium chloride appears to be the reagent of choice since ammonium chloride can buffer the pH of the endosome within 1 min after its addition to cells (77). To measure the timing of baculovirus nucleocapsid release from the endosome, we used ammonium chloride inhibition in combination with the single cell infectivity assay. vAchsZ BV binding at the cell surface was synchronized by binding virions at 4° for 1 hour, then shifting the cells to 27°. After various intervals at 27° (0-120 min), ammonium chloride was added to a final concentration of 25 mM and cells were incubated for up to 24 hours. At 24 h after shifting to 27°, plates were scored for infected cells. When ammonium chloride was added immediately after the 4° BV binding period, an ~ 98% inhibition of virion infectivity was observed. With increasing intervals of incubation at 27° prior to ammonium chloride addition, the numbers of infected cells detected increased (Fig. 7B). Escape from ammonium chloride inhibition was first detected after 16 minutes and was near maximal levels after ~ 28 minutes of incubation at 27°. Within 30 min at 27°, infectivity had increased to ~ 90% of that from cells in which no ammonium chloride was added. Thus, after binding of BV at the cell surface, the estimated half-time for triggering of membrane fusion and release of BV nucleocapsids from the endosome in Sf9 cells was ~ 25 min (Fig. 7B).

Discussion

The process of baculovirus entry by receptor-mediated endocytosis may be subdivided into several discrete steps: virion binding at the cell surface, formation of clathrin coated pits and uptake of the virion into a vesicle (endosome), triggering of membrane fusion by low pH, and release of the nucleocapsid into the cytoplasm. Although the role of GP64 in membrane fusion has been examined in some detail (10, 25, 171, 172, 195, 196), its role as a potential host cell receptor binding protein has not been previously explored. Several lines of indirect evidence suggested that GP64 might represent the viral encoded host cell receptor binding protein. First, the GP64 protein represents the most abundant viral protein identified from the BV envelope, and BV-neutralizing antibodies recognize the GP64 protein (97, 206). Recent studies of GP64 glycosylation also suggested that the glycosylation state of GP64 may affect virion binding to host cells (115). Second, GP64 homologs (known as GP75) from a small group of arboviruses within the Orthomyxoviridae appear to be involved in receptor

binding. The GP75 proteins from the Thogoto and Dhori viruses show remarkable primary amino acid sequence identity with baculovirus GP64 proteins, and Thogoto virus hemagglutination is inhibited by a monoclonal antibody directed against GP75 (146, 173, 201). Finally, the GP64 protein expressed on the surface of transfected insect cells is capable of mediating low pH-triggered membrane fusion (10). Since prior receptor binding (docking) is usually a requirement for membrane fusion, this final observation strongly suggested that GP64 may also function as the host cell receptor binding protein.

In the current study, we examined the role of GP64 in host cell receptor binding by using a soluble form of OpMNPV GP64 as a competitor for virion binding. To examine competition for virion binding to the host cell, we developed a competition assay in which a recombinant baculovirus (vAchsZ) carrying a marker gene was bound to the cell surface by incubation at 4° in the presence of competitor proteins. Unbound virions were removed by washing cells prior to shifting the temperature to 27°. Successful virus binding was scored by analysis of single cell expression of β -galactosidase from the recombinant virus. In competition experiments, we showed that both AcMNPV and OpMNPV competed with vAchsZ for binding, suggesting that both OpMNPV and AcMNPV utilize the same cellular receptor(s). To examine the role of GP64 in virion binding to host cells, we used a highly purified soluble form of GP64 as a direct competitor for virion binding. The purified soluble GP64 (GP64sol^{Op}) was determined to be structurally indistinguishable from the ectodomain of native GP64 from budded virions, based on oligomerization patterns and their comparative sensitivities to glycosidase, protease cleavage, and reducing agent DTT. Because the soluble form of GP64 specifically competed for vAchsZ binding to Sf9 cells, these data directly implicate GP64 as a host cell receptor binding protein. In addition, reduced GP64sol^{Op} did not exhibit any significant competition in this assay suggesting that disulfide bonds may be required to maintain a structure capable of binding the receptor. Although we did not attempt to measure the affinity of GP64sol^{Op} binding to host cells in the current study, it is likely that GP64sol^{Op} binds to host cells with a lower overall affinity than virions, which contain local concentrations of GP64. Such differences in affinity may explain why we were not able to eliminate virion binding completely in this very sensitive assay. However, our demonstration that GP64sol^{Op} competes for virion binding in this assay provides the best data to date that GP64 serves as a baculovirus virion binding protein.

gp64 genes from several baculoviruses (AcMNPV, BmNPV, OpMNPV, CfMNPV, AfMNPV (*Anagrapha falcifera*), and EpNPV (*Epiphyas postvittana*)) have been identified and these proteins are highly conserved, showing ~ 80% amino acid sequence identity within the predicted ectodomains(9, 93, 155, 273). Because both AcMNPV and OpMNPV are able to enter *Spodoptera frugiperda* cell lines yet are distinctly different viruses with distinct host ranges, the differences in host range may be explained by factors other than virion binding. Indeed, our previous studies have shown that two OpMNPV late promoters are not fully functional in the AcMNPV genome (62). Studies of host range determinants in AcMNPV and other baculoviruses have identified

critical host range factors that do not appear to be associated with virion entry into the host cell (32, 44, 125, 152, 154, 168). Those studies indicate that baculovirus host specificity can be determined at levels other than virion binding at the cell surface. However, identification of the host receptor for AcMNPV BV will be important for understanding whether viral entry may influence tissue specificity within the infected host and for applications of AcMNPV BV for gene delivery in biotechnological applications such as gene therapy. BV from AcMNPV are infectious to cells of many insect tissues and are highly infectious in insect cell culture. Several early studies showed that BV entered cells of diverse organisms that were non-permissive for viral replication (16, 19), although the mechanisms of entry were not examined. Recent studies of several mammalian cell types showed that AcMNPV BV efficiently entered primary cultures of human hepatocytes and cell lines derived from hepatocytes (3, 12, 96, 218). Other recent studies have reported BV entry into a broad range of mammalian cell lines (227). The apparently wide array of potential cell types that AcMNPV BV can enter suggests that the BV interaction with the host cell may involve recognition of a host receptor molecule that is highly conserved and present on many cell types, or that the interaction may be relatively non-specific.

In the current studies, we also examined the kinetics of two successive steps in baculovirus BV entry by receptor-mediated endocytosis: 1) uptake into the endosome and 2) release from the endosome by membrane fusion. vAchsZ entry was analyzed by synchronizing BV entry by binding virions to cells at 4°, then using a protease resistance assay to measure virions internalized after various periods of incubation at 27° C. The measured half-time required for virus uptake was 12.5 minutes. This rate of entry is similar to those reported from adenovirus, Influenza virus and SFV, which have uptake half-times of 12.5, 10 and 3-5 min, respectively (69, 77, 160). Release of baculovirus virions from endosomes was measured using inhibitors of low pH-triggered membrane fusion. The measured half-time for nucleocapsid release from the endosome was 25 minutes. This is similar to release times reported from several enveloped viruses, including Influenza, VSV, Reovirus and West Nile Virus (159, 162, 240). In an earlier study (261), it was estimated that significantly longer times (half-times of 1-1.5 hours) were necessary for AcMNPV BV release from the endosome. The differences may result from differences in the assay techniques used in the two studies. In the current study, we used a sensitive single cell infectivity assay that detects viral entry and early gene expression in single cells, thus isolating virion entry from subsequent steps such as late gene expression, viral replication, and plaque formation. The current data on BV entry and nucleocapsid release correspond well with data reported from other enveloped viruses.

In summary, we identified GP64 as a protein involved in AcMNPV binding to host cell receptors and we characterized two steps in AcMNPV entry into host cells: internalization into and release from endosomes. Because the GP64 proteins are highly conserved in several baculoviruses, and share a common ancestry with the GP75 envelope proteins from several orthomyxoviruses that are transmitted by ticks, it is

possible that a common entry mechanism is shared by these disparate groups that both infect arthropods. Future studies that identify and characterize the host cell receptor for baculovirus binding will be important for understanding how these very different viruses are adapted to their invertebrate hosts.

Materials and methods

Cells, viruses, and recombinant virus construction. *Spodoptera frugiperda* (Sf9) and *Lymantria dispar* (Ld652Y) cells were cultured at 27° in TNM-FH complete medium (95) containing 10% FBS. Viruses AcMNPV (strain E2) and vAchsZ (172, 256), were titered on Sf9 cells, and OpMNPV was titered on Ld652Y cells as described previously (9). To construct a recombinant virus expressing soluble GP64, a stop codon was engineered into the OpMNPV *gp64* gene in plasmid p64-166 (10) immediately upstream of the predicted transmembrane domain. A synthetic oligonucleotide (5'CTCAACGCCACGCTCTgaTCATTTATGCTGGGGCAC-3') was used to convert the codon for Tyr478 (TAC) to TGA, using site directed mutagenesis (39, 203). Next, the synthetic antisense oligonucleotide 5'-ACCATCTGTAGATCTTGTAGTGT-3' was used for site directed mutagenesis to introduce a BglII restriction site just upstream of the *gp64* ATG, and the resulting plasmid was named p64-BglATG-STOP. The ~1700 bp BglII/Spel fragment containing the *gp64* ORF from p64-BglATG-STOP was cloned into BamHI/XbaI digested transfer vector pAcDZ1, replacing the lacZ ORF and placing the modified *gp64* ORF under control of the very late polyhedrin promoter. The resulting plasmid was named (pAcGP64STOP). A recombinant virus was generated by co-transfection of Sf9 cells with pAcGP64STOP and Bsu36I-digested BacPAK6 viral genomic DNA (Clontech) and the virus was named vAcGP64sol^{Op}. Recombinant viruses were isolated by 3 rounds of limiting-dilution cloning. Recombinant viral genomes were confirmed by restriction enzyme analysis and by PCR using primers homologous to the polyhedrin promoter and the OpMNPV *gp64* gene.

Purification of GP64sol^{Op}. For biochemical studies requiring high purity GP64sol^{Op} and to confirm biological assays, a highly purified preparation of GP64sol^{Op} was prepared. A four step protocol was developed to purify GP64sol^{Op} from tissue culture supernatants of vAcGP64sol^{Op}-infected cells. Insect cells (Tn5B1-4) were grown in serum-free media (Excell 405; JRH Biosciences), and infected at an MOI of 10 with vAcGP64sol^{Op}. After infection, the cells were diluted to a density of 1 x 10⁶ cells/ml and maintained in spinner culture at 27° for 48 h. Cells and debris were removed by low speed centrifugation, supernatants were collected, and sodium azide was added to 0.02% w/v. Sodium azide was present at all times throughout the purification, except for ion-exchange loading, wash and elution. ConA-agarose beads (Sigma) equilibrated in ConA wash buffer (150 mM NaCl, 20 mM NaPi pH 7.0) were added to the supernatant (~ 143 mg beads/liter) and mixed gently overnight at ~ 4 rpm at 7° in a roller bottle. The beads were collected in a large buchner funnel, transferred to a glass column (3 cm

diameter), and washed extensively with ConA wash buffer. Bound glycoproteins were eluted with two bed volumes of 0.5 M glucose, 0.5 M methyl -D-mannopyranoside, 20 mM NaPi pH 7.0, followed by three bed volumes of ConA wash buffer. The eluate and first bed volume of wash were pooled and dialyzed overnight against 200 mM NaCl, 20 mM NaPi pH 7.0. The dialyzed pool was centrifuged (27,000 x g for 30 min at 4° C) to remove precipitated material. For hydrophobic interaction chromatography, the supernatant was applied to a column composed of phenyl-Sepharose CL-4B equilibrated with 200 mM NaCl, 20 mM NaPi, pH 7.0. After sample application the column was washed with one bed volume of 200 mM NaCl, 20 mM NaPi, pH 7.0 followed by one bed volume of 20 mM Tris-HCl, pH 8.0. The bound proteins were eluted by washing with two bed volumes of distilled H₂O. The bound GP64sol^{Op} eluted as a major peak at the 20 mM Tris-HCl-dH₂O transition, followed by a very broad tail. The fractions were analyzed on SDS-PAGE gels and the fractions containing GP64sol^{Op} were pooled and dialyzed against 20 mM Tris-HCl, pH 8.0. For anion-exchange chromatography, the pooled fractions were applied to a DEAE-Memsep cartridge (Millipore) equilibrated with 20 mM Tris-HCl, pH 8.0. After sample application, the cartridge was washed with 20 mM Tris-HCl, pH 8.0. Bound proteins were eluted with a linear salt gradient (0 to 250 mM NaCl) in 20 mM Tris-HCl, pH 8.0. GP64sol^{Op} eluted as several peaks at salt concentrations from 75 to 150 mM NaCl. The fractions containing GP64sol^{Op} were pooled, and Tween 20 was added to 0.1% vol/vol and sodium azide was added to 0.02% wild-type/vol. The pooled fractions were concentrated with Centriprep 30k MWCO ultrafiltration units. For gel filtration chromatography, the concentrated fractions were applied to a 94 cm x 2 cm column of Sephacryl S400HR equilibrated with 200 mM NaCl, 20 mM NaPi, pH 7.0. The peak fractions containing GP64sol^{Op} were pooled and concentrated as above, and aliquots of GP64sol^{Op} were stored at -80°. The final purity of GP64sol^{Op} was ≥ 95% as judged by densitometric quantification of Coomassie-blue stained SDS-PAGE gels. For protease resistance assays, a partially purified preparation of GP64sol^{Op} was prepared and used. Supernatants of cells infected with vAcGP64sol^{Op} were collected as before and incubated with ConA beads as described above, then protein was precipitated in 10% ammonium sulfate. GP64sol^{Op} was further purified by gel filtration chromatography as described above. Purity of partially purified GP64sol^{Op} was estimated at ~ 60% by Bradford assay and Coomassie stained SDS-PAGE gels, and confirmed by Western blot analysis.

Glycosidase treatment, protease resistance, and reduction of GP64sol^{Op}. For glycosidase digestions, 2 µg of purified GP64sol^{Op} was digested with either 0.5 units of Endo F (Boehringer) or 0.01 units of Endo H (Boehringer) for 1 hour in 10 mM sodium phosphate buffer pH 7.0 at 37 °, then electrophoresed on 6% SDS-PAGE gels.

To compare the protease resistance profiles of GP64sol^{Op} and native OpMNPV GP64, 0.5 µg of secreted soluble GP64 (GP64sol^{Op}) and 1.0 µg of OpMNPV budded virions were each treated with 0.1 mg/ml proteinase K for 10 min at 56°. Digestion products were examined by electrophoresis on SDS-PAGE gels and Western blot

analysis with MAb AcV5 (97). For comparisons of oligomerization and the susceptibility of oligomers to reduction by DTT, purified GP64sol^{Op} (0.5 µg) or OpMNPV budded virions (1.0 µg) were incubated with increasing concentrations of DTT at 37° for 5 min. Trimerization and reduction were examined by preparing proteins in 37.5 mM Iodoacetamide, 2% SDS (no β-mercaptoethanol) and electrophoresing proteins on a 6% nonreducing polyacrylamide gel as described earlier (184), followed by Western blot analysis using MAb AcV5.

Binding, infectivity, and competition assays. To measure the effects of GP64sol^{Op} competition on BV binding, we used recombinant virus vAchsZ (which constitutively expresses β-galactosidase in the early phase) for a sensitive single cell infection assay. To demonstrate the linearity of the assay, Sf9 cells (3 X 10⁵) were infected with various concentrations of vAchsZ virions (MOIs ranging from 0.0125 to 0.2) by incubating virus with cells for 1 hour at 4°. Cells were washed three times in complete TNM-FH medium at 4°, then incubated for 24 h in complete TNM-FH medium at 27°, fixed 10 min in 0.5% gluteraldehyde in PBS at RT, and stained for β-galactosidase activity using 1 mg/ml X-gal in PBS + 5 mM potassium ferricyanide, 5 mM potassium ferrocyanide, and 1mM MgSO₄ (247). For each virus dilution, three wells of cells were infected and the number of stained cells in each well were counted. Data presented (Fig. 3) represent the average and standard deviation (error bars) of data from three wells. For competition assays, Sf9 cells (3 or 6 x 10⁵) were preincubated with various concentrations of competitors for 1.5 h at 4°, then BV of vAchsZ were added and incubated with agitation for 1 h at 4°, and cells were processed and assayed as described above. For some experiments, higher or lower MOIs of vAchsZ were used but in all cases, MOIs fell within the linear range of the assay (as established above, Fig. 3A). Viruses (AcMNPV and OpMNPV) used as competitors in binding assays were inactivated by addition of psoralen (4'-aminomethyl-Triosalen, Sigma) to a final concentration of 1 mg/ml followed by crosslinking for 10 minutes with a UV transilluminator (312 nm). Inactivation of viral infectivity was confirmed by examining infectivity on Sf9 or Ld652Y cells as described above.

For competition assays, protein competitors consisted of highly purified GP64sol^{Op} and a negative control, Bovine Serum Albumin (BSA; Sigma Chemicals). As additional controls, protein competitors were also treated with chymotrypsin (2 mg/ml) at 37° for 30 min. Reactions were terminated with 1 µM Leupeptin, 1 µM Pepstatin A and 4 µM Pefabloc. Complete proteolysis of GP64sol^{Op} was assessed by electrophoresis and examination on 8% polyacrylamide gels. As an additional control, DTT was added to a final concentration of 10 mM, and samples were incubated at 95° for 20 min. After treatment in DTT, protein samples were diluted 100x to a final concentration of 0.1 mM DTT and applied to cells as competitors. To confirm that this concentration of DTT did not interfere with infection, cells were also preincubated with 0.1 mM DTT prior to infection with vAchsZ in the absence of competition.

BV binding, entry, and endocytosis assays. For analysis of virion binding at the cell surface and entry after binding, BV of virus vAchsZ was bound to Sf9 cells at 4° for 1

h, and cells were washed in complete TNM-FH at 4°. In initial experiments, subtilysin was added to a final concentration of 2 mg/ml either before, or after shifting cells to 27° and incubating 1 h. As controls, BV were also pretreated with subtilysin (2 mg/ml) prior to binding BV to Sf9 cells. For studies of virion entry, BV of vAchsZ were bound to Sf9 cells at 4° for 1 h, then the temperature was shifted to 27° for increasing periods of time. At the end of each time interval at 27°, cells were treated with 2 mg/ml subtilysin for 15 min at 37° to inactivate or remove virions remaining at the cell surface. This concentration of subtilysin was previously determined to inactivate BV when BV were treated prior to binding to host cells (not shown). Cells were then washed three times with complete TNM-FH medium, incubated for 20 h at 27° in TNM-FH complete medium, then fixed and stained as described above, and scored for single infected cells. To examine the kinetics of virion release from the endosome, virions were bound to cells for 1 h at 4°. The temperature was then shifted to 27° for increasing time intervals as described above. At the end of each interval, media was exchanged for TNM-FH containing 25 mM ammonium chloride or 0.75 mM chloroquine, then incubated 20 h at 27° and assessed for single cells expressing β -galactosidase activity.

Acknowledgements

The authors thank Guangyun Lin and Marlinda Lobo de Souza for assistance with competition experiments and Jeffrey Slack for technical assistance. This work was supported by NIH grant AI 33657.

Chapter 6

Characterization of the *ORF119-gp64-p74* locus of *Anticarsia gemmatalis* Multicapsid Nucleopolyhedrovirus

Abstract

The *Anticarsia gemmatalis* Multicapsid Nucleopolyhedrovirus (AgMNPV) is successfully utilized in biological insect pest control but little is known of its molecular biology and its relatedness to other better characterized baculoviruses. In this study, we examined a 12.5 kbp area of the AgMNPV genome which contains homologs to the *lef-7*, *gp64*, *p24*, *gp16*, *pp34*, *alkaline exonuclease*, *p26*, *p10*, and *p74* genes of *Autographa californica* Multicapsid Nucleopolyhedrovirus (AcMNPV). Comparison of AgMNPV genes to homologs from four other Nucleopolyhedroviruses (AcMNPV, *Bombyx mori* MNPV (BmNPV), *Orgyia pseudotsugata* MNPV (OpMNPV), and *Choristoneura fumiferana* MNPV (CfMNPV)), suggests that AgMNPV is most closely related to OpMNPV and CfMNPV. Gene organization in the *lef7-gp64-p74* region was generally similar with several notable differences. Among these differences were the absence of homologs to the *chitinase*, *cathepsin*, and *p35* genes of AcMNPV, the presence of a small ORF with homology to the 3' end of the AcMNPV *p94* gene, and the presence of a 195 nt *hr*-like repeat region between the homologs of AcMNPV *ORF119* and *120*. This repeat region was unable to support plasmid replication in a transient replication assay. Comparison of AgMNPV GP64 to six other baculovirus GP64s showed that a) the ectodomain is highly conserved (~ 77 to 82% amino acid identity between the various GP64s), b) the AgMNPV GP64 transmembrane (TM) domain is the least conserved among the various GP64 TM domains, and c) the cytoplasmic tail domain (CTD) of AgMNPV is truncated, consisting of only two arginines. To examine functional similarities between the AgMNPV GP64 protein and other baculovirus GP64s, we examined the pH requirements for triggering membrane fusion in syncytium formation assays. The maximum pH required for triggering AgMNPV GP64-mediated membrane fusion was identical to that determined for OpMNPV GP64, and similar to that for AcMNPV GP64. Implications of these observations are discussed.

Manuscript in preparation:

Oomens, A.G.P., M. Lobo de Souza, J.M. Slack, B.M. Ribeiro, and Gary W. Blissard. Characterization of the *ORF119-gp64-p74* locus of *Anticarsia gemmatalis* Multicapsid Nucleopolyhedrovirus.

Introduction

Baculoviruses are large double stranded DNA viruses of invertebrates that have been used as biological control agents and as vectors for eukaryotic gene expression and protein production. Most detailed studies of baculovirus molecular biology have focussed on the following baculoviruses: *Autographa californica* Multicapsid Nucleopolyhedrovirus (AcMNPV), *Bombyx mori* NPV (BmNPV), *Orgyia pseudotsugata* MNPV (OpMNPV), and *Lymantria dispar* MNPV (LdMNPV), of which the complete genomic sequences are now available ((2); Accession number L33180; (1, 141)). Because in most cases, wild-type AcMNPV is not sufficient for effective biological control in commercial agricultural settings, many studies have attempted to improve its properties as a biological control agent by adding foreign genes. In contrast, a related baculovirus, *Anticarsia gemmatalis* MNPV (AgMNPV), has been highly successful as a biological control agent in agriculture and is currently used for insect control on over one million hectares of soybeans in Brazil. Thus, AgMNPV may represent the most successfully used baculovirus in agriculture worldwide. Unlike AcMNPV, little is known of the molecular biology of AgMNPV and its degree of relatedness to other better characterized baculoviruses.

AgMNPV is classified as a member of the Nucleopolyhedroviruses (NPVs), one of two genera within the family Baculoviridae. Because of a lack of extensive sequence data outside the few well studied viruses above, the degree of relatedness of viruses within the NPVs is not well understood. Studies of the AgMNPV genome to date have focused on restriction enzyme mapping (120), examination of repeated sequences homologous to the AcMNPV and OpMNPV *hr* regions (33, 59), and physical mapping and characterization of the *polyhedrin* gene (287). Comparison of *polyhedrin* gene sequences suggested that within the Lepidopteran NPVs, at least two evolutionarily divergent groups exist, and that AgMNPV clustered with AcMNPV, OpMNPV, and BmNPV, designated NPV group I (286). Those studies also showed that AgMNPV appears more distantly related to baculoviruses of designated NPV group II, such as *Mamestra brassicae* MNPV (MbMNPV), *Panolis flammea* MNPV (PfmNPV), *Spodoptera frugiperda* MNPV (SfMNPV), and *Spodoptera exigua* MNPV (SeMNPV). The division of the NPVs into groups I and II, and the placement of AgMNPV within the group I viruses was supported by a recent phylogenetic study (17), in which PCR amplified sequences based on *polyhedrin* and *DNA polymerase* genes were examined.

All previous phylogenetic studies were based on the comparison of a single AgMNPV gene with that of other baculoviruses. In the study presented here, we examine a continuous 12.5 kbp region of the AgMNPV genome, which contains the *gp64* gene, plus homologs to the *ORF119*, *ORF120*, *ORF121*, *lef-7*, *gp64*, *p24*, *gp16*, *pp34*, *alkaline exonuclease*, *p26*, *p10*, and *p74* genes of AcMNPV. This region is compared to four other NPVs, AcMNPV, BmNPV, OpMNPV, and *Choristoneura fumiferana* (CfMNPV), generating a view of the comparative gene organization of this genomic region. One observed difference was the presence of a short sequence with

homology to various baculovirus *hrs*. This sequence was subcloned and analysed in a transient replication assay (134). Other observed differences include the absence of *chitinase*, *cathepsin*, and *p35* genes, the presence of a short sequence encoding a protein with homology to the C-terminus of AcMNPV P94, and the presence of a homolog to (CfMNPV) hypothetical protein P22.2. Hypothetical translation products of the AgMNPV ORFs were subjected to Blast searches, and sequence alignments between the putative AgMNPV proteins and homologs from other baculoviruses revealed that the highest average degree of amino acid identity occurred between AgMNPV, OpMNPV, and CfMNPV proteins. Among all the putative AgMNPV protein homologs examined, GP64 displayed the highest amino acid identity between the different viruses. Analysis of AgMNPV virion-associated GP64 revealed that its molecular weight is similar to GP64 of AcMNPV and OpMNPV, and syncytium formation assays based on transient expression of the AgMNPV *gp64* gene show that the pH requirement for GP64-induced membrane fusion is identical to that of OpMNPV GP64 and similar to that of AcMNPV GP64, despite significant differences in the TM and CTD domains. A multiple sequence alignment with all known baculovirus GP64s and two distant GP64 homologs in Thogoto-like orthomyxoviruses, Thogoto (THO) virus envelope protein (THO env; (201)) and Dhori (DHO) virus envelope protein (DHO env; (54)), identified seven blocks of high amino acid identity, and displays a general GP64 structural organization which may yield insight into the structure-function of the GP64 protein.

Results

To address the relatedness between AgMNPV and other, well characterized baculoviruses, we selected the highly conserved *gp64* gene and flanking regions for analysis of gene organization. To locate the *gp64* gene, a probe based on three overlapping portions of the AcMNPV *gp64* gene, was used for moderate-stringency Southern blot hybridizations. Using this technique, a 5.4 kb HindIII fragment of the AgMNPV genome was identified. Because preliminary analysis showed that the HindIII-I fragment contained only a portion of the *gp64* ORF (3' end), a larger AgMNPV fragment (12.5 kb, BamHI-D) containing the entire *gp64* ORF was subcloned from the AgMNPV genome. This 12.5 kb BamHI-D fragment was subsequently sequenced.

Gene organization in the ORF119-gp64-p74 region. The arrangement of genes in the selected 12.5 kb genomic segment of AgMNPV was compared to corresponding regions of OpMNPV, CfMNPV, AcMNPV, and BmNPV in Fig. 1. The complete corresponding loci are available from complete genomic sequences for OpMNPV, AcMNPV, and BmNPV. For CfMNPV, the majority of the corresponding locus was assembled from overlapping sequences available in the GenBank database (see Materials and Methods), resulting in a genomic segment from *gp64* to *p74*. While in

general the region was found to be similar in gene order and orientation, several striking differences were observed:

- *Chitinase* and *cathepsin* genes are absent from this region of the AgMNPV genome. In AcMNPV, BmNPV, OpMNPV, and CfMNPV, GP64, chitinase, and cathepsin are highly conserved baculovirus proteins, and the genes encoding these proteins are found clustered together. In the corresponding location of the AgMNPV genome however, *chitinase* and *cathepsin* genes are absent. In addition, attempts to locate a *cathepsin* gene homolog in the AgMNPV genome using an AcMNPV-*cathepsin* probe in Southern blot hybridization assays, identified no cross-hybridizing DNA fragments (data not shown). Because like *gp64*, the *cathepsin* gene is highly conserved between AcMNPV, BmNPV, OpMNPV, and CfMNPV, and stringency hybridization conditions were used similar to those used to locate the *gp64* gene, these data suggest that the *cathepsin* gene may not be present in the AgMNPV genome. Attempts to detect cathepsin activity from AgMNPV-infected cells were also negative (J. Slack, personal communication).

- A small ORF encoding a protein with similarity to the C-terminus of AcMNPV *p94* is located immediately upstream of the *p26* gene. This is particularly interesting because the presence of *p94* varies considerably between AcMNPV, BmNPV and OpMNPV. While the AcMNPV genome contains two major ORFs (*p35* and *p94*) between the *alk-exo* and *p26* ORFs, the OpMNPV genome contains neither the *p35* nor *p94* ORF, and the BmNPV genome contains the *p35* ORF and a small portion of the *p94* ORF (Fig. 1). Like AgMNPV, the BmNPV *p94* portion maps to the C-terminus of the AcMNPV P94 homolog, however to a different location than the BmNPV *p94* portion. Unlike AcMNPV *p94*, the ATG codon of the small AgMNPV ORF does not conform to Kozak's rules and an early (or late) consensus transcription motif (TATA; CAGT) is not present, suggesting that it may not be transcribed. A larger (and perhaps functional) AcMNPV P94 homolog has been identified only in *Leucania separata* NPV (LsNPV)(119), but this *p94* homolog is located in a different locus since it is found adjacent to AcMNPV *ORF61*, *60*, and *59* (*lef8* locus) homologs from LsNPV. The presence of *p94* in AcMNPV and LsNPV, the absence of *p94* in OpMNPV, and the presence of portions of *p94* in AgMNPV and BmNPV suggests the possibility that the AcMNPV or LsNPV genome may more closely

FIG. 1. Genomic heterogeneity in the *ORF119-gp64-p74* genomic region of five distinct Nucleopolyhedroviruses. The 12.5 kb BamHI-D fragment of AgMNPV (isolate 2D) was sequenced and compared to the corresponding region in OpMNPV (1), AcMNPV (2), BmNPV (GenBank accession number L33180) and CfMNPV (see Materials and Methods). Positions indicated at the beginning and end of each genomic fragment are the positions within the complete genomes, except for AgMNPV and CfMNPV. At the bottom, a bar indicates the scale (basepairs). Large differences between the genomic regions are illustrated by shaded areas. (**Insert**) Two regions (represented by horizontal bars) with significant sequence similarity to a previously identified AgMNPV tandem repeat region ((59), are present between *ORF119* and *120* (boxed area within AgMNPV sequence), and are designated repeat-1 and repeat-2. Both repeat regions display significant nucleotide identity with various baculovirus *hrs* (see text). Numbers indicated represent the position of these repeat regions within the 12.5 kb AgMNPV genomic fragment. The positions of two imperfect palindromes, located within these repeat regions, are indicated.

resemble an ancestral state in which the large *p94* gene was present. Subsequently, *p94* may have been relocated or partially or completely lost as these viruses diverged.

- AgMNPV contains a homolog to hypothetical protein p22.2 of CfMNPV, while a P22.2 homologous ORF is absent from OpMNPV and AcMNPV (Fig. 1). The AgMNPV homolog encodes a predicted protein of 211 amino acids displaying 61.6% identity with CfMNPV P22.2. The functional relevance of *p22.2* is not known.

- Putative *hr* sequences. AgMNPV contains a sequence, located between *ORF119* and *120* homologs, with similarity to various baculovirus *hr* regions. This area displays two regions, (nt 891 to 992 and 1005 to 1084), with a high degree of nt identity to each other, each containing an ~ 40 nt imperfect palindrome (Fig. 1). Both regions show similarity to nt 488-564 of a previously published AgMNPV genomic repeat region (59), and are designated repeat-1 (102 nt) and repeat-2 (80 nt). In addition, Blast searches reveal homology of repeat-1 to an OpMNPV enhancer region downstream of the *IE2* gene (250), and to the 3' end of the CfMNPV *IE2* ORF (GenBank accession number U72030). AgMNPV repeat-2 shows homology to the same OpMNPV enhancer region, CfMNPV *IE1*-enhancer region (GenBank accession number L04945), CfMNPV *hr1* region (282), BmNPV *hr1* region (156), and AcMNPV *hr4* region (80). It has been speculated that *hrs* may serve as hot spots for genomic rearrangements (167), and they can serve as enhancers of transcription (81, 250) and putative origins of replication (135). Although this region is small in comparison to characterized *hr* sequences from AcMNPV and other repeats in AgMNPV, we examined whether the short AgMNPV repeat sequences could serve as an origin of replication in an infection-dependent, transient replication assay (135). Both AgMNPV repeat-1 and -2 were examined separately as well as combined (as present within the AgMNPV 12.5 kb sequence). Repeats were PCR amplified and cloned into pGEM-T vector plasmids. A known AcMNPV *hr* (*hr5*) was cloned into the same plasmid as a positive control. Unlike the AcMNPV *hr5*-containing plasmid which displayed substantial replication, neither of the plasmids containing AgMNPV repeats was able to support plasmid replication in the context of AgMNPV or AcMNPV viral infection (data not shown). It is possible that additional factors are necessary to allow replication of the AgMNPV repeat regions in a transient assay, but the above result suggests that these small regions alone do not serve as origins for AgMNPV viral replication.

Amino acid identities show that AgMNPV is closely related to OpMNPV and CfMNPV, and confirm the proposed phylogenetic placement of AgMNPV within one NPV subgroup. Figure 2A shows amino acid sequence identities between all proteins (50 amino acids or longer) predicted by the ORFs in the AgMNPV 12.5 kb sequence and their homologs in other baculoviruses. Protein homologs were identified from the GenBank database by Advanced Blast searches. *ORF119* and *p74* from the AgMNPV sequence are incomplete: The protein predicted by AgMNPV *ORF119* constitutes ~ 50% (the C-terminal half) of its AcMNPV homolog, whereas AgMNPV *P74* represents the C-terminal ~ 29% of AcMNPV *P74*. Figure 2B graphically displays percent identity

A

position	hAc ORF	name	length (aa)	baculovirus											orthomyxovirus						
				Op	Cf	Ac	Bm	Bs	Ld	Spil	Ls	Pn	Split	Ep	Se	Af	DHO	THO	Batken		
1 - 828	119	-	274 (p)			75.2		77	67.2	44.2	32.8	27.4									
1107 - 1358	120	U1	83			60.2		54.2	63												
1625 - 1341	-	U2	94																		
1471 - 1815	-	-	114																		
1764 - 1567	122	-	65			52.3		38.5	43.1												
1917 - 2645	124	-	242			62		40.5	40.1												
3394 - 2702	-	U3	230																		
4067 - 3420	125	lef7	215			54.4		30.7	30.2												
5781 - 4282	128	gp64	499			78.6	77	76	74.5						75.8		75.2	32.3	32.1	23.7*	
6118 - 6687	129	p24	192			79.2	77.8	62.5	59.4			40*									
6712 - 7026	130	gp16	104			83.7	82.7	76	76												
7074 - 7955	131	pp34	283			84	77.1	61.8	61.8	31*		29.4									
7958 - 8614	132	-	218			41.3	43.1	28.4	32.1												
8620 - 9882	133	alk-exo	420			70.7	68.3	56.7	56.7			42.4									
10563 - 9928	-	(Or) p22.2	211				61.6														
10896 - 10682	134	p84	74				29.7*					29.7*									
10898 - 11008	136	p26	236			64.4	72	51.3	49.2	34.3							35.2*				
11684 - 11945	137	p10	93			83.9	44.1	38.7	32.3	32.3*				80.6			22.0				
12516 - 11948	138	p74	188 (p)			86.8	86.2	75.5	73.9	47.8	49.5	42	36.3		44.1						

(* Derived from partial sequence)

B

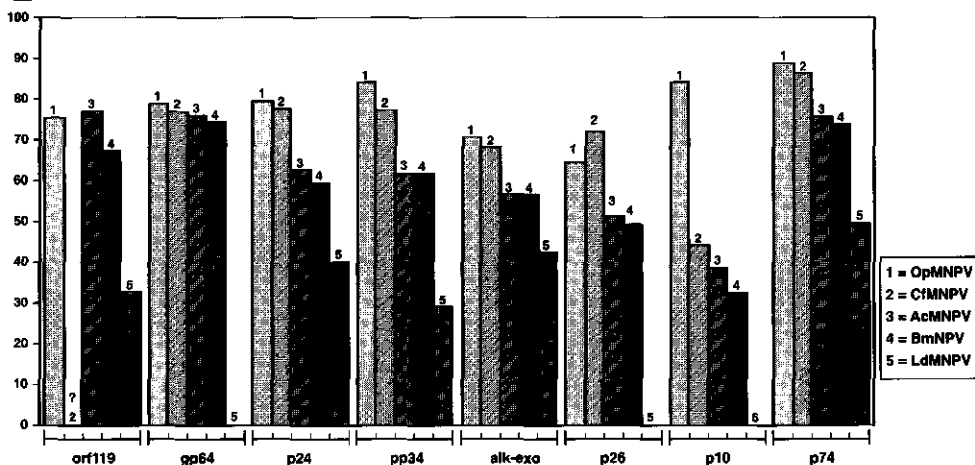


FIG. 2. (A) Amino acid identities between translated putative ORFs of AgMNPV and other baculoviruses. Positions of the putative ORFs within the 12.5 kb sequence are indicated in column 1. In column 2 (hAc ORF) the AcMNPV homologs to the AgMNPV ORFs are indicated according to Ayres (2), except position 10563-9928 (homolog to CfMNPV hypothetical 22.2kD protein), and three ORFs (U1, 2 and 3) with no observed homologies. Column 3 shows commonly used names of some of the proteins. Column 4 shows the length of the predicted AgMNPV proteins in amino acids. Displayed percentages are the number of identical amino acids between AgMNPV and a homolog/total number of amino acids of the AgMNPV protein x 100%. Where homologies were to partial proteins only, the percentage is followed by *, see specific comments in 'Results' section. **(B)** Graphic representation of selected amino acid identities of Figure 2A, with amino acid identities on the Y-axis and selected viral proteins of five different viruses (OpMNPV [1], CfMNPV [2], AcMNPV [3], BmNPV[4], LdMNPV [5]) on the X-axis. A possible CfMNPV homolog to ORF119 is indicated by '?', as the ORF119-genomic region of CfMNPV is not available in the GenBank database.

for a selection of proteins from Figure 2A, and demonstrated that AgMNPV is closely related to OpMNPV and CfMNPV: Except for P10 and ORF132, all identities are higher than 64%. Between AgMNPV and two other proposed NPV group I viruses, AcMNPV and BmNPV, amino acid identities are also high (ranging from 28.4 to 77%), but lower than the identities between AgMNPV and OpMNPV or CfMNPV. Analysis of the complete LdMNPV genome sequence (141) revealed homologs to 95 AcMNPV ORFs, although there was only limited similarity in the organization and order of genes. Out of the 19 selected ORFs within the AgMNPV sequence, homologs for only five (*ORF119*, *p24*, *pp34*, *alk-exo.*, and *p74*) were found in LdMNPV, with identities ranging from 29.4 to 49.5%. Relatively low identities with LdMNPV support the conclusion that LdMNPV is phylogenetically relatively distant from the proposed group I NPVs (141). Relatively low amino acid identities are also observed between proteins of AgMNPV and group II NPVs (*Buzura suppressaria* SNPV [BsNPV], SeMNPV, *Spodoptera litura* MNPV [SpltNPV], *Spodoptera littoralis* MNPV [SpliNPV]). This, combined with the high identity between AgMNPV and OpMNPV/CfMNPV/AcMNPV/BmNPV correlates well with the placement of the latter viruses within one subgroup (I) of the NPVs.

Specific comments on amino acid identities of selected individual proteins:

ORF129/p24: Only a partial AgMNPV P24 protein (C-terminal amino acids 125 to 192) showed significant homology to a hypothetical LdMNPV 11k protein with unknown function.

ORF131/pp34: Protein alignments revealed an unusually large difference in the C-terminus between AcMNPV and BmNPV, two viruses that otherwise display a very high degree of amino acid identity. AcMNPV PP34 appeared truncated at cys249, compared to other PP34 proteins. Screening for alternate reading frames in the C-terminus of this AcMNPV PP34 coding sequence revealed that possibly a frame shift was introduced due to a one bp deletion at position 111647 (2). Introduction of one nt (arbitrarily an 'A') at that position increased the length of AcMNPV PP34 from 252 to 322 amino acids (similar to BmNPV PP34: 315 amino acids) and amino acid identity from 36.9 to 61.9%. In Gombart *et al.* (70), a frame shift-corrected version of AcMNPV PP34 was used for alignments with OpMNPV PP34; However, the source of AcMNPV PP34 however was reportedly the same as the one used in the complete genome of (2, 178), with no mention of the discrepancy in the C-terminus. Because we consider the frameshift-corrected version (322 amino acids) more likely than the shorter version of 252 amino acids, the data reported in Fig. 2 reflect identity with an AcMNPV PP34 protein of 322 amino acids (61.9%). The BsNPV PP34 sequence (102) lacked an N-terminal methionine and aligned with the AgMNPV PP34 sequence starting at amino acid 86. The BsNPV PP34 sequence therefore appeared incomplete and was aligned with a partial AgMNPV PP34 protein only (amino acid 86 to 293).

ORF133/alk-exo: In addition to the baculovirus homologies, alignments showed similarities with two different herpesvirus proteins: a bovine herpes virus 1 DNAse protein (257) and the pseudoRabies *UL12* gene product (with alkaline exonuclease

function; (40)). Although average amino acid identities (22.4% and 18.6% for bovine herpes 1 and Pseudorabies respectively, not shown in Fig. 2A) were relatively low, a cluster of amino acids with high identity was found in the same region of the putative AgMNPV alk-exo protein: amino acids 55 to 89. These amino acids may represent a conserved domain in AgMNPV ORF133 involved in its putative function.

hCf p22.2: and **ORF134/p94:** See earlier.

ORF137/p10: Sizes of P10 proteins of the various NPVs are uniform (~ 90 amino acids). One exception is BmNPV, of which P10 (from complete genome (100, 155)) is a truncated version with a length of 70 amino acids. This truncation is the result of a stop codon introduced by a frameshift ~ 20 amino acids before the C-terminus. This truncation was found in several natural isolates and does not seem to be a cloning artefact (100), perhaps most convincingly shown by the fact that a one bp change in the downstream sequence creates a putative polyA signal, conserving well the spacing between stop codon and polyA signal (90 nt compared to ~ 88 nt for AcMNPV). Therefore, the truncated P10 version from the complete BmNPV genome was used for the alignments in Fig. 2. There are however reports of full length BmNPV P10 proteins (189, 289). It is possible that the P10 C-terminus (which is involved in the formation of fibrillar structures) is not essential for the survival of the virus or that the truncation is an adaptation to a particular environment.

ORF138/p74: Homologs to the partial sequence of AgMNPV P74 were found through Blast searches in 9 different baculoviruses, belonging to both postulated NPV groups (I and II). Across NPV group I and II, P74 is the most conserved protein of the examined AgMNPV sequence, with identities ranging from 49.5 to 88.8%.

ORF128/gp64: Fig. 2B shows amino acid identities ranging from 74.5 to 78.6% between AgMNPV and four other GP64s, however in contrast to P74, GP64 has been found within proposed group I of the NPVs only. The fact that GP64 is so highly conserved between the different baculoviruses, (all known GP64s display between 70 and 80% amino acid identity), suggests that GP64 is either a extremely critical factor in their life cycles, or that the acquisition of GP64 is a relatively recent event in baculovirus evolution. GP64 is a key factor in systemic spread of the virus within the insect host (172). The absence of *gp64* from the genome of the evolutionarily distant LdMNPV suggests that GP64 may be an attribute specific to one subgroup (I) only, and raises the question of whether all baculoviruses have common strategies for cell-to-cell transmission or whether alternate mechanisms exist for these important steps in the baculovirus life cycle. Previous data indicate that GP64 structure and function is conserved not only between the group I NPVs but also between baculoviruses and a Thogoto-like genus within the Orthomyxoviridae. A remarkable similarity (~32% overall amino acid identity, local clusters of strong amino acid identity, conserved cysteine residues and hydrophobicity profiles; (173)) between GP64 and the envelope protein of two tick-transmitted orthomyxoviruses: Thogoto (THO) and Dhori (DHO) virus. This homology strongly suggests a common ancestry for GP64 and the THO and DHO envelope proteins.

Comparison of GP64 homologs from different baculoviruses and THO-like orthomyxoviruses. Among baculovirus GP64s, amino acid identity is exceptionally high throughout the ectodomain. The multiple sequence alignment (Fig. 3) demonstrates that this is also the case for AgMNPV GP64, with ectodomain amino acid identities ranging from 77.5 to 81.9% between AgMNPV and other GP64s. In contrast, among all GP64 proteins, the AgMNPV GP64 transmembrane (TM) domain is the least conserved, with only ~22% identity with other GP64s, although most substitutions are of a conservative nature, retaining the overall hydrophobicity of the domain. In addition, the AgMNPV CTD is

B

		Percent Similarity									
	1	2	3	4	5	6	7	8	9		
1	█	77.9	76.4	74.1	74.5	73.5	75.0	27.6	27.0	1	Ag GP64
2	25.2	█	88.9	78.8	79.1	78.8	78.9	28.0	26.0	2	Op GP64
3	27.5	12.1	█	80.1	80.5	79.5	79.7	27.8	26.6	3	Cf GP64
4	31.5	24.6	22.9	█	98.7	94.9	74.4	27.7	25.8	4	Af GP64
5	31.1	24.2	22.6	1.2	█	95.9	74.6	27.8	25.7	5	Ac GP64
6	32.4	24.9	24.0	5.3	4.1	█	74.4	27.7	25.7	6	Bm GP64
7	29.6	25.1	24.5	31.2	31.1	31.2	█	27.1	26.0	7	Ep GP64
8	165.1	162.7	164.0	166.1	165.2	166.1	169.5	█	33.5	8	DHO Env
9	164.8	178.0	173.4	176.5	176.5	178.0	179.6	134.6	█	9	THO Env
	1	2	3	4	5	6	7	8	9		

C

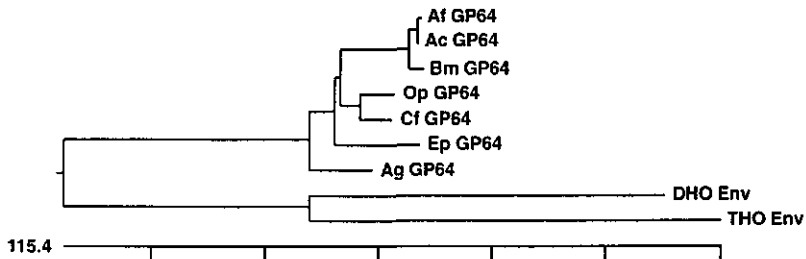


FIG. 3. (A) Multiple amino acid sequence alignment (Clustal method with PAM250 weight residue table) of seven different baculovirus GP64s (AgMNPV, OpMNPV, CfMNPV, AcMNPV, BmNPV, EpNPV, and AfNPV) and envelope proteins from two THO-like orthomyxoviruses (Thogoto [THO] and Dhori [DHO] virus). The display of identities is based on comparison with AcMNPV GP64 (center sequence). Amino acids differing from those of AcMNPV GP64 are indicated as shaded boxes. Numbered boxes represent areas of high amino acid identity (area 1 to 7). Boxes named 'fusion' and 'trimerization' represent a predicted hydrophobic domain of OpMNPV GP64 involved in membrane fusion (171), and a predicted hydrophobic domain of OpMNPV GP64 involved in trimerization (171). Signal peptide of AcMNPV GP64 (chapter 5) and predicted AcMNPV GP64 TM domain are also indicated. **(B)** Percentages similarity and divergence between the GP64 homologs based on the alignment of Fig. 3A. Similarity is calculated as 100x sum of the matches/length - individual gap residues. Divergence is calculated as 100x the distance of individual sequences divided by the total distance (see Materials and Methods). **(C)** GP64 phylogenetic tree based on similarities and divergence of Fig. 3B. The length of a pair of branches represents the relative distance between a pair of sequences. The scale beneath the tree indicates the relative distance between all sequences involved.

truncated, consisting of only two arginines. The CTD truncation correlates well with our previous demonstration that, although the CTD increases budding efficiency, this domain is dispensable for propagation of the virus in cell culture. The functional homology and sequence conservation between baculovirus GP64 and THO and DHO envelope proteins can be used as a tool to identify functional domains within GP64. At least seven clusters of relatively high amino acid sequence identity can be identified among baculovirus GP64 and THO/DHO env proteins. Based on amino acid numbers from the AcMNPV GP64 protein, these are designated: region 1 (aa 21-33), region 2 (aa 66-86), region 3 (aa 102-128), region 4 (aa 142-165), region 5 (aa 340-372), region 6 (aa 381-402), and region 7 (aa 438-465). A region that contains a predicted coiled-coil motif (amino acids 301-337) displays lower amino acid sequence identity, but leucine and methionine residues predicted to constitute the hydrophobic face of the alpha helix, are conserved. Notably also throughout the GP64 ectodomain is the conservation of the location of cysteine residues. This conservation is also evident in the THO and DHO env proteins, and suggests conserved locations of disulfide bridges. The strong conservation in the ectodomain does not include a membrane fusion and oligomerization domain previously characterized in OpMNPV GP64 (171). Although these two functional domains (corresponding to AcMNPV amino acids 229/230 and 330-338 respectively) are well conserved among baculoviruses, they are only poorly to moderately conserved between GP64 and the envelope proteins of the THO-like viruses.

The phylogenetic tree in Fig. 3C, projects large evolutionary distances between the baculovirus GP64s as a group and DHO/THO envelope proteins. The THO and DHO envelope proteins also appear to be diverged significantly. In comparing and interpreting these projected distances, one should keep in mind the fact that THO and DHO virus are segmented ssRNA viruses. Their mutation and recombination frequencies may differ substantially from the ds DNA baculoviruses. Thus evolutionary rates may differ and divergence may be difficult to compare between these two groups. While the remaining conservation between envelope proteins of two such distant virus families suggests an essential nature and/or a relatively high intolerance for amino acid substitutions, recently completed baculovirus genomes demonstrate that at least some baculoviruses do not possess a *gp64* gene.

Molecular mass of AgMNPV GP64 from virions and pH requirement for membrane fusion of AgMNPV-gp64 transfected Sf9 cells. To compare the size of virion-associated AgMNPV GP64 to that of AcMNPV and OpMNPV, partially purified budded virions were electrophoresed on SDS-PAGE, transferred to membranes (Western blot), and incubated with MAb AcV5. The epitope recognized by MAb AcV5 (SWKDASGWS) is conserved between AgMNPV, AcMNPV, and OpMNPV, and resulted in detection of an AgMNPV GP64 protein band of ~ 60 kD, slightly smaller than the AcMNPV and OpMNPV GP64 proteins. The predicted AgMNPV GP64 protein is 13 amino acids shorter than AcMNPV GP64. In addition, carbohydrate modifications or phosphorylation

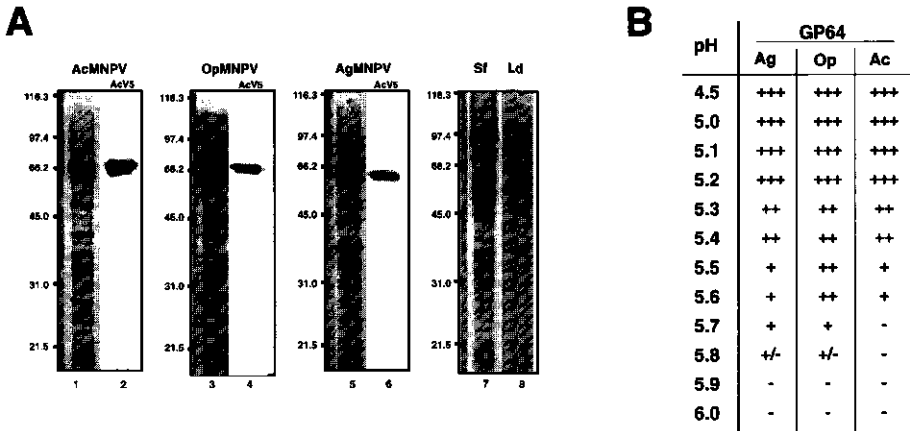


FIG. 4. (A) Detection of GP64 from budded virions of AcMNPV, OpMNPV, and AgMNPV. Sf9 cells (AcMNPV, AgMNPV), or Ld cells (OpMNPV) were infected at low moi and supernatants harvested at 4 days pi. Virions were isolated by centrifugation through a 20% sucrose cushion, resuspended in Laemli buffer and electrophoresed on 10% SDS-PAGE gels. Gels were stained with Coomassie blue (lanes 1, 3, 5, 7, and 8), or transferred to membranes, incubated with MAb AcV5 and visualized with an anti-mouse AP conjugate (lanes 2, 4, and 6). Lane 1 and 2: AcMNPV GP64; Lane 3 and 4: OpMNPV GP64; Lane 5 and 6: AgMNPV GP64. Lanes 7 and 8 are Coomassie stained uninfected Sf9 and Ld cell lysates respectively. **(B)** Syncytium formation after transient expression of AcMNPV, OpMNPV, and AgMNPV *gp64* in Sf9 cells. AcMNPV and AgMNPV *gp64* gene expression was driven by their respective wild-type promoters; OpMNPV *gp64* by a truncated OpMNPV *gp64* promoter construct. Amounts of GP64 on the cell surface for each construct were monitored by CELISA and adjusted to similar levels. At 36 h post transfection, cells were exposed to a range of pH values (4.5 to 6) for 5 min, further incubated in TNM-FH for 2 h, fixed, and scored for syncytium formation. Syncytium formation required ≥ 5 nuclei in each syncytial mass (++ syncytia abundant; + syncytia present but not abundant; +/- syncytia rare but present; - no syncytia observed).

may also cause variability in the molecular mass measured by SDS-PAGE electrophoresis. Low pH-induced membrane fusion is a function of GP64 necessary for its mechanism of entry by adsorptive endocytosis. Because truncations in the CTDs of some viral envelope proteins can modulate the ability to fuse membranes (174, 205, 235), the fusogenic capacity of AgMNPV GP64 and the pH value at which fusion is triggered, were compared to that of OpMNPV and AcMNPV GP64. First, AgMNPV GP64 was subcloned in a pBS-based plasmid vector with 392 nt of upstream sequence corresponding to nt 4037 to 6168 in the 12.5kb AgMNPV sequence (pBS-AgGP64). Because the level of GP64 expressed at the cell surface may be a factor in whether membrane fusion can be induced, MAb AcV5 was used in a modified cell ELISA assay (CELISA; (171)) to monitor the amount of each GP64 at the cell surface (data not shown). Based on the CELISA data, plasmid concentrations for cell transfections were adjusted, so that very similar levels of the various GP64s were present at the plasma membrane. AgMNPV, OpMNPV, or AcMNPV GP64-transfected cells were then exposed to a range of pH values (4.5-6.0) at 36 h. post transfection for 5 min, incubated in TNM-

FH for 2 hrs, and fixed with 0.5% glutaraldehyde in PBS (Fig. 4B). Syncytium formation was scored based on ≥ 5 nuclei per syncytial mass. The range of pH values at which AgMNPV GP64 induced membrane fusion was identical to that of OpMNPV and similar to that of AcMNPV. For AgMNPV and OpMNPV GP64s, the maximum pH at which syncytia were formed was 5.8, whereas for AcMNPV GP64 no membrane fusion was observed above pH 5.6. It is possible that the identical range of pH values at which AgMNPV and OpMNPV GP64 induced fusion, is a reflection of their high level of amino acid identity.

Discussion

Identities and similarities based on single proteins or genes are a useful tool to study phylogeny of baculoviruses. However these need to be considered jointly with other approaches for a broader view of baculovirus evolution. Analysis of multiple genes within a large genomic segment represents a more powerful approach, because it combines conservation between individual homologous genes and conservation of gene organization. Comparative analysis of the genomic structure of the 12.5 kb region of AgMNPV to OpMNPV, CfMNPV, AcMNPV, and BmNPV, may yield additional insight into the relatedness of the above NPVs and the potential relative importance of individual genes. Our study agrees well with the proposed placement of AgMNPV within one group of the NPVs. Within this subgroup, our data strongly indicates that AgMNPV is most closely related to OpMNPV, to which AgMNPV proteins revealed a high level of amino acid identity. Between AgMNPV and CfMNPV, almost equally high amino acid identities were observed, and (unlike any other NPV of this subgroup) these two viruses both possessed a gene encoding hypothetical protein P22.2. Of the more distantly related baculoviruses, most protein homologs were found among BsNPV and LdMNPV, but this likely reflects the large amount of sequence available from these viruses. For LdMNPV, a virus considered evolutionarily distant from the proposed group I NPVs, homologs were found for ORF119, P24, PP34, alk-exo., and P74. Of these, P74 displayed the highest percentage of amino acid identity. Thus, not only is P74 present across a wide variety of baculoviruses, it is also relatively well conserved. Such characteristics may yield clues to what some of the most conserved and critical functions and processes may be of the baculovirus life cycle. While comparison of the LdMNPV genome to that of AcMNPV revealed an average amino acid identity between homologs of ~ 41%, LdMNPV- and AcMNPV P74 were 61% identical (141). The most conserved proteins were those predicted by the *polyhedrin* and *ORF2* genes, while several other well conserved genes included: *lef 8*, *lef9*, *chitinase*, *cathepsin*, *ubiquitin*, *sod*, and *ctl*. Such proteins were likely acquired in an early evolutionary stage and were perhaps present in an ancestral baculovirus.

The absence of *cathepsin* and *chitinase* genes from this AgMNPV locus is interesting because the location of these genes, adjacent to the *gp64* gene, is very well

conserved in all other NPVs of this subgroup sequenced to date. Chitinase and cathepsin are widespread among the kingdoms and are present in all examined baculoviruses so far, albeit in sometimes different locations in different subgroups. They are known to be involved in viral directed liquefaction of the host, as *cathepsin* and *chitinase* deletion mutants each fail to liquefy infected caterpillars (179, 231) in an otherwise normal infection. Liquefaction is a result of degradation of cuticle and internal insect tissues, which require the synergistic action of cathepsin and chitinase and is thought to enhance the horizontal spread of the virus by increasing availability of polyhedra to feeding caterpillars. While the *cathepsin* gene is highly conserved among baculoviruses, Southern hybridization under moderate stringency conditions failed to detect a cathepsin homolog elsewhere in the AgMNPV genome. Absence or presence of *cathepsin* and *chitinase* genes can be conclusively demonstrated only by sequencing of the entire AgMNPV genome, and a baculovirus lacking chitinase and cathepsin would be exceptional. A possible absence of the *chitinase* and *cathepsin* genes from the AgMNPV genome might indicate that an unrelated functional homolog exists in AgMNPV or that cathepsin and chitinase-like enzymes may not be necessary for efficient propagation of AgMNPV through an insect population. It has been suggested that the *chitinase* gene may have been inserted into an ancestral baculovirus gene containing a signal sequence and a KDEL (ER retention) signal (167). The speculated absence of chitinase and cathepsin then might suggest that this acquisition occurred after the divergence of the AgMNPV lineage, or that the AgMNPV lineage lost the *cathepsin/chitinase* genomic region. Considering that AgMNPV is highly similar to OpMNPV (which like AcMNPV, BmNPV and CfMNPV, possesses both *chitinase* and *cathepsin* genes), the divergence of AgMNPV before acquisition of these genes would seem unlikely.

In several baculoviruses, tandem repeat sequences (*hrs*) have been demonstrated at various locations within the baculovirus genomes. Sequences with similarities to *hrs* have been demonstrated in AgMNPV as well. Past studies of plaque-purified AgMNPV isolates from field samples collected over different years in Brazil, identified repeat regions at four locations throughout the AgMNPV genome, one of which was located immediately upstream of the *p74* gene (map units 88.6 to 90.1, (59, 120)) This region contained repeats of 127 bp sequences each harboring two 30 bp imperfect palindromes and showed homology to *hrs* of AcMNPV and OpMNPV. One of the field isolates (AgMNPV-D7) had developed increased virulence for an alternate host (*Diatraea saccharalis*) after serial passage in this host, without affecting its virulence for *Anticarsia gemmatalis* (192). Upon characterization, a deletion was found consisting of 3 repeats in the *p74* repeat region, compared to prototype AgMNPV-2D (59). Approximately the same region (map units 88.7 to 94.3) had previously been identified as a region associated with genotypic variation (33). Although the deletion in AgMNPV-D7 may or may not be responsible for its increased virulence, the AgMNPV *hrs* may serve a similar role as proposed for other baculoviruses: to serve as prime areas for genomic rearrangements. In the AgMNPV GP64 genomic region examined in this study,

we also identified two short sequences with similarities to various baculovirus *hrs*. The two repeat regions also show strong nucleotide identity with the previously identified sequence within the *p74* repeat region identified in AgMNPV (161). The presence of a region with homology to the *hrs* in this AgMNPV locus may not be too surprising, as between baculoviruses only some *hrs* are conserved in location. In our transient replication assays we could not detect replication from the repeat regions identified in the 12.5 kb AgMNPV genomic segment. This may indicate that these repeat regions alone do not serve as an origin of replication. This does however not fully exclude an origin of replication or other function for this region. LdMNPV *hrs* for example had to be linked to AT-rich sequences before being capable of undergoing replication (194), and it is also possible that this region serves an enhancer function, analogous to AcMNPV (80) and OpMNPV *hrs* (250).

In previous studies, we characterized GP64 proteins of OpMNPV and AcMNPV. In this paper we found that the AgMNPV GP64 protein is very similar to the previously characterized GP64 proteins, displaying 78.5% amino acid identity with OpMNPV GP64, and 76% with AcMNPV GP64. Predicted TM domains and CTDs display less amino acid identity than seen with any of the other published GP64 sequences, while syncytium formation assays show that the maximum pH at which membrane fusion is induced is identical to OpMNPV GP64. Although GP64 is known to be an essential baculovirus protein (171), the recently completed LdMNPV genome contains no potential protein with homology to GP64. This brings forth the question whether LdMNPV (and possible other baculoviruses not containing a *gp64* gene) contains a functional homolog of GP64, or whether it uses alternate strategies for entry and exit of its host cell. It also raises the question of how widespread presence of the *gp64* gene is within the Baculoviridae. Although extensive sequence data are available for only a few baculoviruses, all viruses to date shown to contain a *gp64* gene, are phylogenetically placed within one proposed subgroup of the NPVs (group I; (286)). It is generally believed that MNPVs are not a monophyletic group, except for the proposed group I. If GP64 is restricted to the proposed group I baculoviruses only, it is possible that the acquisition of the *gp64* gene at some point in evolution may be a key factor in the existence of this subgroup I as a monophyletic group. The strong conservation between GP64 from the various baculoviruses may reflect its essential nature and with it an intolerance for amino acid substitutions. It is however also possible that the *gp64* gene was acquired at a relatively late stage in baculovirus evolution, and insufficient time has elapsed to allow divergence of the individual *gp64* genes. The latter fits well with previous suggestions (101, 286), whose phylogenetic studies indicate distinct evolutionary rates for proposed groups I and II, with radiation in group I apparently slower than in group II or occurring later. The phylogenetic tree in Fig. 3C suggests that, among the viruses in proposed NPV group I, AgMNPV GP64 may have been the first to branch from the ancestral GP64 protein.

A hint towards the evolutionary origin of GP64 was the finding that a GP64 homolog exists in the THO-like orthomyxoviruses THO, DHO, and Batken virus (only a

partial *gp64* ORF is available for Batken virus; (55)). A striking structural and functional homology between their envelope proteins and baculovirus GP64 points to a common ancestor for these proteins (173, 201). In interpreting the phylogenetic tree of Fig. 3C, one should keep in mind that the THO and DHO virus are single-stranded RNA viruses, with a mutation rate possibly higher than that of the double-stranded DNA baculoviruses. This may explain why a large evolutionary distance is projected between DHO and THO env in Fig 3C, and why amino acid identity between DHO and THO envelope proteins is only 33%, very low compared to the identity between baculovirus GP64s. Consequently though, individual amino acids and clusters of amino acids that are conserved between DHO/THO envelope proteins and GP64 may represent residues or domains that are extremely important to functions conserved between the envelope proteins of these two virus families: Fig. 3A demonstrates that the signal peptide and TM domain are the least conserved domains between all the shown homologs, although most substitutions are of a conservative nature, retaining the overall hydrophobicity of the domain. Several blocks of strong conservation in the ectodomain do not include a membrane fusion and oligomerization domain previously characterized in OpMNPV GP64 (171). These two functional domains (corresponding to AcMNPV amino acids 229/230 and 330-338 respectively) are well conserved among baculoviruses, but only poorly to moderately conserved between GP64 and the envelope protein of the THO-like viruses. With regard to the fusion domain, this may reflect the capacity of THO-like viruses to function in mammalian cells, at a physiological pH different than that from insect cells. Beside the domains demonstrated to be involved in OpMNPV GP64 fusion and trimerization, little is known about how and which regions of the protein are involved in which functions. Identification of the above clusters of amino acids, conserved between baculoviruses and THO-like orthomyxoviruses, may be helpful to further unravel the structure/function relationship of the GP64 protein.

Materials and methods

Cells, virus, infections, and transfections. *Spodoptera frugiperda* (Sf9) cells, *Lymantria dispar* (Ld) cells, and *Trichoplusia ni* (Tn5B1-4) (75) cells were used to propagate wild-type AcMNPV (strain E2), OpMNPV, and AgMNPV (isolate 2D) virus. Cells were cultured at 27°C in TNM-FH medium (95) containing 10% fetal bovine serum. For viral infections, virus was incubated on cells for a 1 hr viral adsorption period. For transient transfections, 6 µg of DNA was introduced into 0.6×10^6 Sf9 cells by CaPO₄ precipitation as described earlier (8).

Southern blot hybridizations. AgMNPV genomic DNA was used to screen for presence of a *cathepsin* gene homolog. A 1 kb AcMNPV *v-cath* PCR fragment (400 ng) was ³²P-labelled using the Rediprime kit (Amersham), and used to probe 1-2 µg of HindIII or PstI-digested viral DNA (AgMNPV isolate 2D and L1). The viral DNA was transferred to a nylon blot by vacuum transfer (Hybrid transfer apparatus) and

hybridization was done in a Hybaid oven under the following conditions: Pre-hybridization in 50 ml of 6x SSC, 0.5% SDS, 5x Denhardt's solution, 100 µg/ml denatured salmon sperm DNA for 2 h at 60 °C. Hybridization was carried out overnight in 20 ml pre-hybridization solution + 0.01 M EDTA. The membrane was washed for 15 min at 60°C in 50 ml of 2x SSC/0.1%SDS, for another 15 min in 0.1x SSC/0.1%SDS, and exposed to X-ray film for 72 hours. Hybridizations to initially locate the *gp64* gene were carried out similarly, with a probe based on three different but overlapping restriction fragments of the AcMNPV *gp64* gene.

Cloning of AgMNPV 5.4 kb genomic (HindIII-I) fragment. Shotgun cloning was used to clone multiple AgMNPV genomic segments: AgMNPV DNA was digested with HindIII-I, precipitated, and cloned into a HindIII-cut pBS-based plasmid. Clones with various size inserts were recovered. A clone with a 5.4 kb insert, containing a partial *gp64* gene, was named pBS-Ag/HindIII-I.

Cloning of AgMNPV 12.5 kb genomic (BamHI-D) fragment. AgMNPV DNA was digested with BamHI, precipitated, and cloned into a BamHI-cut pBS-based plasmid. Clones with inserts of two different sizes were recovered: A clone with insert size 12.5 kb was named pBS-Ag/BamHI-D, and a clone with insert size 18.2 kb was called pBS-Ag/BamHI-C.

Sequencing, Blast searches, and protein alignments. Sequencing was done of a CsCl-purified plasmid prep of pBS-Ag/BamHI-D on a ABI Prism 310 genetic analyzer (Perkin Elmer). Both strands were sequenced at least once, and DNASTAR SeqMan (Martinez and Needleman-Wunsch algorithms) was used to generate a consensus sequence. DNASTAR MAP was used to locate ORFs coding for proteins equal to or larger than 50 amino acids. A few small ORFs, 50-100 amino acids in length, which overlapped with ORFs with a known function and of which no homologous proteins are known, were disregarded in the analysis, resulting in a total of 19 ORFs of ≥ 50 amino acids. These selected ORFs were translated and used to find protein homologs through 'Advanced Blast' searches in the GenBank database. Three ORFs, Unknown 1, 2 and 3 (U1,2,3), did not display homology to any baculovirus or other proteins. Blast hits with significant homology were aligned individually with the corresponding predicted proteins of the AgMNPV sequence by the Clustal method (91) with the use of an identity residue weight table and default settings for pairwise alignment: gap penalty 3, window 5, diagonals saved 5, ktuple 1 (DNASTAR Megalign). Percentage identity was calculated as number of identical amino acids/total number of amino acids of the AgMNPV protein $\times 100\%$, and all baculovirus homologs, as well as other homologs with an amino acid identity of $> 22.5\%$, were selected and used for Figure 2. The multiple sequence alignment of GP64 (Figure 3) was performed by the Clustal method with a PAM 250 residue weight table and default settings for multiple alignments (gap penalty 10, gap length penalty 10)(DNASTAR Megalign). Percentages similarity and divergence between the GP64 homologs were determined based on the alignment of Fig. 3A. Similarity is a gross measure of similarity between sequences, and is calculated as $100 \times \text{sum of the matches} / \text{length} - \text{individual gap residues}$. Divergence is

calculated as 100x the distance of individual pairs of sequences divided by the total distance of all sequences. Distance between two sequences = sum of the residue distances + (gaps x gaps penalty) + (gap residues x gap length penalty).

Assembly of the genomic segment (chitinase to p74) of CfMNPV. The genomic segment around the *gp64* gene of CfMNPV was constructed by overlapping of the various sequences available in the GenBank database. These overlaps were determined through DNA alignments by the Wilbur-Lipman method with default settings, and were always larger than 100 nt with 98 to 100% identity. References used for the various DNA segments are: *gp64* (93); *p24/gp16/pp34/ORF132/alk-exo/p22.2/p26* (198, 199); *p10* (280); *p74* (94).

Origin of replication assay. AgMNPV repeat regions, as well as AcMNPV *hr5* were PCR amplified, and cloned into the pGEM-T vector (Promega). Amplified regions from AgMNPV corresponded to nt 808-1024 (217 bp, includes repeat 1), nt 1002-1163 (162 bp, includes repeat 2), and nt 808-1163 (366 bp, includes repeat 1+2). Infection-dependent plasmid replication assays were performed as described by (135). Briefly, Sf9 cells were transfected with plasmids containing the AgMNPV repeat 1, 2 or a combination of 1 and 2, or AcMNPV *hr5* as a control, 5 $\mu\text{g}/2 \times 10^6$ cells. Transfected Sf9 cells were superinfected with AgMNPV or AcMNPV (control) at MOI 10 at 24 h post transfection, and further incubated at 27°C. DNA was extracted according to (177) at 48-72 h post super infection, and 13 μg of DNA per sample was digested at 37°C for 12 h with DpNI, followed by a 12 h digest with PstI. DNA fragments were transferred to Genescreen Plus membrane, and hybridized with a pGEM-T vector-based probe, P32-labelled with the Prime-it Rmt kit (Stratagene). The following conditions were used for hybridization: Pre-hybridization was carried out in a Hybaid oven for 2 h at 65°C in prehybridization solution (5x SSC, 0.1% laurylsarcosine, 0.02% SDS, 10% blocking reagent [Boehringer Mannheim]). Hybridization was carried out for 14 h at 65°C, in prehybridization solution + probe. After hybridization, membranes were washed in 2x SSC/0.1% SDS at RT, followed by a wash step in 5x SSC/0.1%SDS at 65°C. Membranes were scanned on a phosphorimager and analyzed with the Imagequant software (Molecular Dynamics).

CELISA and Western blots. Western blots were carried out as described previously (10). For detection and quantification of GP64 surface levels, a cell ELISA (CELISA) protocol was used as previously described (171): Cells were fixed in 0.5% glutaraldehyde for 10 min at RT, washed once with phosphate buffered saline (PBS pH 7.4) and blocked by incubation in PBS + 1% gelatin for 2 h at 27°C. Cells were then incubated for 45 min at 27°C in Mab AcV5 tissue culture supernatant diluted 1:25 in PBS + 0.5% gelatin. Cells were washed once in PBS for 2 min, followed by incubation for 45 min at 27°C in a secondary goat-anti-mouse antibody conjugated to alkaline phosphatase (GAM-AP, Promega) diluted 1:7500 in PBS + 0.5% gelatin. Cells were then washed four times (5 min/wash) in PBS, and incubated in 1 mM p-nitrophenyl phosphate (Boehringer) in alkaline substrate buffer (100 mM Tris; 100 mM NaCl, 5 mM

MgCl₂ [pH 9.5]) at 37°C. After addition of the substrate, the OD₄₀₅ was determined at several timepoints using an ELISA plate reader.

Syncytium formation assays. Syncytium formation assays were done as follows: Sf9 cells were transfected with p64-166 (OpMNPV GP64 with a truncated wild-type promoter), pBS-Ag-Xba/Pst (AgMNPV GP64 with wild-type promoter), or pAcEcoHΔCla (AcMNPV GP64 with wild-type promoter). Based on the CELISA data, plasmid concentrations for cell transfections were adjusted, so that very similar levels of the various GP64s were present at the plasma membrane. At 48 hr post transfection, supernatant was replaced with PBS-citrate buffer titrated to a range of pHs (4.5 - 6). The PBS-citrate buffer was incubated on the cells for 5 min, replaced with TNM-FH, and cells were further incubated for 2 h. Cells were then fixed in 0.5% glutaraldehyde (10 min) and scored for the presence of syncytia. Syncytium formation required ≥ 5 nuclei in each syncytial mass (++ syncytia abundant; + syncytia present but not abundant; +/- syncytia rare but present; - no syncytia observed).

Chapter 7

General discussion

In addition to the individual discussions of chapters 2 to 6, I will address a few selected topics below. A part of these regard aspects of GP64 that have not been experimentally addressed in this thesis, and supplement the understanding acquired from the previous chapters. The topics are 'Carbohydrate and lipid modifications of GP64', 'Glycoprotein targeting in polarized epithelial cells', 'Evolution of GP64', and 'The role of viral spike proteins and their cytoplasmic tail domains in virus budding. In the latter section I will review virus budding models and mechanisms and speculate on how they may apply to baculovirus BV budding. A list of CTDs and TM domains of spike proteins from the virus families addressed in this chapter, can be found in Fig. 2. The chapter is concluded with a note on future perspectives of GP64.

Carbohydrate and lipid modifications of GP64 and their role in GP64 function

Carbohydrate modifications. With the use of baculoviruses as protein expression systems there has been an interest in knowing the capacity of insect cells to glycosylate foreign gene products, and in the biological effects of carbohydrate modifications. When N-linked oligosaccharides of three insect cell lines were examined, carbohydrate modification pathways similar to those of mammalian cells were suggested (138). Insect cells are able to glycosylate heterologous proteins but their capacity to process carbohydrates to complex forms differs from mammalian cells. Some galactose was found on human plasminogen produced in insect cells (37) however most often, complex carbohydrate modifications such as sialic acid and galactose, are not found (for example (140)). GP64 can serve as a model for studies of the capacity of insect cells to produce and modify carbohydrates, and for the role of carbohydrates in structure and function of glycoproteins, because GP64 is extensively modified with carbohydrates. Characterization of AcMNPV BV glycoproteins by (237) and immunoprecipitation of AcMNPV BV proteins, labeled with N-acetyl-D-[^3H]glucosamine, by MAb AcV1 (264) first indicated that GP64 was a glycoprotein. This is consistent with the presence of a signal peptide, directing GP64 into the secretory pathway where carbohydrate additions and modifications take place. The amino acid sequence of AcMNPV GP64 (after signal peptide cleavage) contains five potential N-linked glycosylation sites (N-X-S/T) (273) whereas the OpMNPV GP64 coding sequence contains 7 (9). While O-linked glycosylation clearly takes place in baculovirus infected cells (177) and some viral proteins have been reported to contain O-linked

sugars (for example ODV structural protein GP41 (271)), no reports on O-linked carbohydrate modification of GP64 have been published. Consensus sites for O-linked glycosylation are not well defined, and it is therefore difficult to predict whether any potential sites on GP64 exist. The site for O-linked glycosylation, similar to the one seen in baculovirus GP41 (N-acetyl glucosamine addition), was mapped for a nuclear pore protein (34) and found to be attached to a serine residue. In mucins, O-linked N-acetyl glucosamine addition is known to occur in proline/serine-rich regions (284). Although some of these N-linked glycosylation sites may be critical for GP64 structure or function, only moderate conservation is apparent. For DHO env, the locations of two and three glycosylation sites are conserved with AcMNPV and OpMNPV respectively. Only one site is conserved between THO env and OpMNPV GP64, and none between THO env and AcMNPV GP64. Between DHO and THO env, only one putative N-linked glycosylation site is conserved. The study presented in chapter 2 (184) indicates that, shortly after production, the observed mass of a GP64 subunit is ~ 67. During transport to the cell surface, carbohydrate processing shifts the observed molecular weight from 67 to 64. When a mature, 64 kD, OpMNPV GP64 protein subunit was deglycosylated, an approximate 8 kD size shift was observed. Compared to synthesis, folding, oligomerization and carbohydrate addition, the carbohydrate processing events are relatively slow, and may be rate-limiting steps in GP64 maturation and transport to the cell surface, although it was also demonstrated that processing may not be necessary for functional maturation (114). Resistance to endoglycosidase H shows that at least some of the GP64 carbohydrates are processed to a more complex form (113, 184). In a recent report (115) the positions of N-linked glycans on AcMNPV GP64 were mapped, showing that 4 out of 5 consensus sites are used for carbohydrate addition (amino acid positions 198, 355, 385, and 426). These carbohydrates were processed to various degrees (suggested to be partly due to their relative position in GP64) with most containing fucose but none containing complex modifications such as β -linked galactose or alpha2,6-linked sialic acid.

Carbohydrate modification of a protein may be necessary for proper progression of the folding process. There are several reports on the biological effects of tunicamycin on GP64 production and function. For example AcMNPV GP64, produced in the presence of tunicamycin, could still be immuno-precipitated by AcV1 (which recognizes a conformational epitope that is lost upon exposure to 1% SDS) (264). This would indicate that the AcV1 epitope is intact, and that at least some GP64 must be properly folded in the absence of carbohydrate addition. In similar experiments, it was demonstrated that transport of GP64, its incorporation into BV, and infectious BV production, are all dramatically reduced in the presence of tunicamycin (23, 114). However the interpretation of these results is complex as tunicamycin may have additional effects on cells due to inhibition of glycosylation of all newly synthesized glycoproteins. These biological effects were again addressed in a study using site directed mutagenesis to knock out individual or combinations of glycosylation sites, and generation of recombinant viruses containing these mutant GP64 proteins (115). A very

similar study had previously been reported for the Influenza HA protein, in which a series of mutants were generated to knock out individual, groups, or all of the 7 N-linked glycosylation sites (58). No individual oligosaccharide side chain was necessary or sufficient for folding, intracellular transport, or function of HA. At least five of the seven oligosaccharide chains were necessary to transport HA through the secretory pathway. If less than five sites were glycosylated, intracellular aggregates were formed and HA was retained in the ER. When a variety of GP64 glycosylation-recombinant viruses were examined, expression of GP64 and transport to the cell surface were unaffected, while oligomerization was not addressed. Incorporation of GP64 into BV seemed unaffected, but it should be noted that the examined progeny BV was only partially purified. All constructs possessed fusogenic activity that could not be distinguished from wild-type GP64 by the syncytium formation assay used in this study. However, because this assay was not quantitative, one cannot eliminate the possibility of subtle effects on the function of the mutant GP64 proteins. These new data indicate that the earlier data (23, 114) in which transport and incorporation of GP64 into BV were drastically reduced in the presence of tunicamycin, were not an effect caused by absence of carbohydrate on GP64. Comparisons of infectivity between GP64 glycosylation-recombinant viruses and wild-type virus agreed with earlier data, and indicated reduced infectivity for all mutants. Whether this effect is due to reduced binding of virus to cells, or to inhibition of a stage of entry between initial binding and fusion of the viral and endosomal membrane, remains to be determined.

Lipid modifications. Many membrane associated viral proteins contain modifications consisting of fatty acid chains, or are 'acylated'. Most of these acylations occur post-translationally with use of the most abundant cellular fatty acid chains: palmitic acid (C16, saturated), stearic acid (C18, saturated), and oleic acid (C18, unsaturated) via ester or thio-ester bonds with amino acids. A relatively rare acylation is the co-translational linkage of the saturated myristic acid (C14) to amino-terminal glycine residues by amide bond. It is thought that acylation of membrane proteins may be involved in anchoring to membranes, membrane mobility, membrane fusion, or regulation of intracellular transport (for example targeting to the plasma membrane). The fatty acids are linked to regions of membrane proteins which are in proximity to, or inside the lipid bilayer, and as such can supplement or alter the hydrophobicity of a membrane spanning domain. It is not known if acylation takes place in a preferred cellular compartment, but recent reports on acylated proteins give some insight into the process of fatty acid modification of proteins. Because GP64 is a membrane-anchored protein involved in membrane fusion, it is not an unlikely candidate for acylation. Indeed, it was demonstrated that AcMNPV GP64 is acylated (207). Using ³H-palmitic and myristic acid, GP64 was found to be modified with palmitic acid, most likely through an ester-type linkage. The N-terminus of GP64 was excluded as a candidate for acylation because 1) there is no N-terminal glycine, typical of an amide-bonded modification with myristic acid, and 2) there is no block to amino-terminal Edman

degradation. Therefore the other major membrane-associated area of GP64, the TM domain and surrounding amino acids, was examined for potential acylation sites. Two potential acylation sites were found to be conserved between AcMNPV and OpMNPV: Ser482, located just outside the predicted TM domain in the ectodomain, and cys503, located within the TM domain, near the CTD (Fig. 3, chapter 6). Since fatty acid-derived radioactive label was not removed from GP64 by boiling in Laemli buffer, an oxy-ester linkage was considered more likely than a thio-ester linkage. Ser482 was therefore the preferred candidate for this acylation. Previous reports that associate acylating activity to intracellular compartments such as ER and Golgi (225), might also suggest ser482 to be a good candidate, as topologically this amino acid residue is located inside the secretory pathway compartments during transport to the cell surface. Another study (212) however challenges this hypothesis, as VSV-G protein was found to be palmitylated on a cysteine residue within its 29 amino acid CTD (see Fig. 2) via a thio-ester linkage. In a comprehensive study by Ponimaskin (200), a variety of TM domains and CTDs from viral glycoproteins of different virus families were compared. Nearly all cysteines in the CTD domains and all within the C-terminal 7 amino acids of the TM domain (cytoplasmic border region), were acylated. However, cysteines simply placed close to the cytoplasmic border region were not sufficient to induce acylation, and based on TM and CTD domain swaps, complex conformational signals for palmitylation were suggested to reside mainly in the TM domain, but also in the CTD. Cys503 of baculovirus GP64 is located in the cytoplasmic border region of the predicted TM domain, and is conserved between all known GP64s and DHO env (Orthomyxoviridae). While ser482 is also conserved between these viruses, the conservation of location of cys503 within the various baculovirus GP64s and the fact that its location is very similar to the location of acylated cysteine residues within the TM domains of other viral membrane proteins, makes cys503 (through a thio-ester type linkage) another candidate for acylation. Some reports on viral spike protein acylation mutants demonstrate little effect on spike protein transport to the cell surface (212, 275), while others show controversial effects. In part this may be due to the fact that most studies do not report quantitative data and may therefore fail to detect more subtle effects. VSV G acylation was shown not to be necessary for fusion or incorporation into virions (275). (175) demonstrated a similar result for Influenza HA: palmitylation of 3 cytoplasmic cysteines of HA was not required for HA biosynthesis, function, or incorporation into virions. However, Fischer (50) reported that acylation of Influenza HA does modulate fusion activity. Only marginal effects were reported in alphaviruses (216). Substitution of cysteines in the TM domain (near the CTD domain) of Sindbis virus E1/E2 glycoproteins resulted in non-acylated glycoproteins. Viruses with the mutant E1/E2 glycoprotein grew slightly slower in cell culture and the amount of virus particles secreted was about half that of wild-type. However at later timepoints and in general, the total effects on the infection cycle were marginal. A report by Ivanova (108) somewhat contradicted the report by Ryan (216): Substitution of the same cysteines in Sindbis resulted in aberrant assembly and particle formation. Possible functions of lipid modification of GP64 are

further addressed in section: 'The role of viral spike proteins and their cytoplasmic tail domains in virus budding'.

Glycoprotein targeting in polarized epithelial cells, the initial site of ODV infection: a role for GP64?

Host epithelial cells are one of the first barriers an invading virus will encounter. Midgut epithelial cells are the first cells infected by the ODV phenotype (Fig. 1), and systemic invasion of the caterpillar hinges on successful spread of the baculovirus from the epithelial cell. The question addressed in this section is whether there might be a role for GP64 in asymmetrically directing baculovirus BV budding from infected midgut epithelial cells. Such a role might not be unlikely, as it was demonstrated that HIV env is capable of redirecting an otherwise random gag-induced budding in MDCK cells to the basolateral side exclusively (185), while in chapter 4 it was shown that GP64 is necessary to drive efficient virion budding. Although in several cases viral spike proteins are not necessary for viral budding, a requirement for spike protein for efficient budding, similar to baculovirus BV, was demonstrated for other viruses such as alpha and rhabdoviruses as well (163, 246). Depending on the particular virus, it may be advantageous and/or necessary for progeny virions to exit towards the luminal or basolateral side of the epithelium. For example, VSV (208), type C retroviruses (214), and HIV type 1 (48) have been shown to bud predominantly from the basolateral membrane whereas Sendai virus, Influenza virus (208), and Rotavirus (122) are released exclusively from the apical side. Coronaviruses, for which the final envelopment step occurs by budding into the pre-Golgi compartment, sort preferentially either to the apical or basolateral side, dependent on the virus and cell type (213). If progeny baculoviruses (BV phenotype) were to bud from the apical side of the epithelial cells into the gut, little would be gained since BV are not infectious to midgut cells (128, 265). In this case, selective budding from the basolateral side of midgut epithelial cells (where host cells and tissues are highly susceptible to BV), would confer an advantage, for example accelerating the systemic infection process. Tanada and Hess (249) were one of the first to report baculovirus BV budding through the basal plasma membrane of midgut epithelial cells, in the armyworm *Pseudaletia unipuncta*. Granados and Lawler also observed budding through the basal side of midgut epithelial cells after feeding high doses of ODV to Lepidopteran larvae (74). In addition, they demonstrated that infectious virus could be detected in the hemolymph as early as a few hours after infection. This was unusual considering that viral spread was thought to occur only after viral DNA replication and progeny virus production within the midgut cells. In a more recent report it was shown that apparently, albeit at low frequency, parental NCs are transported through columnar cells to underlying regenerative cells before the onset of viral replication and progeny production (51), closely matching earlier observations in AcMNPV infected- *T. ni* midgut epithelium. All above observations support a mechanism

of rapid traverse through the midgut epithelial cells, which may offer to baculoviruses the advantage of viral spread before the onset of viral DNA replication. In consideration of a role for GP64 in the suggested rapid viral spread, it should be noted that GP64, unlike most other structural protein genes which are expressed from late promoters, has a complex promoter region, active both early and late in the infection cycle. By histochemical staining of AcMNPV infected- *Trichoplusia ni* caterpillars, GP64 was detected in a polar fashion when it was expressed in columnar epithelial cells, but not when expressed in other cells types (127). It is a possibility that this asymmetric targeting is mediated by signals residing within the GP64 protein. A domain shown to contain such sorting motifs in other viral spike proteins, is the CTD. For example, the VSV-G protein CTD possesses a basolateral targeting motif, able to confer basolateral targeting to a normally apical protein (251). A tyrosine residue at position 19 of the 29 amino acid CTD domain, proved essential. A membrane-proximal tyrosine residue in the CTD domains of two retroviruses (Human T-cell leukemia virus type 1 (HTLV 1) and Moloney murine leukemia virus (MoMuLV)) appeared crucial in conferring basolateral targeting in a similar study by (150). This led to suggestions of a consensus motif for basolateral targeting present in the CTD domain of type 1 membrane glycoproteins. However, except for the presence of a tyrosine residue and its relative location, neither a consensus sequence nor a specific structural element of such signals has been conclusively determined (139), although some believe that Y-X-X-aliphatic/aromatic may represent such a motif (150, 251). (While CTDs are often implicated in targeting of type 1 membrane proteins, an example of a targeting domain in a type II membrane protein was reported in a study by Huang (103). In type II membrane proteins, the signal peptide sequence also represents the membrane-anchoring portion of the protein. The signal peptide/anchor region of paramyxovirus SV5 hemagglutinin-neuraminidase (HN) appeared to contain independent sorting information for apical specific targeting.) With the occlusion bodies harvested from an AcMNPV recombinant virus lacking the predicted 7 amino acid CTD (vAc-C-7, see chapter 4), we have performed neonate droplet feeding assays (Oomens, unpublished data) to determine whether the absence of the GP64 CTD would have an effect on *in vivo* mortality. No significant differences however were observed in mortality of *T. ni* larvae between the recombinant viruses and a control virus containing full length GP64. These data are however by no means conclusive, as the assay may not be ideally suited to detect such differences. It is also possible that GP64 is targeted to the basolateral side, but the CTD domain is not involved in this targeting. Given that the CTD is the only GP64 domain predicted to be in direct cytoplasmic contact, this may seem unlikely. However, it cannot be excluded that the GP64 ectodomain may interact with targeting factors in the ER lumen or that the TM domain of GP64 plays a dominant role. Alternatively, GP64 may not contain any targeting signals. For example, one possibility is that NCs or components of NCs contain basolateral targeting signals and that GP64 is detected at the basolateral membrane by virtue of association with NCs. It is also possible that the basolateral membrane may be the default target membrane for proteins entering the secretory

pathway in midgut epithelial cells. However, the demonstration of basolateral targeting signals in the spike protein CTDs within several virus families, may suggest that the default sorting pathway for type 1 membrane glycoproteins in epithelial cells may be apical. Unlike in the mammalian systems, where polarized cell lines such as the Madin Darby canine kidney (MDCK) cell line are utilized, polarized insect cell lines to address this question for baculoviruses are not available. It nevertheless remains plausible that GP64 is selectively targeted to the basolateral side of epithelial cells to facilitate efficient spread, and that signals determining this selectivity, reside within the GP64 protein.

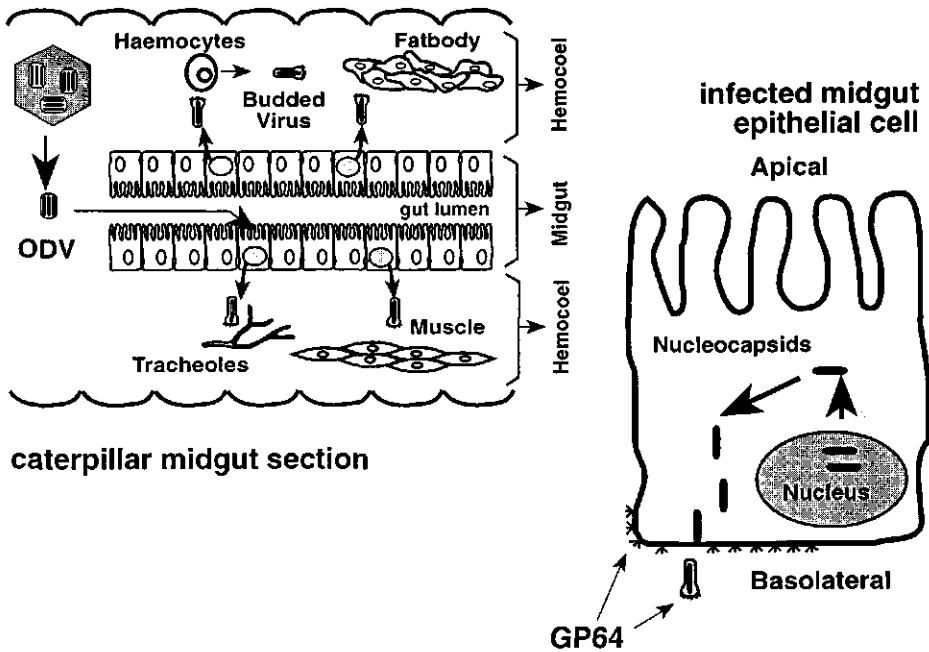


FIG. 1. GP64 and basolateral targeting in the midgut epithelium. The left panel represents a longitudinal section of a baculovirus-infected caterpillar. The single enlarged cell on the right represents an infected midgut epithelial cell. Frequently, epithelial cells are the first host cells targeted by an invading virus. In most cases, depending on the virus, budding occurs preferentially on either the apical or basolateral side of the infected epithelial cell. Viral spike proteins, and in particular their CTD and TM domains, may aid in driving virus budding to the desired location by being asymmetrically targeted (see text). Baculovirus budding has been observed by EM from the basolateral side of insect midgut epithelial cells only. GP64 is necessary for efficient BV budding (chapter 4), and in AcMNPV infected- Tn columnar epithelial cells GP64 was detected in a polar fashion, appearing at the basolateral side (127). It is possible that, within midgut epithelial cells, a selective basolateral targeting mechanism is mediated by signals residing within the GP64 protein.

The role of viral spike proteins and their cytoplasmic tail domains in virus budding

Due to the size of this section, page numbers of subtitles are shown below:

	<u>page</u>
- <i>Introduction</i>	132
- <i>Requirement for spike proteins in virus budding</i>	133
- <i>The role of the spike protein CTD in virus budding</i>	133
- <i>Budding and spike-NC interaction models for alphaviruses (Togaviridae)</i>	135
- <i>Budding and spike-NC/matrix interaction models for rhabdoviruses and orthomyxoviruses</i>	136
- <i>Budding and spike-NC/matrix interaction models for retroviruses</i>	139
- <i>Incorporation of (heterologous) spike proteins in virus particles</i>	141
- <i>New concepts in virus budding</i>	142
- <i>A baculovirus BV budding model?</i>	144

Introduction. The term 'virus budding', as I have used it throughout this thesis, refers to the final envelopment step within the overall assembly of a virion. For enveloped viruses, budding as a final envelopment step may be the last step in the maturation of a virion, however in some cases additional maturation events (for example proteolytic cleavage in retroviruses) occurring after budding, have been demonstrated. Enveloped animal viruses may target different host cellular membranes for their final envelopment step. With few exceptions, most members of the Orthomyxoviridae, Rhabdoviridae, Retroviridae, and Togaviridae have been shown to use the plasma membrane, whereas others belonging to the Coronaviridae, Bunyaviridae, Herpesviridae, and Flaviviridae seem to utilize intracellular membranes for the final envelopment step. There does not appear to be a single budding model that fits each member of a virus family, but the majority of viruses within one family often fit one model. Sometimes, different viruses within one family display unique budding properties; in contrast, certain generic steps of a budding mechanism may be shared by relatively unrelated viruses. Below I review budding models for a number of virus families. Although these may differ from baculoviruses by complexity, size and nature of the viral genome and the type of host they infect, they represent some of the best described, and perhaps relatively simple budding mechanisms that can serve as a model for baculoviruses. Described are: alphaviruses (Semliki Forest virus [SFV], Sindbis virus; Togaviridae), rhabdoviruses (Vesicular Stomatitis virus [VSV], Rabies virus), orthomyxoviruses (Influenza virus), and retroviruses (Human Immunodeficiency virus type 1 [HIV-1], MoMuLV). Specifically, because GP64 seems to play a major role in BV budding, I will compare the roles of the spike proteins and their CTD domains in virus budding, with the aim of defining general processes that may help design strategies to further address baculovirus budding. Only viral spike protein and spike protein CTD functions that pertain to a role in virus budding will be explored. Some

other hypothetical roles of the GP64 CTD domain that will not be addressed are: Endocytosis for the purpose of degradation or recycling, modulation of the membrane fusion capacity upon entry, and modulation of membrane mobility of GP64.

Requirement for spike proteins in virus budding. The earliest budding models were based on SFV, an alphavirus, and derived from the demonstration that observed virion spikes were composed of transmembrane proteins (61). Interactions between NC and spike proteins were thought to initiate and drive the budding process, and both components appeared essential. While this crude model currently still applies to alphaviruses and has been further refined among others by cryo-EM observations (24), recent genetic studies have clearly shown that various other types of interactions and viral components are major players in the viral budding process in general as well. Matrix proteins of several virus families (for example retroviruses, rhabdoviruses) have been shown to be major organizers in virus budding, and lateral interactions between core, matrix, membrane proteins, and lipid bilayer have been proposed to be a major force in virus budding in general (60). In some cases (for example retroviruses (64)) it has been shown that spike proteins are altogether dispensable for budding; however, even in these cases and in general, interactions that involve the spike proteins or spike protein complexes facilitate efficient virus budding. In viruses for which spike glycoproteins are required for efficient virus budding (such as Rabies virus (163) and AcMNPV (chapter 4), the requirement for spike protein may not be absolute, as a low level of virus budding was detected in the complete absence of spike protein ((163), chapter 4). In the case of AcMNPV, this low level of virus budding could potentially be explained by recycled GP64 from the inoculum (see chapter 4). Although GP64 was undetectable by Western blot, whether the low level virus budding represents virion budding in the complete absence of GP64 versus a strongly reduced plasma membrane level of inoculum-derived GP64 remains undetermined. A requirement of viral spike proteins for efficient budding may seem beneficial, as it assures spike protein incorporation into virions. In most cases, spike protein incorporation is critical as virions lacking spike proteins are typically non-infectious. For herpesviruses, this may not necessarily be so: Pseudorabies encodes a series of different glycoproteins involved in entry and exit processes, and gK for example was shown to be involved in virus release but not required for entry (130). Despite the fact that retrovirions lacking the spike protein (*env*) are non-infectious, *env* is dispensable in virus egress as the gag polyprotein (Pr55^{gag} or gag) itself is sufficient to induce budding of virus-like particles (64). By virtue of its matrix protein region at the N-terminus, gag is able to associate with the plasma membrane without the need for spike protein (293). Since *env* is not required for budding, additional factors must be in place to ensure *env* incorporation and infectivity of the virion.

The role of the spike protein CTD domain in virus budding. Particularly (but not only) in cases where budding at the plasma membrane relies heavily on the spike

ectodomain	transmembrane domain	cytoplasmic tail domain
AcMNPV GP64	F M F G H V V N F V I I L I V I L F L Y C M I	R N R N R Q Y
OpMNPV GP64	F M L G H G F T F V L I V G V I L F L Y C M L	R N R P S H Y
AgMNPV GP64	Y G S F G S Y T I V F C I I A F L A F M M C T	R R
DHO Env	G L L L N G A I S W V V V I G V V L V G C V L M	R R V F
THO GP75	G G L L Y G N I G V Y L L I A F A F V L L I	R L I K S A G L C
Sindbis E1	L F G G A S S L L I I G L M I F A C S M M L T S T	R R
Sindbis E2	V Y T I L A V A S A T V A M M I G V T V A V L C A C K A	R R E C L T P Y A L A P N A V I P T S L A L L C C V R S A N A
SFV E1	I S G G L G A L F A I G A I L V L V V V T C I G L	R R
SFV E2	A A T V S A V V G M S L L A L I S I F A S C Y M L V A A	R S K C L T P Y A L T P G A A V P W T L G I L C C A P R A H A
Infl. HA (H7)	V I L W F S F G A S C F L L L A I A M G L V F I C V	K N G N M R C T I C I
VSV G	S S I A S F F F I I G L I I G L F L V L	R V G I H L C I K L K H T K K R Q I Y T D I E M N R L G K
HIV Env	I F I M I V G G L V G L R I V A F V L S I V N	R V R Q G Y S P L S F Q R R I R Q G L E R I L L
MoMuLV Env	F T T L I S T I M G P L I I L L L I L L F G P C I L N	R L V Q F V K D R I S V V Q A L V L T Q Q Y H Q L K P I E Y E P

FIG. 2. Cytoplasmic tail domains (CTDs) and transmembrane (TM) domains of viral spike proteins described in this chapter. All depicted proteins are type 1 transmembrane proteins (see Fig. 5 of chapter 1). A TM domain of a type I membrane envelope protein is generally defined as a highly hydrophobic domain near the C-terminus. Whereas definition of its N- and C-termini may be somewhat arbitrary, for AcMNPV GP64 (see chapter 6, Fig. 3 for full amino acid sequence), residues leu480 to phe483 (1st residue depicted) may represent the N-terminal end, whereas the first charged residue beyond the hydrophobic domain, arg506, likely represents the C-terminal boundary and start of the cytoplasmic tail domain (CTD)(chapter 4). Of the CTD of HIV env. (150 amino acids long), only the N- and C-terminal 12 amino acids are depicted. For full virus names, see page 'abbreviations'. References: GP64s and DHO/THO env, see elsewhere; Sindbis and Semliki forest virus (SFV) E1 and E2, (204); Influenza HA, (200); VSV G, (121, 200); HIV env, (269); Moloney Murine Leukemia virus env [MoMuLV], (110).

protein, the spike protein CTD may constitute one of the most critical domains. Figure 2 displays spike protein CTD and TM domains of viruses addressed in this chapter. Because the CTD seems to occupy a strategic position with regard to interactions between spike proteins and other viral components, several studies have examined the effect of deletion of the spike protein CTD on virus budding. Often, the rate of transport to the surface of non-polarized cells is not or only marginally affected by deletion of the CTD domain, hence these deletions are considered suitable for studies on the effect on virus budding from the plasma membrane or intracellular membranes. In the study in chapter 4, AcMNPV budding was found to be reduced by ~ 50% in the absence of the GP64 CTD, whereas in a similar study for Rabies virus this reduction was 84% (163), and for VSV 90% (221). These results confirm that the CTDs can be major contributors to efficient virus budding, but how these domains exert their effect on budding efficiency is not well understood. It may appear that budding efficiency is determined by the efficiency of membrane anchoring, however in most cases subtle differences raise additional questions. For example, AcMNPV GP64 surface expression and growth characteristics of the vAc-C-7 virus (chapter 4) are near wild-type levels, however budding is reduced by 50% and GP64 incorporation into the virion by 63 to 70%. This indicates that, in addition to possible involvement in membrane anchoring, the CTD plays other, yet undefined roles in budding and incorporation of GP64 into the virion. It

also implicates that the CTD may not be the only domain necessary for efficient budding. Fuel to this fire is added by the differences observed in virus budding between the vAc-C-11 and vAc-C-14 CTD mutants in chapter 4. The fact that they are equally represented on the surface (Fig. 5, chapter 4) yet exhibit remarkably different growth characteristics (Fig. 6, chapter 4), cannot be explained by effects on membrane-anchoring only, and suggests a possible specific role for sequences within the TM domain. Another demonstration that the CTD may not be the only determinant in efficiency of budding, is that budding in the total absence of the spike protein is more strongly reduced (98% for AcMNPV GP64 and 97% for Rabies virus) than budding in the presence of CTD-less spike proteins (50 and 84% for AcMNPV and Rabies virus respectively). Based on these numbers also, the relative importance of the CTD in budding seems to vary between different viruses. For Rabies virus, the reduction by spikeless versus CTD-less spike proteins differs by 13%, whereas for AcMNPV, the difference in budding in the absence of GP64 (2%) and in the presence of tailless GP64 (50%) is much larger.

Budding and spike-NC interaction models for alphaviruses (Togaviridae). For GP64, no studies to date have experimentally addressed the role of domains other than the CTD in virus budding, and any imaginable interactions between individual viral or cellular components have yet to be demonstrated. For a number of other virus families, elaborate budding models have been proposed. One of the first described and best understood budding mechanisms is that of alphaviruses. In alphaviruses, the spike glycoprotein consists of three heterodimers of E1 and E2 proteins. E2 is produced by cleavage from a precursor protein p62. This cleavage is not necessary for particle formation or release but is important for infectivity (252). The E2/E1 spikes form a rigid protein lattice of which the E1 subunits reorganize into more labile fusogenic homotrimers upon exposure to low pH (268). An early hypothetical model based on SFV (61), in which interactions between two essential components, NC and spike proteins, initiate and drive the budding process, has been confirmed and further elaborated on for alphaviruses by several important observations. For example it was convincingly demonstrated that NC-spike interactions drive the budding process (246), and such an interaction was mapped to the CTD of the spike protein E2 (165). A tyrosine based motif within that CTD was shown to be essential for budding (292). In the absence of capsid protein, spike protein was produced and localized to the plasma membrane normally, but unexpectedly, instead of accumulating at the plasma membrane, spike protein was degraded rapidly with characteristic degradation products (291). Since in wild-type virus, degradation products of the spike protein are never found, it was suggested that the spike protein is very efficiently captured by NCs into budding complexes. In a study on another alphavirus, Sindbis virus, an interaction between the spike protein and the viral capsid was also demonstrated (283). Mutants or recombinant viruses were obtained in which interaction between NC and spike protein was compromised due to the nature of modified E2. Revertants of this

assembly/budding-compromised phenotype were then selected and when analysed, all revertants displayed mutations in the capsid protein. In particular, the mutations were localized near a hydrophobic pocket of the capsid, postulated to be the site for docking of amino acids of the E2 cytoplasmic domain. (The E1 cytoplasmic tail plays no significant role in SFV multiplication in cell culture (4)). Another big step towards the understanding of interactions necessary for budding was taken when the first detailed structure of a complete enveloped virion (Ross River virus, an alphavirus) was revealed by a combination of cryo-EM and image processing (24). This structure revealed an elaborate pattern of interactions between the capsid and spike proteins stabilizing the connections between the capsomers. Interestingly, the skirt regions of the spike proteins (i.e. the regions close to the lipid bilayer) were shown to entertain extensive lateral interactions. These lateral interactions are conceptually interesting and form the basis of one of the most recent alphavirus budding model (60). In this hypothetical model, lateral interactions between the spike proteins facilitate budding in two ways: 1) the interactions form of a larger membrane protein unit with a polyvalent NC-binding site. (A few studies indirectly support this hypothesis, for example (46)), 2) the interactions assist in formation of a so-called protein 'lattice' or 'cage', and may thereby provide a force for membrane bending. Budding then is initiated by binding of the NC to a cluster of heterodimers at the PM. The cluster could be a trimer or multimer through lateral interactions in the skirt region of the spikes. The multivalent nature of this initial protein-NC interaction is strong enough to maintain a complex, and additional spike clusters bind by cooperative spike-spike and spike-capsid interactions. It is likely that formation of the spike protein icosahedral lattice directly promotes membrane bending, but NC-spike interaction cooperate and are necessary in the formation of the lattice.

Alphaviruses have a wide host range and replicate in a variety of different species ranging from mammals to insects. Interestingly, in a report on Sindbis virus replication in mosquito cells, the final envelopment step occurred intracellularly rather than at the plasma membrane, and virus was subsequently secreted via vesicles of the secretory pathway (169). The basis of the difference in cell compartments in which final budding takes place, is not known.

Budding and spike-NC/matrix interaction models for rhabdoviruses and orthomyxoviruses. The negative-stranded RNA viruses rhabdoviruses, orthomyxoviruses and paramyxoviruses all encode multi-functional matrix proteins which form a dense layer tightly associated with the inner leaflet of the lipid bilayer. These matrix proteins also bind to liposomes, and have a tendency to polymerize (63, 88, 290). These similarities may indicate that these viruses have similar budding mechanisms, which so far have been found to differ significantly from the earlier described alphavirus model. The basis for this difference lies in the fact that for some well studied viruses of this group (for example VSV (123)), the encoded matrix proteins were shown to independently (i.e. expressed alone in host cells and without the presence of envelope G protein!) bind to the plasma membrane, and induce slow but

efficient release of M protein containing vesicles. Expression of deletion and substitution recombinants suggested that an N-terminal binding site may be necessary, and that a specific structural conformation was required for vesicle budding. Interestingly, when G protein was coexpressed with matrix protein, it was not included in the budding vesicles, suggesting that the nucleocapsid may be necessary to organize matrix-G collaboration. Rhabdovirus budding in the absence of spike protein had been previously demonstrated in a study using temperature-sensitive mutants of VSV (131, 224), however subsequent work (166) showed that the temperature sensitive mutants of VSV still contained the C-terminal fragment of VSV G including the cytoplasmic tail. The development of reverse genetics systems for negative-stranded RNA viruses enabled researchers to generate recombinant viruses completely lacking G protein. For Rabies virus, another rhabdovirus, virus budding in the complete absence of spike protein was found to be reduced 30-fold (163). When only the CTD of Rabies spike protein was absent, budding was reduced 6-fold, indicating a role in budding for this domain. The observed difference in reduction (30-fold versus 6-fold) suggests that, beside the CTD, other domains of G protein are involved in budding as well. For VSV, remaining budding was detected in the absence of G protein (221), however G protein had been replaced by a heterologous protein (CD4). Therefore efficiency of budding in the complete absence of spike protein (i.e. without the co-expression of a heterologous membrane protein) has not yet been conclusively determined. The importance of the VSV G protein CTD was also addressed, and demonstrated to be necessary for efficient budding and spike protein incorporation (221): While the wild-type CTD of VSV G protein is 29 amino acids, a mutant 1 amino acid tail did not support VSV budding, whereas a 9 amino acid VSV G tail did. In addition, a VSV G protein in which the CTD was replaced with the CTD from CD4 (of approximately equal length) supported efficient virus budding, and Respiratory Syncytial virus (RS virus, a paramyxovirus) G and F proteins were also successfully incorporated into VSV virions (124). With regards to a rhabdovirus budding model, the above mentioned capacity of matrix protein to induce independent budding (123) and the strategic position of the matrix protein within the virion, might suggest that the matrix protein plays a central role in rhabdovirus budding, and that it may form a protein 'lattice' similar to that described for alphaviruses. Based on the CTD studies by Schnell (221), a relatively non-specific interaction between the spike protein CTD and a pocket or groove in the viral NC/matrix structure was proposed and is thought to generate a glycoprotein array that promotes viral budding (Fig. 4). Optimal budding efficiency and G protein incorporation is achieved by a concerted action of G, matrix protein, and/or nucleocapsid. An interesting twist to this hypothetical model was a study by Rolls (211). The VSV-G protein gene was engineered into an SFV-based replicon, possessing no structural proteins genes other than the introduced G protein. Not only was G protein expressed in cells transfected with this replicon, but infectious virus-like particles were produced capable of propagating in cell culture. While these results seem significant, another study (60) suggested that the produced particles may have resulted from a generic cellular

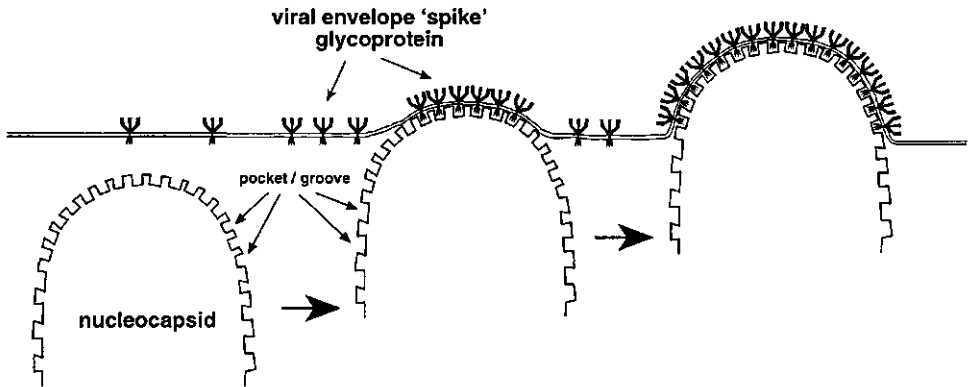


FIG. 3. Virus budding model for Vesicular Stomatitis virus (VSV), a rhabdovirus, by Schnell (221). A relatively non-specific interaction between the spike protein cytoplasmic tail domain (CTD) and a pocket or groove in the viral nucleocapsid or matrix protein is thought to generate a glycoprotein array that promotes viral budding. In this model, VSV matrix protein is not depicted separately, however matrix protein has the capacity to induce budding independent of G or other viral proteins, and a tendency to polymerize (see text). It has therefore been proposed that matrix protein, in cooperation with G protein and/or nucleocapsid, may form a protein 'lattice' as proposed for the alphaviruses, which may aid in inducing membrane curvature during budding (60). Optimal budding efficiency and G protein incorporation is achieved by a concerted action of G protein, matrix protein, and nucleocapsid.

process called membrane vesiculation, blebbing, or ectocytosis, thereby perhaps leaving a proposed independent vesicle budding capacity for the G protein inconclusive.

Similar to rhabdoviruses, for Influenza viruses it is known that matrix protein M1 can associate with the lipid bilayer. The role of the spike proteins, though thoroughly examined, remains somewhat controversial. Influenza A virus envelopes contain two major envelope glycoproteins, neuraminidase (NA, a type 2 membrane protein) and hemagglutinin (HA, a type 1 membrane protein), and a much less abundant non-glycosylated small membrane protein with ion-channel activity (M2). With its neuraminidase activity, NA is important for the release of virus particles from the cell surface but its role in budding and assembly is not well understood. Early studies were compromised due to lack of a suitable genetics system: Virus budding of NA-minus mutants appeared to take place (149, 188), however these mutants apparently still possessed the capacity to express the NA TM domain and CTD, (149). According to Jin (116), the same potential problem applied to a study of temperature-sensitive mutants of the HA protein, in which efficient assembly and budding were observed at the non-permissive temperature (191). In 1989, a reverse genetics system for Influenza virus greatly improved (153) the possibilities to introduce a cDNA derived RNA gene segment into an infectious genome. With this improved technology it was shown that deletion of

the CTD of the NA protein resulted in 86% less incorporation of NA into virions and large aggregates of progeny virions (probably due to insufficient cleavage of sialic acid by NA), while the amount of budding did not seem drastically affected (170). In Influenza HA, five residues of the 10 to 11 amino acid CTD of HA are well conserved between most subtypes (230), among which two cysteines which are post-translationally modified by covalent linkage of palmitate. This conservation was thought to be indicative of an important function of the HA tail. Simpson and Lamb (230) examined alterations of the HA tail, and found that HA proteins with substitutions or deletions in the CTD were still incorporated into the virion, and all altered HAs were also biologically active in hemadsorption and fusion assays. However, deletion of residues within the CTD resulted in delayed cell-surface expression, and no infectivity could be detected from virions containing these HA CTD deletions. In another study however, tailless-HA viruses assembled and replicated almost as efficiently as viruses containing a wild-type HA, contradicting the necessity of the HA CTD for viral infectivity (116). For the above studies, it should be noted that most assays in these studies were not quantitative and may not be sensitive enough to reveal subtle but perhaps significant differences. An importance for the HA CTD in virus propagation may be reflected in the fact that in the tailless-HA studies by Jin (116) a revertant virus was recovered, suggesting that possession of a cytoplasmic tail does indeed confer an advantage. When the CTDs of HA and NA were both absent, particle production was reduced ~ 10-fold. However, particles were no longer spherical but displayed an elongated irregular shape (117), indicating a role in virion morphology for HA and NA CTDs.

Budding and spike-NC/matrix interaction models for retroviruses. A very clear deviation from the earliest alphavirus-based budding models was demonstrated through retrovirus studies, in which it was shown that polyprotein Pr55^{gag} (gag) constitutes the budding apparatus. A basic domain in conjunction with several other basic residues throughout gag is thought to promote membrane binding by interacting with acidic phospholipids on the inner face of the lipid bilayer (182, 294). A myristate moiety at the N-terminus (with a proposed myristyl switch mechanism (187, 234)) is also necessary for membrane binding (64). Matrix protein seems to form an icosahedral 'lattice' (176) (which may initiate virus budding), and also appears to have the capacity to direct virus budding (53): Mutations between amino acids 84 and 88 of matrix protein redirected HIV-1 assembly to an intracellular compartment. The capacity for env protein to direct virus budding was addressed by Salzwedel (217) who expressed an HIV-1 mutant env protein that was strictly retained in the ER. In the presence of this mutant env, HIV-1 budding was not redirected to the ER but was still only observed at the plasma membrane, which might argue that matrix and not env is the major determinant in directing virus budding. Contrary to this data however, it was previously shown that env was capable of concentrating HIV-1 budding to the basolateral side in polarized epithelial cells (185). Moreover, this capacity to redirect was lost when the env CTD was deleted (and also by certain mutations in the matrix protein) suggesting a role for env

CTD-gag interaction in budding (151). Other studies have shown equally contradicting data for env incorporation into the retrovirus. For example, the CTD of GP41 (which, with 150 amino acids is unusually long for a viral spike protein; see Fig. 2) was not required for the incorporation of the HIV-1 envelope glycoprotein into virions (57, 277) whereas for Moloney Murine Leukemia Virus (MoMuLV) the opposite was found (110). Although a direct interaction between HIV-1 matrix and GP41 was detected *in vitro* (31) this has not yet been demonstrated in infected cells. Taken together, specific interactions between the env CTD and gag may occur, but may not be critical in all retroviruses. In one retrovirus model (based on (110)), and other available data, the capsid is assembled at the plasma membrane concomitant with, or prior to (for the B- and D-type viruses), budding from the cell plasma membrane. The matrix region of the gag precursor polyprotein locates to the plasma membrane by virtue of a specific interaction with the plasma membrane, and may form a protein 'lattice'. Depending on the virus, glycoproteins may or may not interact with the matrix region of gag and accumulate at the plasma membrane. Based on x-ray crystal structures (92, 202), SIV and HIV matrix protein were determined to be trimeric proteins, and an interaction was proposed between the long cytoplasmic tail of GP41 and holes present in the 'lattice'-like structure formed upon matrix trimerization (92). The timing of this interaction and the relative importance of env and gag in driving budding remains somewhat controversial yet may be critical for efficient incorporation of env into the budding virion. A report by Egan (45) may help find explanations of some of the observed data. HIV-1 env was found to be endocytosed from the plasma membrane in the absence of other viral proteins by means of an intrinsic signal in the CTD domain. However, in the presence of gag, endocytosis of env was not observed. It is possible that, since env is not required for retrovirus budding, early gag-env interaction is an additional factor to assure env incorporation into the virion. Should this interaction not occur, then env is not incorporated into the virion and is endocytosed for either degradation or recycling for another opportunity to interact with gag. This observed endocytosis of unincorporated env may also serve to evade detection by the immune system. An exception to the above retrovirus model are the foamy viruses. The env proteins contain ER retention signals in their CTD which drive maturation to intracellular membranes (67). Because spike protein is not required for budding of retrovirus-like particles, retroviruses are well suited to study the effect of spike protein absence on virion morphology. For HIV-1, the lack of env in the virion had no morphological consequences. Virus particles were indistinguishable from wild-type virions, and thus env may not be involved in the structural integrity of the virion. In addition to retroviruses, effects of deletion of the spike protein or the spike protein CTD on virion morphology have only been examined for Influenza viruses (see earlier). EM studies on a gp64null virus might reveal possible effects of GP64 deletion on baculovirus morphology, however these particles are far less abundant as budding in the absence of GP64 is drastically reduced. If GP64 is directly or indirectly (via interaction with the envelope or other viral proteins) involved in the integrity or stability of the BV virion, the isolation of properly enveloped GP64-

lacking virions may prove difficult. The budding studies in chapter 4 do indicate that small amounts of virus particles with a density similar to that of wild-type AcMNPV can be purified in the absence of GP64 or with strongly reduced amounts of GP64 incorporated per virion.

Incorporation of (heterologous) spike proteins in virus particles. The stringency at which viruses sort host and viral proteins at membranes, in preparation for budding, differs. For Sindbis, cellular proteins are almost completely displaced by viral proteins (239), whereas retro- or rhabdoviruses appear less selective (see below). Little is understood with regard to these differences, but available space within the viral envelope during or after budding may be a factor. For VSV, foreign viral glycoproteins as well as a cellular glycoproteins can be incorporated into virions in the absence of specific incorporation signals (222). In contrast, the HN protein of the paramyxovirus Newcastle Disease virus (NDV) was not incorporated into Sendai virus (another paramyxovirus), unless its cytoplasmic domain was replaced with that of Sendai virus (248). An example of selective exclusion of homologous virus-encoded proteins is Influenza M2 protein. Although expressed at the plasma membrane at levels fourfold higher than HA, M2 is greatly underrepresented in the virion (145, 288). When Influenza HA and NA genes were added to the VSV genome, they were expressed at high levels in infected cells but there was a preference for incorporation of VSV G protein over HA and NA (137), also indicating that certain specific signals may be required for efficient incorporation. A similar conclusion was drawn for a retrovirus when it was found that homologous proteins were incorporated efficiently into MoMuLV virions even when present at a relatively low density at the plasma membrane, whereas heterologous proteins were incorporated only when expressed at high densities (245). One possible mechanism for selective exclusion or inclusion of spike proteins was suggested by Johnson *et al.* (121), who examined why HIV1 env protein could not be incorporated into VSV virions unless its cytoplasmic tail was replaced with that of VSV G (186). They found that amino acids between position 3 and 10 in the HIV env tail were responsible for an inhibition of incorporation into VSV. By confocal microscopy, the authors concluded that this inhibition occurred because the HIV env CTD signal directed the protein to plasma membrane locations distinct from the sites where VSV proteins were concentrated for budding. The data may be explained by their conclusion but the evidence for the existence of distinct microdomains was however not compelling, and their conclusion therefore appears somewhat speculative. Nevertheless, the implications of this study are interesting: Within the plasma membrane, distinct domains may exist, and specific incorporation signals in the CTD and /or TM domain of viral spike proteins may target spike proteins to such microdomains to possibly enhance the rate of incorporation. For Influenza, a perhaps related membrane-distribution effect was observed. HA appeared to be diffusely distributed over the surface, whereas M2 and NA seemed to cluster in patches (144). With regard to the existence of membrane microdomains, a very novel and interesting concept has emerged in protein targeting,

involving so-called 'rafts' (15, 229). Rafts are dense lipid complexes that are resistant to solubilization at 4°C in triton X-100. They represent tightly-packed, cholesterol- and sphingomyelin-enriched membrane microdomains. Certain viral glycoproteins (for example GPI-anchored proteins and Influenza HA) have been shown to be associated with raft domains during transport to the cell surface, and Influenza HA and NA are recovered in rafts after entering the Golgi complex, and from the plasma membrane (220). The current hypothesis is that raft-domains are formed in the trans Golgi network from lipids with preferentially saturated acyl chains, and are dependent on, and interspersed with cholesterol. These rafts are less fluid due to the tight lipid packing, and function as platforms for intracellular protein sorting and signal transduction events (Simons and Ikonen, 1997). Viral spike proteins that pass through the secretory pathway may be selectively associated with rafts or forming rafts, and therefore end up selectively within or outside of raft domains in the plasma membrane. The significance for viral spike protein incorporation may be in the fact that the raft domains at the plasma membrane, depending on the virus, may represent preferred or non-preferred sites of viral budding and thus influence which membrane-associated proteins are incorporated. For example, Influenza HA proteins from purified virions were associated with raft domains, whereas SFV and VSV spike proteins were not (219). It has also been suggested that acyl modifications of proteins may influence their affinity for raft domains. It was for example reported that the acyl groups of HA, a protein that associates with rafts, are highly ordered, whereas those of VSV G, a spike protein that does not associate with rafts, were more mobile (219). Although lipid modifications (or protein-lipid interactions) were implicated as a possible factor in the raft concept, they may also modulate the efficiency of the budding process in different ways. Lipid modifications may be involved in the positioning of envelope proteins in a budding-favorable conformation, or preparing the plasma membrane for budding by altering plasma membrane curvature (necessary for viral envelopment), for example by changing protein-to-lipid ratio or overall lipid content. Lipid content and the amount of protein influence the fluidity of a membrane, and significant differences in the lipid content of BV and ODV phenotypes of baculoviruses have already been demonstrated (14). Fig. 1 of chapter 1 shows the percentages of the various fatty acids found in the BV membrane, and it is thought that the BV membrane is more fluid than the ODV membrane. AcMNPV GP64 is acylated (207) and this acylation may influence the overall fluidity of the BV membrane. One of the proposed candidate residues for GP64 acylation, cys503, was deleted in AcMNPV-viruses vAc-C-11 and vAc-C-14, described in chapter 4). Both of these recombinant viruses display strongly reduced amounts of surface-anchored GP64 and a drop in virus budding to below 10% of that of wild-type, however vAc-C-11 still propagated efficiently in Sf9 cell culture.

New concepts in virus budding (see also 'Requirement for spike proteins in virus budding', page 132). Since the early alphavirus budding models, in which spike-nucleocapsid interactions were proposed to be the major force in driving the budding

process, new concepts in budding have emerged. In particular, the role of spike proteins as generic promoters of virus budding has been called into question, as in several cases viral matrix proteins (as separate proteins or within gag) have been shown to independently induce vesicle budding. For the alphaviruses, the early budding hypotheses still seem to hold but have been further refined, giving indications that extensive lateral interactions between spike proteins may play a significant role. These lateral interactions may be partly responsible for, and organize the formation of a protein 'lattice' or 'cage' seen in the icosahedral high resolution structure of a mature alphavirus virion (24). Because similar protein 'lattices' are seen in retroviruses, and because matrix proteins of retroviruses and several negative-stranded RNA viruses bind to membranes and have a tendency to polymerize (see earlier), the formation of a protein 'cage' has been proposed as a generic mechanism for virus budding (60). This 'cage' would be organized through extensive interactions between integral or peripheral membrane proteins. Interactions between capsid or nucleocapsid and spike proteins cooperate in this process, but matrix proteins may be the central organizers in this process. Also hypothetical is the idea that these 'lattices' or 'cages' may structurally alter/prepare the host plasma membrane for the budding process by sorting host and viral proteins via protein-protein or other interactions with stringencies that differ depending on the virus. In the cage-formation process, the membrane may adopt the curvature of the 'cage' and initiate the movement of the nucleocapsid outward. In contrast to the proposed roles for matrix proteins in budding, for coronaviruses coexpression of the envelope proteins alone resulted in the release of membrane particles indistinguishable from authentic virions (254), thus demonstrating that viral budding mechanisms may vary substantially between different virus families.

Recent research highlights additional potential components of the budding machinery: the use of host membrane proteins in pinching off the budding virion, and the involvement of the host cytoskeleton in budding and morphogenesis. Pinching off constitutes the final step in the dissociation of the virion from the host cell. Very little is known about the process of pinching off, but a few interesting observations have been reported. One of these observations regards the mapping of a late assembly domain in the p2b region of the Rous Sarcoma virus gag protein (278, 281). Mutations in this region caused a block in pinching off and the mutant virions remain attached to the plasma membrane by a thin membrane stalk. The identified domain contains a sequence motif PPPY, which is found in gag proteins of many retroviruses. In HIV, a similar pro-rich domain with late assembly function has been identified in a different location within gag (71, 190). Most interestingly, the pro-rich sequence motif is similar to a consensus motif required to interact with WW domains of cellular proteins. The WW domain is a highly structured domain that mediates protein-protein interactions in a wide range of cellular proteins with unrelated functions (241). Indeed, the late domain of Rous Sarcoma virus gag has been shown to interact with the WW domain of a signalling molecule associated with the plasma membrane called YAP (Yes-kinase associated protein) (242). In addition, a very similar motif (PPxY) with similar functional

characteristics has been demonstrated in VSV and Rabies matrix proteins (86). Mutations in this motif abolish binding to WW domains and interfere with the release of VSV M protein in a functional budding assay. It is therefore conceivable that both retroviruses and rhabdoviruses utilize host cellular proteins for parts of the budding process. Other studies have been performed that indicate the participation of the host cytoskeleton in virus budding: Both paramyxovirus matrix protein and gag form complexes with actin in vitro (36, 66), actin filaments have been seen by EM in association with budding virions (11), and purified virus particles have been found to contain actin. In brief, there is good evidence to suggest that host cytoskeletal components are indeed involved in virus budding, however the mechanisms underlying these involvements are not understood.

A baculovirus BV budding model? Because so little is known about baculovirus budding, it is difficult to relate the above described virus budding concepts to baculoviruses. Early observations (90, 249, 258, 260) show NCs lining up and budding through the plasma membrane of insect cells, and a seemingly independent transport to the cell surface and membrane fusion capacity of GP64 (Fig. 4)(9, 10). One can only speculate as to what constitutes the driving force in baculovirus BV budding. A baculovirus protein with a matrix-like function has not yet been identified, but given its abundance, VP39 might be a candidate. In the absence of GP64, budding is significantly (but not completely (98%)) reduced, suggesting that budding is either critically dependent on GP64 (and the remaining 2% budding is artefactual) or that other viral components are capable of inducing budding but efficiency is greatly enhanced in the presence of GP64. It is possible that baculoviruses form a protein structure, 'lattice' or 'cage', in or near the plasma membrane, analogous to the models described for alpha- and retroviruses. If so, it is likely that GP64 would be a constituent of the 'lattice', and interactions between GP64 and other components might initiate such a structure. No such interactions have been demonstrated to date, but the data in chapter 4 indirectly indicate that the CTD may play an interactive role. Despite being present at the surface at wild type levels, deletion of the CTD leads to an ~63 to 70% decrease in the number of GP64 molecules per virion, suggestive of specific interactions for preferential incorporation of membrane proteins. The GP64 C-terminal residues between -11 and -14 may also be involved in interactions, as vAc-C-14 (see chapter 4) was unable to efficiently propagate in Sf9 cells, whereas vAc-C-11, while present in equivalent amounts on the cell surface, did efficiently propagate. One of the current hypotheses for the initiation of membrane deformation in preparation for viral budding is that the membrane follows the curvature induced by the proposed protein 'lattice'. An interesting phenomena in that regard may be the apparent asymmetrical distribution of GP64 within the BV phenotype. If induction of membrane curvature would be a function of GP64, presence of GP64 on one side of the virion only might be explained by the fact that GP64, after interaction with the NC and induction of the initial membrane curvature, would no longer be needed until the end of the virion structure

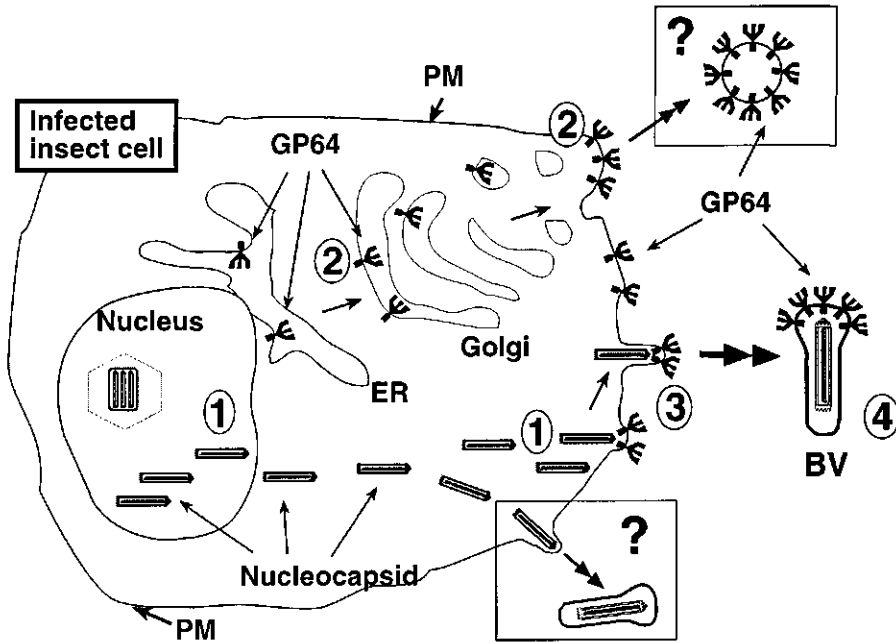


FIG. 4. Baculovirus BV budding. In the figure, observed phenomena involving budding are depicted: 1) In an infected cell, nucleocapsids (NCs) are seen in the nucleus, cytoplasm, and lining up along the plasma membrane, 2) In infected cells, but also when expressed in the absence of viral infection, GP64 follows the secretory pathway and accumulates at the plasma membrane, 3) NCs bud through the plasma membrane at sites where GP64 has accumulated, and acquire an envelope in the process, 4) Spike-like structures are seen at one end of the resulting BV virions, and are thought to be composed of GP64.

Few experimental data are available to understand what constitutes the driving force in baculovirus BV budding. Two hypothetical phenomena (boxed; with ?) that may be involved in driving virus budding are shown. The top scenario depicts budding of GP64-enriched lipid vesicles. Such a phenomenon has been demonstrated for Mouse Hepatitis virus, a coronavirus, in which envelope proteins M and E are together capable of inducing budding of virus-like particles (254). It is not known whether GP64 alone has the capacity to induce vesicle budding, however this would be an inefficient process as only trace quantities of GP64 are detected from the supernatant of GP64 transfected cells. One study (263) suggests that GP64, in cooperation with other viral proteins, may be able to induce budding in the absence of the viral nucleocapsid. The bottom (boxed) scenario depicts budding in the absence of GP64, resulting in GP64-lacking virions. Chapter 4 demonstrated that GP64 is necessary for efficient budding, but it is possible that a low level of virus budding occurs in the absence of GP64. This would however also be a highly inefficient process. In addition to the two depicted phenomena, matrix-like proteins have been demonstrated in other viruses such as rhabdo- and retroviruses, with the capacity to induce vesicle budding independent of other viral spike proteins. Similar matrix-like proteins have not yet been demonstrated in baculoviruses.

due to the virion's rod shape. Pinching off then might then be accomplished in cooperation with host cellular proteins, analogous to the proposed utilization of host membrane proteins for pinching off of retro- and rhabdovirions (278, 281). It is possible that baculoviruses utilize host cellular proteins for additional steps of the budding process, such as the interactions described between matrix proteins and actin for retro- and paramyxoviruses (36, 66). The involvement of the cytoskeleton in virus maturation has been addressed for baculovirus AcMNPV (263). In those studies, the effects of cytochalasins B and D (CB and CD) were determined. These compounds are inhibitors of microfilament elongation, and have been shown to interfere with budding for a number of viruses (for example (11, 193) but not for others (for example Sindbis, (28)). When added to cells infected with AcMNPV, particles lacking nucleocapsids are observed budding from the plasma membrane by EM. Conclusions from these studies included that budding remained unaffected by cytochalasin, whereas the inhibitory effect was likely on the synthesis, transport and/or assembly of viral components. Although these results may hold some very interesting implications for baculovirus BV budding, their interpretation is not straight forward. CD has been shown to cause secondary effects, not directly related to transport or budding (41, 79), and significant quantitative effects may not be easily detected by EM. Also, the absence of nucleocapsid at the plasma membrane due to the presence of CB or CD may lead to an artefactual overrepresentation of budded empty particles. Nevertheless, the apparent budding of core-less particles may hold interesting implications, in particular that the baculovirus nucleocapsid may not be essential for budding. The most abundant protein detected in the particles produced in the presence of CD is GP64, suggesting that GP64 may be involved in nucleocapsid-independent virus budding. While I have never detected large amounts of GP64 in supernatants from GP64-transfected cells, and consider it therefore unlikely that vesicle budding induced by GP64 alone is a significant mechanism, it is possible that GP64, in cooperation with other viral or cellular proteins, may be capable of inducing budding without the need for nucleocapsid. It has been reported that, even in a normal infection, empty particles bud to a limited extent (126, 263). However, whether these represent an insignificant minority within the total population of budded particles, or whether this is a significant mechanism in baculovirus propagation remains to be determined.

Finally, a recent publication (181) identified a baculovirus protein that is necessary for a different step in the assembly process: egress of NC from the nucleus. At the non-permissive temperature, NCs of a temperature sensitive mutant of AcMNPV were found to be retained in the nucleus and, contrary to wild-type, no interaction with the nuclear membrane was observed by EM. This mutation was mapped to GP41, an O-linked protein previously suspected to reside in the space between the NC and viral envelope (defined as the 'tegument') of the ODV phenotype exclusively (272). Studies using highly purified rat liver subcellular fractions demonstrated that the majority of proteins with O-linked sugars similar to GP41 (O-linked N acetyl-glucosamine) are found in the nucleus, with the highest density associated with the nuclear membrane

(e.g. nuclear pore proteins; (85)). GP41 is found in the nucleus and in the ODV phenotype, but did not fractionate with viral membrane fractions (272). It is however possible that GP41 is loosely associated with the nuclear membrane but that membrane association was lost in the procedure of fractionation, or that the presence of GP41 in ODV is a consequence of its presence in the nucleoplasm when NC are assembled. Several functions for GP41 were postulated: GP41 may be involved in movement of NCs from the virogenic stroma to the nuclear membrane, or in facilitating movement of NCs through the nuclear membrane. GP41 may also be directly involved in assembly of NCs, as the EM resolution may not have been sensitive enough to detect possible aberrations in the formed NCs in its absence. It is not known whether baculovirus NCs use the nuclear pores to migrate from the nucleus to the cytoplasm. Because sometimes, enveloped NCs are seen within the cytoplasm, and this envelope is lost before reaching the plasma membrane (52), it is possible that baculovirus NCs bud through the nuclear membrane. Herpesviruses are an example of how egress from the nucleus may occur. Although herpesvirus assembly differs significantly from baculovirus assembly, both have a need to transport newly assembled NCs from the nucleus, and herpes simplex virus NCs are thought to bud through the inner nuclear lamella and then deenvelop by budding through the outer nuclear lamella. Because several findings support this process of nuclear exit yet it is only rarely seen in herpesvirus infected cells, it is suggested to be a process much more rapid than some other envelopment processes (210). Since baculovirus NCs are usually seen naked in the cytoplasm of infected cells, and if the process is similarly rapid and difficult to observe, the same mechanism might apply to baculoviruses.

Evolution of GP64, and current and future avenues of GP64 research

A *gp64* gene has been identified in the genomes of a number of baculoviruses that taxonomically fall within proposed group I of the genus Nucleopolyhedrovirus: AcMNPV, BmNPV, OpMNPV, CfMNPV, AfMNPV, EpNPV, and AgMNPV. These GP64s display an ~ 77 to 82 % amino acid identity within the predicted ectodomain. Besides baculoviruses, genes with homology to baculovirus GP64 were demonstrated only in the genomes of three related arboviruses of the family Orthomyxoviridae (see introduction, and chapter 6). It is extremely interesting to find the homology of a viral envelope gene between viruses of two so profoundly different groups. A factor that possibly links the two is the fact that both baculoviruses and the THO/DHO viruses replicate in invertebrate hosts (THO/DHO viruses also replicate in mammalian cells). Because of the remarkable sequence similarity, a common ancestor for the GP64 homologs has been suggested and seems likely. Several schemes of acquiring the gene are possible, but at this point one can only speculate as to which virus first possessed the gene. Certain considerations may be helpful in understanding how the two virus families can share this envelope gene. For example, other orthomyxoviruses

such as the Influenza viruses are notorious for their capacity to acquire genes by reassortment when multiple viruses infect one host. Although this is described between two segmented RNA viruses, it may be possible that the segmented THO/DHO virus acquired GP64 (presumably as an mRNA) from a baculovirus by a mechanism similar to RNA-RNA reassortment, while sharing the same host. Alternatively, DHO/THO virus may have first acquired the gene or both viruses may have independently acquired the gene from an ancestor, to which mechanisms such as recombination may have contributed. Sharing the same host is not unlikely since they both infect invertebrate cells, and since AcMNPV for example has a relatively broad host range. Although only a speculation, is it possible that the acquisition of GP64 may have been a contributing factor to expanding AcMNPV's host range? And because a large group of baculoviruses may not possess a *gp64* gene, is it possible that the primordial baculovirus was gut (epithelium)-limited and radiated in different directions perhaps upon acquisitions of different envelope genes that permitted systemic infection? If this would be the case, one would expect the existence of phylogenetic subgroups based on the various acquired envelope genes.

In the determination of what (evolutionarily) the most critical domains in GP64 function may be, conservations between the baculovirus and THO/DHO genes are likely to be a good indicator. After the *gp64* ancestral gene was acquired, it may have diverged within baculoviruses and THO/DHO viruses at different rates. Considering that THO/DHO are RNA viruses, their mutation/evolutionary rates may differ from that of the double-stranded DNA baculoviruses. A consequence of this may be that the level of amino acid identity between the GP64 homologs of DHO and THO viruses is relatively low (33%) compared to the high level of conservation (70-80% amino acid identity) between baculovirus GP64s. It is altogether likely that those residues that are unchanged between baculovirus GP64 and THO/DHO env, represent key amino acids in the most conserved functions. Of course, functions may have diverged based on requirements of the different viruses or adaptations to a particular host, however the structural similarities between them suggest remaining functional conservation. For both, induction of low-pH membrane fusion and involvement in receptor binding have been demonstrated ((10, 201) Chapter 5). We do not know whether GP64 or THO/DHO env are important for the structural integrity of the virion in the extracellular environment, however baculovirus virions could be isolated carrying only 30 to 37% of the level of GP64 in the envelope of a wild-type virion (Chapter 4). In any case, GP64 and THO/DHO envelope proteins appear to share a common ancestry, and both proteins play critical roles in the respective infection cycles of their viruses.

What is the evolutionary significance of the GP64 CTD? The basic character (due mainly to arginine residues) and small size of 2 to 8 amino acids, may be important characteristics of the GP64 CTD domain since this is conserved between baculovirus GP64s and the related orthomyxovirus DHO virus. Based on a statistical analysis of membrane protein topology and the role of TM domains and their flanking regions (267), a 'positive inside' rule was proposed. This rule says that the transmembrane

orientation of an apolar segment is not determined by the apolar region itself, but by the charge content of the flanking regions. Positively charged residues were almost always found on the non-translocated side of the apolar segment, with a majority of these residues being arginines and lysines. This was true for membrane proteins of different organisms and a variety of cellular locations: bacterial inner-membrane proteins, and eukaryotic proteins from the ER, plasma membrane, mitochondrial and chloroplast membrane. These findings suggest that an apolar segment followed by polar and charged residues (mostly arginines) is a generic signal for membrane anchoring rather than a specific signal for other processes. In that regard, the overall charge of the viral spike protein tail or the charge at the cytoplasmic border region (arg506) may aid in effective membrane anchoring of GP64. In addition, it is possible that the basic charge of the CTD has an undetermined function in the infection process of larvae, however the observation that the recombinant virus vAc-CΔ3Ra (in which all arginines were replaced with alanines, see chapter 4) was in all measurable aspects indistinguishable from virus carrying a wild-type GP64, demonstrates that the charge is not necessary for viability of AcMNPV in cell culture. Not only the charge, but the complete predicted CTD was shown to be dispensable for survival of the virus in cell culture. Nevertheless in the presence of the CTD domain, despite GP64 surface levels equivalent to those in the absence of the CTD, the amount of budding and incorporation of GP64 into virions are significantly higher, indicative of a role for the CTD beyond membrane anchoring. Because incorporation of GP64 into the virion is important for subsequent entry, the CTD thus seems to confer an advantage to AcMNPV. In conclusion, the size and charge of the CTD may represent a domain involved in evolutionary conserved functions that confer a significant advantage to the virus, or may be a domain with only a marginal impact on overall survival.

Current and future avenues of GP64 research. Most of the GP64 research in the past decade has addressed, directly or indirectly, the role of GP64 in the baculovirus infection cycle. This is an area that still needs considerable attention, particularly in determining the role of GP64 in BV assembly and the mechanism of BV host cell receptor binding. Determination of the 3-dimensional structure of GP64 would be extremely valuable, especially in the area of receptor binding and structural requirements for budding. Attempts to crystallize the soluble form of OpMNPV GP64 that was described in chapter 2 and 5, have not yet been successful. Another fundamental line of GP64 research that has developed in recent years and which is not addressed in this thesis, concerns the bio-physical aspects of GP64 membrane fusion. Because of the robust fusion mediated by GP64, baculovirus GP64 is becoming a model for studies of fusion pore formation during the process of membrane fusion. Typically, BV-infected insect cells are used in electrophysiological experiments of membrane fusion with the use of so-called 'patch-clamping' technique. This resulted in reports on the role of lipid composition in fusion pore formation (25), and how size, timing and reversibility ('pore-flickering') of the initial fusion pore induced by AcMNPV GP64, compares to Influenza

HA (197). The stably transfected cell line Sf9^{Op1D}, designed to complement GP64 in the gp64null virus system (chapter 4), has proved useful in these studies. Upon characterization, these uninfected cells showed a relatively uniform distribution of GP64 at the plasma membrane, and were successfully used in additional fusion pore studies (195), and also in studies examining the multimeric requirements for GP64-induced fusion (157).

There are other, more applied, potential avenues for GP64. Among them is the possibility to utilize AcMNPV in human gene therapy-related applications. AcMNPV is nonpathogenic to humans, but the BV can enter a large variety of cell types including mammalian cells (12, 16, 19, 96, 227) and can efficiently deliver genes (12, 27, 227). A very recent example of the use of baculoviruses for gene delivery is a study by Delaney and Isom (38). Insertion of the entire hepatitis B virus (HBV) genome into AcMNPV, followed by 'infection/transfection' of this recombinant virus, drastically improved the very low efficiency of HBV infection of liver cells *in vitro*. Despite efficient gene delivery in some cell types, expression of the genes in mammalian cells from mammalian promoters in a recombinant virus, has been more challenging. A recent study (27) applied two novel ideas to the baculovirus gene delivery concept: 1) treatment of certain mammalian cells with trichostatin A, a selective histone deacetylase inhibitor, significantly increased expression levels of a foreign gene from a mammalian promoter in recombinant baculovirus infected cells, 2) incorporation of a selectable marker (*neomycin* resistance gene) into a recombinant virus followed by incubation with G418, selected transformed lines incorporating a portion of the baculovirus genome and still expressing a gene of interest after 25 passages. Another interesting potential research avenue for GP64 involves pseudotyping and selective targeting of diseased cells (222). VSV, a virus non-pathogenic to humans, was designed to express the HIV-1 receptor CD4 and co-receptor CXCR4, and was shown to infect, propagate, and kill T cells infected with HIV. For similar potential baculovirus applications, studies of GP64 could be particularly helpful as it itself accumulates at the cell surface, and possesses all the signals necessary for cell surface display and for effective incorporation into baculovirus virions. Currently, commercial vectors are already available that utilize GP64 signals to display glycoproteins of interest at the cell surface in a eukaryotic virus display system. The above examples of applied GP64 research are encouraging and may in the future yield many practical uses. A continued fundamental approach to the study of GP64 structure and function will be essential to provide the framework for such applications, in particular to understand the requirements for virion entry into host and non-host cells, and the role of GP64 in the production of budded virions. Hopefully, continued GP64 research will also yield clues towards the intriguing questions of when and how GP64 was acquired, and how this acquisition may have impacted the evolution of the family of viruses we now know as the Baculoviridae.

References

1. Ahrens, C. H., R. L. Q. Russell, C. J. Funk, J. T. Evans, S. H. Harwood, and G. F. Rohrmann (1997). The sequence of the *Orgyia pseudotsugata* Multinucleocapsid Nuclear Polyhedrosis virus genome. *Virology*. 229: 381-399.
2. Ayres, M. D., S. C. Howard, J. Kuzio, M. Lopez-Ferber, and R. D. Possee (1994). The complete DNA sequence of *Autographa californica* Nuclear Polyhedrosis virus. *Virology*. 202: 586-605.
3. Barsoum, J., R. Brown, M. McKee, and F. M. Boyce (1997). Efficient transduction of mammalian cells by a recombinant baculovirus having the vesicular stomatitis virus G glycoprotein. *Hum. Gene Ther.* 8: 2011-8.
4. Barth, B. U., M. Suomalainen, P. Liljestrom, and H. Garoff (1992). Alphavirus assembly and entry role of the cytoplasmic tail of the E1 Spike subunit. *J. Virology*. 66: 7560-7564.
5. Blissard, G. W. (1996). Baculovirus - Insect Cell Interactions. *Cytotechnology*. 20: 73-93.
6. Blissard, G. W., P. H. Kogan, R. Wei, and G. F. Rohrmann (1992). A synthetic early promoter from a baculovirus: Roles of the TATA box and conserved start site CAGT sequence in basal levels of transcription. *Virology*. 190: 783-793.
7. Blissard, G. W., and G. F. Rohrmann (1990). Baculovirus diversity and molecular biology. *Annu. Rev. Entomol.* 35: 127-155.
8. Blissard, G. W., and G. F. Rohrmann (1991). Baculovirus *gp64* gene expression: Analysis of sequences modulating early transcription and transactivation by IE1. *J. Virology*. 65: 5820-5827.
9. Blissard, G. W., and G. F. Rohrmann (1989). Location, sequence, transcriptional mapping, and temporal expression of the *gp64* envelope glycoprotein gene of the *Orgyia pseudotsugata* Multicapsid Nuclear Polyhedrosis virus. *Virology*. 170: 537-555.
10. Blissard, G. W., and J. R. Wenz (1992). Baculovirus GP64 envelope glycoprotein is sufficient to mediate pH-dependent membrane fusion. *J. Virology*. 66: 6829-6835.
11. Bohn, W., G. Rutter, H. Hohenberg, K. Mannweiler, and P. Nobis (1986). Involvement of actin filaments in budding of Measles virus: studies on cytoskeletons of infected cells. *Virology*. 149: 91-106.
12. Boyce, F. M., and N. L. R. Bucher (1996). Baculovirus-mediated gene transfer into mammalian cells. *Proc. Natl. Acad. Sci. USA*. 93: 2348-2352.
13. Bradford, M. B., G. W. Blissard, and G. F. Rohrmann (1990). Characterization of the infection cycle of the *Orgyia pseudotsugata* Multicapsid Nuclear Polyhedrosis virus in *Lymantria dispar* cells. *J. Gen. Virology*. 71: 2841-2846.
14. Braunagel, S. C., and M. D. Summers (1994). *Autographa californica* nuclear polyhedrosis virus, PDV, and ECV viral envelopes and nucleocapsids: Structural proteins, antigens, lipid and fatty acid profiles. *Virology*. 202: 315-328.
15. Brown, D. A., and J. K. Rose (1992). Sorting of GPI-anchored proteins to glycolipid-enriched membrane subdomains during transport to the apical cell surface. *Cell*. 68: 533-44.
16. Brusca, J., M. Summers, J. Couch, and L. Courtney (1986). *Autographa californica* Nuclear Polyhedrosis virus efficiently enters but does not replicate in poikilothermic vertebrate cells. *Intervirology*. 26: 207-222.
17. Bulach, D. M., C. A. Kumar, A. Zaia, B. Liang, and D. E. Tribe (1999). Group II nucleopolyhedrovirus subgroups revealed by phylogenetic analysis of polyhedrin and DNA polymerase gene sequences [In Process Citation]. *J. Invert. Pathol.* 73: 59-73.
18. Bullough, P. A., F. M. Hughson, J. J. Skehel, and D. C. Wiley (1994). Structure of influenza haemagglutinin at the pH of membrane fusion. *Nature*. 371: 37-43.

19. Carbonell, L. F., and L. K. Miller (1987). Baculovirus interaction with nontarget organisms: a virus-borne reporter gene is not expressed in two mammalian cell lines. *Appl. Environ. Microbiol.* 53: 1412-1417.
20. Carr, C. M., and P. S. Kim (1994). Flu virus invasion: halfway there. *Science.* 266: 234-236.
21. Carstens, E. B., S. T. Tjia, and W. Doerfler (1979). Infection of *Spodoptera frugiperda* cells with *Autographa californica* Nuclear Polyhedrosis virus. I. Synthesis of intracellular proteins after virus infection. *Virology.* 99: 368-398.
22. Casadaban, M. J. J., A. Martinez-Arias, S. K. Shapira, and J. Chou (1981). Beta-galactosidase gene fusions for analyzing gene expression in *Escherichia coli* and yeast. *Meth. Enzymol.* 100: 293-308.
23. Charlton, C. A., and L. E. Volkman (1986). Effect of tunicamycin on the structural proteins and infectivity of budded *Autographa californica* nuclear polyhedrosis virus. *Virology.* 154: 214-218.
24. Cheng, R. H., R. J. Kuhn, N. H. Olson, M. G. Rossmann, H. K. Choi, T. J. Smith, and T. S. Baker (1995). Nucleocapsid and glycoprotein organization in an enveloped virus. *Cell.* 80: 621-30.
25. Chernomordik, L., E. Leikina, M. Cho, and J. Zimmerberg (1995). Control of baculovirus GP64-induced syncytium formation by membrane lipid composition. *J. Virology.* 69: 3049-3058.
26. Clerx, J. M. P., F. Fuller, and D. H. L. Bishop (1983). Tick-borne viruses structurally similar to the orthomyxoviruses. *Virology.* 127: 295-279.
27. Condreay, J. P., S. M. Witherspoon, W. C. Clay, and T. A. Kost (1999). Transient and stable gene expression in mammalian cells transduced with a recombinant baculovirus vector. *Proc. Natl. Acad. Sci. U S A.* 96: 127-32.
28. Coombs, K., E. Mann, J. Edwards, and D. T. Brown (1981). Effects of chloroquine and cytochalasin B on the infection of cells by Sindbis virus and Vesicular Stomatitis virus. *J. Virology.* 37: 1060-5.
29. Copeland, C. S., R. W. Doms, E. M. Bolzau, R. G. Webster, and A. Helenius (1986). Assembly of Influenza hemagglutinin trimers and its role in intracellular transport. *J. Cell. Biol.* 103: 1179-1192.
30. Copeland, C. S., K. P. Zimmer, K. R. Wagner, G. A. Healey, I. Mellman, and A. Helenius (1988). Folding trimerization and transport are sequential events in the biogenesis of Influenza virus hemagglutinin. *Cell.* 53: 197-210.
31. Cosson, P. (1996). Direct interaction between the envelope and matrix proteins of HIV-1. *EMBO J. Journal.* 15: 5783-5788.
32. Croizier, G., L. Croizier, O. Argaud, and D. Poudevigne (1994). Extension of *Autographa californica* Nuclear Polyhedrosis virus host range by interspecific replacement of a short DNA sequence in the p143 Helicase Gene. *Proc. Natl. Acad. Sci. USA.* 91: 48-52.
33. Croizier, G., and H. C. T. Ribeiro (1992). Recombination as a possible major cause of genetic heterogeneity in *Anticarsia gemmatilis* nuclear polyhedrosis virus. *Virus Res.* 26: 183-196.
34. D'Onofrio, M., C. M. Starr, M. K. Park, G. D. Holt, R. S. Haltiwanger, G. W. Hart, and J. A. Hanover (1988). Partial cDNA sequence encoding a nuclear pore protein modified by O-linked N-acetylglucosamine. *Proc. Natl. Acad. Sci. U S A.* 85: 9595-9.
35. Dahlberg, J. E. (1974). Quantitative electron microscopic analysis of the penetration of VSV into L cells. *Virology.* 58: 250-62.
36. Damsky, C. H., J. B. Sheffield, G. P. Tuszyński, and L. Warren (1977). Is there a role for actin in virus budding? *J. Cell. Biol.* 75: 593-605.
37. Davidson, D. J., and F. J. Castellino (1991). Asparagine-linked oligosaccharide processing in lepidopteran insect cells. Temporal dependence of the nature of the oligosaccharides assembled on asparagine-289 of recombinant human plasminogen produced in baculovirus vector infected *Spodoptera frugiperda* (IPLB-SF-21AE) cells. *Biochem.* 30: 6165-74.
38. Delaney, W. E. t., and H. C. Isom (1998). Hepatitis B virus replication in human HepG2 cells mediated by hepatitis B virus recombinant baculovirus. *Hepatology.* 28: 1134-46.
39. Deng, W. P., and J. A. Nickoloff (1992). Site-directed mutagenesis of virtually any plasmid by eliminating a unique site. *Anal. Biochem.* 200: 81-8.

40. Dijkstra, J. M., N. Visser, T. C. Mettenleiter, and B. G. Klupp (1996). Identification and characterization of pseudorabies virus glycoprotein gM as a nonessential virion component. *J. Virol.* 70: 5684-8.
41. Dix, R. D., and R. J. Courtney (1976). Effects of cytochalasin B on Herpes Simplex virus type 1 replication. *Virology*. 70: 127-35.
42. Doms, R. W., D. S. Keller, A. Helenius, and W. E. Balch (1987). Role for adenosine triphosphate in regulating the assembly and transport of Vesicular Stomatitis virus G protein trimers. *J. Cell. Biol.* 105: 1957-1970.
43. Doms, R. W., R. A. Lamb, J. K. Rose, and A. Helenius (1993). Folding and assembly of viral membrane proteins. *Virology*. 193: 545-562.
44. Du, X., and S. M. Thiem (1997). Characterization of host range factor 1 (hrf-1) expression in *Lymantria dispar* M nucleopolyhedrovirus- and recombinant *Autographa californica* M nucleopolyhedrovirus-infected IPLB-Ld652Y. *Virology*. 227: 420-430.
45. Egan, M. A., L. M. Carruth, J. F. Rowell, X. Yu, and R. F. Siliciano (1996). Human immunodeficiency virus type 1 envelope protein endocytosis mediated by a highly conserved intrinsic internalization signal in the cytoplasmic domain of gp41 is suppressed in the presence of the Pr55gag precursor protein. *J. Virol.* 70: 6547-56.
46. Ekstrom, M., P. Liljestrom, and H. Garoff (1994). Membrane protein lateral interactions control Semliki Forest virus budding. *Embo J.* 13: 1058-64.
47. Engelhard, E. K., L. N. W. Kam-Morgan, J. O. Washburn, and L. E. Volkman (1994). The insect tracheal system: A conduit for the systemic spread of *Autographa californica* M nuclear polyhedrosis virus. *Proc. Natl. Acad. Sci. USA.* 91: 3224-3227.
48. Fantini, J., S. Baghdiguan, N. Yahi, and J. C. Chermann (1991). Selected human immunodeficiency virus replicates preferentially through the basolateral surface of differentiated human colon epithelial cells. *Virology*. 185: 904-7.
49. Federici, B. A., and R. H. Hice (1997). Organization and molecular characterization of genes in the polyhedrin region of the *Anagrapha falcifer* multinucleocapsid NPV. *Arch. Virol.* 142: 333-348.
50. Fischer, C., B. Schroth-Diez, A. Herrmann, W. Garten, and H. D. Klenk (1998). Acylation of the influenza hemagglutinin modulates fusion activity. *Virology*. 248: 284-94.
51. Flipsen, J. T. M., J. W. M. Martens, M. M. Van-Oers, J. M. Vlask, and J. W. M. Van-Lent (1995). Passage of *Autographa californica* Nuclear Polyhedrosis virus through the midgut epithelium of *Spodoptera exigua* larvae. *Virology*. 208: 328-335.
52. Fraser, M. J. (1986). Ultrastructural observations of virion maturation in *Autographa californica* nuclear polyhedrosis virus infected *Spodoptera frugiperda* cell cultures. *J. Ultrastr. Mol. Struct. Res.* 95: 189-195.
53. Freed, E. O. (1998). HIV-1 gag proteins: diverse functions in the virus life cycle. *Virology*. 251: 1-15.
54. Freedman-Faulstich, E. Z., and F. J. Fuller (1990). Nucleotide sequence of the tick-borne, orthomyxo-like Dhori/Indian/1313/61 virus envelope gene. *Virology*. 175: 10-18.
55. Frese, M., M. Weeber, F. Weber, V. Speth, and O. Haller (1997). Mx1 sensitivity: Batken virus is an orthomyxovirus closely related to Dhori virus. *J. Gen. Virol.* 78: 2453-8.
56. Fuchs, L. Y., M. S. Woods, and R. F. Weaver (1983). Viral transcription during *Autographa californica* nuclear polyhedrosis virus infection: A novel RNA polymerase induced in infected *Spodoptera frugiperda* cells. *J. Virol.* 48: 641-646.
57. Gabuzda, D. H., A. Lever, E. Terwilliger, and J. Sodroski (1992). Effects of deletions in the cytoplasmic domain on biological functions of human immunodeficiency virus type 1 envelope glycoproteins. *J. Virol.* 66: 3306-15.
58. Gallagher, P. J., J. M. Henneberry, J. F. Sambrook, and M. J. H. Gething (1992). Glycosylation requirements for intracellular transport and function of the hemagglutinin in Influenza virus. *J. Virol.* 66: 7136-7145.

59. Garcia Maruniak, A., O. H. O. Pavan, and J. E. Maruniak (1996). A variable region of *Anticarsia gemmatalis* nuclear polyhedrosis virus contains tandemly repeated DNA sequences. *Virus Res.* 41: 123-132.
60. Garoff, H., R. Hewson, and D. J. E. Opstelten (1998). Virus maturation by budding. *Microbiol. Mol. Biol. Rev.* 62: 1171-90.
61. Garoff, H., and K. Simons (1974). Location of the spike glycoproteins in the Semliki Forest virus membrane. *Proc. Natl. Acad. Sci. U S A.* 71: 3988-92.
62. Garrity, D. B., M.-J. Chang, and G. W. Blissard (1997). Late promoter selection in the baculovirus *gp64 envelope fusion protein* gene. *Virology* 231: 167-181.
63. Gaudin, Y., J. Sturgis, M. Doumith, A. Barge, B. Robert, and R. W. Ruigrok (1997). Conformational flexibility and polymerization of Vesicular Stomatitis virus matrix protein. *J. Mol. Biol.* 274: 816-25.
64. Gheysen, D., E. Jacobs, F. De Foresta, C. Thiriart, M. Francotte, D. Thines, and M. De Wilde (1989). Assembly and release of HIV-1 precursor Pr55gag virus-like particles from recombinant baculovirus-infected insect cells. *Cell.* 59: 103-112.
65. Gill, S. C., and P. H. von Hippel (1989). Calculation of protein extinction coefficients from amino acid data. *Anal. Biochem.* 182: 319-326.
66. Giuffre, R. M., D. R. Tovell, C. M. Kay, and D. L. Tyrrell (1982). Evidence for an interaction between the membrane protein of a paramyxovirus and actin. *J. Virol.* 42: 963-8.
67. Goepfert, P. A., G. Wang, and M. J. Mulligan (1995). Identification of an ER retrieval signal in a retroviral glycoprotein. *Cell.* 82: 543-4.
68. Goldstein, N. I., and A. H. McIntosh (1980). Glycoproteins of nuclear polyhedrosis viruses. *Arch. Virol.* 64: 119-26.
69. Gollins, S. W., and J. S. Porterfield (1986). The uncoating and infectivity of the flavivirus West Nile on interaction with cells: effects of pH and ammonium chloride. *J. Gen. Virol.* 67: 1941-1950.
70. Gombart, A. F., G. W. Blissard, and G. F. Rohrmann (1989). Characterization of the genetic organization of the Hind-III M region of the multicapsid nuclear polyhedrosis virus of *Orgyia pseudotsugata* reveals major differences among baculoviruses. *J. Gen. Virol.* 70: 1815-1828.
71. Gottlinger, H. G., T. Dorfman, J. G. Sodroski, and W. A. Haseltine (1991). Effect of mutations affecting the p6 gag protein on Human Immunodeficiency virus particle release. *Proc. Natl. Acad. Sci. U S A.* 88: 3195-9.
72. Gottlinger, H. G., J. G. Sodroski, and W. A. Haseltine (1989). Role of capsid precursor processing and myristoylation in morphogenesis and infectivity of human immunodeficiency virus type 1. *Proc. Natl. Acad. Sci. U S A.* 86: 5781-5.
73. Granados, R. R. (1978). Early events in the infection of *Heliothis zea* midgut cells by a baculovirus. *Virology* 90: 170-174.
74. Granados, R. R., and K. A. Lawler (1981). In vivo pathway of *Autographa californica* baculovirus invasion and infection. *Virology* 108: 297-308.
75. Granados, R. R., G. X. Li, A. C. G. Derksen, and K. A. McKenna (1994). A new insect cell line from *Trichoplusia ni* (BTI-Tn-5B1-4) susceptible to *Trichoplusia ni* single enveloped nuclear polyhedrosis virus. *J. Invert. Pathol.* 64: 260-266.
76. Granados, R. R., and K. A. Williams (1986). In vivo infection and replication of Baculoviruses, vol. 1. Biological properties and molecular biology. *CRC Press*, Boca Raton, Florida.
77. Greber, U. F., M. Willetts, P. Webster, and A. Helenius (1993). Stepwise dismantling of adenovirus 2 during entry into cells. *Cell.* 75: 477-486.
78. Greenspan, G. L., B. G. Corsaro, P. R. Hughes, and R. R. Granados (1991). In-vivo enhancement of baculovirus infection by the viral enhancing factor of a granulosis virus of the cabbage looper *Trichoplusia ni* (Lepidoptera: noctuidae). *J. Invert. Pathol.* 58: 203-210.
79. Griffin, J. A., and R. W. Compans (1979). Effect of cytochalasin B on the maturation of enveloped viruses. *J. Exp. Med.* 150: 379-91.

80. Guarino, L. A., M. A. Gonzalez, and M. D. Summers (1986). Complete sequence and enhancer function of the homologous DNA regions of *Autographa californica* nuclear polyhedrosis virus. *J. Virol.* 60: 224-229.
81. Guarino, L. A., and M. D. Summers (1986). Functional mapping of a trans-activating gene required for expression of a baculovirus delayed-early gene. *J. Virol.* 57: 563-571.
82. Guarino, L. A., B. Xu, J. Jin, and W. Dong (1998). A virus-encoded RNA polymerase purified from baculovirus-infected cells. *J. Virol.* 72: 7985-91.
83. Guinea, R., and L. Carrasco (1995). Requirement for vacuolar proton-ATPase activity during entry of influenza virus into cells. *J. Virol.* 69: 2306-12.
84. Hall, D. C. A., K. M. B. Caradoc-Davies, and V. K. Ward (1998). Analysis of the *Epiphyas postvittana* nucleopolyhedrovirus *gp64* gene, vol. 1998.
85. Hart, G. W., R. S. Haltiwanger, G. D. Holt, and W. G. Kelly (1989). Glycosylation in the nucleus and cytoplasm. *Annu. Rev. Biochem.* 58: 841-874.
86. Harty, R. N., J. Paragas, M. Sudol, and P. Palese (1999). A proline-rich motif within the matrix protein of Vesicular Stomatitis virus and Rabies virus interacts with WW domains of cellular proteins: implications for viral budding. *J. Virol.* 73: 2921-9.
87. Hefferon, K. L., A. G. P. Oomens, S. A. Monsma, C. M. Finnerty, and G. W. Blissard (1999). Host cell receptor binding by baculovirus GP64 and kinetics of virion entry. *Virology* 258: 455-68.
88. Heggeness, M. H., P. R. Smith, and P. W. Choppin (1982). In vitro assembly of the nonglycosylated membrane protein (M) of Sendai virus. *Proc. Natl. Acad. Sci. U S A.* 79: 6232-6.
89. Helenius, A., M. Marsh, and J. White (1982). Inhibition of Semliki Forest virus penetration by lysosomotropic weak bases. *J. Gen. Virol.* 58 Pt 1: 47-61.
90. Hess, R. T., and L. A. Falcon (1977). Observations on the interaction of baculoviruses with the plasma membrane. *J. Gen. Virol.* 36: 525-530.
91. Higgins, D. G., and P. M. Sharp (1989). Fast and sensitive multiple sequence alignments on a microcomputer. *Comput. Appl. Biosci.* 5: 151-3.
92. Hill, C. P., D. WorthyLake, D. P. Bancroft, A. M. Christensen, and W. I. Sundquist (1996). Crystal structures of the trimeric Human Immunodeficiency virus type 1 matrix protein: implications for membrane association and assembly. *Proc. Natl. Acad. Sci. U S A.* 93: 3099-104.
93. Hill, J. E., and P. Faulkner (1994). Identification of the *gp67* gene of a baculovirus pathogenic to the spruce budworm, *Choristoneura fumiferana* multinucleocapsid nuclear polyhedrosis virus. *J. Gen. Virol.* 75: 1811-1813.
94. Hill, J. E., J. Kuzio, J. A. Wilson, E. A. Mackinnon, and P. Faulkner (1993). Nucleotide sequence of the p74 gene of a baculovirus pathogenic to the spruce budworm *Choristoneur fumiferana* multicapsid nuclear polyhedrosis virus. *Biochim. Biophys. Acta.* 1172: 187-189.
95. Hink, W. F. (1970). Established insect cell line from the cabbage looper, *Trichoplusia ni*. *Nature.* 226: 466-467.
96. Hofmann, C., V. Sandig, G. Jennings, M. Rudolph, P. Schlag, and M. Strauss (1995). Efficient gene transfer into human hepatocytes by baculovirus vectors. *Proc. Natl. Acad. Sci. USA.* 92: 10099-10103.
97. Hohmann, A. W., and P. Faulkner (1983). Monoclonal antibodies to baculovirus structural proteins: Determination of specificities by Western blot analysis. *Virology* 125: 432-444.
98. Hong, T., M. D. Summers, and S. C. Braunagel (1997). N-terminal sequences from *Autographa californica* Nuclear Polyhedrosis virus envelope proteins ODV-E66 and ODV-E25 are sufficient to direct reporter proteins to the nuclear envelope, intranuclear microvesicles, and the envelope of occlusion derived virus. *Proc. Natl. Acad. Sci. USA.* 94: 4050-4055.
99. Horton, H. M., and J. P. Burand (1993). Saturable attachment sites for polyhedron-derived baculovirus on insect cells and evidence for entry via direct membrane fusion. *J. Virol.* 67: 1860-1868.

100. Hu, N. T., Y. F. Lu, Y. Hashimoto, S. Maeda, and R. F. Hou (1994). The *p10* gene of natural isolates of *Bombyx mori* Nuclear Polyhedrosis virus encodes a truncated protein with an M(r) of 7700. *J. Gen. Virol.* 75: 2085-8.
101. Hu, Z. (1998). Ph.D. thesis, ISBN 90-5485-917-2. Agricultural University Wageningen, the Netherlands.
102. Hu, Z. H., B. M. Arif, J. S. Sun, X. W. Chen, D. Zuidema, R. W. Goldbach, and J. M. Vlak (1998). Genetic organization of the HindIII-I region of the Single-nucleocapsid Nucleopolyhedrovirus of *Buzura suppressaria*. *Virus Res.* 55: 71-82.
103. Huang, X. F., R. W. Compans, S. Chen, R. A. Lamb, and P. Arvan (1997). Polarized apical targeting directed by the signal-anchor region of simian virus 5 hemagglutinin-neuraminidase. *J. Biol. Chem.* 272: 27598-27604.
104. Hughes, P. R., N. A. M. VanBeek, and H. A. Wood (1986). A modified droplet feeding method for rapid assay of *Bacillus thuringiensis* and baculoviruses in Noctuid larvae. *J. Invert. Pathol.* 48: 187-192.
105. Hughes, P. R., and H. A. Wood (1981). A synchronous peroral technique for the bioassay of insect viruses. *J. Invert. Pathol.* 37: 154-159.
106. Hurlley, S. M., D. G. Bole, H. Hoover Litty, A. Helenius, and C. S. Copeland (1989). Interactions of misfolded Influenza virus hemagglutinin with binding protein Bip. *J. Cell. Biol.* 108: 2117-2126.
107. Hurlley, S. M., and A. Helenius (1989). Protein oligomerization in the endoplasmic reticulum. *Ann. Rev. Cell. Biol.* 5: 277-307.
108. Ivanova, L., and M. J. Schlesinger (1993). Site-directed mutations in the Sindbis virus E2 glycoprotein identify palmitoylation sites and affect virus budding. *J. Virol.* 67: 2546-51.
109. Jansen, J. J. M., W. R. Mulder, C. G. L. J. De, J. M. Vlak, and G. W. J. De (1991). In-vitro expression of bovine opsin using recombinant baculovirus and the role of glutamic acid 134 in opsin biosynthesis and glycosylation. *Biochim. Biophys. Acta.* 1089: 68-76.
110. Januszkeski, M. M., P. M. Cannon, D. Chen, Y. Rozenberg, and W. F. Anderson (1997). Functional analysis of the cytoplasmic tail of Moloney murine leukemia virus envelope protein. *J. Virol.* 71: 3613-9.
111. Jarvis, D. L., J. A. G. W. Fleming, G. R. Kovacs, M. D. Summers, and L. A. Guarino (1990). Use of early baculovirus promoters for continuous expression and efficient processing of foreign gene products in stably transformed lepidopteran cells. *Bio/Technology.* 8: 950-955.
112. Jarvis, D. L., and A. Garcia (1994). Biosynthesis and processing of the *Autographa californica* Nuclear Polyhedrosis virus GP64 protein. *Virology.* 205: 300-313.
113. Jarvis, D. L., and L. A. Guarino (1995). Continuous foreign gene expression in transformed Lepidopteran insect cells, p. 187-202. In: *Baculovirus Expression Protocols*. C. Richardson (ed.), vol. Methods in Molecular Biology Vol. 39. *Humana Press Inc.*, Totowa, NJ.
114. Jarvis, D. L., C. Oker-Blom, and M. D. Summers (1990). Role of glycosylation in the transport of recombinant glycoproteins through the secretory pathway of lepidopteran insect cells. *J. Cell. Biochem.* 42: 181-191.
115. Jarvis, D. L., L. Wills, G. Burow, and D. A. Bohimeyer (1998). Mutational analysis of the N-linked glycans on *Autographa californica* nucleopolyhedrovirus gp64. *J. Virol.* 72: 9459-9469.
116. Jin, H., G. P. Leser, and R. A. Lamb (1994). The Influenza virus hemagglutinin cytoplasmic tail is not essential for virus assembly or infectivity. *EMBO J. Journal.* 13: 5504-5515.
117. Jin, H., G. P. Leser, J. Zhang, and R. A. Lamb (1997). The Influenza virus hemagglutinin and neuraminidase cytoplasmic tails control particle shape. *EMBO J.* 16: 1236-1247.
118. Jin, H., K. Subbarao, S. Bagai, G. P. Leser, B. R. Murphy, and R. A. Lamb (1996). Palmitoylation of the Influenza virus hemagglutinin (H3) is not essential for virus assembly or infectivity. *J. Virol.* 70: 1406-1414.
119. Jin, T., B. Qi, and Y. Qi (1998). *Leucania separata* multiple nuclear polyhedrosis virus genome DNA 3336bp fragment including p94 gene and another four ORFs.

120. Johnson, D. W., and J. E. Maruniak (1989). Physical map of *Anticarsia gemmatalis* Nuclear Polyhedrosis virus AgMNPV-2 DNA. *J. Gen. Virol.* 70: 1877-1884.
121. Johnson, J. E., W. Rodgers, and J. K. Rose (1998). A plasma membrane localization signal in the HIV-1 envelope cytoplasmic domain prevents localization at sites of vesicular stomatitis virus budding and incorporation into VSV virions. *Virology* 251: 244-52.
122. Jourdan, N., M. Maurice, D. Delautier, A. M. Quero, A. L. Servin, and G. Trugnan (1997). Rotavirus is released from the apical surface of cultured human intestinal cells through nonconventional vesicular transport that bypasses the Golgi apparatus. *J. Virol.* 71: 8268-78.
123. Justice, P. A., W. Sun, Y. Li, Z. Ye, P. R. Grigera, and R. R. Wagner (1995). Membrane vesiculation function and exocytosis of wild-type and mutant matrix proteins of Vesicular Stomatitis virus. *J. Virol.* 69: 3156-60.
124. Kahn, J. S., M. J. Schnell, L. Buonocore, and J. K. Rose (1999). Recombinant Vesicular Stomatitis virus expressing Respiratory Syncytial virus (RSV) glycoproteins: RSV fusion protein can mediate infection and cell fusion. *Virology* 254: 81-91.
125. Kamita, S. G., and S. Maeda (1993). Inhibition of *Bombyx mori* Nuclear Polyhedrosis virus (NPV) replication by the putative DNA helicase gene of *Autographa californica* NPV. *J. Virol.* 67: 6239-6245.
126. Kawamoto, F., C. Suto, N. Kumada, and M. Kobayashi (1977). Cytoplasmic budding of a Nuclear Polyhedrosis virus and comparative ultrastructural studies of envelopes. *Microbiol. Immunol.* 21: 255-65.
127. Keddie, B. A., G. W. Aponte, and L. E. Volkman (1989). The pathway of infection of *Autographa californica* nuclear polyhedrosis virus in an insect host. *Science*. 243: 1728-1730.
128. Keddie, B. A., and L. E. Volkman (1985). Infectivity difference between the two phenotypes of *Autographa californica* nuclear polyhedrosis virus: Importance of the 64K envelope glycoprotein. *J. Gen. Virol.* 66: 1195-1200.
129. Klenk, H. D., and R. Rott (1980). Cotranslational and posttranslational processing of viral glycoproteins. *Curr. Top. Microbiol. Immunol.* 90: 19-48.
130. Klupp, B. G., J. Baumeister, P. Dietz, H. Granzow, and T. C. Mettenleiter (1998). Pseudorabies virus glycoprotein gK is a virion structural component involved in virus release but is not required for entry. *J. Virol.* 72: 1949-58.
131. Knipe, D. M., D. Baltimore, and H. F. Lodish (1977). Maturation of viral proteins in cells infected with temperature-sensitive mutants of Vesicular Stomatitis virus. *J. Virol.* 21: 1149-58.
132. Kogan, P. H., and G. W. Blissard (1994). A baculovirus *gp64* early promoter is activated by host transcription factor binding to CACGTG and GATA elements. *J. Virol.* 68: 813-822.
133. Kogan, P. H., X. Chen, and G. W. Blissard (1995). Overlapping TATA-dependent and TATA-independent early promoter activities in the baculovirus *gp64* envelope fusion protein gene. *J. Virol.* 69: 1452-1461.
134. Kool, M., C. H. Ahrens, J. M. Vlak, and G. R. Rohrmann (1995). Replication of baculovirus DNA. *J. Gen. Virol.* 76: 2103-2118.
135. Kool, M., J. T. M. Voeten, R. W. Goldbach, J. Tramper, and J. M. Vlak (1993). Identification of seven putative origins of *Autographa californica* multiple nucleocapsid nuclear polyhedrosis virus DNA replication. *J. Gen. Virol.* 74: 2661-2668.
136. Kornfeld, R., and S. Kornfeld (1985). Assembly of asparagine-linked oligosaccharides. *Ann. Rev. Biochem.* 54: 631-664.
137. Kretzschmar, E., L. Buonocore, M. J. Schnell, and J. K. Rose (1997). High-efficiency incorporation of functional Influenza virus glycoproteins into recombinant Vesicular Stomatitis viruses. *J. Virol.* 71: 5982-5989.

138. Kubelka, V., F. Altmann, G. Kornfeld, and L. Marz (1994). Structures of the N-linked oligosaccharides of the membrane glycoproteins from three lepidopteran cell lines (*Sf-21*, *IZD-Mb-0503*, *Bm-N*). *Arch. Biochem. Biophys.* 308: 148-57.
139. Kundu, A., R. T. Avalos, C. M. Sanderson, and D. P. Nayak (1996). Transmembrane domain of Influenza virus neuraminidase, a type II protein, possesses an apical sorting signal in polarized MDCK cells. *J. Virol.* 70: 6508-15.
140. Kuroda, K., H. Geyer, R. Geyer, W. Doerfler, and H.-D. Klenk (1990). The oligosaccharides of Influenza virus hemagglutinin expressed in insect cells by a baculovirus vector. *Virology*. 174: 418-429.
141. Kuzio, J., M. N. Pearson, S. H. Harwood, C. J. Funk, J. T. Evans, J. M. Slavicek, and G. F. Rohrmann (1999). Sequence and analysis of the genome of a baculovirus pathogenic for *Lymantria dispar*. *Virology*. 253: 17-34.
142. Kyte, J., and R. F. Doolittle (1982). A simple method for displaying the hydropathic character of a protein. *J. Mol. Biol.* 157: 105-132.
143. Lamb, R. A. (1993). Paramyxovirus fusion: A hypothesis for changes. *Virology*. 197: 1-11.
144. Lamb, R. A., and R. M. Krug (1996). Orthomyxoviridae, p. 1353-1396. In: Fields Virology. . *Lippincott-Raven*, Philadelphia.
145. Lamb, R. A., S. L. Zebedee, and C. D. Richardson (1985). Influenza virus M2 protein is an integral membrane protein expressed on the infected-cell surface. *Cell*. 40: 627-33.
146. Leahy, M. B., J. T. Dessens, F. Weber, G. Kochs, and P. A. Nuttall (1997). The fourth genus in the Orthomyxoviridae: Sequence analyses of two Thogoto virus polymerase proteins and comparison with Influenza Viruses. *Virus Res.* 50: 215-224.
147. Leikina, E., H. O. Onaran, and J. Zimmerberg (1992). Acidic pH induces fusion of cells infected with baculovirus to form syncytia. *FEBS Letters*. 304: 221-224.
148. Lenard, J., and D. K. Miller (1982). Uncoating of enveloped viruses. *Cell*. 28: 5-6.
149. Liu, C., and G. M. Air (1993). Selection and characterization of a neuraminidase-minus mutant of Influenza virus and its rescue by cloned neuraminidase genes. *Virology*. 194: 403-7.
150. Lodge, R., L. Delamarre, J. P. Lalonde, J. Alvarado, D. A. Sanders, M. C. Dokhelar, E. A. Cohen, and G. Lemay (1997). Two distinct oncornaviruses harbor an intracytoplasmic tyrosine-based basolateral targeting signal in their viral envelope glycoprotein. *J. Virol.* 71: 5696-702.
151. Lodge, R., H. Gottlinger, D. Gabuzda, E. A. Cohen, and G. Lemay (1994). The intracytoplasmic domain of gp41 mediates polarized budding of human immunodeficiency virus type 1 in MDCK cells. *J. Virol.* 68: 4857-61.
152. Lu, A., and L. K. Miller (1996). Species-specific effects of the *hcf-1* gene on baculovirus virulence. *J. Virol.* 70: 5123-5130.
153. Luytjes, W., M. Krystal, M. Enami, J. D. Pavin, and P. Palese (1989). Amplification, expression, and packaging of foreign gene by Influenza virus. *Cell*. 59: 1107-13.
154. Maeda, S., S. G. Kamita, and A. Kondo (1993). Host range expansion of *Autographa californica* Nuclear Polyhedrosis virus (NPV) following recombination of a 0.6-Kilobase-pair DNA fragment originating from *Bombyx mori* NPV. *J. Virol.* 67: 6234-6238.
155. Majima, K., S. Gomi, T. Ohkawa, S. G. Kamita, and S. Maeda (1996). Complete nucleotide sequence of the 128,413 bp-long genome of the baculovirus BmNPV.
156. Majima, K., R. Kobara, and S. Maeda (1993). Divergence and evolution of homologous regions of *Bombyx mori* Nuclear Polyhedrosis virus. *J. Virol.* 67: 7513-7521.
157. Markovic, I., H. Pulyaeva, A. Sokoloff, and L. V. Chernomordik (1998). Membrane fusion mediated by baculovirus gp64 involves assembly of stable gp64 trimers into multiprotein aggregates. *J. Cell. Biol.* 143: 1155-66.
158. Marsh, M., and A. Helenius (1980). Adsorptive endocytosis of Semliki Forest virus. *J. Mol. Biol.* 142: 439-54.

159. Marsh, M., and A. Helenius (1989). Virus entry into animal cells. *Advances in Virus Research*. 36: 107-151.
160. Martin, K., and A. Helenius (1991). Transport of incoming Influenza virus nucleocapsids into the nucleus. *J. Virol.* 65: 232-244.
161. Maruniak, J. W., and M. D. Summers (1981). *Autographa californica* nuclear polyhedrosis virus phosphoproteins and synthesis of intracellular proteins after virus infection. *Virology*. 109: 25-34.
162. Matlin, K. S., H. Reggio, A. Helenius, and K. Simons (1982). Pathway of Vesicular Stomatitis virus entry leading to infection. *J. Mol. Biol.* 156: 609-31.
163. Mebatsion, T., M. Konig, and K. K. Conzelmann (1996). Budding of Rabies virus particles in the absence of the spike glycoprotein. *Cell*. 84: 941-951.
164. Melikyan, G. B., H. Jin, R. A. Lamb, and F. S. Cohen (1997). The role of the cytoplasmic tail region of Influenza virus hemagglutinin in formation and growth of fusion pores. *Virology*. 235: 118-128.
165. Metsikko, K., and H. Garoff (1990). Oligomers of the cytoplasmic domain of the p62/E2 membrane protein of Semliki Forest virus bind to the nucleocapsid in vitro. *J. Virol.* 64: 4678-83.
166. Metsikko, K., and K. Simons (1986). The budding mechanism of spikeless Vesicular Stomatitis virus particles. *EMBO J.* 5: 1913-20.
167. Miller, L. K. (ed.) (1997). *The Baculoviruses*. Plenum Press, New York.
168. Miller, L. K., and A. Lu (1997). The molecular basis of baculovirus host range, p. pp 217-236. In: *The Baculoviruses*. L. K. Miller (ed.). Plenum Press, New York.
169. Miller, M. L., and D. T. Brown (1992). Morphogenesis of Sindbis virus in three subclones of *Aedes albopictus* (mosquito) cells. *J. Virol.* 66: 4180-90.
170. Mitnaul, L. J., M. R. Castrucci, K. G. Murti, and Y. Kawaoka (1996). The cytoplasmic tail of influenza A virus neuraminidase (NA) affects NA incorporation into virions, virion morphology, and virulence in mice but is not essential for virus replication. *J. Virol.* 70: 873-879.
171. Monsma, S. A., and G. W. Blissard (1995). Identification of a membrane fusion domain and an oligomerization domain in the baculovirus GP64 Envelope Fusion Protein. *J. Virol.* 69: 2583-2595.
172. Monsma, S. A., A. G. P. Oomens, and G. W. Blissard (1996). The GP64 Envelope Fusion Protein is an essential baculovirus protein required for cell to cell transmission of infection. *J. Virol.* 70: 4607-4616.
173. Morse, M. A., A. C. Marriott, and P. A. Nuttall (1992). The glycoprotein of Thogoto virus (a tick-borne orthomyxo-like virus) is related to the baculovirus glycoprotein gp64. *Virology*. 186: 640-646.
174. Mulligan, M. J., G. V. Yamshchikov, G. D. Ritter, Jr., F. Gao, M. J. Jin, C. D. Nail, C. P. Spies, B. H. Hahn, and R. W. Compans (1992). Cytoplasmic domain truncation enhances fusion activity by the exterior glycoprotein complex of Human Immunodeficiency virus type 2 in selected cell types. *J. Virol.* 66: 3971-5.
175. Naim, H. Y., B. Amareh, N. T. Kistakis, and M. G. Roth (1992). Effects of altering palmitoylation sites on biosynthesis and function of the Influenza virus hemagglutinin. *J. Virol.* 66: 7585-8.
176. Nermut, M. V., D. J. Hockley, J. B. Jowett, I. M. Jones, M. Garreau, and D. Thomas (1994). Fullerene-like organization of HIV gag-protein shell in virus-like particles produced by recombinant baculovirus. *Virology*. 198: 288-96.
177. O'Reilly, D. R., L. K. Miller, and V. A. Luckow (1992). Baculovirus expression vectors, a laboratory manual. *W. H. Freeman and Co., New York*.
178. Oellig, C., B. Happ, T. Mueller, and W. Doerfler (1987). Overlapping sets of viral RNA species reflect the array of polypeptides in the Eco-RI J and N fragments, map positions 81.2 to 85.0 of the *Autographa californica* nuclear polyhedrosis virus genome. *J. Virol.* 61: 3048-3057.
179. Ohkawa, T., K. Majima, and S. Maeda (1994). A cysteine protease encoded by the baculovirus *Bombyx mori* Nuclear Polyhedrosis virus. *J. Virol.* 68: 6619-25.
180. Ohuchi, M., C. Fischer, R. Ohuchi, A. Herwig, and H. D. Klenk (1998). Elongation of the cytoplasmic tail interferes with the fusion activity of Influenza virus hemagglutinin. *J. Virol.* 72: 3554-9.

181. Olszewski, J., and L. K. Miller (1997). A role of baculovirus GP41 in budded virus production. *Virology* 233: 292-301.
182. Ono, A., M. Huang, and E. O. Freed (1997). Characterization of human immunodeficiency virus type 1 matrix revertants: effects on virus assembly, Gag processing, and Env incorporation into virions. *J. Virology* 71: 4409-18.
183. Oomens, A. G. P., and G. W. Blissard (1999). Requirement for GP64 to drive efficient budding of *Autographa californica* Multicapsid Nucleopolyhedrovirus. *Virology* 254: 297-314.
184. Oomens, A. G. P., S. A. Monsma, and G. W. Blissard (1995). The baculovirus GP64 Envelope Fusion Protein: synthesis, oligomerization, and processing. *Virology* 209: 592-603.
185. Owens, R. J., J. W. Dubay, E. Hunter, and R. W. Compans (1991). Human Immunodeficiency virus envelope protein determines the site of virus release in polarized epithelial cells. *Proc. Natl. Acad. Sci. U S A* 88: 3987-91.
186. Owens, R. J., and J. K. Rose (1993). Cytoplasmic domain requirement for incorporation of a foreign envelope protein into Vesicular Stomatitis virus. *J. Virology* 67: 360-5.
187. Paillart, J. C., and H. G. Gottlinger (1999). Opposing effects of Human Immunodeficiency virus type 1 matrix mutations support a myristyl switch model of gag membrane targeting. *J. Virology* 73: 2604-12.
188. Palese, P., K. Tobita, M. Ueda, and R. W. Compans (1974). Characterization of temperature sensitive Influenza virus mutants defective in neuraminidase. *Virology* 61: 397-410.
189. Palhan, V. B., and K. P. Gopinathan (1996). The p10 gene of *Bombyx mori* nuclear polyhedrosis virus is highly conserved amongst baculoviruses and hypertranscribed from the TAAG motif, vol. 1996.
190. Parent, L. J., R. P. Bennett, R. C. Craven, T. D. Nelle, N. K. Krishna, J. B. Bowzard, C. B. Wilson, B. A. Puffer, R. C. Montelaro, and J. W. Wills (1995). Positionally independent and exchangeable late budding functions of the Rous sarcoma virus and Human Immunodeficiency virus Gag proteins. *J. Virology* 69: 5455-60.
191. Pattnaik, A. K., D. J. Brown, and D. P. Nayak (1986). Formation of Influenza virus particles lacking hemagglutinin on the viral envelope. *J. Virology* 60: 994-1001.
192. Pavan, O. H. P., and H. C. T. Ribeiro (1989). Selection of a baculovirus strain with a bivalent insecticidal activity. *Mem. Inst. Oswaldo Cruz* 84: 63-65.
193. Payne, L. G., and K. Kristensson (1982). The effect of cytochalasin D and monensin on enveloped Vaccinia virus release. *Arch. Virology* 74: 11-20.
194. Pearson, M. N., and G. F. Rohrmann (1995). *Lymantria dispar* Nuclear Polyhedrosis virus homologous regions: Characterization of their ability to function as replication origins. *J. Virology* 69: 213-221.
195. Plonsky, I., M. S. Cho, A. G. P. Oomens, G. W. Blissard, and J. Zimmerberg (1999). An analysis of the role of the target membrane on the gp64-induced fusion pore. *Virology* 253: 65-76.
196. Plonsky, I., E. Leikina, A. G. P. Oomens, G. W. Blissard, J. Zimmerberg, and L. Chernomordik (1997). The target membrane influences the pH-dependence and kinetics of viral fusion. *Biophys. J.* 72: A300.
197. Plonsky, I., and J. Zimmerberg (1996). The initial fusion pore induced by baculovirus GP64 is large and forms quickly. *J. Cell. Biol.* 135: 1831-1839.
198. Poloumienko, A., and P. Krell (1996). Identification of the putative p22, gp16, calyx protein, p25, exonuclease and p26 genes of a baculovirus pathogenic to the spruce budworm, CfMNPV.
199. Poloumienko, A., and P. Krell (1997). New protein in the p22-gp67 intergenic region of the CfMNPV.
200. Ponimaskin, E., and M. F. Schmidt (1998). Domain-structure of cytoplasmic border region is main determinant for palmitoylation of Influenza virus hemagglutinin (H7). *Virology* 249: 325-35.
201. Portela, A., L. D. Jones, and P. Nuttall (1992). Identification of viral structural polypeptides of Thogoto virus, a tick-borne orthomyxo-like virus and functions associated with the glycoprotein. *J. Gen. Virology* 73: 2823-2830.
202. Rao, Z., A. S. Belyaev, E. Fry, P. Roy, I. M. Jones, and D. I. Stuart (1995). Crystal structure of SIV matrix antigen and implications for virus assembly. *Nature* 378: 743-7.

203. Ray, F. A., and J. A. Nickoloff (1992). Site-specific mutagenesis of almost any plasmid using a PCR-based version of unique site elimination. *Biotechniques*. 13: 342-346.
204. Rice, C. M., and J. H. Strauss (1981). Nucleotide sequence of the 26S mRNA of Sindbis virus and deduced sequence of the encoded virus structural proteins. *Proc. Natl. Acad. Sci. U S A*. 78: 2062-6.
205. Ritter, G. D., Jr., M. J. Mulligan, S. L. Lydy, and R. W. Compans (1993). Cell fusion activity of the Simian Immunodeficiency virus envelope protein is modulated by the intracytoplasmic domain. *Virology*. 197: 255-64.
206. Roberts, S. R., and J. S. Manning (1993). The major envelope glycoprotein of the extracellular virion of *Autographa californica* Nuclear Polyhedrosis virus possesses at least three distinct neutralizing epitopes. *Virus Res*. 28: 285-297.
207. Roberts, T. E., and P. Faulkner (1989). Fatty acid acylation of the 67K envelope glycoprotein of a baculovirus *Autographa californica* nuclear polyhedrosis virus. *Virology*. 172: 377-381.
208. Rodriguez-Boulan, E., and D. D. Sabatini (1978). Asymmetric budding of viruses in epithelial monolayers: a model system for study of epithelial polarity. *Proc. Natl. Acad. Sci. USA*. 75: 5071-5075.
209. Rohrmann, G. F. (1992). Baculovirus structural proteins. *J. Gen. Virol.* 73: 749-761.
210. Roizman, B., and A. E. Sears (1996). Herpes Simplex viruses and their replication, p. 2231-2295. In: *Fields Virology*. . Lippincott-Raven, Philadelphia.
211. Rolls, M. M., P. Webster, N. H. Balba, and J. K. Rose (1994). Novel infectious particles generated by expression of the Vesicular Stomatitis virus glycoprotein from a self-replicating RNA. *Cell*. 79: 497-506.
212. Rose, J. K., G. A. Adams, and C. J. Gallione (1984). The presence of cysteine in the cytoplasmic domain of the Vesicular Stomatitis virus glycoprotein is required for palmitate addition. *Proc. Natl. Acad. Sci. U S A*. 81: 2050-4.
213. Rossen, J. W., R. de Beer, G. J. Godeke, M. J. Raamsman, M. C. Horzinek, H. Vennema, and P. J. Rottier (1998). The viral spike protein is not involved in the polarized sorting of Coronaviruses in epithelial cells. *J. Virol.* 72: 497-503.
214. Roth, M. G., R. V. Srinivas, and R. W. Compans (1983). Basolateral maturation of retroviruses in polarized epithelial cells. *J. Virol.* 45: 1065-1070.
215. Ruta, M., M. J. Murray, M. C. Webb, and D. Kabat (1979). A Murine Leukemia virus mutant with a temperature-sensitive defect in membrane glycoprotein synthesis. *Cell*. 16: 77-88.
216. Ryan, C., L. Ivanova, and M. J. Schlesinger (1998). Effects of site-directed mutations of transmembrane cysteines in Sindbis virus E1 and E2 glycoproteins on palmylation and virus replication. *Virology*. 249: 62-7.
217. Salzwedel, K., J. T. West, Jr., M. J. Mulligan, and E. Hunter (1998). Retention of the human Immunodeficiency virus type 1 envelope glycoprotein in the endoplasmic reticulum does not redirect virus assembly from the plasma membrane. *J. Virol.* 72: 7523-31.
218. Sandig, V., C. Hofmann, S. Steinert, G. Jennings, P. Schlag, and M. Strauss (1996). Gene transfer into hepatocytes and human liver tissue by baculovirus vectors. *Hum. Gene Ther.* 7: 1937-45.
219. Scheiffele, P., A. Rietveld, T. Wilk, and K. Simons (1999). Influenza viruses select ordered lipid domains during budding from the plasma membrane. *J. Biol. Chem.* 274: 2038-44.
220. Scheiffele, P., M. G. Roth, and K. Simons (1997). Interaction of Influenza virus haemagglutinin with sphingolipid- cholesterol membrane domains via its transmembrane domain. *EMBO J.* 16: 5501-8.
221. Schnell, M. J., L. Buonocore, E. Boritz, H. P. Ghosh, R. Chernish, and J. K. Rose (1998). Requirement for a non-specific glycoprotein cytoplasmic domain sequence to drive efficient budding of Vesicular Stomatitis virus. *EMBO J.* 17: 1289-1296.

222. Schnell, M. J., L. Buonocore, E. Kretzschmar, E. Johnson, and J. K. Rose (1996). Foreign glycoproteins expressed from recombinant Vesicular Stomatitis viruses are incorporated efficiently into virus particles. *Proc. Natl. Acad. Sci. USA.* 93: 11359-11365.
223. Schnell, M. J., J. E. Johnson, L. Buonocore, and J. K. Rose (1997). Construction of a novel virus that targets HIV-1-infected cells and controls HIV-1 infection. *Cell.* 90: 849-857.
224. Schnitzer, T. J., C. Dickson, and R. A. Weiss (1979). Morphological and biochemical characterization of viral particles produced by the tsO45 mutant of Vesicular Stomatitis virus at restrictive temperature. *J. Virol.* 29: 185-95.
225. Schultz, A. M., L. E. Henderson, and S. Oroszlan (1988). Fatty acylation of proteins. *Annu. Rev. Cell Biol.* 4: 611-47.
226. Shields, A., W. N. Witte, E. Rothenberg, and D. Baltimore (1978). High frequency of aberrant expression of Moloney Murine Leukemia virus in clonal infections. *Cell.* 14: 601-9.
227. Shoji, I., H. Aizaki, H. Tani, K. Ishii, T. Chiba, I. Saito, T. Miyamura, and Y. Matsuura (1997). Efficient gene transfer into various mammalian cells, including non-hepatic cells, by baculovirus vectors. *J. Gen. Virol.* 78: 2657-2664.
228. Silverstein, S. C., R. M. Steinman, and Z. A. Cohn (1977). Endocytosis. *Annu. Rev. Biochem.* 46: 669-722.
229. Simons, K., and E. Ikonen (1997). Functional rafts in cell membranes. *Nature.* 387: 569-72.
230. Simpson, D. A., and R. A. Lamb (1992). Alterations of Influenza virus hemagglutinin cytoplasmic tail modulate virus infectivity. *J. Virol.* 66: 790-803.
231. Slack, J. M., J. Kuzio, and P. Faulkner (1995). Characterization of v-cath, a cathepsin L-like proteinase expressed by the baculovirus *Autographa californica* Multiple Nuclear Polyhedrosis virus. *J. Gen. Virol.* 76: 1091-1098.
232. Smith, G. E., and M. D. Summers (1978). Analysis of baculovirus genomes with restriction endonucleases. *Virology.* 89: 517-527.
233. Southern, P. J., and P. Berg (1982). Transformation of mammalian cells to antibiotic resistance with a bacterial gene under control of the SV40 early region promoter. *J. Mol. Appl. Gen.* 1: 327-341.
234. Spearman, P., R. Horton, L. Ratner, and I. Kuli-Zade (1997). Membrane binding of Human Immunodeficiency virus type 1 matrix protein in vivo supports a conformational myristyl switch mechanism. *J. Virol.* 71: 6582-92.
235. Spies, C. P., and R. W. Compans (1994). Effects of cytoplasmic domain length on cell surface expression and syncytium-forming capacity of the Simian Immunodeficiency virus envelope glycoprotein. *Virology.* 203: 8-19.
236. Stephens, E. B., and R. W. Compans (1988). Assembly of animal viruses at cellular membranes. *Annu. Rev. Microbiol.* 42: 489-516.
237. Stiles, B., and H. A. Wood (1983). A study of the glycoproteins of *Autographa californica* Nuclear Polyhedrosis virus (AcNPV). *Virology.* 131: 230-241.
238. Straubinger, R. M., K. Hong, D. S. Friend, and D. Papahadjopoulos (1983). Endocytosis of liposomes and intracellular fate of encapsulated molecules: encounter with a low pH compartment after internalization in coated vesicles. *Cell.* 32: 1069-79.
239. Strauss, E. G. (1978). Mutants of Sindbis virus. III. Host polypeptides present in purified HR and ts103 virus particles. *J. Virol.* 28: 466-74.
240. Sturzenbecker, L. J., M. Nibert, D. Furlong, and B. N. Fields (1987). Intracellular digestion of Reovirus particles requires a low pH and is an essential step in the viral infectious cycle. *J. Virol.* 61: 2351-61.
241. Sudol, M. (1996). Structure and function of the WW domain. *Prog. Biophys. Mol. Biol.* 65: 113-32.
242. Sudol, M., P. Bork, A. Einbond, K. Kastury, T. Druck, M. Negrini, K. Huebner, and D. Lehman (1995). Characterization of the mammalian YAP (Yes-associated protein) gene and its role in defining a novel protein module, the WW domain. *J. Biol. Chem.* 270: 14733-41.

243. Summers, M. D. (1971). Electron microscopic observations of granulosis virus entry, uncoating and replication processes during infection of the midgut cells of *Trichoplusia ni*. *J. Ultrastr. Res.* 35: 606-625.
244. Summers, M. D., and G. E. Smith (1987). A manual of methods for baculovirus vectors and insect cell culture procedures. *Texas Agricultural Experiment Station Bulletin*.
245. Suomalainen, M., and H. Garoff (1994). Incorporation of homologous and heterologous proteins into the envelope of Moloney Murine Leukemia virus. *J. Virol.* 68: 4879-4889.
246. Suomalainen, M., P. Liljestrom, and H. Garoff (1992). Spike protein-nucleocapsid interactions drive the budding of alphaviruses. *J. Virol.* 66: 4737-4747.
247. Sussman, D. J. (1995). 24-hour assay for estimating the titer of beta-galactosidase expressing baculovirus. *Biotechniques.* 18: 50-51.
248. Takimoto, T., T. Bousse, E. C. Coronel, R. A. Scroggs, and A. Portner (1998). Cytoplasmic domain of Sendai virus HN protein contains a specific sequence required for its incorporation into virions. *J. Virol.* 72: 9747-54.
249. Tanada, Y., R. T. Hess, and E. M. Ormi (1975). Invasion of a nuclear polyhedrosis virus in midgut of the armyworm *Pseudaletia unipuncta*, and the enhancement of a synergistic enzyme. *J. Invert. Pathol.* 26: 99-104.
250. Theilmann, D. A., and S. Stewart (1992). Molecular analysis of the trans-activating *ie-2* gene of *Orgyia pseudotsugata* Multicapsid Nuclear Polyhedrosis virus. *Virology.* 187: 84-96.
251. Thomas, D. C., C. B. Brewer, and M. G. Roth (1993). Vesicular Stomatitis virus glycoprotein contains a dominant cytoplasmic basolateral sorting signal critically dependent upon a tyrosine. *J. Biol. Chem.* 268: 3313-20.
252. Tubulekas, I., and P. Liljestrom (1998). Suppressors of cleavage-site mutations in the p62 envelope protein of Semliki Forest virus reveal dynamics in spike structure and function. *J. Virol.* 72: 2825-31.
253. Van Oers, M. M., J. T. M. Flipsen, C. B. E. M. Reusken, E. L. Sliwinsky, R. W. Goldbach, and J. M. Vlak (1993). Functional domains of the p10 protein of *Autographa californica* Nuclear Polyhedrosis virus. *J. Gen. Virol.* 74: 563-574.
254. Vennema, H., G. J. Godeke, J. W. Rossen, W. F. Voorhout, M. C. Horzinek, D. J. Opstelten, and P. J. Rottier (1996). Nucleocapsid-independent assembly of Coronavirus-like particles by co-expression of viral envelope protein genes. *Embo J.* 15: 2020-8.
255. Vlak, J. M., and G. F. Rohrmann (1985). The nature of polyhedrin. In: *Viral insecticides of biological control*. K. Maramorosch and K. E. Sherman (ed.). *Academic Press*, New York.
256. Vlak, J. M., A. Schouten, M. Usmany, G. J. Belsham, E. C. Klinge Roode, A. J. Maule, J. W. M. VanLent, and D. Zuidema (1990). Expression of Cauliflower Mosaic virus Gene I using a baculovirus vector based upon the P10 gene and a novel selection method. *Virology.* 179: 312-320.
257. Vlcek, C., V. Benes, Z. Lu, G. F. Kutish, V. Paces, D. Rock, G. J. Letchworth, and M. Schwyzer (1995). Nucleotide sequence analysis of a 30-kb region of the bovine herpesvirus 1 genome which exhibits a colinear gene arrangement with the UL21 to UL4 genes of Herpes Simplex virus. *Virology.* 210: 100-8.
258. Volkman, L. E. (1986). The 64K envelope protein of budded *Autographa californica* Nuclear Polyhedrosis virus. *Curr. Top. Microbiol. Immunol.* 131: 103-118.
259. Volkman, L. E., G. W. Blissard, P. Friesen, B. A. Keddie, R. Possee, and D. A. Theilmann (1995). Baculoviridae: Taxonomic structure and properties of the family. *Arch. Virol. Sixth report of the international committee for the taxonomy of viruses.* Supplement 10: 104-113.
260. Volkman, L. E., and P. A. Goldsmith (1984). Budded *Autographa californica* NPV 64K protein: further biochemical analysis and effects of postimmunoprecipitation sample preparation conditions. *Virology.* 139: 295-302.

261. Volkman, L. E., and P. A. Goldsmith (1985). Mechanism of neutralization of budded *Autographa californica* Nuclear Polyhedrosis virus by a monoclonal antibody: Inhibition of entry by adsorptive endocytosis. *Virology* 143: 185-195.
262. Volkman, L. E., and P. A. Goldsmith (1988). Resistance of the 64K protein of budded *Autographa californica* nuclear polyhedrosis virus to functional inactivation by proteolysis. *Virology* 166: 285-289.
263. Volkman, L. E., P. A. Goldsmith, and R. Hess (1987). Evidence for microfilament involvement in budded *Autographa californica* Nuclear Polyhedrosis virus production. *Virology* 156: 32-39.
264. Volkman, L. E., P. A. Goldsmith, R. T. Hess, and P. Faulkner (1984). Neutralization of budded *Autographa californica* NPV by a monoclonal antibody: Identification of the target antigen. *Virology* 133: 354-362.
265. Volkman, L. E., and M. D. Summers (1977). *Autographa californica* nuclear polyhedrosis virus: Comparative infectivity of the occluded, alkali-liberated, and nonoccluded forms. *J. Invert. Pathol.* 30: 102-103.
266. Volkman, L. E., M. D. Summers, and C. H. Hsieh (1976). Occluded and nonoccluded nuclear polyhedrosis virus grown in *Trichoplusia ni* comparative neutralization, comparative infectivity, and in vitro growth studies. *J. Virology* 19: 820-832.
267. Von Heijne, G., and Y. Gavel (1988). Topogenic signals in integral membrane proteins. *Eur. J. Biochem.* 174: 671-678.
268. Wahlberg, J. M., and H. Garoff (1992). Membrane fusion process of Semliki Forest virus. I: Low pH-induced rearrangement in spike protein quaternary structure precedes virus penetration into cells. *J. Cell. Biol.* 116: 339-48.
269. Wain-Hobson, S., P. Sonigo, O. Danos, S. Cole, and M. Alizon (1985). Nucleotide sequence of the AIDS virus, LAV. *Cell* 40: 9-17.
270. Wang, P., D. A. Hammer, and R. R. Granados (1997). Binding and fusion of *Autographa californica* nucleopolyhedrovirus to cultured insect cells. *J. Gen. Virology* 78: 3081-9.
271. Whitford, M., and P. Faulkner (1992). Nucleotide sequence and transcriptional analysis of a gene encoding gp41 a structural glycoprotein of the baculovirus *Autographa californica* nuclear polyhedrosis virus. *J. Virology* 66: 4763-4768.
272. Whitford, M., and P. Faulkner (1992). A structural polypeptide of the baculovirus *Autographa californica* Nuclear Polyhedrosis virus contains O-linked N-acetylglucosamine. *J. Virology* 66: 3324-3329.
273. Whitford, M., S. Stewart, J. Kuzio, and P. Faulkner (1989). Identification and sequence analysis of a gene encoding gp67, an abundant envelope glycoprotein of the baculovirus *Autographa californica* Nuclear Polyhedrosis virus. *J. Virology* 63: 1393-1399.
274. Whitt, M. A., and J. S. Manning (1988). A phosphorylated 34-kDa protein and a subpopulation of polyhedrin are thiol linked to the carbohydrate layer surrounding a baculovirus occlusion body. *Virology* 163: 33-42.
275. Whitt, M. A., and J. K. Rose (1991). Fatty acid acylation is not required for membrane fusion activity or glycoprotein assembly into VSV virions. *Virology* 185: 875-8.
276. Wickham, T. J., M. L. Shuler, D. A. Hammer, R. R. Granados, and H. A. Wood (1992). Equilibrium and kinetic analysis of *Autographa californica* Nuclear Polyhedrosis virus attachment to different insect cell lines. *J. Gen. Virology* 73: 3185-3194.
277. Wilk, T., T. Pfeiffer, and V. Bosch (1992). Retained in vitro infectivity and cytopathogenicity of HIV-1 despite truncation of the C-terminal tail of the env gene product. *Virology* 189: 167-77.
278. Wills, J. W., C. E. Cameron, C. B. Wilson, Y. Xiang, R. P. Bennett, and J. Leis (1994). An assembly domain of the Rous sarcoma virus Gag protein required late in budding. *J. Virology* 68: 6605-18.
279. Wilson, I. A., J. J. Skehel, and D. C. Wiley (1981). Structure of the haemagglutinin membrane glycoprotein of influenza virus at 3 Å resolution. *Nature* 289: 366-73.

280. Wilson, J. A., J. E. Hill, J. Kuzio, and P. Faulkner (1995). Characterization of the baculovirus *Choristoneura fumiferana* multicapsid Nuclear Polyhedrosis virus p10 gene indicates that the polypeptide contains a coiled-coil domain. *J. Gen. Virol.* 76: 2923-2932.
281. Xiang, Y., C. E. Cameron, J. W. Wills, and J. Leis (1996). Fine mapping and characterization of the Rous sarcoma virus Pr76gag late assembly domain. *J. Virol.* 70: 5695-700.
282. Xie, W. D., B. Arif, P. Dobos, and P. J. Krell (1995). Identification and analysis of a putative origin of DNA replication in the *Choristoneura fumiferana* Multicapsid Nuclear Polyhedrosis virus genome. *Virology*. 209: 409-419.
283. Yao, J., E. G. Strauss, and J. H. Strauss (1998). Molecular genetic study of the interaction of Sindbis virus E2 with Ross River virus E1 for virus budding. *J. Virol.* 72: 1418-23.
284. Young, J. D., D. Tsuchiya, D. E. Sandlin, and M. J. Holroyde (1979). Enzymic O-glycosylation of synthetic peptides from sequences in basic myelin protein. *Biochem.* 18: 4444-8.
285. Yu, Y. G., D. S. King, and Y. K. Shin (1994). Insertion of a coiled-coil peptide from Influenza virus hemagglutinin into membranes. *Science*. 266: 274-276.
286. Zanutto, P. M., B. D. Kessing, and J. E. Maruniak (1993). Phylogenetic interrelationships among baculoviruses: evolutionary rates and host associations. *J. Invert. Pathol.* 62: 147-164.
287. Zanutto, P. M. D. A., M. J. Sampaio, D. W. Johnson, T. L. Rocha, and J. E. Maruniak (1992). The *Anticarsia gemmatilis* Nuclear Polyhedrosis virus polyhedrin gene region: sequence analysis, gene product and structural comparisons. *J. Gen. Virol.* 73: 1049-1056.
288. Zebedee, S. L., and R. A. Lamb (1988). Influenza A virus M2 protein: monoclonal antibody restriction of virus growth and detection of M2 in virions. *J. Virol.* 62: 2762-72.
289. Zhang, Y., X. Wu, and Z. Li (1995). *P10* genes of BmNPV and AcMNPV, vol. 1995.
290. Zhao, H., M. Ekstrom, and H. Garoff (1998). The M1 and NP proteins of Influenza A virus form homo-but not heterooligomeric complexes when coexpressed in BHK-21 cells. *J. Gen. Virol.* 79: 2435-46.
291. Zhao, H., and H. Garoff (1992). Role of cell surface spikes in alphavirus budding. *J. Virol.* 66: 7089-7095.
292. Zhao, H., B. Lindqvist, H. Garoff, C. H. Von Bonsdorff, and P. Liljestrom (1994). A tyrosine-based motif in the cytoplasmic domain of the alphavirus envelope protein is essential for budding. *EMBO J.* 13: 4204-4211.
293. Zhou, W., L. J. Parent, J. W. Wills, and M. D. Resh (1994). Identification of a membrane-binding domain within the amino-terminal region of Human Immunodeficiency virus type 1 Gag protein which interacts with acidic phospholipids. *J. Virol.* 68: 2556-69.
294. Zhou, W., and M. D. Resh (1996). Differential membrane binding of the Human Immunodeficiency virus type 1 matrix protein. *J. Virol.* 70: 8540-8.
295. Zuidema, D., A. Schouten, M. Usmany, A. J. Maule, G. J. Belsham, J. Roosien, E. C. Klinge Roode, J. W. M. VanLent, and J. M. Vlak (1990). Expression of Cauliflower Mosaic virus gene I in insect cells using a novel polyhedrin-based baculovirus expression vector. *J. Gen. Virol.* 71: 2201-2210.

Summary

The Baculoviridae are a family of large, enveloped, double-stranded DNA viruses, that cause severe disease in the larvae of mostly lepidopteran insects. Baculoviruses have been studied with the aim of developing alternatives to chemical pest control, and later for their potential as systems for foreign gene expression and to address fundamental virological questions. The Baculoviridae are divided into two genera: the Granuloviruses (GVs) and the Nucleopolyhedroviruses (NPVs). The viruses studied in this thesis, *Autographa californica*, *Orgyia pseudotsugata*, and *Anticarsia gemmatilis* Multicapsid Nucleopolyhedroviruses (AcMNPV, OpMNPV and AgMNPV), fall within the NPV genus. A striking characteristic of the NPVs is the presence of two different phenotypes with distinct roles in the infection cycle. Important differences between these two phenotypes are the lipid and protein compositions of their envelopes and the type of host cells they infect. Budded virus (BV) is the phenotype responsible for systemic infection of the insect host, and GP64 is the major envelope glycoprotein of this phenotype. GP64 is absent from the envelope of the other phenotype, the occlusion-derived virus (ODV), which serves to initiate baculovirus infection in midgut epithelial cells. GP64 was shown to be a glycosylated, phosphorylated and acylated protein, present at early and late stages of the infection cycle. Based on estimations of mass on non-reducing SDS-PAGE, GP64 was speculated to exist as both trimeric and tetrameric forms. Several observations contributed to the belief that GP64 was important for BV entry into the host cell by endocytosis: 1) antibodies to GP64, as well as lipophilic amines, inhibited BV infectivity at a step beyond virus binding to host cells, 2) GP64 induced low-pH mediated membrane fusion when expressed alone at the surface of cells, 3) a monoclonal antibody to GP64 inhibited this low pH-induced membrane fusion capacity. Because of GP64's presence at sites where viral budding occurred, roles for GP64 in virus exit were suspected, but never demonstrated. In this thesis, structural and functional aspects of GP64 were examined with the aim to expand our knowledge about the role of GP64 in BV exit/transmission and entry, within the baculovirus infection cycle.

In the first experimental chapter (chapter 2), an anti-GP64 antiserum was generated, and used to examine the kinetics of OpMNPV GP64 synthesis, oligomerization, and carbohydrate processing. Immunoprecipitation, pulse label, and pulse-chase analyses showed that OpMNPV GP64 is produced during a large part of the infection cycle, and undergoes a rapid but inefficient oligomerization step. While carbohydrate addition was rapid, carbohydrate processing occurred with half-times of 45 to 75 min and appeared to be the rate-limiting step in maturation of GP64. In addition, a difference in carbohydrate processing efficiency was demonstrated between the early and late phases of the infection cycle. Mass spec of a highly purified, soluble form of OpMNPV GP64 revealed that two high molecular weight forms of GP64, typically

observed on non-reducing gels, are both homotrimers. The different forms may be the result of differential disulfide bonding.

Next, the role of GP64 in the infection cycle was addressed by examining AcMNPV infectivity in the complete absence of GP64 (chapter 3). Because GP64 was suspected to be an essential BV protein, OpMNPV GP64- expressing Sf9 cells were generated for complementation during propagation of an AcMNPV recombinant gp64null virus (vAc^{64Z}). This gp64null virus was able to propagate in Sf9 cells when GP64 was complemented. However, by detection of an included *lacZ* marker gene and comparison to wild-type AcMNPV, vAc^{64Z} failed to transmit from Sf9 to Sf9 cell in the absence of GP64 complementation, both in cell culture as in *Trichoplusia ni* larvae. Thus, this result demonstrated a critical role for GP64 in virus transmission.

Whether the block in virus transmission was due to a defect in BV production or to production of non-infectious BV, was the next question we sought to address (chapter 4). A budding assay was designed to compare BV budding in the presence (wild-type AcMNPV) or absence of GP64 (gp64null virus). A second generation gp64null virus (vAc^{64*}) was generated and used for these studies. In the absence of GP64, budding appeared to be reduced by ~ 98%. Hence, the earlier observed block in viral transmission was likely and predominantly a result of decreased virus budding. Because the highly charged GP64 cytoplasmic tail domain (CTD) is predicted to be in a position to interact with cytoplasmic viral and/or cellular factors, it became the next target in the pursuit of the role of GP64 in BV budding. Recombinant viruses carrying deletions or modifications in the GP64 CTD and/or portions of the transmembrane (TM) domain were generated and examined by the earlier developed budding assay. The complete, seven amino acid, predicted CTD was found to be dispensable for propagation of AcMNPV in cell culture, for GP64 surface localization, and low pH-induced membrane fusion. Virus budding however was reduced by ~ 50%, and incorporation of GP64 into virions by 63%, thus indicating that the presence of the CTD domain may confer an advantage. Removal of 11 and 14 amino acids resulted in more dramatic effects. Membrane-anchoring of these GP64s was significantly affected, and viral budding was 4-22% and 2% respectively compared to a control virus with a wild-type GP64. The virus carrying a truncation of 14 amino acids was unable to propagate efficiently in Sf9 cells, indicating a possible role for amino acids -12, -13, and -14 from the C-terminus. A recombinant virus, vAc-CΔ3Ra, in which all arginines were replaced with alanines, was in all measurable aspects indistinguishable from virus carrying a wild-type GP64, demonstrating that the CTD charge is not essential.

In chapter 5, the role of GP64 in BV binding and entry into host cells was examined by a single cell infectivity assay. In this assay, inactivated virus as well as a highly purified, soluble form of OpMNPV GP64, competed with AcMNPV BV during a 1 hr viral adsorption period at 4°C, resulting in a reduced number of infected Sf9 cells. This suggests that AcMNPV GP64 is a host cell receptor binding protein. In addition, entry kinetics of the BV phenotype were examined. After binding, BV entered Sf9 cells

with a half-time of ~ 12.5 min, and fusion of the viral and endosomal membrane (presumably to release the NC into the cytoplasm) occurred with a half-time of ~ 25 min.

The last experimental chapter (chapter 6) describes the mapping and analysis of the *gp64* genomic region in baculovirus *Anticarsia gemmatalis* Multicapsid Nucleopolyhedrovirus (AgMNPV). This virus is extensively utilized in the protection of soybean crop in Brazil, and demonstrates well the baculovirus potential for insect pest control. To examine the relatedness of AgMNPV to other NPVs, the *gp64* genomic region of AgMNPV (containing 19 ORFs of ≥ 50 amino acids) was analyzed and compared to the corresponding regions in four other baculoviruses. In addition, a multiple alignment of GP64s from seven baculoviruses and envelope proteins of two orthomyxoviruses was performed, demonstrating that 1) baculovirus GP64s are highly conserved (74.5 to 78.6% amino acid identity), 2) among baculoviruses, AgMNPV GP64 is the least conserved in the TM domain and its CTD is truncated, 3) between baculovirus GP64 and Thogoto/Dhori virus envelope proteins, clusters of amino acid conservation can be identified, which may be useful in designing approaches to map key functional domains of GP64.

Finally, because virus budding is a poorly understood area of baculovirology, the general discussion includes a review of selected literature regarding the role of viral spike proteins in exit of enveloped viruses from host cells. In addition, a few GP64 research topics that are not addressed experimentally in this thesis, are included to complement our understanding of GP64. Next, evolutionary implications of the various experimental results are discussed with regard to the significance of the GP64 protein, and the relationship between GP64 and Thogoto and Dhori virus envelope proteins. The discussion is concluded with a note on what the current avenues of GP64 research are and what these may lead to in the future.

Samenvatting

Virussen behorende tot de familie Baculoviridae bezitten een dubbelstrengs DNA genoom en zijn van een lipidemembraan voorzien. Baculovirussen infecteren alleen geleedpotigen, voornamelijk rupsen van insecten uit de orde Lepidoptera. Zij werden bestudeerd met als doel het ontwikkelen van alternatieven voor chemische insectenbestrijding, en later vanwege hun potentieel als eiwitproductiesystemen en ter beantwoording van fundamenteel virologische vraagstukken. De Baculoviridae worden verdeeld in twee genera, de Granulovirussen (GVs) en de Kernpolyedervirussen (NPVs). De virussen die ik in dit proefschrift behandel, *Autographa californica*, *Orgyia pseudotsugata*, and *Anticarsia gemmatalis* Multicapsid Nucleopolyhedroviruses (AcMNPV, OpMNPV en AgMNPV), behoren tot de NPVs. Een opvallende karakteristiek van de NPVs is het voorkomen van twee verschillende phenotypen, die een afzonderlijke rol spelen in de infectiecyclus. Belangrijke verschillen tussen deze twee phenotypen zijn de lipide- en eiwitcompositie van hun membraan en het type gastheercel dat zij infecteren. Budded virus (BV) is het phenotype verantwoordelijk voor de systemische infectie van de gastheer, en GP64 is een viraal membraan glycoproteïne dat in relatief grote hoeveelheid aanwezig is in de lipidemembraan van dit phenotype. GP64 komt niet voor in het tweede phenotype, het occlusion-derived virus (ODV), welk tot doel heeft de gastheerinfectie te initiëren in de epitheelcellen van het darmkanaal. Door anderen werd reeds aangetoond dat GP64 geglycosileerd, gefosforileerd en geacyleerd is, en aanwezig is gedurende de vroege en late stadia van de infectiecyclus. Gebaseerd op de relatieve molecuulmassa op niet-reducerende eiwitgels, werd gespeculeerd dat GP64 voorkomt als trimeren en tetrameren. Een aantal observaties resulteerden in de hypothese dat GP64 een belangrijke factor is in het binnendringen van het BV phenotype in de gastheercel d.m.v. endocytose: 1) anti-GP64 antilichamen, en ook lipofiele aminegroepen, blokkeren infectiviteit van BV in een stadium voorbij de binding van virus aan cellen, 2) GP64 veroorzaakt lage pH-afhankelijke membraanfusie, wanneer het afzonderlijk in Sf9 cellen tot expressie wordt gebracht, 3) een monoclonaal antilichaam, gericht tegen GP64, blokkeert deze membraanfusiecapaciteit. Omdat GP64 voorkomt op locaties waar virusbudding plaatsvindt, vermoedde men ook een rol in het naar buiten treden uit de gastheercel. Zo'n rol werd echter nog niet gedemonstreerd. In dit proefschrift worden structurele en functionele aspecten van GP64 onderzocht, met als doel onze kennis uit te breiden omtrent de rol van GP64 in het binnendringen en uit treden van de gastheercel, binnen de infectiecyclus.

In het eerste experimentele hoofdstuk (2) werd een anti-OpMNPV GP64 polyclonaal antilichaam geproduceerd. Dit werd gebruikt om de synthese, de oligomerisatie en de carbohydraat-modificatie van GP64 te bestuderen. Analyses m.b.v. immunoprecipitatie, 'pulse label', en 'pulse-chase' technieken, toonden aan dat GP64 gedurende het grootste gedeelte van de infectiecyclus geproduceerd wordt, en dat het

een snelle maar inefficiënte oligomerisering ondergaat. Het aanhechten van carbohydraatgroepen geschiedt snel. Echter, de modificatie van die groepen is een relatief langzaam proces en is mogelijk de stap die de snelheid van maturatie en transport van GP64 het meest beïnvloedt. Bovendien werd een verschil aangetoond in efficiëntie van GP64-carbohydraatmodificatie tussen het vroege en late stadium van de infectiecyclus. Een gezuiverde vorm van OpMNPV GP64 in oplossing werd onderworpen aan massaspectrometrie. Daarmee werd duidelijk dat twee verschillende vormen van GP64 met hoog-moleculaire massa, zoals die op een niet-reducerende eiwitgel worden waargenomen, beide homo-trimeren zijn. De twee waargenomen vormen zijn waarschijnlijk het gevolg van alternatief gevormde zwavelbruggen.

Vervolgens werd de rol van GP64 in de infectiecyclus bekeken, door de infectiviteit van AcMNPV te onderzoeken in de afwezigheid van GP64 (hoofdstuk 3). Omdat werd vermoed dat GP64 een essentieel baculoviruseiwit is, werden GP64-producerende Sf9 cellen geproduceerd ter aanlevering van GP64 tijdens de productie van een gp64-negatief virus (vAc^{gp64Z}). D.m.v. een *lacZ* markergen werd aangetoond dat dit gp64-negatief virus zich zonder problemen replicateerde, wanneer GP64 door de cellijn werd aangeleverd. Wanneer GP64 niet werd aangeleverd, bleek het gp64-negatieve virus niet in staat naburige Sf9 cellen te infecteren, zowel in celcultuur als in *Trichoplusia ni* rupsen. Hiermee werd een belangrijke rol voor GP64 gedemonstreerd, namelijk het verbreiden van de infectie van cel tot cel.

Het was niet bekend of dit defect in het verbreiden van infectie veroorzaakt werd door een gebrek aan virusbudding, of dat de budding onveranderd was maar dat de gevormde virussen niet infectieus waren. Deze vraag werd beantwoord in hoofdstuk 4. Een budding-assay werd opgezet, waarin AcMNPV en het gp64-negatief virus konden worden vergeleken. Een tweede generatie gp64-negatief virus (vAc^{gp64}) werd gebruikt voor die studie. Bij afwezigheid van GP64 bleek virusbudding gereduceerd te zijn met 98%. Het virustransmissiedefect van het gp64-negatief virus was daarom hoogstwaarschijnlijk een buddingdefect. Omdat het positief geladen, cytoplasmatische domein (CTD) van GP64 mogelijk interacties aangaat met cytoplasmatische factoren (viraal of cellulair), werd het CTD het volgende doel van onderzoek naar virus budding. Recombinante virussen met een *gp64* gen, gemodificeerd in CTD of transmembraan (TM) domein, werden geproduceerd en onderworpen aan het eerdergenoemde budding-assay. Dit wees uit dat het zeven aminozuren lange, hypothetische CTD niet nodig was voor vermeerdering van AcMNPV in celcultuur, voor GP64-transport naar het plasmamembraan en voor de lage pH-geïnduceerde membraanfusie functie. Echter, virusbudding was met 50% gereduceerd en de opname van GP64 in het BV met 63%, wat erop duidde dat het bezit van een CTD voor AcMNPV mogelijk een voordeel oplevert. Verwijdering van 11 en 14 aminozuren van het C-terminale eind van GP64 (virussen vAc-C-11 en vAc-C-14) had verdergaande gevolgen. Membraanverankering in deze mutanten was drastisch gereduceerd en virusbudding was respectievelijk 4-22% en 2%, vergeleken met niet-gemodificeerd GP64. Het virus vAc-C-14 was bovendien als enige niet in staat zich efficiënt te vermeerderen in Sf9 cellen, wat op

een mogelijke rol duidt voor aminozuren op positie 12, 13, en 14 van het C-terminale eind. Een recombinant virus, waarin alle arginine-residuen van het CTD waren vervangen door alanine, gedroeg zich in alle meetbare aspecten identiek aan wild-type AcMNPV. Dit betekent dat de lading van het CTD niet essentieel is.

In hoofdstuk 5 werd de rol van GP64 in het binden aan, en binnendringen van de gastheercel onderzocht, d.m.v. een 'single-cell infectivity assay'. In dit assay competeerden zowel geïnactiveerd virus als gezuiverd OpMNPV GP64 in oplossing, met AcMNPV gedurende een virusinfectieperiode van 1 uur bij 4°C, resulterend in een reductie van het aantal geïnfecteerde Sf9 cellen. Dit suggereert dat GP64 een gastheercelreceptor-bindend eiwit is. Ook werd de kinetiek van een aantal stappen in het virusendocytose proces gemeten. Na binding werd virus met een half-time van 12.5 minuten opgenomen door de gastheercel en fusie van de viraal en endosoom membranen (vermoedelijk ter introductie van het nucleocapside in het cytoplasma) geschiedde met een half-time van 25 minuten.

In het laatste experimentele hoofdstuk werd een genomisch segment, waarin het *gp64* gen, van AgMNPV gelocaliseerd en geanalyseerd. Dit virus wordt uitgebreid toegepast bij het beschermen van soyaboon gewas in Brazilië, en is een goed voorbeeld van het potentieel van baculovirussen voor insectenbestrijding. Om de verwantschap van AgMNPV met andere baculovirussen te bepalen werd dit genomisch segment, dat 19 leesramen van ≥ 50 aminozuren bevat, geanalyseerd en vergeleken met de corresponderende genoomregio's in vier andere baculovirussen. Ook werd een verwantschapsanalyse uitgevoerd met zeven baculovirus GP64 eiwitten en twee verwante membraanglycoproteïnen van de Thogoto-achtige virussen Thogoto virus (THO) en Dhori virus (DHO) (familie Orthomyxoviridae). Deze analyse toonde aan dat 1) baculovirus GP64 eiwitten zijn zeer geconserveerd (74.5 tot 78.6% aminozuuridentiteit), 2) bij de baculovirussen is AgMNPV GP64 het minst geconserveerd in het TM-domein, en het CTD is slechts 2 aminozuren lang, 3) Tussen baculovirus GP64 en THO- en DHO- membraanglycoproteïnen kunnen lokale gebieden onderscheiden worden met een hoog percentage identieke aminozuren. Deze lokale gebieden kunnen mogelijk behulpzaam zijn bij het bedenken van strategieën om de locatie en functie van belangrijke, geconserveerde domeinen van GP64 te bepalen.

Omdat in het onderzoek van baculovirussen weinig bekend is over virusbudding, wordt in de algemene discussie (hoofdstuk 7) een overzicht gegeven van geselecteerde literatuur betreffende budding van virussen met een lipidemembraan en de rol van het CTD daarin. Daarnaast wordt een aantal GP64 onderzoeksgebieden behandeld die in dit proefschrift niet aan de orde zijn gekomen, maar een belangrijke aanvulling zijn op de gepresenteerde experimentele resultaten. Vervolgens wordt de evolutionaire implicatie van de experimentele resultaten besproken, betreffende de betekenis van GP64 voor de Baculoviridae en de relatie tussen GP64 en de membraanglycoproteïnen van THO- en DHO- virussen. De discussie wordt besloten met een korte omschrijving van het huidige GP64 onderzoek, en waar dit in de toekomst toe kan leiden.

List of publications

- Oomens, A.G.P., S.A. Monsma, and G.W. Blissard. (1995). The baculovirus GP64 envelope fusion protein: Synthesis, oligomerization, and processing. *Virology* 209, 592-603
- Monsma, S.A., A.G.P. Oomens, and G.W. Blissard. (1996). The GP64 envelope fusion protein is an essential baculovirus protein required for cell-to-cell transmission of infection. *Journal of Virology* 70, 4607-4616
- Plonsky, I., E. Leikina, A.G.P. Oomens, G.W. Blissard, J. Zimmerberg, and L. Chernomordik (1997). The target membrane influences the pH-dependence and kinetics of viral fusion. *Biophysical Journal* 72 (2), A300
- Plonsky, I, M-S. Cho, A.G.P. Oomens, G.W. Blissard, and J. Zimmerberg (1999). An analysis of the role of the target membrane on the GP64-induced fusion pore. *Virology* 253, 65-76
- Oomens, A.G.P., and G.W. Blissard (1999). Requirement for GP64 to drive efficient budding of *Autographa californica* Multicapsid Nucleopolyhedrovirus. *Virology* 254, 297-314.
- Hefferon, K.L., A.G.P. Oomens, S.A. Monsma, C.M. Finnerty, and G.W. Blissard (1999). Host cell receptor binding by baculovirus GP64 and kinetics of virion entry. *Virology* 258, 455-468
- Oomens, A.G.P., M. Lobo de Souza, J.M. Slack, B.M. Ribeiro, and Gary W. Blissard. (1999). Characterization of the *ORF119-gp64-p74* locus of *Anticarsia gemmatalis* Multicapsid Nucleopolyhedrovirus. *Manuscript in preparation*.

Curriculum vitae

Antonius G.P. (Tom) Oomens werd geboren in Nederland op 15 September 1963 te Oosterhout, alwaar in 1980 het VWO diploma werd behaald aan het Mgr. Frencken College. Vervolgens werden enige jaren doorgebracht studierend aan de HBO-Verpleegkunde (eerste drie jaar), en werkend voor Philips, te Eindhoven. In 1986 werd begonnen aan de studie Biologie aan de Landbouwniversiteit Wageningen. Doctoraal onderzoek werd verricht bij de toenmalige vakgroepen Celbiologie (immunologie) en Virologie, alsmede aan de Universidad de Murcia, Spanje, en in het Boyce Thompson Institute te Ithaca, New York, Verenigde Staten. In 1992 studeerde hij af en bleef hij werkzaam in het laboratorium van Dr. Gary W. Blissard in het bovengenoemde Boyce Thompson Institute. Na een aantal jaren als 'technician' aan baculovirussen gewerkt te hebben, werd een Ph.D. studie begonnen betreffende de structuur en functie van het baculovirus eiwit GP64, onder supervisie van Dr. Just M. Vlak, leerstoelgroep Virologie, Universiteit Wageningen, en Dr. Gary W. Blissard. De resultaten van deze studie zijn in dit proefschrift weergegeven.

In augustus 1999 werd een post-doctorale studie begonnen aan Respiratory Syncytial virus (een paramyxovirus) in het laboratorium van Dr. Gail W. Wertz, Department of Microbiology, aan de University of Alabama Medical School, Birmingham, Alabama, Verenigde Staten.